

**STRUCTURE-FUNCTION RELATIONSHIPS OF
BOLAAMPHIPHILIC PEPTIDES AND PEPTIDE HYBRIDS**

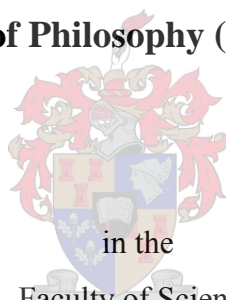
by

Marco Martari

Laurea in Chemistry and Pharmaceutical Technology,
University of Padua, Italy

Dissertation presented for the degree of

Doctor of Philosophy (Chemistry)



in the
Faculty of Science

at the

University of Stellenbosch

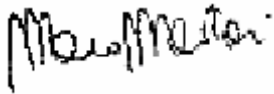
Promoter: **Prof. RD Sanderson**
Chemistry and Polymer Science
University of Stellenbosch

December 2006

Declaration

I, the undersigned, hereby declare that the work contained in this dissertation is my own original work and that I have not previously in its entirety or in part submitted it at any university for a degree.

Marco Martari



Date

31.08.06

Abstract

Synthetic peptides derived from the active core of a natural antimicrobial peptide were used as a template for the design of novel bolaamphiphilic peptides and hybrid molecules. The amphiphilic character of the original compounds was modified by using non-natural amino acids (AAs) – such as ω -AA – and varying the hydrophobic content. The outcomes of these modifications were studied focusing on structural and biological properties.

Because of the bolaamphiphilic character, the alternation of polar and non-polar AAs and the use of hydrophobic AAs such as tyrosine and leucine, these novel molecules were designed to undergo self-assembly in response to certain stimuli (e.g. a pH increase). This significant property was investigated by means of different tools, such as fluorescence measurements, electron microscopy (EM), Fourier transform infrared spectroscopy (FT-IR) and circular dichroism (CD). By using fluorescence it was possible to determine the critical aggregation concentration (CAC) of the new compounds. Differences in amino acid composition, which were reflected into diverse secondary structures and hydrophobicity (H), resulted in different CAC values and aggregation profiles. The data were consistent with the literature and showed that (i) the aggregation of these basic compounds was triggered by a pH increase, (ii) the use of hydrophobic AA highly augmented the self-assembly tendency while (iii) the presence of proline strongly reduced it. EM revealed the morphology of the peptide assemblies: microtubes and microvesicles were identified and characterised by dimensions of 500 nm to 2 μ m. The presence of 3-way junctions and vesicles budding out of the microtubes demonstrated that the self-assembly is a dynamic process. The aggregation was confirmed by FT-IR spectroscopy, by studying the dried peptide assemblies and the significant spectral signs the process left, especially in the amide II envelope.

The relationship between hydrophobicity and self-assembly was expanded by experimentally and theoretically determining the hydrophobic content of the novel bolaamphiphiles. Data from liquid chromatography and computational calculations (two common ways used to determine the hydrophobicity of a given molecule) correlated well with the tendency to self-assemble, as expressed by CAC values. Importantly, some structural parameters (such as the presence of β -turn induced by proline) also showed significant influence on the aggregation, highly limiting the role of the peptides' hydrophobicity.

These novel peptide bolaamphiphiles displayed a very low haemolytic action and retained some antimicrobial activity at high concentrations against both Gram-positive and -negative bacteria. Unfortunately, the activity was greatly reduced at low concentrations, as clearly demonstrated by the use of two antimicrobial tests. The inability to provoke cell lysis was also evident when using liposomes mimicking a negative bacterial membrane.

The loss of activity is possibly related to the modifications of the three-dimensional structure caused by the use of ω -AA and proline, which strongly alter the secondary structure.

The results of this study were valuable in terms of understanding the relationships between self-assembly and structural parameters, such as AA compositions, hydrophobicity and secondary structure. Possible applications of the synthesised compounds were however limited as a result of the loss of the biological activity at low concentrations.

Opsomming

Sintetiese peptiede verkry vanaf die aktiewe kern van 'n natuurlike antimikrobiese peptied is as 'n templaar gebruik vir die ontwerp van nuwe bola-amfifiliese peptiede en hibriedmolekule. Die amfifiliese karakter van die oorspronklike verbindings is verander met behulp van nie-natuurlike aminosure (ASe), soos byvoorbeeld ω -AS, en deur die hidrofobiese inhoud te verander. Die gevolge van hierdie veranderinge is bestudeer, met die fokus op strukturele en biologiese eienskappe.

As gevolg van die bola-amfifiliese karakter, die afwisseling van polêre en nie-polêre ASe en die gebruik van hidrofobiese ASe, soos tirosien en leusien, is hierdie unieke molekules ontwerp om selfmontering te ondergaan in reaksie op sekere stimuli (bv. 'n verhoging in pH). Hierdie belangrike eienskap is met verskeie tegnieke ondersoek, soos byvoorbeeld fluoressensie-metings, elektronmikroskopie (EM), Fourier-transform infrarooispektrometrie (FT-IR), en sirkulêre dichroïsme (CD). Fluoressensie is gebruik om die kritieke aggregasie konsentrasie van die nuwe verbindings te bepaal. Verskille in aminosuursamestelling, wat gereflekteer is in 'n verskeidenheid sekondêre strukture en hidrofobisiteit (H), het aanleiding gegee tot verskillende kritieke aggregasie konsentrasiewaardes en aggregasieprofiel. Die data was in pas met die literatuur en het gewys dat (i) die aggregasie van hierdie basiese verbindings veroorsaak is deur 'n verhoging in die pH, (ii) die gebruik van hidrofobiese ASe die selfmonteringstendens baie versterk het, terwyl (iii) die teenwoordigheid van prolien dit sterk laat afneem het. EM het die morfologie van die peptiedsamestellings uitgewys: mikrobuisies en mikrobliasies is geïdentifiseer en gekarakteriseer met afmetings van 500 nm tot 2 μ m. Die teenwoordigheid van 3-richtingverbindings, en blasies wat uit die mikrobuisies groei, toon aan dat die selfmontering 'n dinamiese proses is. Die aggregasie is bevestig met FT-IR, deur bestudering van die gedroogde peptiedmonterings en die opmerklieke spektrale tekens wat die proses nagelaat het, veral in die amied-II-omhulsel.

Die verwantskap tussen hidrofobisiteit en selfmontering is verder ondersoek deur die eksperimentele en teoretiese bepaling van die hidrofobiese inhoud van die nuwe bola-amfifiliese. Resultate vanuit vloeistofchromatografie en rekenaarmatige berekeninge (twee metodes wat algemeen gebruik word om hidrofobisiteit van 'n spesifieke molekule te bepaal), het goed ooreengestem met die tendens tot selfmontering, soos uitgedruk in die kritieke aggregasie konsentrasie-waardes. Dit is belangrik om ook daarop te let dat sekere strukturele parameters (soos die teenwoordigheid van 'n β -draai, geïnduseer deur prolien) ook 'n sterk invloed op aggregasie getoon het, met gevolglike beperking van die rol van die hidrofobisiteit van die peptied.

Hierdie unieke peptied-bola-amfifiele het 'n baie lae hemolitiese aksie getoon, en behou gedeeltelike antimikrobiese aktiwiteit by hoë konsentrasies teen beide Gram-positiewe en -negatiewe bakterieë. Die aktiwiteit is egter baie laer teen lae konsentrasies, soos duidelik blyk uit

twee antimikrobiese toetse. Die onvermoë om sel-liesse te veroorsaak is ook uitgewys met die gebruik van liposome wat 'n negatiewe bakterie-membraan nageboots het.

Die verlies aan aktiwiteit is moontlik verwant aan veranderinge aan die drie-dimensionele struktuur veroorsaak deur die gebruik van ω -AS en prolien, wat die sekondêre struktuur aansienlik verander het.

Die resultate van hierdie studie is waardevol in terme van die verstaan van die verwantskappe tussen selfmontering en strukturele parameters, soos AS-samestellings, hidrofobisiteit en sekondêre struktuur. Moontlike aanwending van die gesintetiseerde verbindings was egter beperk, weens die verlies van biologiese aktiwiteit by lae konsentrasies.

Acknowledgments

Prof RD Sanderson – my promoter – for allowing me to creatively and independently develop this research project.

Dr M Rautenbach (Biochemistry, US) for giving helpful inputs about peptide synthesis, providing some crude peptides and discussing some of the biological results.

Dr J Juodaityte for her help in setting up peptide synthesis and purification facilities and her kind cooperation during the final submission of my thesis.

Dr MJ Hurdall for her words of wisdom, the valuable thesis writing assistance and appreciated suggestions during the preparation of this manuscript.

Dr HC Hoppe (Clinical Pharmacology, UCT) for his kind collaboration during the haemolysis tests and allowing me to work in his lab. Dr AC Withelaw (Microbiology, UCT) for his help during the antimicrobial tests. Ms M Chauhan (Molecular and Cellular Biology, UCT) for her cooperation with the CD analysis. Dr M Stander (Central Analytical Facilities, US) for performing the ESI-MS analyses. Ms M Waldron (Physics, UCT) for SEM and cryo-SEM work. Drs T Nell and TA Kohn (Physiological Sciences, US) for the use of the Kontron microplate fluorescence reader.

Institute for Polymer Science/UNESCO-Associated Centre for Macromolecules and Materials for financial assistance.

Jurjen and Noki, Sibuy, Sonto, Jos, Maggie, Nagarayu, Gertrude and Bettinah for their friendship and caring support. Laura, for her encouragement, strength and positive thinking.

Dr R Salvatori (Medicine, Johns Hopkins University) for welcoming into his group before the formal end of my doctoral studies.

Fiorella and Giuseppe, Sara and Gianluca for accepting my decisions and for their unconditional love.

The last but not the least, Ale, for driving me so far away from my small nest, teaching me how to open my mind and see the world from a different point of view, for being at my side, supporting and listening to me at any time. This thesis is dedicated to you. Grazie.

Table of contents

List of abbreviations	XII
List of figures	XVI
List of tables	XXII
Structures, three-letter and single-letter codes for proteinogenic amino acids	XXIV
Structures and three-letter codes for non-proteinogenic amino acids used in this study	XXV
Preface	XXVII
Chapter 1 Introduction	1
1.1 Background	1
1.2 Objectives	2
1.3 Layout of the dissertation	3
1.4 References	5
Chapter 2 Theoretical framework	7
2.1 Cationic antimicrobial peptides	7
2.1.1 Sources and characteristics	7
2.1.2 Structures and classification	8
2.1.3 Mechanisms of antibacterial activity	9
2.1.4 Antimicrobial peptides as next generation therapeutics	12
2.2 Antimicrobial peptides derived from <i>Sarcophaga peregrina</i>	13
2.3 Peptide bolaamphiphiles	16
2.3.1 Bolaamphiphiles	16
2.3.2 Self-assembly properties	17
2.4 References	19
Chapter 3 Synthesis of novel bolaamphiphilic peptides and peptide hybrids	26
3.1 Introduction	26
3.1.1 Amino acids, peptides and proteins	26
3.1.2 Principle and development of solid-phase peptide synthesis	28
3.1.2.1 Side-chain protecting groups	31
3.1.2.2 Fmoc deprotection	33
3.1.2.3 Activation strategies	33
3.1.2.4 Racemisation	35

3.2 Design of novel peptide bolaamphiphiles	36
3.2.1 Guidelines	36
3.2.2 Library of peptides	37
3.3 Materials and instrumentation	39
3.3.1 Chemicals	39
3.3.1.1 Solvents and general reagents	39
3.3.1.2 Protected amino acids, resins and coupling reagents	39
3.3.2 Instrumentation	40
3.3.2.1 Bench solid-phase peptide synthesis	40
3.3.2.2 Reversed-phase high performance liquid chromatography	40
3.3.2.3 Electrospray ionisation mass spectrometry	41
3.4 Experimental methods	41
3.4.1 Preparation of solvents	41
3.4.2 Peptide synthesis	41
3.4.2.1 Attachment of the first amino acid	42
3.4.2.2 Capping	42
3.4.2.3 Elongation of the peptide chain	43
3.4.2.4 Deprotection of the attached Fmoc-amino acid	43
3.4.2.5 Cleavage of the peptide from the resin	43
3.4.2.6 Ninhydrin test	43
3.4.2.7 Chloranil test	44
3.4.2.8 Determination of coupling efficiency	44
3.4.3 Peptide purification	45
3.4.4 Analysis of purified peptides	45
3.5 Results and discussion	46
3.5.1 Peptide synthesis	46
3.5.2 Peptide purification and analysis	50
3.6 Conclusions	53
3.7 References	54

Chapter 4 Self-assembly behaviour and structural characterisation of novel bolaamphiphiles

4.1 Introduction	58
4.2 Materials	59
4.3 Experimental methods	59
4.3.1 Steady-state fluorescence measurements	59
4.3.2 Self-assembly experiments	60

4.3.3 Congo red staining and optical microscopy	60
4.3.4 Scanning electron microscopy	60
4.3.5 Cryo-fracture scanning electron microscopy	60
4.3.6 Fourier transform photoacoustic infrared spectroscopy	60
4.3.7 Circular dichroism spectroscopy	61
4.4 Results and discussion	62
4.4.1 Steady-state fluorescence measurements	62
4.4.2 Self-assembly through microscopy	69
4.4.3 Gels from peptide bolaamphiphiles	73
4.4.4 Fourier transform photoacoustic infrared spectroscopy	75
4.4.5 Circular dichroism spectroscopy	78
4.5 Conclusions	81
4.6 References	83
Chapter 5 Hydrophobic characterisation and correlation with self-assembly behaviour	86
5.1 Hydrophobicity in peptide chemistry	86
5.2 Materials	89
5.3 Methods	90
5.3.1 Theoretical determination of the hydrophobic content	90
5.3.2 Experimental determination of the hydrophobic content by RP-HPLC	90
5.3.3 Critical aggregation concentration	91
5.4 Results and discussion	91
5.4.1 Theoretical determination of the hydrophobic content	91
5.4.2 Experimental determination of the hydrophobic content by RP-HPLC	92
5.4.3 Correlation between hydrophobicity and aggregation behaviour	96
5.5 Conclusions	99
5.6 References	100
Chapter 6 Determination of biological properties of peptides and peptide hybrids	102
6.1 Introduction	102
6.2 Materials	103
6.3 Experimental methods	104
6.3.1 Antimicrobial activity	104
6.3.1.1 Bauer-Kirby disk diffusion test	104
6.3.1.2 MIC determination (I)	104
6.3.1.3 MIC determination (II)	104

6.3.2 Haemolytic activity	105
6.3.3 Dye-leakage assay from liposomes	106
6.3.3.1 Preparation of liposomes	106
6.3.3.2 Determination of lipid concentration	107
6.4 Results and discussion	108
6.4.1 Antimicrobial properties	108
6.4.2 Haemolytic activity	112
6.4.3 Interaction with model membranes	114
6.5 Conclusions	117
6.6 References	119
Chapter 7 Conclusions and recommendations	121
7.1 Conclusions	121
7.1.2 Understanding of the self-assembly behaviour	121
7.1.3 Morphological study of the supramolecular assemblies	122
7.1.4 Hydrophobic content and its correlation to the self-assembly	122
7.1.4 Influence of non-natural amino acid on the biological activity	123
7.2 Limitations	124
7.3 Recommendations for future work	125
7.4 References	126
Appendix A Examples of natural antimicrobial peptides	A-1
Appendix B Additional mass spectra of peptide bolaamphiphiles	B-1
Appendix C CLOGP calculations by Bio-Loom software	C-1

List of abbreviations

3D	three-dimensional
A	absorbance
Å	angstrom
AA	amino acid
ACN	acetonitrile
AcOH	acetic acid
amu	atomic mass unit
ATCC	American type culture collection
Boc	<i>tert</i> -butoxycarbonyl
BOP	benzotriazol-1-yloxytris(dimethylamino)phosphoniumhexafluorophosphate
BSA	bovine serum albumin
C5	6-aminohexanoic acid (also 6-Ahx)
C8	9-aminononanoic acid (also 9-Anc)
CAC	critical aggregation concentration
Calcd	calculated
CAMPs	cationic antimicrobial peptides
CD	circular dichroism
CF	5(6)-carboxyfluorescein
CFU/ml	colony forming unit per millilitre
CHOL	cholesterol
CL	cardiolipin
CLOGP	calculated Log <i>P</i>
CMC	critical micelle concentration
CR	Congo red
CV	cone voltage
Da	dalton
DCC	1,3-dicyclohexylcarbodiimide
DCM	dichloromethane
DIC	1,3-diisopropylcarbodiimide
DIEA	N,N'-diisopropylethyl amine
DMF	N,N'-dimethylformamide
<i>E. coli</i>	<i>Escherichia coli</i>
<i>E. faecalis</i>	<i>Enterococcus faecalis</i>
ELISA	enzyme-linked immunosorbent assay
EL-SD	evaporative light-scattering detector

EM	electron microscopy
EPC	egg phosphatidylcholine
EPG	egg phosphatidylglycerol
em	emission
eq.	equivalent
ex	excitation
ESI-MS	electrospray ionisation mass spectrometry
Fmoc	<i>N</i> ⁹ -fluorenylmethyloxycarbonyl
FT-IR PAS	Fourier-transform infrared photoacoustic spectroscopy
H	hydrophobicity
HATU	<i>N</i> -[(dimethylamino)-1 <i>H</i> -1,2,3-triazolo[4,5- <i>b</i>]pyridin-1-yl-methylene]- <i>N</i> -methylmethanaminium hexafluorophosphate <i>N</i> -oxide
HBTU	<i>N</i> -[(1 <i>H</i> -benzotriazol-1-yl)(dimethylamino) methylene]- <i>N</i> -methylmethanaminium hexafluorophosphate <i>N</i> -oxide
HC ₅₀	peptide concentration leading to 50% haemolysis
HOBt	1-hydroxybenzotriazole
HPLC	high performance liquid chromatography
hRBCs	human red blood cells
k'	isocratic capacity factor
I ₁	pyrene first vibrionic band (373 nm)
I ₃	pyrene third vibrionic band (384 nm)
LMVs	large multilamellar vesicles
log <i>k</i>	logarithm of isocratic capacity factor
Log <i>P</i>	logarithm of partition coefficient
LUVETs	large unilamellar vesicles by extrusion technique
M	molar
[M+H] ⁺	molecular ion
[M-H+Na] ⁺	sodium salt of the molecular ion
MHA	Mueller-Hinton agar
MHB	Mueller-Hinton broth
MIC	minimum inhibitory concentration
mdeg	millidegree
mM	millimolar
mmol	millimole
mol	mole
mQ	milli Q
ms	molecular sieves

MW	molecular weight
<i>m/z</i>	mass over charge ratio
N	normal
Na ₂ EDTA•2H ₂ O	disodium ethylenediaminetetraacetate dihydrate
OD	optical density
OM	optical microscopy
<i>P. aeruginosa</i>	<i>Pseudomonas aeruginosa</i>
PBS	phosphate-buffered saline
PDB ID	protein data bank identification number
PE	phosphatidylethanolamine
PS	phosphatidylserine
PyBOP [®]	benzotriazol-1-yloxytris(pyrrolidino)phosphonium hexafluorophosphate
RP-HPLC	reversed-phase high performance liquid chromatography
rpm	revolutions per minute
RT	room temperature
SAR	structure-activity relationship
<i>S. aureus</i>	<i>Staphylococcus aureus</i>
<i>S. marcescens</i>	<i>Serratia marcescens</i>
SEM	scanning electron microscopy
Sph	sphingomyelin
SPPS	solid-phase peptide synthesis
<i>t</i> -Bu	<i>tert</i> -butyl
TBTU	<i>N</i> -[(1 <i>H</i> -benzotriazol-1-yl)(dimethylamino)methylene]- <i>N</i> -methylmethanaminium tetrafluoroborate <i>N</i> -oxide
TEA	triethylamine
TFA	trifluoroacetic acid
TFE	trifluoroethanol
TFFH	tetramethylfluoroformamidinium hexafluorophosphate
TIS	triisopropyl silane
<i>t</i> _R	HPLC retention time
Tris	tris(hydroxyethyl) amino methane
TSA	triptone soy agar
TSB	triptone soy broth
USB	United States Biochemical
UV	ultraviolet
VIS	visible
λ_{em}	emission wavelength

λ_{exc}	excitation wavelength
λ_{max}	maximum emission wavelength
μg	microgram
μl	microlitre
μm	micron/micrometre
μM	micromolar
μmol	micromole

List of figures

Chapter 2

Fig. 2.1: Actions naturally performed by cationic antimicrobial peptides (adapted from Sugiarto and Yu, 2004).

Fig. 2.2: Molecular models of the different structural classes of antimicrobial peptides: a) β -sheet structure of human β -defensin-2, b) α -helical structure of magainin 2, c) looped structure of bovine bactenecin and d) extended structure of bovine indolicidin. Models are taken from the NMR structural database and based on two-dimensional NMR spectroscopy of the peptides in water (a) or in a membrane mimetic condition (b, c and d) (adapted from Hancock, 2001).

Fig. 2.3: Barrel-stave model. Peptides reach the membrane either as monomers or oligomers and first assemble on the surface of the membrane (A), then insert into the lipid core of the membrane following recruitment of additional monomers (B). Colour designation: black, hydrophobic surface; grey, hydrophilic surface (adapted from Shai, 2002).

Fig. 2.4: Carpet model. The peptides reach the membrane either as monomers or oligomers and then bind to the surface of the membrane with their hydrophobic surfaces facing the membrane and their hydrophilic surfaces facing the solvent (A). When a threshold concentration of peptide monomers is reached, the membrane is permeated and transient pores can be formed (B), a process that can lead also to membrane disintegration (C). Colour designation: black, hydrophobic surface; grey, hydrophilic surface (adapted from Shai, 2002).

Fig. 2.5: Toroidal pore model. Peptides interact with the membranes with their hydrophilic regions (a) and positively modify the membrane curvature (b). With a flip-flop mechanism they translocate and act on intracellular targets(c) (adapted from Matsuzaki, 1999).

Fig. 2.6: Comparison of primary structures of sapecin A and its homologues. Identical amino acids are highlighted (modified from Yamada and Natori, 1993).

Fig. 2.7: Primary structure of sapecin B. Disulfide bridges are indicated (modified from Yamada and Natori, 1993).

Fig. 2.8: Synthetic peptides derived from sapecin B. From sapecin B, the first generation peptides are in the first line (I), the second generation compounds in the second line (II) and the third generation peptides in the last 6 cells (III). The rational path between sapecin B and the leader antimicrobial sequence used in the present study is shown by the grey boxes.

Fig. 2.9: Chemical structure of the hydrophobic backbones that can be obtained by hydrolysis of archaeal tetraether lipids (after Gliozzi et al., 2002).

Fig. 2.10: Molecular structure of oligopeptides bolaamphiphiles synthesised by Shimizu's group in the late 1990s (modified from Kogiso et al., 1998).

Chapter 3

Fig. 3.1: Zwitterionic structure of a general amino acid at pH 7.

Fig. 3.2: The peptide bond forms the backbone of peptides and proteins.

Fig. 3.3: The peptide bond (adapted from: www.codefun.com/Genetic_tRNA.htm, 25/11/05).

Fig. 3.4: Protein and peptide structures: primary, secondary, tertiary and quaternary (adapted from: www.geneticsolutions.com, 24/10/05).

Fig. 3.5: Principle of SPPS. P and P': permanent protecting group; T: temporary protecting group; X: activating group.

Fig. 3.6: Boc SPPS (Merrifield's SPPS) (Merrifield, 1963). P and P' are permanent protecting groups removed by HF while the Boc group is removed by TFA. Activation strategy shown: preformed symmetrical anhydrides.

Fig. 3.7: Fmoc SPPS. P and P' are permanent protecting groups removed by the final TFA cleavage while the Fmoc group is removed by piperidine. Activation strategy shown: active esters.

Fig. 3.8: Reactions involved in the Fmoc deprotection.

Fig. 3.9: Racemisation via oxazolone formation.

Fig. 3.10: Library of synthesised compounds: the original amino acid pattern is shown at the top of the diagram. For shortness, C8 and C5 represent 9-aminononanoic acid and 6-aminohexanoic acid respectively.

Fig. 3.11: Shake-flask method used for manual solid-phase peptide synthesis.

Fig. 3.12: A) RP-HPLC chromatogram of crude OY2 on system 1 (C₁₂ column) eluted with gradient C. Note the difference between the signal of the UV detector and the one from the EL-SD (refer to Section 4.2.2.2 for details about UV/EL-SD settings). B) RP-HPLC chromatogram of pure OY2 (same conditions).

Fig. 3.13: RP-HPLC chromatogram of crude OL1 on system 1 (C₁₂ column) eluted with gradient C. B) RP-HPLC chromatogram of pure OL1 (same conditions).

Fig. 3.14: ESI-MS spectrum of crude KL3. Isotope variations are marked by i_1 , i_2 and i_3 corresponding to m/z -values with 1, 2 or 3 amu higher than the mass calculated from the monoisotopic residue mass (unknown fragments are indicated by *).

Fig. 3.15: ESI-MS spectrum of crude LO1. Isotope variations are marked by i_1 , i_2 and i_3 corresponding to m/z -values with 1, 2 or 3 amu higher than the mass calculated from the monoisotopic residue mass (unknown fragments are indicated by *).

Fig. 3.16: ESI-MS spectrum of crude LY1. Isotope variations are marked by i_1 , i_2 and i_3 corresponding to m/z -values with 1, 2 or 3 amu higher than the mass calculated from the monoisotopic residue mass (unknown fragments are indicated by *).

Fig. 3.17: ESI-MS spectrum of crude KL2. Isotope variations are marked by i_1 , i_2 and i_3 corresponding to m/z -values with 1, 2 or 3 amu higher than the mass calculated from the monoisotopic residue mass (unknown fragments are indicated by *).

Fig. 3.18: ESI-MS spectrum of pure KL1. Isotope variations are marked by i_1 , i_2 and i_3 corresponding to m/z -values with 1, 2 or 3 amu higher than the mass calculated from the monoisotopic residue mass.

Chapter 4

Fig. 4.1: Pyrene fluorescence emission spectra in water, OY1 in 0.1% TEA ($[OY1] < CAC$) [A] and OY1 in 0.1% TEA ($[OY1] > CAC$) [B]. Differences in I_3 intensity are underlined by the dotted line. $\lambda_{exc} = 334$ nm, emission recorded between 350 and 450 nm on a LS50B Fluorescence Spectrometer (Perkin Elmer, UK), scan speed 500 nm/min.

Fig. 4.2: Change of pyrene I_1/I_3 ratios with peptide concentration in 0.1% TEA. $\lambda_{exc} = 334$ nm; detection wavelengths: $I_1 = 373$ nm; $I_3 = 384$ nm. The arrows graphically indicate the CAC values.

Fig. 4.3: Effect of pH on the aggregation process of OY1. The arrows graphically indicate the CAC values.

Fig. 4.4: Effect of pH on the aggregation process of OY2. The arrows graphically indicate the CAC values.

Fig. 4.5: Despite small differences in the primary structure, KL peptide hybrids (KL1, KL2, KL3, KL4) show a similar behaviour in 0.1% TEA.

Fig. 4.6: Role of three-dimensional structure on the aggregation behaviour of OY1 and OY2 in 0.1% TEA. The arrows graphically indicate the CAC values.

Fig. 4.7: Role of three-dimensional structure on the aggregation behaviour of OL1 and OL2 in 0.1% TEA. The arrows graphically indicate the CAC values.

Fig. 4.8: Effect of Leu→Tyr substitution on the aggregation behaviour in 0.1% TEA of OL1 and OY1. The arrows graphically indicate the CAC values.

Fig. 4.9: Effect of Leu→Tyr substitution on the aggregation behaviour in 0.1% TEA of OL2 and OY2. The arrows graphically indicate the CAC values.

Fig. 4.10: Assembly of OY1 in 0.1% TEA (after 7 days at 25 °C) upon treatment with CR (left) and birefringence under polarised light (right). The scale bar represents 100 μ m.

Fig. 4.11: Assembly of OY2 in 0.1% TEA (after 7 days at 25 °C) upon treatment with CR (left) and birefringence under polarised light (right). The scale bar represents 100 μ m.

Fig. 4.12: SEM images of dried assemblies from KL1. [A] Vesicles budding out of interwoven microtubes.

Fig. 4.13: SEM images of dried assemblies from KL4.

Fig. 4.14: SEM images of dried assemblies from OY2. [A] Vesicles budding out of microtubes.

- Fig. 4.15:** SEM images of 3-way junctions (arrows) from dried assemblies: OL2 [A] and OL1 [B].
- Fig. 4.16:** Microtubes from OY1 [A] and OY2 assemblies [B] after 15 days in 0.1% TEA.
- Fig. 4.17:** Microtubes from KL4 assemblies after 15 days in 0.1% TEA.
- Fig. 4.18:** Microtubes from OL1 [A] and OL2 assemblies [B] after 15 days in 0.1% TEA.
- Fig. 4.19:** Light microscope images showing birefringence from OY1 gel, observed under cross-polarised light. The bar scale represents 100 μm .
- Fig. 4.20:** FT-IR spectrum of the dried OY1 assemblies in the region 500-4500 cm^{-1} .
- Fig. 4.21:** FT-IR spectrum of the dried KL2 assemblies in the region 500-4500 cm^{-1} .
- Fig. 4.22:** Amide I bands (black) and deconvolved amide I bands (grey) of dried peptide assemblies (1700-1600 cm^{-1}).
- Fig. 4.23:** CD spectra of peptide bolaamphiphiles [A] in a watery system and [B] in a more hydrophobic environment.
- Fig. 4.24:** CD spectra of peptide bolaamphiphiles [A] in a watery system and [B] in a more hydrophobic environment.
- Fig. 4.25:** Hypothetical self-assembly mechanism of tubule formation (modified from Matsui and Douberly, 2001).
- Fig. 4.26:** Potential mechanism of tubule formation. Red: hydrophilic; blue: hydrophobic. [A] Each peptide may interact with one another to form closed rings, which stack on top of one another to give a nanotube. [B] Three nanotubes are connected by a three-way junction (modified from Vauthey et al., 2002).

Chapter 5

- Fig. 5.1:** Hydrophobicity contribution of single amino acids (Tao et al., 1999).
- Fig. 5.2:** Linear correlation between the two sets of CLOGP values (calculated with the residue addition method and the fragment addition method) for peptides L3, L4, L5, OL2, OY2.
- Fig. 5.3:** Linear correlation between RP-HPLC retention times of bolaamphiphilic peptides and hybrids in a C_{12} column and CLOGP values (fragment addition method). The two circles indicate L3, L4 and L5 peptides.
- Fig. 5.4:** Graphical correlation between RP-HPLC retention times of bolaamphiphilic peptides and hybrids in a C_{12} column (gradient C_1 and H_1) and CLOGP values (fragment addition method).
- Fig. 5.5:** Linear correlation between RP-HPLC retention times of bolaamphiphilic peptides and hybrids in a C_{18} column and CLOGP values (fragment addition method). The two circles indicate L3, L4 and L5 peptides.

Fig. 5.6: Graphical correlation between RP-HPLC retention times of bolaamphiphilic peptides and hybrids in a C₁₈ column and CLOGP values (fragment addition method).

Fig. 5.7: Helical wheel representation of L3, L4 and L5 peptides. Colour code: black = Lys; white = Leu. Computer-generated helical wheels were obtained by Peptide Companion software (CSPS, Tucson, AZ, USA).

Fig. 5.8: Aggregation behaviour (expressed by CAC values) compared to hydrophobic content (expressed by retention times in RP-HPLC).

Fig. 5.9: Aggregation behaviour (expressed by CAC values) compared to hydrophobic content (expressed by CLOGP_{FRAGMENTS} values).

Fig. 5.10: Aggregation behaviour (expressed by CAC values) compared to hydrophobic content (expressed by CLOGP_{FRAGMENTS} values) for peptide bolaamphiphiles including 9-Anc.

Chapter 6

Fig. 6.1: Examples of results obtained with Bauer-Kirby test on antimicrobial compounds (kindly provided by Dr A Whitelaw).

Fig. 6.2: MIC determination of peptides L3, L4 and L5 with the same micro-well diffusion assay (modified from Rautenbach et al., 2006).

Fig. 6.3: MIC determination of KL2 (Gram S plot adapted from Rautenbach et al., 2006).

Fig. 6.4: MIC determination of OY1 (Gram S plot adapted from Rautenbach et al., 2006).

Fig. 6.5: MIC determination of LO1 (Gram S plot adapted from Rautenbach et al., 2006).

Fig. 6.6: Haemolytic activity of the synthesised compounds against hRBCs after 24 h at 37 °C. Saponin (0.5%) and 0.01% AcOH / 0.2% BSA were used as positive and negative controls.

Fig. 6.7: Carboxyfluorescein leakage from liposomes with different lipid composition challenged by KL1, KL2, KL3 and KL4. [A] Negatively charged liposomes (PC:PG, 10:1, lipid concentration 13 µM) and [B] neutrally charged liposomes (PC:CHOL, 10:1, lipid concentration 16 µM).

Fig. 6.8: Carboxyfluorescein leakage from liposomes with different lipid composition challenged by OL1, OL2, OY1, OY2, LO1 and LY1. [A] Negatively charged liposomes (PC:PG, 10:1, lipid concentration 13 µM) and [B] neutrally charged liposomes (PC:CHOL, 10:1, lipid concentration 16 µM).

Fig. 6.9: Time course of carboxyfluorescein leakage from liposomes induced by L5. Lipid composition: [A] PE:PG (7:3) and [B] PC:PG (7:3) (after Hirakura et al., 1996).

Fig. 6.10: Carboxyfluorescein leakage from liposomes with different lipid composition challenged by L5. [A] Negatively charged liposomes and [B] neutrally charged liposomes (after Hirakura et al., 1996).

Fig. 6.11: Schematic representation of the correlation between secondary structure and biological activity for the compounds studied. Images were modified from Hancock, 2001.

Chapter 7

Fig. 7.1: Correlation between hydrophobicity ($\text{CLOGP}_{\text{FRAGMENTS}}$) and CAC for 9-Anc containing molecules.

List of tables

Chapter 2

Tab. 2.1: List of CAMP drugs, companies responsible for commercialization, testing status, and the disease they are designed to treat (adapted from Breithaupt, 1999 and McPhee and Hancock, 2005)

Chapter 3

Tab. 3.1: Common protecting groups for routine synthesis of peptides (adapted from Chan and White, 2000a)

Tab. 3.2: Coupling methods used in Fmoc SPPS: methods using active esters are shown in grey (adapted from Chan and White, 2000a)

Tab. 3.3: Distillation of solvents used in SPPS

Tab. 3.4: Gradient A

Tab. 3.5: Gradient B

Tab. 3.6: Gradient C

Tab. 3.7: Gradient C₁ for analytical RP-HPLC analysis

Tab. 3.8: Gradient H₁ for analytical RP-HPLC analysis

Chapter 4

Tab. 4.1: CAC values (in water and 0.1% TEA) for the synthesised compounds determined by fluorescence spectroscopy using pyrene as fluorescent probe (n.d. = not determined)

Tab. 4.2: FT-IR bands for the dried peptide assemblies (cm⁻¹)

Chapter 5

Tab. 5.1: Peptides and peptide hybrids used in this study

Tab. 5.2: [a] Hydrophobicity contributions of common amino acids, [b] for N-acetyl-peptide amides, and [c] for free peptides (adapted from Tao et al., 1999)

Tab. 5.3: Gradient C₁

Tab. 5.4: Gradient H₁

Tab. 5.5: CLOGP values (residue and fragment addition methods) for the synthesised compounds and the parent peptides (L3, L4 and L5) (n.d.= not determined)

Tab. 5.6: CLOGP_{FRAGMENTS} values and RP-HPLC retention times (in minutes)

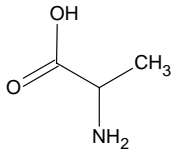
Chapter 6

Tab. 6.1: Antimicrobial activity of the synthesised compounds according to the Bauer-Kirby disk diffusion test performed against [a] *E. coli*, [b] *S. aureus*, [c] *P. aeruginosa*, [d] *E. faecalis* and [e] *S. marcescens* (diameters of inhibition areas are reported in mm; - = no inhibition)

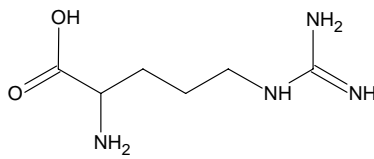
Tab. 6.2: MIC values for peptides and peptide hybrids (MIC values in square brackets are taken from Naidoo, 2004)

Tab. 6.3: Haemolytic activity of bolaamphiphilic peptides and peptide hybrids

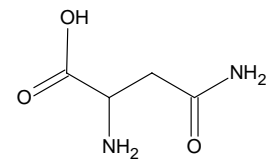
**Structures, three-letter and single-letter codes
for the proteinogenic amino acids**



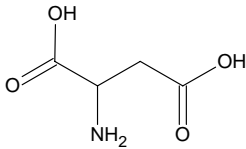
Alanine Ala A



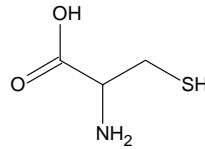
Arginine Arg R



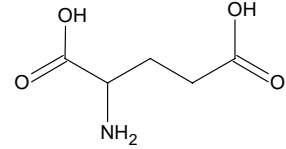
Asparagine Asn N



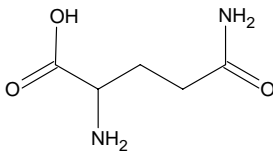
Aspartic acid Asp D



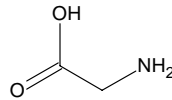
Cysteine Cys C



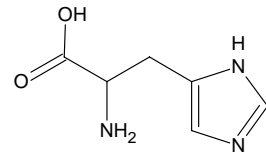
Glutamic acid Glu E



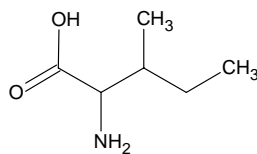
Glutamine Gln Q



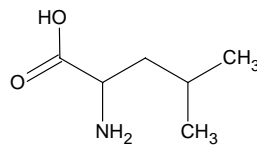
Glycine Gly G



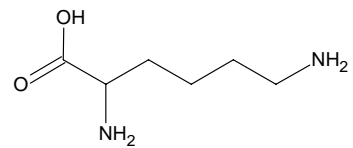
Histidine His H



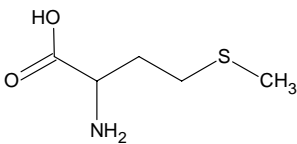
Isoleucine Ile I



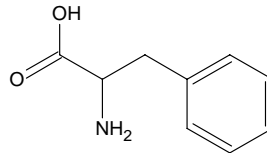
Leucine Leu L



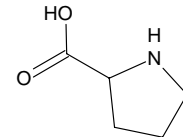
Lysine Lys K



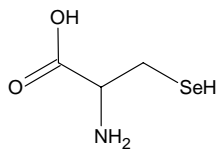
Methionine Met M



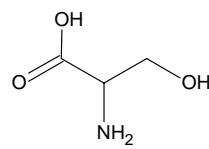
Phenylalanine Phe F



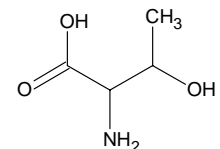
Proline Pro P



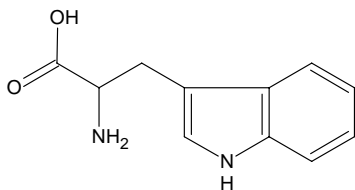
Selenocysteine Sec U



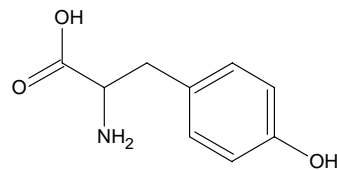
Serine Ser S



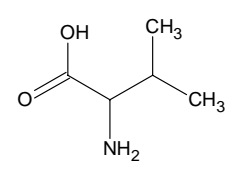
Threonine Thr T



Tryptophan Trp W

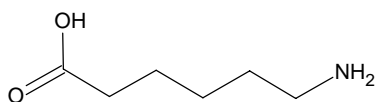


Tyrosine Tyr Y

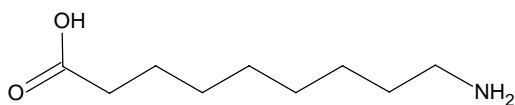


Valine Val V

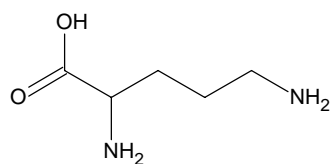
Structures and three-letter codes for the non-proteinogenic amino acids used in this study



6-Aminohexanoic acid 6-Ahx



9-Aminononanoic acid 9-Anc



Ornithine Orn O

Marco Polo descrive un ponte, pietra per pietra.

- Ma qual è la pietra che sostiene il ponte? - chiede Kublai Kan.

- Il ponte non è sostenuto da questa o da quella pietra, - risponde Marco, - ma dalla
linea dell'arco che esse formano.

Kublai Kan rimase silenzioso, riflettendo. Poi soggiunse: - Perché mi parli delle pietre?
è solo dell'arco che mi importa.

Polo risponde: - Senza pietre non c'è arco.

Italo Calvino
"Le città invisibili", 1972

Marco Polo describes a bridge, stone by stone.

- But which is the stone that sustains the bridge? Asks Kublai Kan.

- The bridge is not sustained by this or that stone, - replies Marco, - but by the line
of the arch they form.

Kublai Kan kept silent, thinking. Then he added: - Why do you speak about the
stones?

I only care about the arch.

Polo answers: - Without stones there is no arch.

Italo Calvino
"Le città invisibili", 1972

Preface

The work presented in this dissertation was planned and performed by the author at the Institute for Polymer Science (IPS) UNESCO-Associated Centre for Macromolecules and Materials, Department of Chemistry and Polymer Science (Stellenbosch University, South Africa). This project developed from a previous study carried out at the Department of Biochemistry of the same university by VB Naidoo and M Rautenbach in a collaboration with IPS. When the project was entirely moved to IPS, this institution was mainly involved in research dealing with membranes for water purification, new polymeric materials, their synthesis and characterisation, new polymerisation techniques, development of polymeric and magnetic nanoparticles for coatings and packaging, polymeric nanomaterials, (co)polymerisation of activated amino acids, polymers for paper production. Hence, with this project, the IPS entered for the very first time into the field of the synthesis and characterisation of peptides. Peptides can be considered as polymers (or rather, biopolymers), but synthesis and purification, materials, conditions of work and analytical techniques are very different from those ones commonly used in a polymer chemistry laboratory.

A laboratory was dedicated to solid-phase peptide synthesis and bioorganic chemistry in general. Since then, J Juodaityte and the author dedicated many efforts upgrading the lab and setting up of a suitable work space with adequate facilities for peptide synthesis, purification, analysis and characterisation, for part of the biological work and for the self-assembly studies. Solvents and chemicals generally used in polymer chemistry that could affect the synthesis were removed, distillation apparatuses for high quality solvents were set up, an existing HPLC system was fixed, upgraded and dedicated to peptide analysis and purification, a vacuum system for solvent removal and a freeze-drier were acquired. Because of the need to perform biological tests and use instrumentation unavailable at IPS, collaborations with other institutions were created by the author, within the University of Stellenbosch (Biochemistry, Microbiology) and with the University of Cape Town (Microbiology, Molecular and Cellular Biology, Clinical Pharmacology).

Thanks to all these efforts a bio-organic laboratory is now established and operational at the Institute for Polymer Science, providing facilities for peptide chemistry and peptide-related research.

Chapter 1

Introduction

1.1 Background

The recent interest in cationic antimicrobial peptides (CAMPs) is mainly due to the lack of efficacy of traditional synthetic antibiotics and to the increase of bacterial resistance to standard drugs (WHO, 2002a; WHO, 2002b). Over the past decades the development of new antibiotics has been accompanied by a parallel growth of bacterial resistance and now for nearly every drug a certain degree of resistance is reported. Hence, the scientific community and pharmaceutical industries are investing resources into and making efforts towards the discovery of new products to be used as antimicrobial agents, for humans, animals and plants.

Unfortunately, many cationic peptides cannot be used as drugs because of their indiscriminate action against prokaryotic and eukaryotic cells. Therefore, research now focuses on the modification of active compounds in order to increase the killing action towards pathogens. In this way it is also possible to obtain a selective action against bacteria/fungi/viruses, avoiding any dangerous interactions with mammalian cells.

Over the past twenty years structure-activity relationship (SAR) studies have discovered many active sequences commonly found in natural antimicrobial peptides (Hancock et al., 2006; Zelezetsky and Tossi, 2006). These patterns are frequently used in the development of new molecules. An interesting approach to the design of novel peptide-based antimicrobial drugs involves the creation of hybrid molecules that combine active sequences of CAMPs with non-natural features. Examples include the conjugation to fatty acids (Mak et al., 2003; Oh et al., 2004; Thennarasu et al., 2005) and biopolymers (Guiotto et al., 2003), with the aim to change peptides' pharmacokinetic and pharmacodynamic profiles. Other techniques involve the replacement of the amide bond with other unusual bonds (Lee and Oh, 2000) and the use of non-standard amino acids (AA) – such as D-amino acids or chemically modified AA – instead of the natural ones (Hong et al., 1999; Kawai et al., 2003).

The research work that is detailed in this dissertation developed from previous investigations made at the University of Stellenbosch (Department of Biochemistry, in collaboration with the Institute for Polymer Science). Here new molecules were designed focusing on the use of non-

natural amino acids, such as ω -amino acids, and bifunctional organic molecules, such as α - ω -dicarboxylic acids (Naidoo, 2004). Such molecules were created starting from a common antimicrobial motif made of different combinations of lysine and leucine and derived from the active core of an insect defensin, named sapecin B (Hirakura et al., 1996; Naidoo, 2004).

Peptides derived from sapecin B (Alvarez-Bravo et al., 1994; Nakajima et al., 1997) are natural bolaamphiphiles. A bolaamphiphile is a molecule made of two hydrophilic groups connected by a hydrophobic frame. In this case the hydrophilic group was a lysyl-leucyl-lysine (KLK) tripeptide and the hydrophobic region comprised a poly-leucine chain with 3 to 5 residues. The substitution of this hydrophobic region by α - ω -dicarboxyl acids and ω -amino acids led to the creation of peptide hybrids (Naidoo, 2004). The design of these initial compounds also considered the work carried out by Shimizu's group during the past decade, which was focused on oligopeptide bolaamphiphiles (Shimizu et al., 1996; Kogiso et al., 1998; Kogiso et al., 2000; Kogiso et al., 2004). Those peptide bolaamphiphiles showed strong self-assembly properties and, under certain conditions, gave supramolecular architectures such as micro/nanotubes, vesicles and nano/microfibres (Shimizu et al., 1996).

Peptide fibres and peptide aggregates are often studied as scaffolds for tissue regeneration, cell growth and other nanobiotechnological applications (Hartgerink et al., 2001; Niece et al., 2003; Gao and Matsui, 2005). Macromolecular structures formed by peptides and proteins in solutions offer a three-dimensional network for cells to grow. Additionally, if bioactive sequences are used, they can act at a molecular level boosting cell adhesion, differentiation and growth (Silva et al., 2004). In other cases, starting from antimicrobial self-assembling compounds, the creation of supramolecular architectures gives networks of antibiotic fibres/aggregates with many possible applications as scaffolds for cell growth and wound healing patches (Fernandez-Lopez et al., 2001).

1.2 Objectives

This research project focused on the design and synthesis of hybrid peptides based on sapecin-derived synthetic peptides. Two main aspects were considered: the study of the aggregation/self-assembly behaviour of peptides and peptide hybrids and the investigation of their biological properties. Within these two areas multiple objectives were pursued and these included:

- I. to understand the self-organisation behaviour of the synthesised bolaamphiphiles by using different tools and determine the propensity towards aggregation according to experimental conditions, amino acid composition and three-dimensional structure,

- II. to evaluate the morphology of the bolaamphiphile supramolecular assemblies by using diverse microscopy techniques,
- III. to evaluate the hydrophobic content of the peptide bolaamphiphiles both theoretically and experimentally and correlate it to the self-assembly process,
- IV. to determine the influence of non-natural amino acids on the biological activity of bolaamphiphilic peptides and peptide hybrids.

1.3 Layout of the dissertation

A general introduction to antimicrobial peptides (sources, actions and applications) and the properties of peptide bolaamphiphiles are presented in Chapter 2.

The entire set of bolaamphiphilic peptides and peptide hybrids is presented in Chapter 3. Solid-phase peptide synthesis (SPPS) using the Fluorenylmethoxycarbonyl (Fmoc) polyamide protocol, purification by semi-preparative reversed-phase high performance liquid chromatography (RP-HPLC) and characterisation by electrospray ionisation mass spectrometry (ESI-MS) are here discussed. The path followed for the design of a new library of compounds, which formed the basis of this study, is also considered.

The aggregation behaviour of the synthesised bolaamphiphiles was investigated by fluorescence measurements, different microscopic tools, such as optical microscopy (OM), scanning electron microscopy (SEM) and cryo-fracture SEM, Fourier transform infrared spectroscopy (FT-IR) and circular dichroism spectroscopy (CD). These techniques are described in Chapter 4.

The structural characterisation of the synthesised peptide bolaamphiphiles was expanded with particular attention to the hydrophobicity of the synthesised molecules. Theoretical methods and HPLC retention times were both used. This further characterisation of the molecules allowed for a consistent correlation between self-assembly and hydrophobicity to be drawn (Chapter 5).

The new peptides and peptide hybrids were biologically tested using different protocols, focusing on interaction with bacteria, human erythrocytes and model membranes (Chapter 6).

Finally, general conclusions, limitations and some recommendations for future work are given (Chapter 7).

The outcomes of this research were publicised and presented to the scientific community in the following formats:

- I. Martari M, Juodaityte J and Sanderson RD, Supramolecular structures and biological properties of novel peptide bolaamphiphiles. Poster presented at the 9th UNESCO-IUPAC Conference “Polymers for advanced applications”, 21-23 November 2006, Stellenbosch, South Africa.
- II. Martari M and Sanderson RD, Amphiphilic peptides and peptide hybrids: A fluorescence study of the aggregation behaviour in water. Poster presented at the 9th Frank Warren Conference 2006 on Organic Chemistry, 22-25 January 2006, Cape Town, South Africa.
- III. Martari M, Bioactive self-assembling peptides. Talk presented at the 3rd IUPAC-Workshop on Advanced Materials (WAM III), 5-8 September 2005, Stellenbosch, South Africa.

Additionally, the following original papers have been recently submitted for publication or are under preparation:

- I. Martari M and Sanderson RD, Steady-state fluorescence measurements to study peptide aggregation in water. SUBMITTED to *Analytical Biochemistry*.
- II. Martari M and Sanderson RD, Hydrophobic content of bolaamphiphilic peptides and correlation to their aggregation behaviour. IN PREPARATION / TO BE SUBMITTED to *Biochemical and Biophysical Research Communications*.
- III. Martari M and Sanderson RD, Supramolecular structures and biological properties of novel peptide bolaamphiphiles. IN PREPARATION / TO BE SUBMITTED to *Macromolecular Symposia*.

1.4 References

Alvarez-Bravo J, Kurata S and Natori S (1994) Novel synthetic peptides effective against methicillin-resistant *Staphylococcus aureus*, *Biochemical Journal*, 302, 535-538.

Fernandez-Lopez S, Kim HS, Choi EC, Delgado M, Granja GR, Khasanov A, Kraehenbuehl K, Long G, Weinberger DA, Wilcoxon KM and Gadiri MR (2001) Antibacterial agents based on the cyclic D,L- α -peptide architecture, *Nature*, 412, 452-455.

Gao X and Matsui H (2005) Peptide-based nanotubes and their applications in bionanotechnology, *Advanced Materials*, 17, 2037-2050.

Guiotto A, Pozzobon M, Canevari M, Manganelli R, Scarin M and Veronese FM (2003) PEGylation of the antimicrobial peptide nisin A: problems and perspectives, *Il Farmaco*, 58, 45-50.

Hancock REW, Brown KL and Mookherjee N (2006) Host defence peptides from invertebrates – emerging antimicrobial strategies, *Immunobiology*, 211, 315-322.

Hartgerink JD, Beniash E and Stupp SI (2001) Self-assembly and mineralization of peptide-amphiphile nanofibers, *Science*, 294, 1684-1688.

Hirakura Y, Alvarez-Bravo J, Kurata S, Natori S and Kirino Y (1996) Selective interaction of synthetic antimicrobial peptides derived from sapecin B with lipid bilayers, *Journal of Biochemistry*, 120, 1130-1140.

Hong SY, Oh JE and Lee KH (1999) Effect of D-amino acid substitution on the stability, the secondary structure and the activity of membrane-active peptide, *Biochemical Pharmacology*, 58, 1775-1780.

Kawai M, Tanaka R, Yamamura H, Yasuda K, Narita, Umemoto H, Ando S and Katsu T (2003) Extra amino group-containing gramicidin S analogues possessing outer membrane-permeabilizing activity, *Chemical Communication (Cambridge)*, 11, 1264-1265.

Kogiso M, Ohnishi S, Yase K, Masuda M and Shimizu T (1998) Dicarboxylic oligopeptides bolaamphiphiles: proton-triggered self-assembly of microtubes with loose solid surfaces, *Langmuir*, 14, 4978-4986.

Kogiso M, Okada Y, Hanada T, Yase K and Shimizu T (2000) Self-assembled fibers from valylvaline bola-amphiphiles by a parallel β -sheet network, *Biochimica et Biophysica Acta*, 1475, 346-352.

Kogiso M, Okada Y, Hanada T, Yase K and Shimizu T (2004) Metal-complexed nanofiber formation in water from dicarboxylic valylvaline bolaamphiphiles, *Journal of Colloid and Interface Science*, 273, 394-399.

Lee K-H and Oh J-E (2000) Design and synthesis of novel antimicrobial pseudopeptides with selective membrane-perturbation activity, *Bioorganic and Medicinal Chemistry*, 8, 833-839.

Mak P, Pohl J, Dubin A, Reed MS, Bowers SE, Fallon MT and Shafer WM (2003) The increased bactericidal activity of a fatty acid-modified synthetic antimicrobial peptide of human cathepsin G correlates with its enhanced capacity to interact with model membranes, *International Journal of Antimicrobial Agents*, 21, 13-19.

Naidoo VB (2004) The supramolecular chemistry of novel synthetic biomacromolecular assemblies, PhD thesis, University of Stellenbosch.

Nakajima Y, Alvarez-Bravo J, Cho J, Homma K, Kanegasaki S and Natori S (1997) Chemotherapeutic activity of synthetic antimicrobial peptides: correlation between chemotherapeutic activity and neutrophil-activating activity, *FEBS Letters*, 415, 64-66.

Niece KL, Hartgerink JD, Donners JJM and Stupp SI (2003) Self-assembly combining two bioactive peptide-amphiphile molecules into nanofibers by electrostatic attraction, *Journal of the American Chemical Society*, 125, 7146-7147.

Oh H, Kim S, Cho H and Lee KH (2004) Development of novel lipid-peptide hybrid compounds with antibacterial activity from natural antimicrobial peptides, *Bioorganic and Medicinal Chemistry*, 14, 1109-1113.

Shimizu T, Kogiso M and Masuda M (1996) Vesicle assembly into microtubes, *Nature*, 383, 487-488.

Silva GA, Czeisler C, Niece KL, Beniash E, Harrington DA, Kessler JA and Stupp SI (2004) Selective differentiation of neural progenitor cells by high-epitope density nanofibers, *Science*, 303, 1352-1355.

Thenarasu S, Lee D, Tan A, Kari UP and Ramamoorthy A (2005) Antimicrobial activity and membrane selective interactions of a synthetic lipopeptide MSI-843, *Biochimica et Biophysica Acta*, 1711, 49-58.

WHO – World Health Organization (2002a) Antimicrobial resistance, Fact sheet No. 194; Geneva.

WHO – World Health Organization (2002b) Use of antimicrobials outside human medicine and resultant antimicrobial resistance in humans, Fact sheet No. 268; Geneva.

Zelezetsky I and Tossi A (2006) Alpha-helical antimicrobial peptides – Using a sequence template to guide structure-activity relationship studies, *Biochimica et Biophysica Acta*, 1758, 1436-1449.

Chapter 2

Theoretical framework

2.1 Cationic antimicrobial peptides

2.1.1 Sources and characteristics

All organisms protect themselves against pathogens thanks to their innate immune system. The latter comprises inducible effectors (non-specific immune response), quickly and easily induced, often within hours or minutes, and adaptive humoral and cellular immune responses, which need several days before being activated (Steiner et al., 1981).

An important part of the non-specific immune response available to organisms is formed by cationic antimicrobial peptides, which represent an ancient mechanism of host defence (Lehrer and Ganz, 1999). This class of molecules includes hundreds of different substances* and they are commonly present in bacteria, insects, plants and mammals, human beings included (Broden et al., 2003; Marshall and Arenas, 2003). They are especially produced in epithelial or mucosal cells (including gastrointestinal, genitourinary and pulmonary epithelia) and phagocytes cells: those cells that first come into contact with bacteria, viruses and pathogens in general (Hancock and Chapple, 1999; Raj and Dentino, 2002).

In many cases CAMPs correspond to the first weapon used by the body when a possible dangerous microorganism is detected. They show minimal inhibitory concentrations (MICs) in the range 0.25–16 µg/ml against many pathogens (Robinson et al., 2005). CAMPs have been found active against Gram-positive and -negative bacteria, fungi, parasites, yeasts (Brown and Hancock, 2006), enveloped viruses (Daher et al., 1986) and tumour cells (Winder et al., 1998). They are easily synthesised in large amounts at low metabolic cost, quickly available and help to protect the organism, killing a wide range of microbes while the immune system prepares an adequate reaction through the adaptive immune response (Shai and Oren, 2001). Moreover, their action is not limited to the elimination of microorganisms, they also have a role in the inflammation process and display chemotactic properties, particularly chemoattracting neutrophils, monocytes, mast cells and T cells, while some of them are believed to promote angiogenesis (Fig. 2.1) (Hancock and Diamond, 2000;

* See Appendix A for an overview of the most important antimicrobial peptides (structures, sources and PDB ID) and also visit the antimicrobial peptide databases at www.bbcm.univ.trieste.it/~tossi/pag1.htm or at <http://aps.unmc.edu/AP/main.php> for more complete and updated lists (last accessed on 11/10/06).

Hancock, 2001; Raj and Dentino, 2002; Sugiarto and Yu, 2004; Izadpanah and Gallo, 2005, Bowdish et al., 2005).

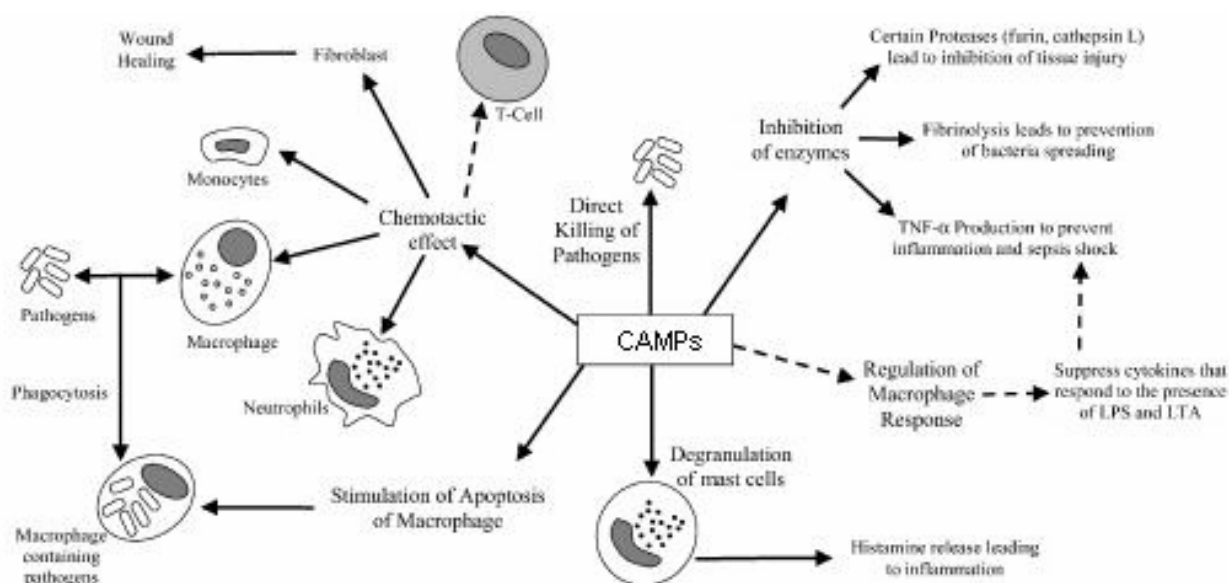


Fig. 2.1 Actions naturally performed by cationic antimicrobial peptides (adapted from Sugiarto and Yu, 2004).

Antimicrobial peptides have been extensively studied in the last two decades and their general characteristics, judged important for the biological activity, can be described as follows (Hancock, 1997a; Rautenbach and Hastings, 1999; Powers and Hancock, 2003; Hancock et al., 2006):

- I. an amino acid sequence with a number of residues between 5 and 50, mostly including L-amino acids
- II. a net positive charge (due to the presence of lysine and arginine residues, less commonly histidine) which gives them the name of ‘cationic antimicrobial peptides’
- III. a three-dimensional amphiphilic structure with a 30-50% content of hydrophobic amino acids and generally an α -helical or β -sheet structure (even if many small CAMPs have little or no structure in solution).

2.1.2 Structures and classification

With almost one thousand compounds recorded as antimicrobial peptides, general considerations about their secondary structure are commonly used to classify them (Epan and Vogel, 1999). Cationic antimicrobial peptides can be divided into four families: β -sheet, α -helical, looped and extended coil peptides (Fig. 2.2) (Hancock, 1997b).

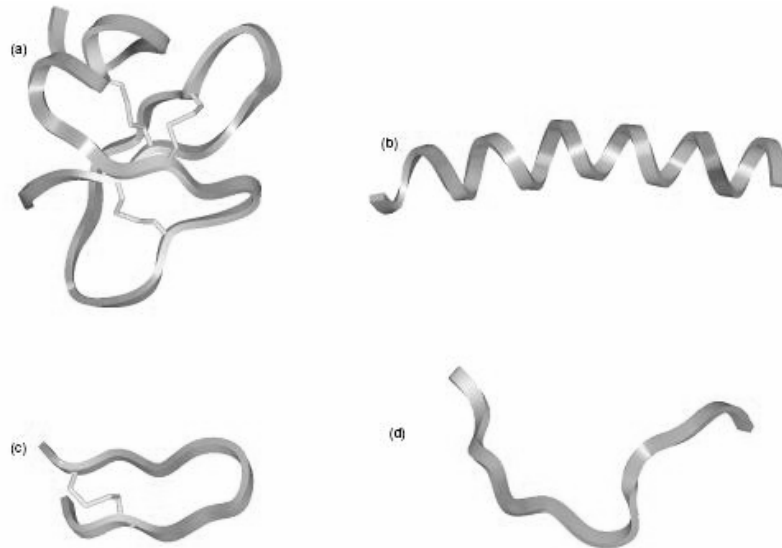


Fig. 2.2: Molecular models of the different structural classes of antimicrobial peptides: a) β -sheet structure of human β -defensin-2, b) α -helical structure of magainin 2, c) looped structure of bovine batenecin and d) extended structure of bovine indolicidin. Models are taken from the NMR structural database and based on two-dimensional NMR spectroscopy of the peptides in water (a) or in a membrane mimetic condition (b, c and d) (adapted from Hancock, 2001).

Peptides belonging to the first group (i.e. human β -defensin-2, tachyplesins, protegrins, lactoferricin) generally exist in the β -sheet conformation and kill bacteria perturbing the membrane or forming channels. On the other hand, α -helical peptides (i.e. magainin, cecropin A, temporins) often only form α -helices upon interaction with the bacterial membrane thanks to their amphipathic character and they can adsorb on the membrane or/and insert into the hydrophobic compartment. Peptides with looped structure (i.e. nisin, bovine batenecin) are usually rich in proline/arginine and therefore cannot form amphipathic structures. Peptides with an extended structure (i.e. histatin, tritrypticin, indolicidin) commonly exhibit the repetition of one or more amino acids (such as His, Trp, Arg/Pro and Pro/Phe) and these patterns are studied as SAR models (Hancock, 2001).

2.1.3 Mechanisms of antibacterial activity

The interest in CAMPs is closely related to their mechanism of action. It is commonly recognised that they interact with the outer membrane of bacterial cells, disorganising the lipid bilayer. This phenomenon leads to the lysis of the cells, depolarization of the membrane and consequently to the death of the microorganism. The interaction is based on electrostatic and hydrophobic interactions (thus partially explaining the selectivity of CAMPs towards prokaryotic cells, which have a negatively charged membrane). However, new studies underlined the presence of various modes of action, like binding to intracellular targets or stimulating host defence systems (Yaeman and Yount, 2003). If the theoretic mechanism of action is widely accepted by the

scientific community, how things happen in the real world is still a source of discussion and hypothesis. Since there are antimicrobial peptides with various secondary structures it can be said that different CAMPs use different mechanisms to express their antimicrobial activity and often, for the same molecule, different mechanisms coexist. To date, four models have been proposed.

A. 'barrel-stave' model

The 'barrel-stave' model describes the formation of transmembrane pores or channels as a result of the self-association of peptides into larger structures (Fig. 2.3) (Ehrenstein and Lecar, 1977; Oren and Shai, 1998). This self-association process occurs on the external surface of the bacterial cell wall and is followed by the insertion of the assembly into the membrane. Cell death is a consequence of leakage of cellular components through the pores. Peptides with a strong amphipathic structure (such as an amphipathic α -helix or β -sheet) are more likely to interact with membranes with this mechanism (Shai, 2002).

B. the 'carpet' model

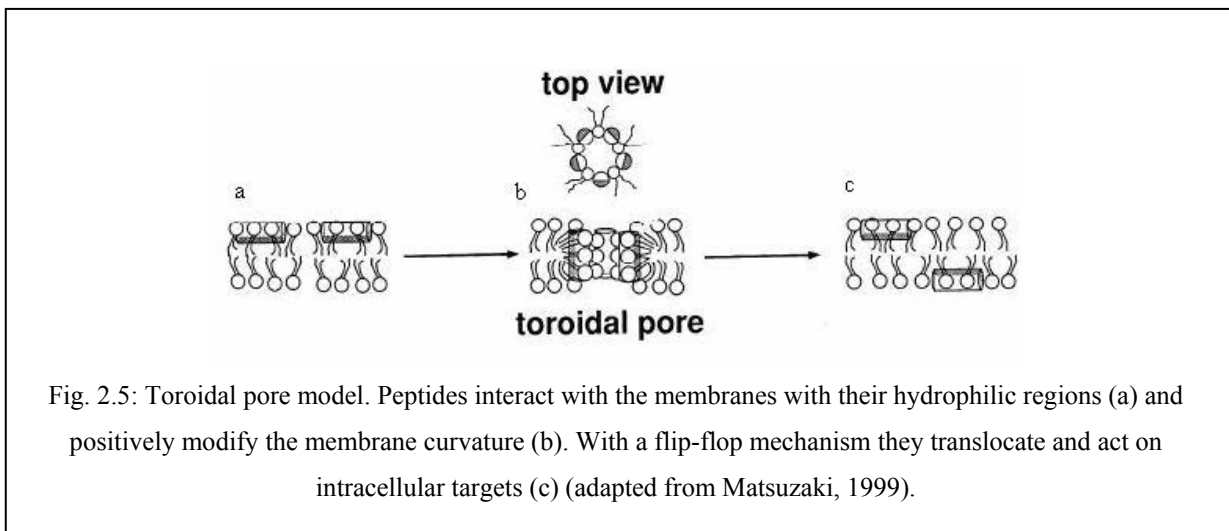
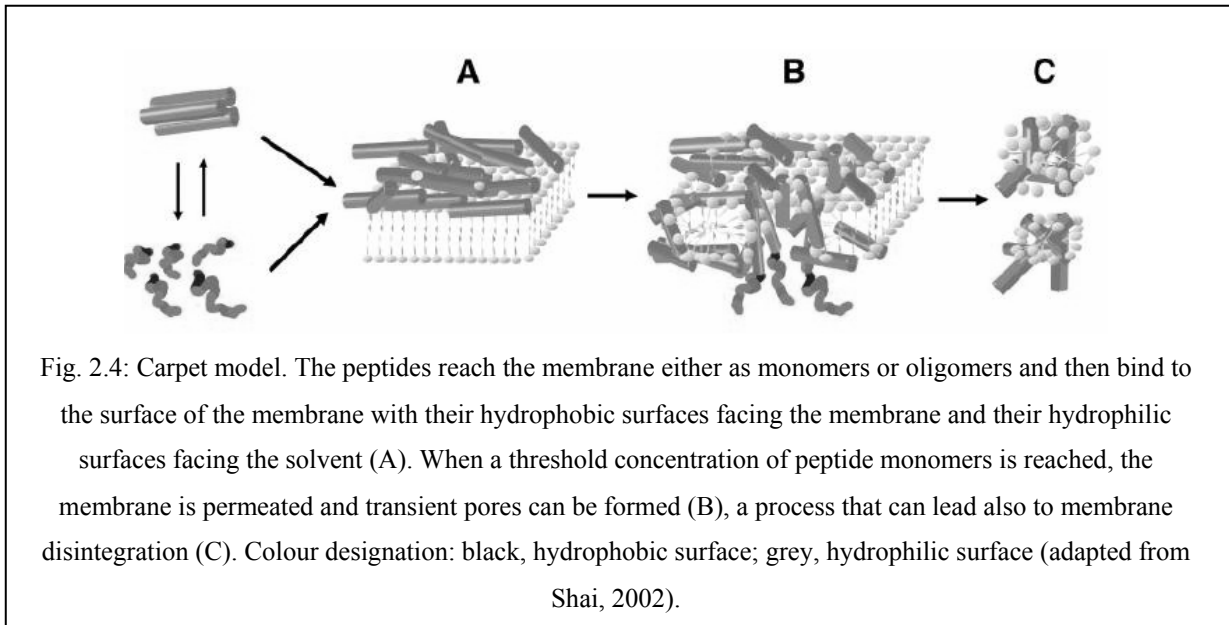
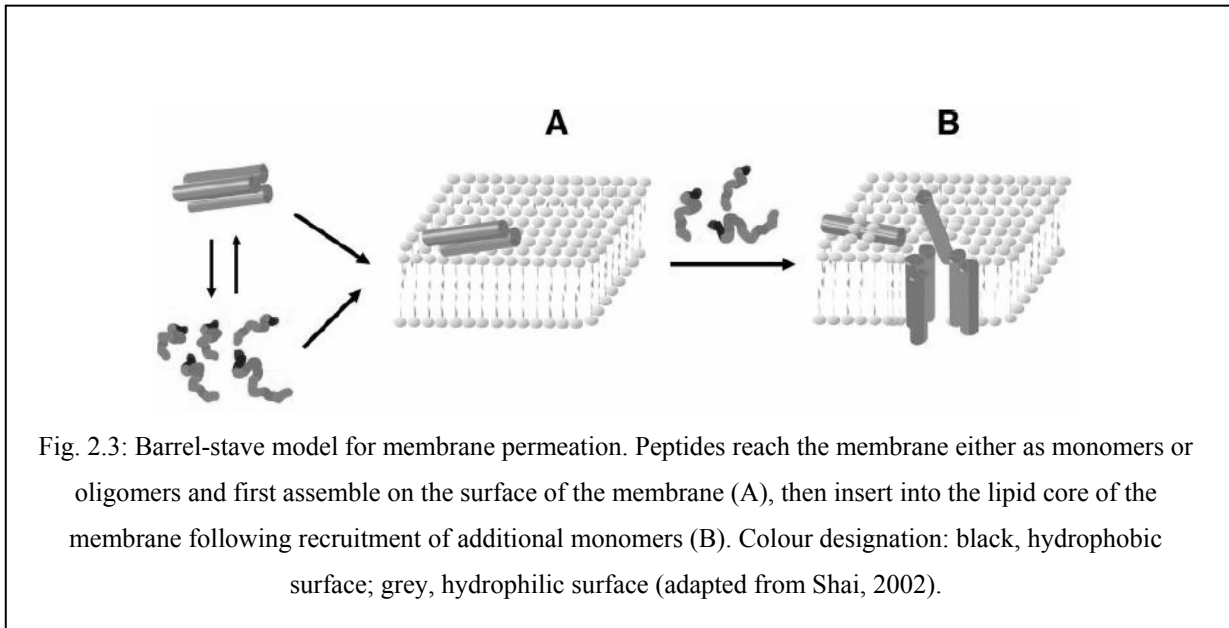
According to the 'carpet' model, peptides first bind to the negatively charged lipids of the bacterial membrane and, after a threshold concentration has been reached, they cause membrane permeation and lysis with a detergent-like mechanism (Fig. 2.4) (Pouny et al., 1992; Shai, 1999). Peptides with a high net positive charge and without a particular structure are more likely to behave in a way similar to this model (Shai, 2002).

C. 'toroidal pore' model

This model was developed to explain how certain peptides could kill bacteria without causing membrane depolarization. According to the 'toroidal pore' model, peptides insert into the membrane creating a positive curvature of the membrane itself and associate into unstructured aggregates and short-lived transmembrane clusters (Fig. 2.5) (Matsuzaki et al., 1996; Matsuzaki, 1998; Matsuzaki, 1999). Peptides can thus cross the membrane with a flip-flop mechanism without provoking depolarization and then act on intracellular targets or facilitate the efflux of intracellular components (Oren and Shai, 1998).

D. alternative mechanisms: intracellular targets

Antimicrobial peptides that do not strongly interact with membrane lipids might target intracellular biomolecules such as DNA, RNA and enzymes, thus inhibiting protein synthesis, interfering with energy transport and metabolism and/or increasing membrane permeability (Reddy et al., 2004; Otvos, 2005). Moreover, CAMPs are also believed to stimulate host defence mechanisms, activate peroxidases and chemoattract neutrophils (Hancock and Rozek, 2002; Yaeman and Yount, 2003; Sugiarto and Yu, 2004).



2.1.3 Antimicrobial peptides as next generation therapeutics

Over the past two decades the interest in CAMPs has been driven by the desperate search for new therapeutic treatments, especially against the spread of bacterial resistance (Dancer, 2004; Alanis, 2005). In particular, antimicrobial peptides' peculiar mechanism of action, based on a physical interaction with membrane lipids, seemed to be a very useful starting point for the development of a new class of antibiotics (Hancock and Lehrer, 1998). The physical disruption of the membrane was thought to make it difficult for bacteria to develop resistance and they are seen as natural antimicrobial agents with minimal or no side effects, high selectivity, low immunogenicity and a significant immunomodulatory action (Hancock et al., 2006).

Antimicrobial peptides have many possible applications, covering a wide potential market: food packaging and food preservation (Ryan et al., 2002), wound dressing and wound healing (Andreu and Rivas, 1998), detergents and gels for topical treatments of skin/mucosa infections (Raj and Dentino, 2002) and contraception (Aranha et al., 2004; Zairi et al., 2005). Some molecules are already on the market such as nisin, pediocin PA-1 (for dairy and canned products) and daptomycin* (derived from vancomycin and used to treat skin Gram-positive infections). A few more compounds are successfully passing clinical trials in phase II and III, such as pexiganan (magainin variant peptide MSI-78), iseganan (a protegrin-derived peptide) and rBPI₂₁ (a modified recombinant fragment of bactericidal/permeability-increasing protein) (Tab. 2.1) (Breithaupt, 1999; Toney, 2002; McPhee and Hancock, 2005).

Systemic administration of CAMPs has been considered as a possible solution for the treatment of systemic resistant infections. The major problems associated with systemic administration are generally correlated to the low half-life of peptides in the blood stream, high clearance, low or impossible absorption through the intestinal tract and potential immunogenicity and/or interferences with metabolic processes (through interactions with receptors). Therefore, their applications have been often limited to topical and external uses.

Other restrictions to the many applications of antimicrobial peptides include their high production costs, especially as inexpensive antibiotics are still produced and used worldwide. Solid-phase synthesis techniques are preferred for R&D studies but these techniques do not seem to be a feasible way for the mass production of antibiotic peptides, because of both high running costs and the environmental impact of the synthesis. Anyway, DNA recombinant technology, enzymatic synthesis and solution phase strategies might yield larger amounts of active peptides from much less expensive processes and more environment-friendly methods (Gill et al., 1996; Hancock and Lehrer, 1998).

* Nisin (Nisaplin[®]) and pediocin PA-1 (ALTA[™]) are currently commercialized by Aplin&Barret (UK) and Quest Intl. (FL, USA) respectively. Daptomycin (Cubicin[®]) is produced by Cubist Pharmaceuticals (MA, USA).

Tab. 2.1: List of CAMP drugs, companies responsible for commercialization, testing status, and the disease they are designed to treat (adapted from Breithaupt, 1999; McPhee and Hancock, 2005)

Compound	Company	Testing status	Target disease
Pexiganan (MSI-78)	Magainin Pharm. & SmithKline Beecham	Phase III completed	Infection of diabetic foot ulcers
Iseganan	IntraBiotics Corp.	Phase III halted prematurely	Oral mucositis resulting from cancer treatment
rBPI ₂₁ (NEUPREX [®])	Xoma & Baxter Intl.	Phase III completed	Severe bacterial meningitis
MBI 594AN	Migenix	Phase IIa completed	Acne
Omiganan (MX-226)	Migenix & Cadence Pharmaceuticals	Phase III completed	Infection at site of indwelling catheter insertion
IMXC001	Inimex Pharmaceuticals	Preclinical	Sepsis

The question of possible resistance is still under discussion. Even if the physical interactions between CAMPs and bacterial membranes do not suggest resistance development, resistance has been nonetheless reported, already several years ago (Guo et al., 1998; Ernst et al., 1999). Bacterial defence mechanisms against antimicrobial peptides might include DNA-expressed superficial peptidases (for the degradation of the peptides before interacting with the membranes) and other mechanisms already active in resistance against traditional antibiotics, such as efflux pumps and modifications of membrane properties (fluidity, charge and lipid composition, membrane potential, reduction of disulfide bonds) (Hancock, 1997a; Andreu and Rivas, 1998; Peschel and Collins, 2001; Nikaido, 2001; Peschel, 2002).

2.2 Antimicrobial peptides from *Sarcophaga peregrina*

Sarcotoxin is a family of antimicrobial peptides discovered during the 1980s in the haemolymph of *Sarcophaga peregrina* larvae (an insect best known as the flesh fly) and produced in response to external injuries (Okada and Natori, 1983; Okada and Natori, 1985). Other proteins were then detected and purified from the culture medium of the embryonic cell line of *Sarcophaga*, some belonged to the sarcotoxin group, another (later sapecin A) to a new family (Matsuyama and Natori, 1988a; Matsuyama and Natori, 1988b). Along with the antibacterial activity, further studies established the role of sapecin in the development and cell proliferation during the embryonic life,

thus suggesting a dual role of this small protein, in the *defence* and in the *development* of *Sarcophaga* larvae (Komano et al., 1991). Other researchers determined different homologues of sapecin A (named sapecin B and sapecin C) (Yamada and Natori, 1993), which led to the total synthesis and characterisation of sapecin A (PDB ID: 1L4V) and sapecin B (Fig. 2.6) (Hanzawa et al., 1990; Kim JI et al., 1994).

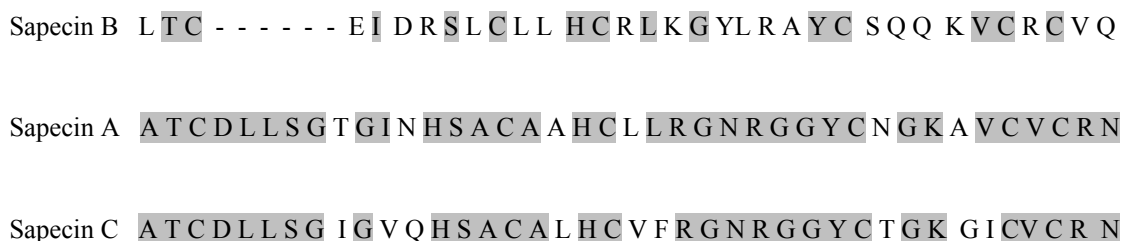


Fig. 2.6: Comparison of primary structures of sapecin A and its homologues. Identical amino acids are highlighted (modified from Yamada and Natori, 1993).

Studies focused on sapecin B which consists of 34 amino acids and has three disulfide bonds that give stability to the secondary structure. It comprises an α -helix from Arg7 to Lys17 and β -sheet structures from Gly18 to Lys28 and from Val29 to Gln34 (Fig. 2.7).



Fig. 2.7: Primary structure of sapecin B. Disulfide bridges are indicated (modified from Yamada and Natori, 1993).

A Japanese research group studied the amino acid composition of sapecin B, looking for its active core, so as to simplify and minimise the structural requirements for the antimicrobial activity (Yamada and Natori, 1994; Alvarez-Bravo et al., 1994; Hirakura et al., 1996). These studies revealed that the minimal structure corresponds to the α -helix region and its simplification led to the determination of a general antimicrobial structure, $KLKL_nKLK-NH_2$ ($n = 3, 4, 5$) (Fig. 2.8) (Nakajima et al., 1997).

This model structure is composed of two hydrophilic and charged sequences (lysyl-leucyl-lysine or arginyl-leucyl-lysine) divided by several hydrophobic amino acids, thus generating peptide bolaamphiphiles.

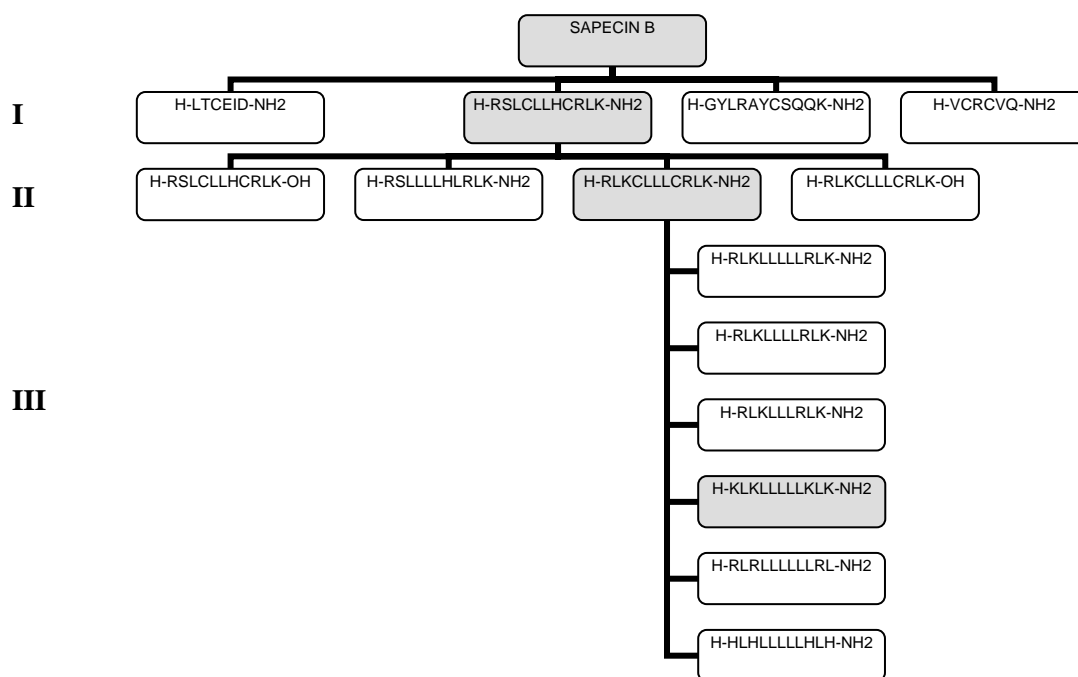


Fig. 2.8: Synthetic peptides derived from sapecin B. From sapecin B, the first generation peptides are in the first line (I), the second generation compounds in the second line (II) and the third generation peptides in the last 6 cells (III). The rational path between sapecin B and the leader antimicrobial sequence is shown by the grey boxes.

Since then, many researchers have tried to further modify the antimicrobial pattern and to test these molecules against a broad spectrum of bacteria and other microorganisms so as to determine better structure-function relationships (Nakajima-Shimada et al., 1998). It should be noted here that antimicrobial properties of lysine/leucine-rich peptides were not new at that time. Basic peptides have been studied since the 1980s for their antibiotic properties and they have been used for many years as model compounds for structure-activity relationships of CAMPs (Lee et al., 1986; Suenaga et al., 1989; Anzai et al., 1991; Castano et al., 2000).

Recently, SAR studies were undertaken at this university (Biochemistry) and focused on the bolaamphiphilic structure of these synthetic sapecin-derived compounds (Naidoo, 2004). Both the biological activity and aggregation properties of these new peptide hybrids were pointed out. Nonetheless, further studies were necessary to corroborate the preliminary results and to have a deeper insight into the influence of the use non-natural amino acid on biological activity and aggregation behaviour.

2.3 Peptide bolaamphiphiles

2.3.1 Bolaamphiphiles

The term ‘bolaamphiphile’ refers to a class of molecules which are formed by two hydrophilic groups linked together by a hydrophobic skeleton (Fuhrhop and Mathieu, 1984). The name comes from a South American hunting weapon made of two balls connected by a string, which is commonly called “bolas”^{*}. Bolaamphiphiles are naturally found in the membranes of archaeobacteria and are responsible for the unusual characteristics of these microorganisms, such as resistance at tremendous temperatures, extreme pH, UV light, radiations (Driessen et al., 1996; Rusterholtz and Pohlschröder, 1999; Gliozzi et al., 2002) (Fig. 2.9).

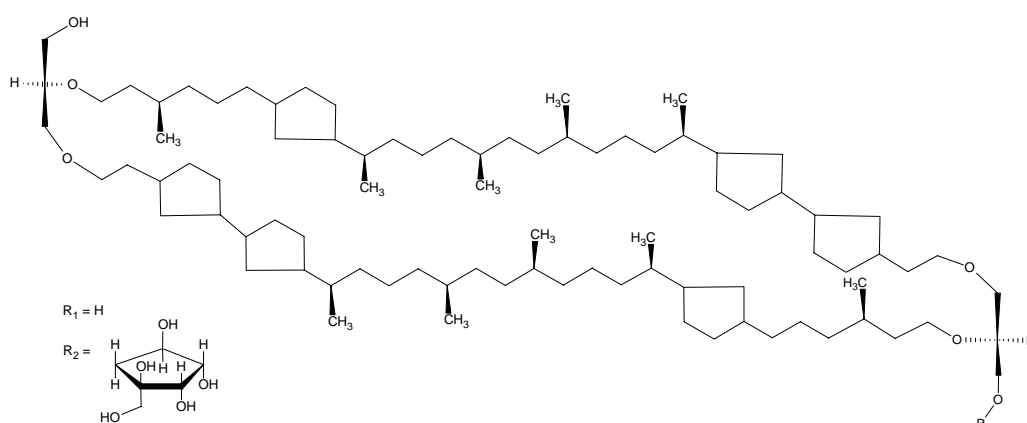


Fig. 2.9: Chemical structure of the hydrophobic backbones that can be obtained by hydrolysis of archaeal tetraether lipids (after Gliozzi et al., 2002).

Synthetic bolaamphiphiles try to mimic these natural compounds, avoiding their structural complexity and including diverse hydrophilic groups. Existing bolaamphiphiles comprise sugars (Masuda and Shimizu, 2004), alcohols (Sirieix et al., 2000), acids, amino acids (Kogiso et al., 1998a; Kogiso et al., 1998b; Kogiso et al., 2000; Matsui and Gologan, 2000; Matsui and Doublerly, 2001) and bioactive di/tripeptides (Claussen et al., 2003). They are made of different building blocks but they share similar physicochemical properties and, once in solution, they tend to spontaneously aggregate and form supramolecular architectures such as nanotubes and nanofibres, fibrils and vesicles: a process known as self-assembly or self-organisation (Shimizu et al., 1996). Figure 2.10 shows some of the peptide-based bolaamphiphiles synthesised by Shimizu’s group.

^{*} Definition from www.en.wikipedia.org/wiki/Bolas (last accessed 09/05/06).

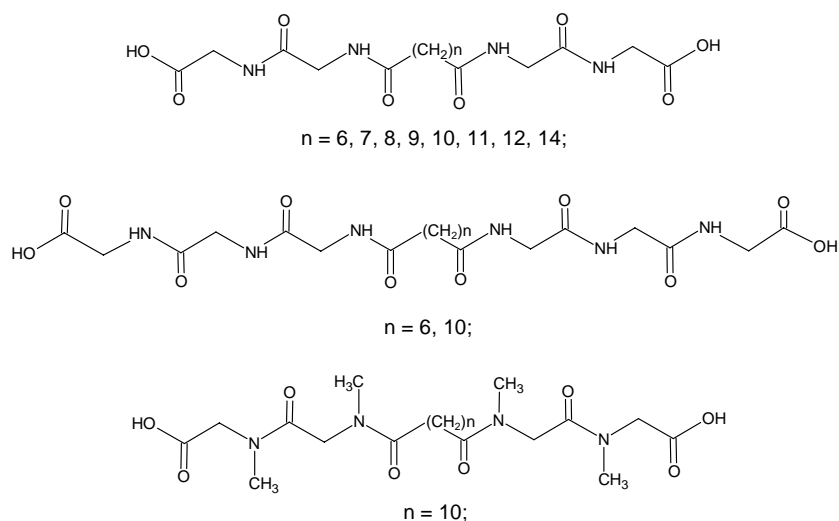


Fig. 2.10: Molecular structure of oligopeptides bolaamphiphiles synthesised by Shimizu's group in the late 1990s (modified from Kogiso et al., 1998).

2.3.2 Self-assembly properties

'Molecular self-assembly is the spontaneous association of molecules under thermodynamic equilibrium conditions into structurally well-defined arrangements due to non-covalent interactions, such as hydrogen and ionic bonds, hydrophobic and van der Waals interactions' (Zhang and Altman, 1999). In nature, self-assembly is a quite diffuse mechanism of molecular organization: DNA, RNA, proteins and lipids spontaneously form supramolecular functional nanostructures (Rajagopal and Schneider, 2004). The packed structure of DNA and RNA inside a nucleus, a folded protein with a specific function and a lipid membrane are natural examples of functional structures in the range of nanometres ($1 \text{ nm} = 10^{-9} \text{ m}$) which depend on a spontaneous process.

Many molecules – such as surfactants and lipids, proteins and peptides, amphiphilic and bolaamphiphilic organic compounds (including peptide bolaamphiphiles) – are studied for their self-assembly properties. In many cases the interest is in how to regulate the process itself and in the understanding of the key elements that move it. Knowing how to trigger the aggregation of a certain kind of molecules – i.e. using pH modifications (Aggeli et al., 2003; Claussen et al., 2003; Niece et al., 2003), ionic strength, metals (Matsui and Douberly, 2001), light (Collier et al., 2001), temperature (Pochan et al., 2003) – permits one to create smart materials which can only form in response to precise conditions or stimuli.

In the last decade, due to the development of nanotechnology, self-assembling peptides and proteins have been extensively studied because of their many possible applications in material science, engineering and manufacture of nanostructured biological materials (Zhang, 2003; Zhang

et al., 2002; Gao and Matsui, 2005). Peptide amphiphiles and bolaamphiphiles were synthesised and studied because of the combination of self-assembly properties and biological activity. Peptides can therefore offer a function and/or a smartness in the scaffold and, being chiral, they can also provide a particular handedness which can amplify the level of recognition (Fairman and Åkerfeldt, 2005). The self-assembly of these amphiphilic molecules is exploited for the creation of nanosized-functional structures, useful as biological scaffolds for tissue regeneration (Silva et al., 2004), mineralization of hydroxyapatite crystals in a particular orientation (Hartgerink et al., 2001), for biocompatible implants and molecular wires (Matsui et al., 2000; Santoso et al., 2002).

Peptide self-assembly can also result in the formation of hydrogels. To date, many amphiphiles and bolaamphiphiles based on peptides have been designed for diverse applications and beautifully combine biological and structural properties leading to the development of next generation biomaterials for regenerative medicine (Holmes et al., 2000; Kisiday et al., 2002; Hartgerink et al., 2002; Kretsinger et al., 2005).

On the other hand, the study of the self-assembly process is also important for the investigation of undesired aggregations. Peptide and protein aggregation in pharmaceuticals is one of the major problems for the production and manufacture of peptide-based drugs (Wang, 2005). It is often regarded as the most frequent type of instability for this class of drugs and it frequently affects their biological activity. For antimicrobial peptides as well, the aggregation has in some cases been correlated to a lower or absent antibiotic activity (Hider et al., 1983; Alvarez-Bravo et al., 1994; Rautenbach et al., 2006). The effects of the spontaneous assembly of peptides inside the human body are even more dramatic: β -amyloid fibril formation *in vivo* has been correlated without doubts to the development of the Alzheimer's disease (Hardy and Selkoe, 2000). Hence, the control over peptide aggregation both *in vitro* and *in vivo* under specific conditions is the focus of the medical research in this field (Pastor et al., 2005).

2.4 References

- Aggeli A, Bell M, Carrick LM, Fishwick CWG, Harding R, Mawer PJ, Radford SE, Strong AE and Boden N (2003) pH as a trigger of peptide β -sheet self-assembly and reversible switching between nematic and isotropic phases, *Journal of the American Chemical Society*, 125, 9619-9628.
- Alanis AJ (2005) Resistance to antibiotics: are we in the post-antibiotics era?, *Archives of Medical Research*, 36, 692-705.
- Alvarez-Bravo J, Kurata S and Natori S (1994) Novel synthetic peptides effective against methicillin-resistant *Staphylococcus aureus*, *Biochemical Journal*, 302, 535-538.
- Andreu D and Rivas L (1998) Animal antimicrobial peptides: an overview, *Biopolymers*, 47, 415-433.
- Anzai K, Hamasuna M, Kadono H, Lee S, Aoyagi H and Kirino Y (1991) Formation of ion channels in planar lipid bilayer membranes by synthetic basic peptides, *Biochimica et Biophysica Acta*, 1064, 256-266.
- Aranha C, Gupta S and Reddy KVR (2004) Contraceptive efficacy of antimicrobial peptide Nisin: in vitro and in vivo studies, *Contraception*, 69, 333-338.
- Bowdish DME, Davidson DJ, Scott MG and Hancock REW (2005) Immunomodulatory activity of small host defence peptides, *Antimicrobial Agents and Chemotherapy*, 49, 1727-1732.
- Breithaupt H (1999) The new antibiotics. Can novel antibacterial treatments combat the rising tide of drug-resistant infections?, *Nature Biotechnology*, 17, 1165-1169.
- Brogden KA, Ackermann M, McCray PB and Tack BF (2003) Antimicrobial peptides in animals and their role in host defences, *International Journal of Antimicrobial Agents*, 22, 465-478.
- Brown KL and Hancock REW (2006) Cationic host defense (antimicrobial) peptides, *Current Opinion in Immunology*, 18, 24-30.
- Castano S, Desbat B and Dufourcq J (2000) Ideally amphipathic β -sheeted peptides at interfaces: structure, orientation, affinities for lipids and hemolytic activity of (KL)_mK peptides, *Biochimica et Biophysica Acta*, 1463, 65-80.
- Claussen RC, Rabatic BM and Stupp SI (2003) Aqueous self-assembly of unsymmetric peptide bolaamphiphiles into nanofibers with hydrophilic cores and surfaces, *Journal of the American Chemical Society*, 125, 12680-12681.
- Collier JH, Hu BH, Ruberti JW, Zhang J, Shum P, Thompson DH and Messersmith PB (2001) Thermally and photochemically triggered self-assembly of peptide hydrogels, *Journal of the American Chemical Society*, 123, 9463-9464.
- Daher KA, Selsted ME and Lehrer RI (1986) Direct inactivation of viruses by human granulocyte defensins, *Journal of Virology*, 60, 1068-1074.
- Dancer SJ (2004) How antibiotics can make us sick: the less obvious adverse affect of antimicrobial chemotherapy, *The Lancet Infectious Diseases*, 4, 611-619.
- Driessen AJ, van de Vossenberg JLCM and Konings WN (1996) Membrane composition and ion-permeability in extremophiles, *FEMS Microbiology Reviews*, 18, 139-148.

- Ehrenstein G and Lecar H (1977) Electrically gated ionic channels in lipid bilayers, *Quarterly Reviews of Biophysics*, 10, 1-34.
- Ernst RK, Guina T and Miller SI (1999) How intracellular bacteria survive: surface modifications that promote resistance to host innate immune responses, *Journal of Infectious Diseases*, 179 (S2), S326-S330.
- Epand RM and Vogel HJ (1999) Diversity of antimicrobial peptides and their mechanism of action, *Biochimica et Biophysica Acta*, 1462, 11-28.
- Fairman R and Åkerfeldt KS (2005) Peptides as novel smart materials, *Current Opinion in Structural Biology*, 15, 453-463.
- Fuhrhop JH and Mathieu J (1984) Routes to functional vesicle membranes without proteins, *Angewandte Chemie, International Edition in English*, 23, 100-113.
- Gao X and Matsui H (2005) Peptide-based nanotubes and their applications in bionanotechnology, *Advanced Materials*, 17, 2037-2050.
- Gill I, López-Fandiño R, Jorba X and Vulfson EV (1996) Biologically active peptide and enzymatic approaches to their production, *Enzyme and Microbial Technology*, 18, 162-183.
- Gliozzi A, Relini A and Chong PL-G (2002) Structure and permeability properties of biomimetic membranes of bolaform archeal tetraether lipids, *Journal of Membrane Science*, 206, 131-147.
- Guo L, Lim KB, Poduje CM, Daniel M, Gunn JS, Hackett M and Miller SI (1998) Lipid A acylation and bacterial resistance against vertebrate antimicrobial peptides, *Cell*, 95, 189-198.
- Hancock REW (1997a) The bacterial outer membrane as a drug barrier, *Trends in Microbiology*, 5, 37-42.
- Hancock REW (1997b) Peptide antibiotics, *The Lancet*, 349, 418-422.
- Hancock REW (2001) Cationic peptides: effectors in innate immunity and novel antimicrobials, *The Lancet Infectious Diseases*, 1, 156-164.
- Hancock REW and Lehrer R (1998) Cationic peptides: a new source of antibiotics, *Trends in Biotechnology*, 16, 82-88.
- Hancock REW and Chapple DS (1999) Peptide antibiotics, *Antimicrobial Agents and Chemotherapy*, 43, 1317-1323.
- Hancock REW and Diamond (2000) The role of cationic antimicrobial peptides in innate host defences, *Trends in Microbiology*, 8, 402-410.
- Hancock REW and Rozek A (2002) Role of membranes in the activities of antimicrobial cationic peptides, *FEMS Microbiology Letters*, 206, 143-149.
- Hancock REW, Brown KL and Mookherjee N (2006) Host defence peptides from invertebrates – emerging antimicrobial strategies, *Immunobiology*, 211, 315-322.
- Hanzawa H, Shimada I, Kuzuhara T, Komano H, Kohda D, Inagaki F, Natori S and Arata Y (1990) ¹H nuclear magnetic resonance study of the solution conformation of an antibacterial protein, sapecin, *FEBS Letters*, 269, 413-420.

- Hardy J and Selkoe GA (2000) The amyloid hypothesis of Alzheimer's disease: progress and problems on the road to therapeutics, *Science*, 297, 353-356.
- Hartgerink JD, Beniash E and Stupp SI (2001) Self-assembly and mineralization of peptide-amphiphile nanofibers, *Science*, 294, 1684-1688.
- Hartgerink JD, Beniash E and Stupp SI (2002) Peptide-amphiphile nanofibers: a versatile scaffold for the preparation of self-assembling materials, *Proceedings of the National Academy of Sciences*, 99, 5133-5138.
- Hider RC, Khader F and Tatham AS (1983) Lytic activity of monomeric and oligomeric mellitin, *Biochimica et Biophysica Acta*, 728, 206-214.
- Hirakura Y, Alvarez-Bravo J, Kurata S, Natori S and Kirino Y (1996) Selective interaction of synthetic antimicrobial peptides derived from sapecin B with lipid bilayers, *Journal of Biochemistry*, 120, 1130-1140.
- Holmes TC, de Lacalle S, Su X, Liu G, Rich A and Zhang S (2000) Extensive neurite outgrowth and active synapse formation on self-assembling peptide scaffolds, *Proceedings of the National Academy of Sciences*, 97, 6728-6733.
- Izadpanah A and Gallo RL (2005) Antimicrobial peptides, *Journal of the American Academy of Dermatology*, 52, 381-390.
- Kim JI, Iwai H, Kurata S, Takahashi M, Masuda K, Shimada I, Natori S, Arata Y and Sato K (1994) Synthesis and characterisation of sapecin and sapecin B, *FEBS Letters*, 342, 189-192.
- Kisiday J, Jin M, Kurz H, Semino C, Zhang S and Grodzinsky (2002) Self-assembling peptide hydrogel fosters chondrocyte extracellular matrix production and cell division: implications for cartilage tissue repair, *Proceedings of the National Academy of Sciences*, 99, 9996-10001.
- Kogiso M, Masuda M and Shimizu T (1998a) Supramolecular polyglycine II-type structure of glycyglycine bolaamphiphiles, *Supramolecular Chemistry*, 9, 183-189.
- Kogiso M, Ohnishi S, Yase K, Masuda M and Shimizu T (1998b) Dicarboxylic oligopeptides bolaamphiphiles: proton-triggered self-assembly of microtubes with loose solid surfaces, *Langmuir*, 14, 4978-4986.
- Kogiso M, Okada Y, Hanada T, Yase K and Shimizu T (2000) Self-assembled fibers from valylvaline bola-amphiphiles by a parallel β -sheet network, *Biochimica et Biophysica Acta*, 1475, 346-352.
- Komano H, Homma K and Natori S (1991) Involvement of sapecin in embryonic cell proliferation of *Sarcophaga peregrina* (flesh fly), *FEBS Letters*, 289, 167-170.
- Kretsinger JK, Haines LA, Ozbas B, Pochan DJ and Schneider JP (2005) Cytocompatibility of self-assembled β -hairpin peptide hydrogel surfaces, *Biomaterials*, 26, 5177-5186.
- Lee S, Mihara H, Aoyagi H, Kato T, Izumiya N and Yamasaki N (1986) Relationships between antimicrobial activity and amphiphilic property of basic model peptides, *Biochimica et Biophysica Acta*, 862, 211-219.
- Lehrer RI and Ganz T (1999) Antimicrobial peptides in mammalian and insect host defense, *Current Opinion in Immunology*, 11, 23-27.

- Marshall SH and Arenas G (2003) Antimicrobial peptides: a natural alternative to chemical antibiotics and a potential for applied biotechnology, *Electronic Journal of Biotechnology*, 6, 272-283.
- Masuda M and Shimizu T (2004) Lipid nanotubes and microtubes: experimental evidence for unsymmetrical monolayer membrane formation from unsymmetrical bolaamphiphiles, *Langmuir*, 20, 5969-5977.
- Matsui H and Gologan B (2000) Crystalline glycyglycine bolaamphiphiles tubules and their pH-sensitive structural transformation, *Journal of Physical Chemistry B*, 104, 3383-3386.
- Matsui H, Pan S, Gologan B and Jonas SH (2000) Bolaamphiphile nanotube-templated metallized wires, *Journal of Physical Chemistry B*, 104, 9576-9579.
- Matsui H and Douberly GE (2001) Organization of peptide nanotubes into macroscopic bundles, *Langmuir*, 17, 7918-7922.
- Matsuyama K and Natori S (1988a) Purification of three antibacterial proteins from the culture medium of NIH-Sape-4, an embryonic cell line of *Sarcophaga peregrina*, *Journal of Biological Chemistry*, 263, 17112-17116.
- Matsuyama K and Natori S (1988b) Molecular cloning of cDNA for sapecin and unique expression of the sapecin gene during the development of *Sarcophaga peregrina*, *Journal of Biological Chemistry*, 263, 17117-17121.
- Matsuzaki K, Murase O, Fujii N and Miyajima K (1996) An antimicrobial peptide, magainin 2, induced rapid flip-flop of phospholipids coupled with pore formation and peptide translocation, *Biochemistry*, 35, 11361-11368.
- Matsuzaki K (1998) Magainins as paradigm for the mode of action of pore forming polypeptides, *Biochimica et Biophysica Acta*, 1376, 391-400.
- Matsuzaki K (1999) Why and how are peptide-lipid interactions utilized for self-defense? Magainins and tachyplesins as archetypes, *Biochimica et Biophysica Acta*, 1462, 1-10.
- McPhee JB and Hancock REW (2005) Function and therapeutic potential of host defence peptides, *Journal of Peptide Science*, 11, 677-687.
- Nakajima Y, Alvarez-Bravo J, Cho J, Homma K, Kanegasaki S and Natori S (1997) Chemotherapeutic activity of synthetic antimicrobial peptides: correlation between chemotherapeutic activity and neutrophil-activating activity, *FEBS Letters*, 415, 64-66.
- Nakajima-Shimada J, Natori S and Aoki T (1998) Effects of synthetic undecapeptides on *Trypanosoma cruzi* in vitro, *Parasitology International*, 47, 203-209.
- Naidoo VB (2004) The supramolecular chemistry of novel synthetic biomacromolecular assemblies, PhD thesis, University of Stellenbosch.
- Niece KL, Hartgerink JD, Donners JJM and Stupp SI (2003) Self-assembly combining two bioactive peptide-amphiphile molecules into nanofibers by electrostatic attraction, *Journal of the American Chemical Society*, 125, 7146-7147.
- Nikaido H (2001) Preventing drug access to targets: cell surface permeability barriers and active efflux in bacteria, *Cell Developmental Biology*, 12, 215-223.

- Okada M and Natori S (1983) Purification and characterization of an antibacterial protein from haemolymph of *Sarcophaga peregrina* (flesh-fly) larvae, *Biochemical Journal*, 211, 727-734.
- Okada M and Natori S (1985) Primary structure of sarcotoxin I, an antibacterial protein induced in the haemolymph of *Sarcophaga peregrina* (flesh fly) larvae, *Journal of Biological Chemistry*, 260, 7174-7177.
- Oren Z and Shai Y (1998) Mode of action of linear amphipathic alpha-helical antimicrobial peptides, *Biopolymers*, 47, 451-463.
- Otvos L (2005) Antibacterial peptides and proteins with multiple cellular targets, *Journal of Peptide Science*, 11, 697-706.
- Pastor MT, Esteras-Chopo A and López de la Paz (2005) Design of model systems for amyloid formation: lessons for prediction and inhibition, *Current Opinion in Structural Biology*, 15, 57-63.
- Peschel A and Collins LV (2001) Staphylococcal resistance to antimicrobial peptides of mammalian and bacterial origin, *Peptides*, 22, 1651-1659.
- Peschel A (2002) How do bacteria resist human antimicrobial peptides?, *Trends in Microbiology*, 10, 179-186.
- Pochan DJ, Schneider JP, Kretsinger J, Ozbas B, Rajagopal K and Haines Lb (2003) Thermally reversible hydrogels via intramolecular folding and consequent self-assembly of a *de novo* designed peptide, *Journal of the American Chemical Society*, 125, 11802-11803.
- Pouny Y, Rapaport D, Mor A, Nicolas P and Shai Y (1992) Interaction of antimicrobial dermaseptin and its fluorescently labelled analogues with phospholipid membranes, *Biochemistry*, 31, 12416-12423.
- Powers JPS and Hancock REW (2003) The relationships between peptide structure and antibacterial activity, *Peptides*, 24, 1681-1691.
- Rautenbach M and Hastings JW (1999) Cationic peptides with antimicrobial activity – The new generation of antibiotics? *Chimica Oggi/Chemistry Today*, Nov/Dec, 81-89.
- Rautenbach M, Gerstner GD, Vlok NM, Kulenkampff J and Westerhoff HV (2006) Analyses of dose-response curves to compare the antimicrobial activity of model cationic α -helical peptides highlights the necessity for a minimum of two activity parameters, *Analytical Biochemistry*, 305, 81-90.
- Raj PA and Dentino AR (2002) Current status of defensins and their role in innate and adaptive immunity, *FEMS Microbiology Letters*, 206, 9-18.
- Rajagopal K and Schneider JP (2004) Self-assembling peptides and proteins for nanotechnological applications, *Current Opinion in Structural Biology*, 14, 480-486.
- Reddy KVR, Yedery RD and Aranha C (2004) Antimicrobial peptides: premises and promises, *International Journal of Antimicrobial Agents*, 24, 536-547.
- Robinson JA, Shankaramma SC, Jetter P, Kienzl U, Schwendener RA, Vrijbloed JW and Obrecht D (2005) Properties and structure–activity studies of cyclic b-hairpin peptidomimetics based on the cationic antimicrobial peptide protegrin, *Bioorganic and Medicinal Chemistry*, 13, 2055–2064.

- Rusterholtz K and Pohlchröder M (1999) Where are the limits of life?, in Horikoshi K and Grant WD (Eds.) *Extremophiles: microbial life in extreme environments*, Wiley-Liss, New York.
- Ryan MP, Hill C and Ross RP (2002) Exploitation of lantibiotic peptides for food and medical uses, in Dutton JC et al. (Eds.) *Peptide antibiotics: discovery, modes of action and applications*, Marcel Dekker; New York.
- Santoso SS, Vauthey S and Zhang S (2002) Structures, function and applications of amphiphilic peptides, *Current Opinion in Colloid and Interface Science*, 7, 262-266.
- Shai Y (1999) Mechanism of the binding, insertion and destabilization of phospholipids membranes by α -helical antimicrobial and cell non-selective membrane-lytic peptides, *Biochimica et Biophysica Acta*, 1462, 55-70.
- Shai Y (2002) Mode of action of membrane active antimicrobial peptides, *Biopolymers*, 66, 236-248.
- Shai Y and Oren Z (2001) From 'carpet' mechanism to de-novo designed diastereomeric cell-selective antimicrobial peptides, *Peptides*, 22, 1629-1641.
- Silva GA, Czeisler C, Niece KL, Beniash E, Harrington DA, Kessler JA and Stupp SI (2004) Selective differentiation of neural progenitor cells by high-epitope density nanofibers, *Science*, 303, 1352-1355.
- Shimizu T, Kogiso M and Masuda M (1996) Vesicle assembly into microtubes, *Nature*, 383, 487-488.
- Sirieux J, Lauth-de Viguerie N, Rivière M and Lattes A (2000) From unsymmetrical bolaamphiphiles to supermolecules, *New Journal of Chemistry*, 24, 1043-1048.
- Steiner H, Hultmark D, Engstrom A, Bennich H and Boman HG (1981) Sequence and specificity of two antimicrobial proteins in insect immunity, *Nature*, 292, 246-248.
- Suenaga M, Lee S, Park NG, Aoyagi H, Kato T, Umeda A and Amako K (1989) Basic amphipathic helical peptides induce destabilization and fusion of acidic and neutral liposomes, *Biochimica et Biophysica Acta*, 981, 143-150.
- Sugiarto H and Yu PL (2004) Avian antimicrobial peptides: the defense role of β -defensins, *Biophysical and Biochemical Research Communications*, 323, 721-727.
- Toney JH (2002) Isegaran. IntraBiotics Pharmaceuticals, *Current Opinion in Investigational Drugs*, 3, 225-228.
- Wang W (2005) Protein aggregation and its inhibition in biopharmaceutics, *International Journal of Pharmaceutics*, 289, 1-30.
- Winder D, Günzburg WH, Erfle V and Salmons B (1998) Expression of antimicrobial peptides has an antitumour effect in human cells, *Biophysical and Biochemical Research Communications*, 242, 608-612.
- Yaeman MR and Yount NY (2003) Mechanisms of antimicrobial peptide action and resistance, *Pharmacology Reviews*, 55, 27-55.

Yamada K and Natori S (1993) Purification, sequence and antibacterial activity of two novel sapecin homologues from *Sarcophaga* embryonic cells: similarity of sapecin B to charybdotoxin, *Biochemical Journal*, 291, 275-279.

Yamada K and Natori S (1994) Characterization of the antimicrobial peptide derived from sapecin B, an antibacterial protein of *Sarcophaga peregrina* (flesh fly), *Biochemical Journal*, 298, 623-628.

Zairi A, Belaïd A, Gahbiche A and Hani K (2005) Spermicidal activity of dermaseptins, *Contraception*, 72, 447-453.

Zhang S (2003) Fabrication of novel biomaterials through molecular self-assembly, *Nature Biotechnology*, 21, 1171-1178.

Zhang S and Altman M (1999) Peptide self-assembly in functional polymer science and engineering, *Reactive and Functional Polymers*, 41, 91-102.

Zhang S, Marini DM, Hwang W and Santoso S (2002) Design of nanostructured biological materials through self-assembling of peptides and proteins, *Current Opinion in Chemical Biology*, 6, 865-871.

Chapter 3

Synthesis of novel bolaamphiphilic peptides and peptide hybrids

3.1 Introduction

3.1.1 Amino acids, peptides and proteins

Amino acids are known as the building blocks of life and they represent the starting units for the assembly of peptides and proteins. They are characterised by two main functional groups, an amino group and a carboxyl group, both linked to a carbon atom which is named the α -carbon or $C\alpha$. They exist as zwitterionic molecules at neutral pH (Fig. 3.1). As $C\alpha$ is also substituted with a hydrogen atom and a side-chain group (R) it forms a chiral centre (except in the case of glycine). Side-chain groups are different for each amino acid, they are essential for the determination of the chemical properties of peptides and proteins and they play an important role in the structure and function of these biomacromolecules (refer to p. XXIV for a complete list of naturally occurring side-chain groups).

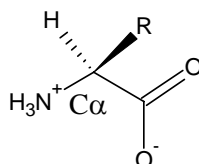


Fig. 3.1: Zwitterionic structure of a general amino acid at pH 7.

In nature there are 21 amino acids encoded by DNA and they are connected to each other to form peptides and proteins by an amide bond (or peptide bond) which links the carboxyl group of one AA to the amino group of the following AA (Fig. 3.2).

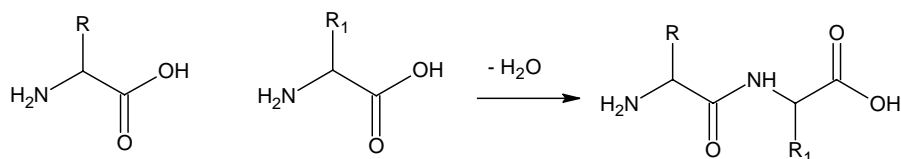


Fig. 3.2: The peptide bond forms the backbone of peptides and proteins.

The atoms involved in the peptide bond (showed in a rectangle in Fig. 3.3, left) form the so called “peptide group”: it comprises the carbonyl carbon and the α -carbon of the first amino acid (C_1 and α_1 respectively) together with the carbonyl oxygen, the amide nitrogen and the α -carbon of the second amino acid (N_2 and α_2) together with the amide hydrogen. These six atoms create a planar structure because of the partial double bond character of the C-N amide bond. Consequently, the peptide bond exists as two rotamers: the *trans* configured (Fig. 3.3 left) – occurring in most of the natural peptides and proteins because of the lower steric hindrance – and the *cis* configured (Fig. 3.3 right).

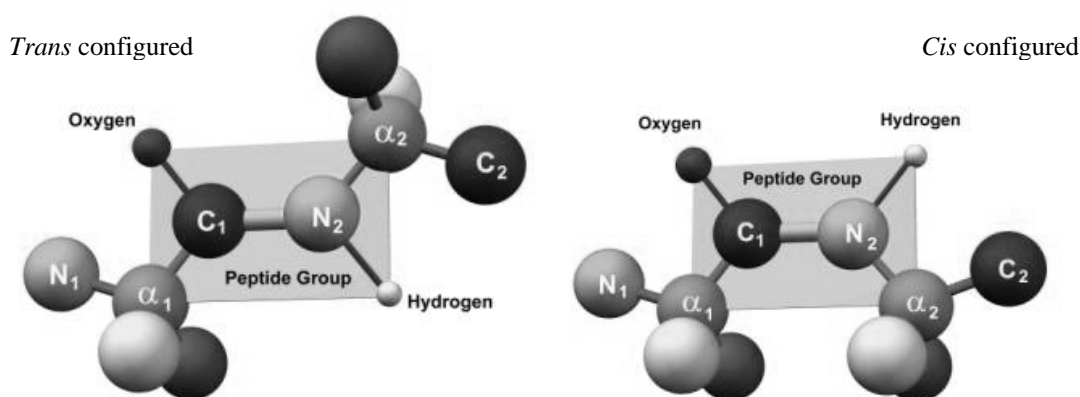


Fig. 3.3: The peptide bond (adapted from: www.codefun.com/Genetic_tRNA.htm, last accessed 25/11/05).

From a structural point of view, peptides and proteins can be described at four different levels of complexity (Fig. 3.4). The linear sequence of amino acids that forms a polypeptide chain gives the *primary structure* of the macromolecule. According to the different composition of amino acids, different three-dimensional structures of the peptide backbone can be obtained (called α -helix and β -sheet) and they create the *secondary structure* of the polypeptide. The secondary structure is mainly based on hydrogen bonds between the amide hydrogen and the carboxyl oxygen. The global organization of an entire protein or peptide is expressed by its *tertiary structure* which is based on the interactions between different amino acids belonging to the same chain. Covalent bonds (i.e. disulfide bridges) and noncovalent interactions (i.e. ionic bonds) are responsible for the tertiary structure. Finally, the term *quaternary structure* refers to the special arrangements of different polypeptide chains associated by noncovalent interaction to form supramolecular assemblies (Sewald and Jakubke, 2002).

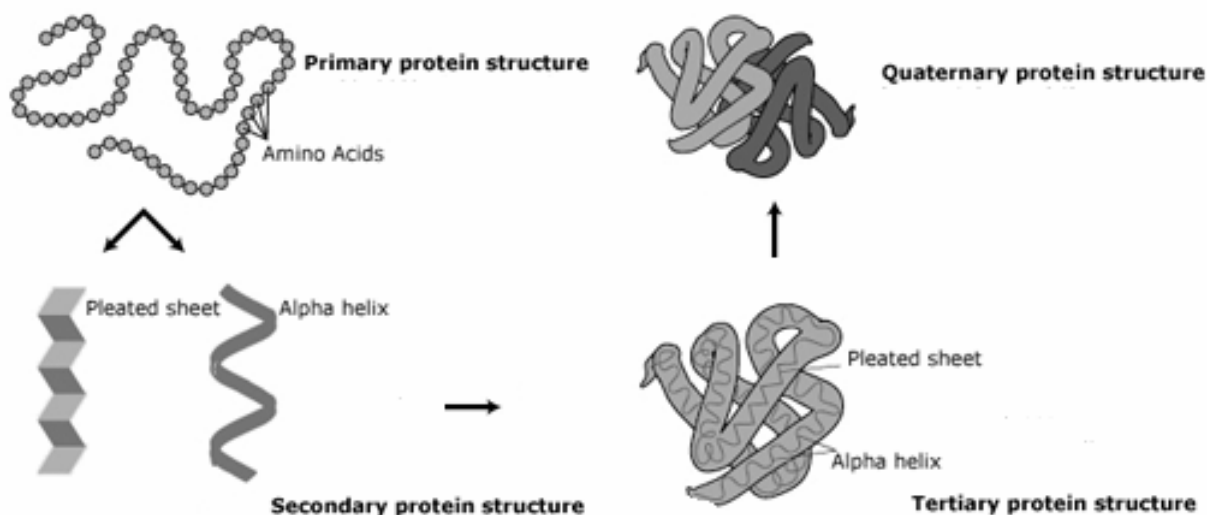


Fig. 3.4: Protein and peptide structures: primary, secondary, tertiary and quaternary
(adapted from: www.geneticsolutions.com, last accessed 24/10/05).

3.1.2 Principles and development of solid-phase peptide synthesis

For centuries the work of chemists and biochemists has been based on semi-synthetic products mainly obtained from natural sources (animals, plants and minerals). During the 1960s, because of an increasing interest in peptide and protein research, these sources were not enough and new synthetic routes for the preparations of such compounds were necessary. Hence, synthetic techniques for the synthesis of polypeptides were developed; they were basically divided into solution and solid-phase approaches. The solid-phase approach, proposed by Merrifield, marked the future of peptide and protein synthesis, and brought the Nobel prize to its developer (Merrifield, 1963; Merrifield, 1964; Merrifield, 1969; Merrifield, 1997).

Solid-phase peptide synthesis soon proved its advantages over solution phase methods: purification steps were performed simply by washing the polymeric support, the amide bond formation was forced by increasing the concentration of reagents and the loss of product was reduced by being attached to the resin beads via a linker. However, SPPS does have some negative aspects. Purity and high yields are possible only if each reaction is quantitative. Supposing only 95% yield is achieved in every coupling and Fmoc deprotection step in the synthesis of a 124-amino acid protein (such as the ribonuclease synthesised by Merrifield), the final yield will then be in the range of 0.0002% (Bayer, 1991). But, on the other hand, in the solution phase methodology it was necessary to isolate and purify the intermediates after each coupling and deprotection, thus requiring more time for reaction work-up, wasting more product and more solvent/chemicals for purification and isolation of the growing peptide chain.

An amide bond is formed by the reaction between a carboxyl group and an amino group belonging to different AAs. Hence, to avoid side reactions, an orthogonal protection scheme is necessary when the building blocks have many functionalities, as do most of the amino acids (α -amino and carboxyl groups, side-chains with amino and carboxyl groups, alcohols, thiols, etc.). During the synthesis, certain groups (i.e. α -amino groups) have to be momentarily protected and others (i.e. those ones on the side-chains) have to be kept permanently protected until the end of the synthesis. Moreover, the temporary protecting group must be easy to remove under conditions that will not affect the permanent protecting groups. Usually the removal of these permanent protecting groups occurs together with the release of the peptide from the solid support (Jones, 2002). A schematic representation of SPPS is shown in Figure 3.5.

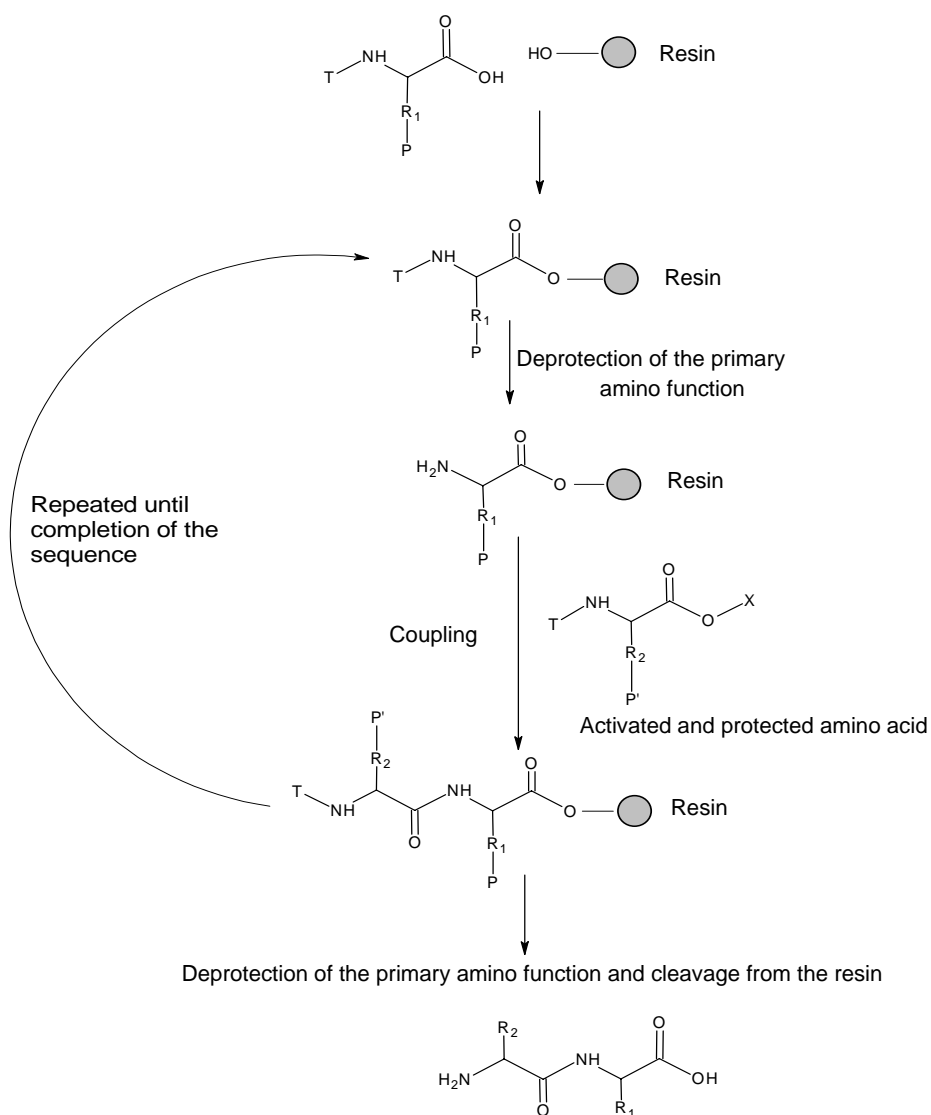


Fig. 3.5: Principle of SPPS.

P and P': permanent protecting group; T: temporary protecting group; X: activating group.

Several protocols have been developed from Merrifield's original idea which was based on the use of a *tert*-butoxycarbonyl (Boc) α -amino protecting group. The polyamide protocol is one of the most widely employed and it is based on the use of the N^9 -fluorenylmethyloxycarbonyl group for the protection of the α -amino function (Carpino and Han, 1970). This protocol, developed by Atherton, Sheppard and Dryland, presents many advantages over the Boc protocol (Atherton et al., 1979; Atherton and Sheppard, 1989; Wellings and Atherton, 1997). First of all it requires only mild chemistry: the Fmoc group is easily and quickly removed in weak basic conditions – 20% v/v piperidine in dimethylformamide (DMF) (Carpino and Han, 1972) – in which the permanent protecting groups are stable. In Merrifield's solid-phase approach the Boc group was removed by treating the resin with trifluoroacetic acid (TFA). Acid-stable permanent protecting groups were used for the side-chains (Fig. 3.6). Cleavage and complete deprotection were performed at the end of the synthesis by HF treatment. This could lead to loss of the growing peptide from the resin and many costly safety measures required when using liquid HF (Pennington, 1997a). A second advantage is that the free Fmoc group reacts with the excess of piperidine and the concentration of this adduct is measurable by ultraviolet (UV) spectrophotometry, thus enabling one to follow the completion of each elongation step and monitor the entire synthesis (see Section 3.3.2.7 for details) (Sheppard, 2003).

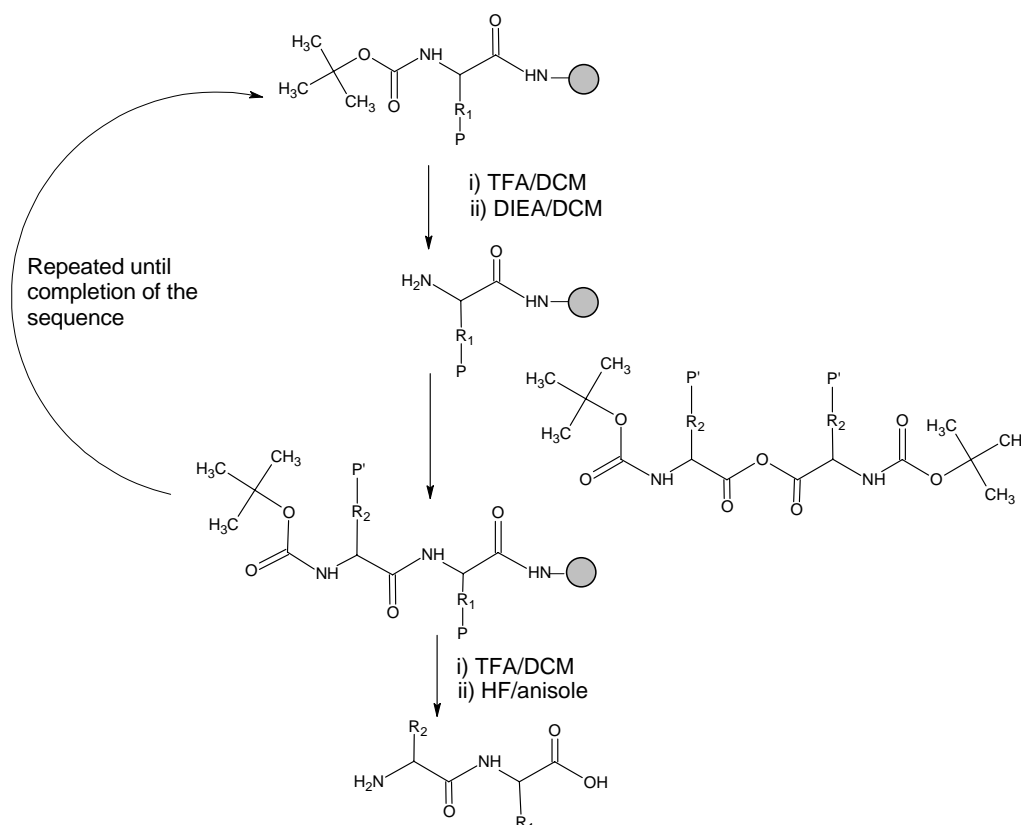


Fig. 3.6: Boc SPPS or Merrifield's SPPS (Merrifield, 1963).

P and P' are permanent protecting groups removed by HF while the Boc group is removed by TFA.

Activation strategy shown: preformed symmetrical anhydrides.

Finally, the use of an acid labile peptide-resin linkage in the Fmoc protocol allows one to cleave the peptide from the resin with a strong acid (i.e. TFA) with the concurrent removal of side-chain protecting groups (Guy and Fields, 1997; Dick, 1997). Therefore, with the Fmoc-polyamide strategy it is possible to avoid some typical problems of the progressive acidolysis of the Merrifield's strategy (Boc removal by TFA and final cleavage with HF). The two different protocols for SPPS are shown in Figures 3.6 and 3.7.

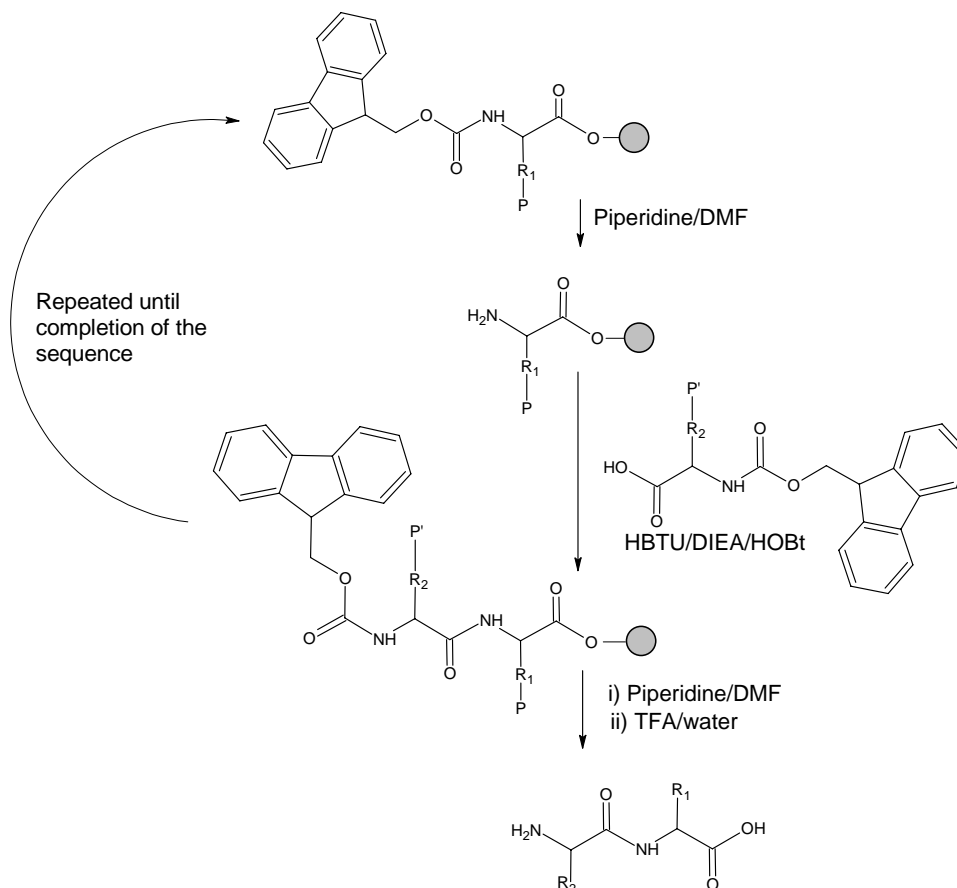


Fig. 3.7: Fmoc SPPS. P and P' are permanent protecting groups removed by the final TFA cleavage while the Fmoc group is removed by piperidine. Activation strategy shown: active esters.

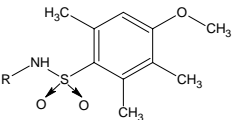
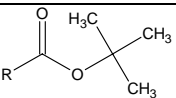
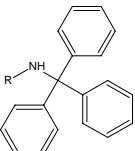
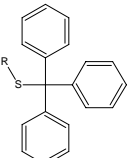
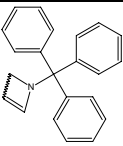
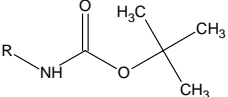
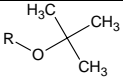
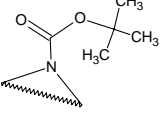
In this study Fmoc-based SPPS was chosen for the synthesis of the designed bolaamphiphilic peptides. It is now quite a common technique for the production of small peptides and proteins, and applying the same principle, different activation strategies and polymeric supports can be utilized (Bayer, 1991; Chan and White, 2000b).

3.1.2.1 Side-chain protecting groups

As about half of the natural amino acids have reactive groups on their side-chains the use of protecting groups during SPPS is essential in order to avoid (or highly reduce) the production of wrong sequences. For the classical Fmoc protocol two important aspects must be considered when

choosing an orthogonal protecting group: (i) it must be stable during the normal coupling/deprotection steps (both carried out in a basic environment) and (ii) it must be easy to remove, preferably during the TFA cleavage (thus achieving simultaneous deprotection and release from the solid support). On the other hand if a selective deprotection of certain amino acids is necessary during the synthesis (i.e. for the synthesis of cyclic peptides, biotinylated peptides or chemically modified peptides) a wide range of protecting groups is available (Pennington, 1997b). The most common side-chain protecting groups are listed in Table 3.1.

Tab. 3.1: Common protecting groups for routine synthesis of peptides
(adapted from Chan and White, 2000a)

SIDE-CHAIN FUNCTIONALITY	PROTECTING GROUP	ABBREVIATION	CLEAVAGE CONDITIONS
Arg		Mtr	90-95% TFA v/v, 4-6 h or TFA-anisole (9:1), 1 h
Asp/Glu		OtBu	90% TFA v/v, 30 min
Asn/Gln		Trt	90% TFA v/v, 1 h
Cys		Trt	90% TFA v/v, 30 min
His		Trt	50% TFA in DCM, 30 min
Lys/Orn		Boc	90% TFA v/v, 30min
Ser/Thr/Tyr		tBu	90% TFA v/v, 30 min
Trp		Boc	(i) 90% TFA, 1 h and (ii) 1% aq.TFA, 1-2 h

3.1.2.2 Fmoc deprotection

The removal of the Fmoc protecting group is performed by treating the resin with 20% (v/v) piperidine in DMF. As shown in Fig. 3.8, the initial step is the deprotonation of the fluorene ring to generate an aromatic intermediate that rearranges, giving the dibenzofulvene (a). The latter reacts with the piperidine (in excess) leading to the formation of the fulvene adduct (b) (Fields, 1997; Chan and White, 2000a).

The product of the deprotection reaction (b) absorbs UV strongly (λ_{\max} at 301 nm) and this characteristic is used to follow both the deprotection and the elongation steps (the millimoles of fulvene-adduct are directly correlated to the millimoles of amino acid coupled during the coupling reaction) (See Section 3.3.2.7 for details).

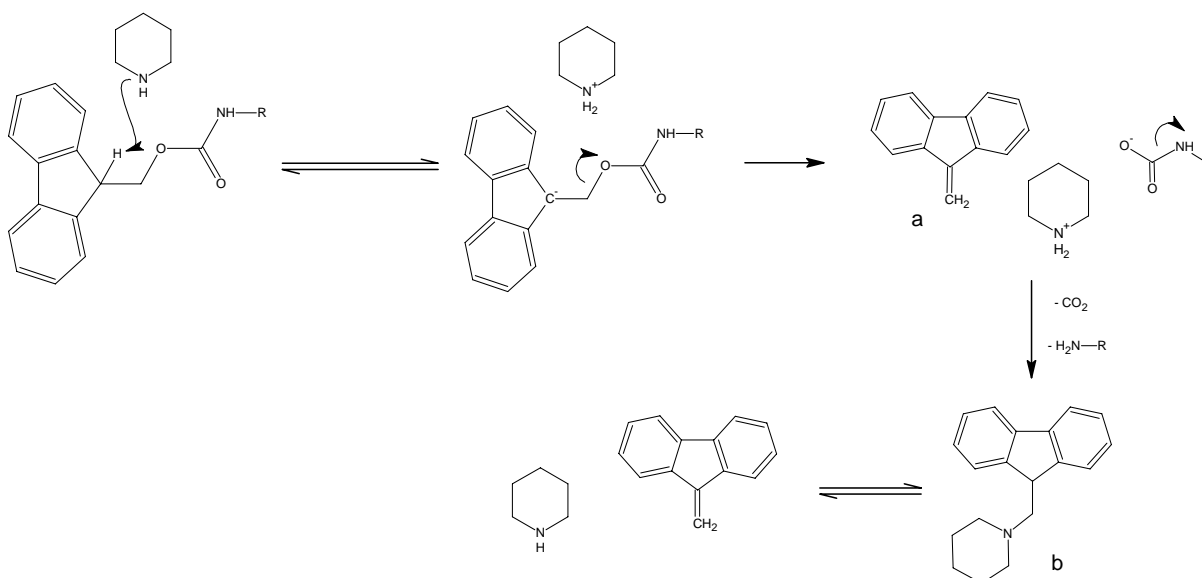


Fig. 3.8: Reactions involved in the Fmoc deprotection.

3.1.2.3 Activation strategies

Considering the main step of the peptide synthesis, the coupling reaction, many approaches and reagents can be employed in Fmoc SPPS (Bailey, 1990; Albericio and Carpino, 1997; Chan and White, 2000a; Chan and White, 2000b). In order to facilitate the formation of the amide bond between the amino group of the growing peptide and the carboxyl group of the incoming Fmoc-protected amino acid (Fmoc-AA), different activation reagents are used (Marder and Albericio, 2003; Montalbetti and Falque, 2005).

Some of the most widely used activation methods for peptide coupling are discussed below.

A. Preformed symmetrical anhydrides

DCC[†] and DIC are used in dichloromethane (DCM) for the preparation of symmetrical anhydrides of the Fmoc-AA (Sheehan and Hess, 1955). They have been widely used in the past

[†] Refer to the list of abbreviations (p. XII) for a complete explanation of the acronyms.

because of their reactivity but their use produces a huge loss of reagents as only one out of two equivalents of protected amino acid reacts. Moreover certain symmetrical anhydrides have a low solubility in DCM.

B. Active esters (HOBt esters and pentafluorophenyl esters)

- HOBt[†] esters are easily prepared in situ using different kinds of carbodiimides (DCC, DIC) or phosphonium/amminium salts (BOP, PyBOP, TBTU, HBTU, HATU)[†] and react quickly with the amino group of the growing peptide (Albericio et al., 1998). Side reactions include the formation of diketopiperazines by intramolecular aminolysis (Fields, 1997).

- Fmoc-protected amino acids can be bought as pentafluorophenyl esters and used directly. They quickly react with no side reactions (Kisfaludy and Schön, 1980; Atherton et al., 1988).

C. Acid fluoride

Acid fluorides of the corresponding amino acid can be generated by using TFFH[†] (Chan and White, 2000b) or cyanuric fluoride (Carpino et al., 1990), they are less reactive than acid chlorides and more stable in the presence of tertiary amines and in the common conditions of SPPS.

A comparison of the coupling methods used in SPPS is given in Table 3.2.

Tab. 3.2: Coupling methods used in Fmoc SPPS: methods using active esters are shown in bold
(adapted from Chan and White, 2000a)

COUPLING REAGENT	ADDITIVE	ACTIVE SPECIES	CONDITIONS	COMMENTS
DCC (or DIC)	/	Symmetrical anhydrides	Fmoc-AA/DIC (2:1) in DCM	1 eq. Fmoc-AA wasted
DCC (or DIC)	HOBt	Benzotriazolyl ester	Fmoc-AA/DIC/HOBt (1:1:1) in DMF	Slow activation in DMF
PyBOP (or TBTU, HBTU)	HOBt	Benzotriazolyl ester	Fmoc-AA/PyBOP/HOBt/DIEA (1:1:1:2) in DMF	Common activation method/fast activation
HATU	/	9-Azabenzotriazolyl ester	Fmoc-AA/HATU/DIEA (1:1:2) in DMF	Excellent for difficult couplings
Fmoc-AA pentafluorophenyl ester	HOBt	Benzotriazolyl ester	Fmoc-AA pentafluorophenyl ester/HOBt (1:1) in DMF	No side-reactions
TFFH	/	Acid fluoride	Fmoc-AA/TFFH/DIEA (1:1:2) in DMF	Useful for <i>N</i> -alkyl and α -substituted residues

[†] Refer to the list of abbreviations (p. XII) for a complete explanation of the acronyms.

3.1.2.4 Racemisation

Most of the natural amino acids, excluding glycine, have a chiral centre of L-configuration on their α -carbon atoms. The presence of such chiral centres is often important for the correct biological functions of peptide and proteins. Possible modifications of the $C\alpha$ chirality can occur during the activation step of the carboxyl group. Due to the activated carboxyl group the hydrogen atom (natural substituent at the asymmetric α -carbon) presents enhanced acidity and can be easily removed by a base. The reattachment of such a proton represents the first mechanism of racemisation (direct enolization). The second more common one, involves deprotonation and ring opening of an oxazolone intermediate, that is generated by attack on the activated carboxy group of the adjacent amide bond (Fig. 3.9) (Chan and White, 2000a).

Oxazolone formation takes place quite easily when using carboxy-activated amino acids especially if the activation strategy includes strong activators (such as DCC). It has been experimentally proved that when utilizing HOBt as catalyst during the coupling step the racemisation reaction is drastically reduced (Gamet et al., 1984; Benoiton et al., 1992). For this reason the chosen activation method for the synthesis of the designed bolaamphiphilic peptides involved the use of HOBt esters generated in situ with ammonium/phosphonium salts. PyBOP[®] has been used for the loading of the first amino acid on the resin and HBTU for the elongation of the peptide chain (Fields, 1991; Angell et al., 2002).

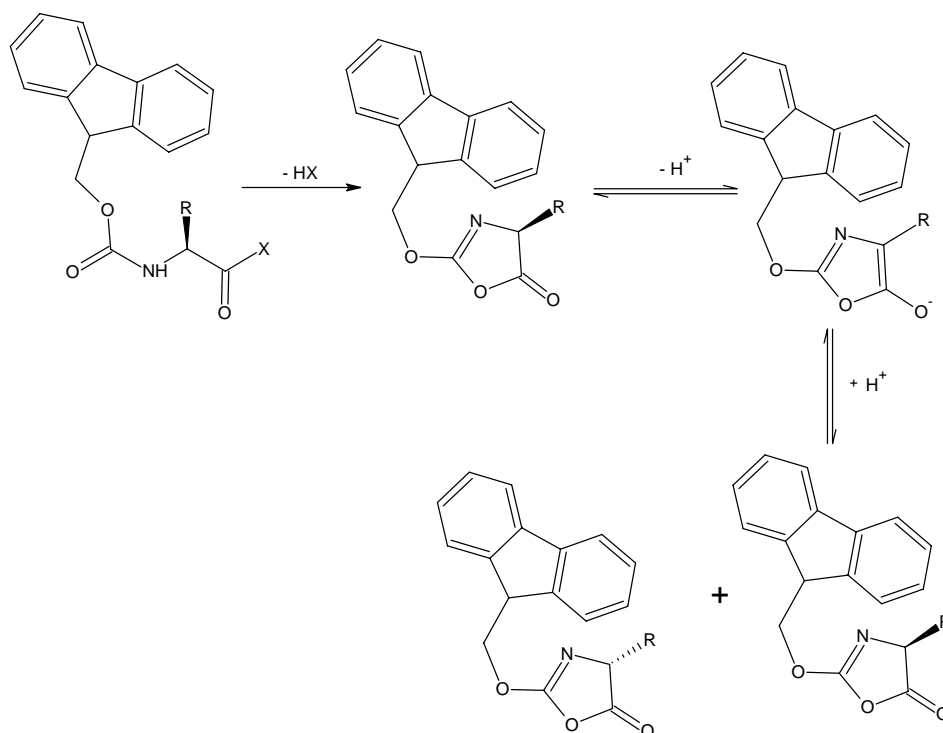
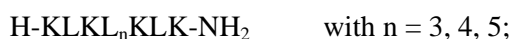


Fig. 3.9: Racemisation via oxazolone formation.

3.2 Design of novel peptide bolaamphiphiles

3.2.1 Guidelines

Peptides derived from the general active motif suggested by Alvarez Bravo et al. (Alvarez-Bravo et al., 1994) were used as parent compounds (L3, L4 and L5):



The design of novel peptides and peptide hybrids took into account:

1. the importance of the KLK moiety and the hydrophobic poly-leucine chain for the antimicrobial activity (Nakajima-Shimada et al., 1998)
2. a library of compounds previously designed at the University of Stellenbosch (Biochemistry) and derived from the abovementioned peptides (Naidoo, 2004)
3. the well-established use of model antimicrobial peptides containing lysine and leucine (Lee et al., 1986; Suenaga et al., 1989; Anzai et al., 1991; Park et al., 2003; Béven et al., 2003).

Moreover, the project also focused on the self-assembly properties of these natural peptide bolaamphiphiles. Special consideration was therefore paid to previous work regarding self-assembling peptides and peptide hybrids (Shimizu et al., 1996; Santoso and Zhang, 2004).

Various modifications were introduced so as to investigate and evaluate the connections between the amino acid composition, the secondary structure and the biological activity. Additionally, for the development of new functional nanomaterials with antibiotic properties, it was important to modify the amino acid composition so as to increase the tendency to self-assemble.

Modifications and changes were applied in different positions along the primary structure of the original model peptides. They are discussed below:

- A) Many synthetic and natural antimicrobial peptides (such as temporin A, magainin II amide, melittin, cecropin, nisin) have an amide functional group at the C terminus, hence, the entire set of peptides was synthesised as peptide amide. Only two compounds (KL1 and KL2[♦]) were designed as peptide acids, thus possibly providing a better understanding of SAR in this position.
- B) The charged amino acid lysine was replaced by the non-proteinogenic amino acid ornithine. The introduction of a non-natural amino acid is often intended to reduce the degradation of the peptide by bacterial hydrolytic enzymes (Hong et al., 1999).
- C) The hydrophobic amino acid leucine was substituted by the amino acid tyrosine. The phenolic functionality of the latter could increase the interactions with bacterial membranes

[♦] Refer to Fig. 3.10 for the primary structure of KL1 and KL2.

because of its ability to disorganise phospholipid bilayers (hence its use as disinfectant since 1867 when Lister first introduced it in the clinical practice). Moreover, it could enhance the self-assembly properties (Zhang, 2003; Santoso and Zhang, 2004).

- D) The poly-leucine chain was changed into a linear spacer using ω -amino acids, more precisely using 6-aminohexanoic acid (with an aliphatic chain made of 5 carbons) and 9-aminononanoic acid (with an aliphatic chain made of 8 carbons) (Naidoo, 2004).
- E) A glycyl-prolyl-glycine (GPG) tripeptide was also used instead of 9-aminononanoic acid, providing the same length (in terms of number of atoms) between the two hydrophilic heads. The use of proline involves the creation of a β -turn in the secondary structure, which influences the interaction with membranes and the self-assembly properties (Rex, 2000).
- F) In order to create a large diversity inside the designed library of peptides and to evaluate the importance of the hydrophobicity in SAR, the charged amino acid (ornithine and lysine) and the hydrophobic amino acids (tyrosine and leucine) were switched.

The outlined changes were not introduced simultaneously in the entire set of molecules. They were applied at different levels in various compounds, creating a series of molecules with some common features (length between 7 and 9 amino acids, net positive charge, general bolaamphiphilic structure) and some differences (amino acid composition, hydrophobicity, three-dimensional structure).

3.2.2 Library of peptides

The library of synthesised compounds can be divided into four smaller families (Fig. 3.10). The first one comprises the parent compounds L3, L4 and L5 representing the original antimicrobial motif. In the second one 6-aminohexanoic acid and 9-aminononanoic acid are used instead of the poly-leucine chain. In the third group, molecules maintain the same overall positive charge (+5) but both ω -amino acid and GPG tripeptide are used. The last group includes peptide hybrids with a higher content in the hydrophobic AA leucine and a lower net positive charge (+3/+1)[§].

The entire library was planned and created focusing on the KL4 peptide hybrid which includes 9-aminononanoic acid (Fig. 3.10). In preliminary studies this compound showed a biological activity higher than other peptide hybrids derived from the same motif and which included 6-aminohexanoic acid and 12-aminododecanoic acid as linear aliphatic skeleton (Naidoo, 2004). Furthermore, the 9-aminononanoic acid provides a distance (in terms of number of atoms) between the two KLK charged motives comparable to the poly-leucine chain of the sapecin's first derivative (L3), the most active peptides derived from sapecin B (Hirakura et al., 1996).

[§] Physicochemical properties of the designed peptides are extensively reviewed later in this chapter.

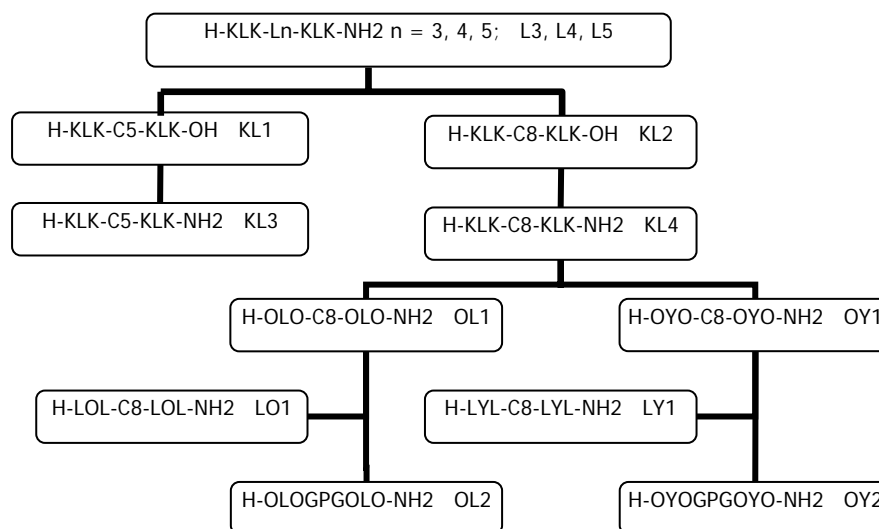


Fig. 3.10: Library of synthesised compounds: the original amino acid pattern is shown at the top of the diagram. For simplicity, C8 and C5 represent 9-aminononanoic acid and 6-aminohexanoic acid respectively.

Therefore, peptides' physicochemical properties changed:

- I. the use of ornithine instead of lysine (OL1 and OL2), besides introducing a non natural AA, means increasing the charge density on the molecule, thus influencing the interaction with negatively charged membranes (such as bacterial cell wall).
- II. the substitution of leucine with tyrosine (OY1 and OY2) implies the possibility of stabilizing intramolecular hydrophobic interactions which can change the three-dimensional structure of the tyrosine-containing peptides.
- III. the diverse hydrophobic content between the various families entails different interactions with membranes and alters the self-organisation behaviour as the use of more hydrophobic amino acids (Tyr, Phe, Trp) increases the self-assembly ability (Santoso and Zhang, 2004).
- IV. not much is known about the effect on the biological activity of non-natural amino acids such as the ω -amino acids used in KL1, KL2, KL3, KL4, OL1, OY1, LO1 and LY1. Their hydrocarbon chain interferes with the classical α -helical structure of the parent peptides but provides a hydrophobic core comparable to that created by the poly-leucine chain.
- V. in OL2 and OY2, the use of a glycyl-prolyl-glycine tripeptide instead of the linear aliphatic ω -amino acid also involves modifications of three-dimensional structural properties, destroying the α -helical conformation.

The modifications experimented in the library of peptides and peptide hybrids allowed us to investigate the effects on biological activity and aggregation properties of the following changes in the 3D-structure: { α -helices (parent peptides) \rightarrow distorted α -helices (peptides including C5 and C8) \rightarrow β -turn (GPG)}. They were later taken into account during the structural and biological characterisation of the novel compounds and correlated to their properties.

3.3 Materials and instrumentation

3.3.1 Chemicals

3.3.1.1 Solvents and general reagents

N,N'-dimethylformamide (99%) and toluene (99%) were supplied by Saarchem (Wadeville, South Africa).

Pyridine (99%) and *t*-amyl alcohol (2-methylbutan-2-ol, 99%) were supplied by Acros Organics (Geel, Belgium).

Glacial acetic acid (AcOH, 99%) was supplied by BDH (Poole, UK).

Trifluoroacetic acid (99.5%) and acetic anhydride (99%) were supplied by Merck (Hohenbrunn, Germany).

Acetonitrile (ACN, HPLC grade) was supplied by Riedel-de Haën (Seelze, Germany).

Methanol (MeOH, 99.9%), *N,N'*-diisopropylethylamine (DIEA, 99.5%) and piperidine (99%) were supplied by Aldrich (Steinheim, Germany).

Technical grade dichloromethane and diethyl ether were used after distillation.

Analytical grade water (Milli-Q® water) was obtained by filtering glass-distilled water with a Millipore Milli-Q® (Bedford, MA, USA) 0.22-µm filtering system.

Potassium cyanide was purchased from Merck (Darmstadt, Germany). Ninhydrin (99%) was from Aldrich (Steinheim, Germany). Phenol (99%) was from Labchem (Edenvale, South Africa). Chloranil (99%) and triisopropylsilane (TIS, 99%) were from Fluka (Buchs, Switzerland).

Drying agents, salts, silica gel, 3 Å and 4 Å molecular sieves (ms) were supplied by Saarchem (Wadeville, South Africa), Fluka (Buchs, Switzerland) and Merck (Darmstadt, Germany).

3.3.1.2 Protected amino acids, resins and coupling reagents

Fmoc-Gly-OH*, Fmoc-Leu-OH, Fmoc-Lys(Boc)-OH, Fmoc-Orn(Boc)-OH, Fmoc-Pro-OH, Fmoc-Tyr(*t*Bu)-OH were supplied by Novabiochem (Laufelfingen, Switzerland).

Fmoc-9-Anc-OH and Fmoc-6-Ahx-OH were supplied by Advanced ChemTech (Louisville, KY, USA).

Novasyn TGA-Fmoc-Lys(Boc)-OH resin (loading capacity 0.21 mmol/g), Novasyn TGA resin (loading capacity 0.25 mmol/g), Novasyn TGR resin (loading capacity 0.23 mmol/g) were from Novabiochem (Laufelfingen, Switzerland).

Benzotriazol-1-yloxytris(pyrrolidino)phosphonium hexafluorophosphate (PyBOP®) and 1-hydroxybenzotriazole (HOBt) were from Novabiochem (Laufelfingen, Switzerland). 2-(1H-benzotriazol-1-yl)-1,1,3,3-tetramethyluronium hexafluorophosphate (HBTU) was supplied by both Advanced ChemTech (Louisville, KY, USA) and Novabiochem (Laufelfingen, Switzerland).

* Amino acid codes denote (S)-amino acids with an L-configuration unless stated otherwise.

Some crude L3, L4 and L5 peptides were kindly provided by Dr M Rautenbach (Department of Biochemistry, Stellenbosch University).

3.3.2 Instrumentation

3.3.2.1 Bench solid-phase peptide synthesis

Solid-phase peptide synthesis was performed using a glass peptide reaction vessel coupled to a vacuum pump for solvents removal.

A Stuart flask shaker SF1 (Bibby Sterilin, UK) was used during the elongation and deprotection reactions to vigorously mix the resin.

The absorbance of the fulvene-piperidine adduct was determined using a Lambda 20 UV-Vis spectrophotometer (Perkin Elmer, UK).

Lyophilization of the final pure products was performed using an Alpha 2-4 LD2 freeze-drier (Christ, Germany).

3.3.2.2 Reversed-phase high performance liquid chromatography

Reversed-phase high performance liquid chromatography was carried out using two different systems:

1. a Waters Alliance 2690 Separations Module (Waters Corp., MA, USA) including an Alliance pump and autosampler connected to an Agilent 1100 Series UV detector (Agilent Technologies, CA, USA) and a PL-ELS 1000 evaporative light-scattering detector (EL-SD) (Polymer Laboratories, UK). The column was eluted at 30 °C. The UV detector was set at 220 nm. The parameters for the EL-SD detector were set as follows: nebuliser 80 °C, evaporator 90 °C, gas flow (N₂) 1.5 l/min. The system was controlled by GPC-7 software (Polymer Laboratories, UK).
2. a Kontron 500 HPLC System (Kontron Instruments, Italy) comprising a Kontron Bio-Tek 522 dual solvent pump, a Kontron HPLC 560 autosampler, a Kontron degasser 3493, a Kontron HPLC 535 dual wavelength UV detector and a PL-ELS 2100 EL-SD (Polymer Laboratories, UK). The column was eluted at 30 °C. The UV detector was set at 220 and 254 nm. The parameters for the EL-SD detector were set as follows: nebuliser 70 °C, evaporator 40 °C, gas flow (N₂) 1 l/min. The system was controlled by Geminix software (Goebel-Instrumentelle Analytik, Germany).

Analytical RP-HPLC was performed on a C₁₂ Proteo Jupiter column (250 x 4.6 mm, 4 µm particle size, 90 Å pore size) (Phenomenex, CA, USA). The purification of the synthesised

products was carried out using a semi-preparative C₁₂ Proteo Jupiter column (250 x 10 mm, 10 µm particle size, 90 Å pore size) (Phenomenex, CA, USA).

3.3.2.3 Electrospray ionisation mass spectrometry

Electrospray ionisation mass spectrometry was performed on the crude peptides and on the pure peptides so as to confirm the mass and the purity of the synthesised compounds. The spectrometer used was a Waters Micromass Q-TOF Ultima API (Waters Corp., MA, USA) fitted with an electrospray source. Peptides were analysed in the positive mode. The parameters for the analysis were set as follows: capillary voltage 3.5 kV, cone voltage 35 kV, source 100 °C, desolvation temperature 350 °C, desolvation gas 400 l/h, cone gas 50 l/h.

3.4 Experimental methods

3.4.1 Preparation of solvents

Solvents employed in solid-phase peptide synthesis were distilled before use and stored in different ways according to the guidelines given in Table 3.3. Solvents not listed in this table were bought of the highest quality commercially available and used without further purification.

Tab. 3.3: Distillation and storage of solvents used for SPPS

<i>SOLVENT</i>	<i>AGENT</i>	<i>BOILING POINT (°C)</i>	<i>CONDITIONS</i>	<i>STORAGE</i>
DMF	Ninhydrin (100 mg/l)	153	Vacuum	4 Å ms, dark bottle
Pyridine	KOH (20 g/l) [∞]	115	N ₂ or Ar	3 Å ms, dark bottle
Piperidine	KOH (20 g/l)	106	N ₂ or Ar	Dark bottle
DCM	CaCl ₂	40	N ₂	/
Acetic anhydride	/	139-140	N ₂	Used immediately
Diethyl ether	P ₂ O ₅	34.5	N ₂	/

ms = molecular sieves

3.4.2 Peptide synthesis

Peptides were synthesised at room temperature (RT) by manual solid-phase peptide synthesis, applying the Fmoc protocol to the shake-flask method (Fig. 3.11) (Chan and White, 2000b).

[∞] Pyridine was kept on KOH (20 g/l) for a few days before the distillation.

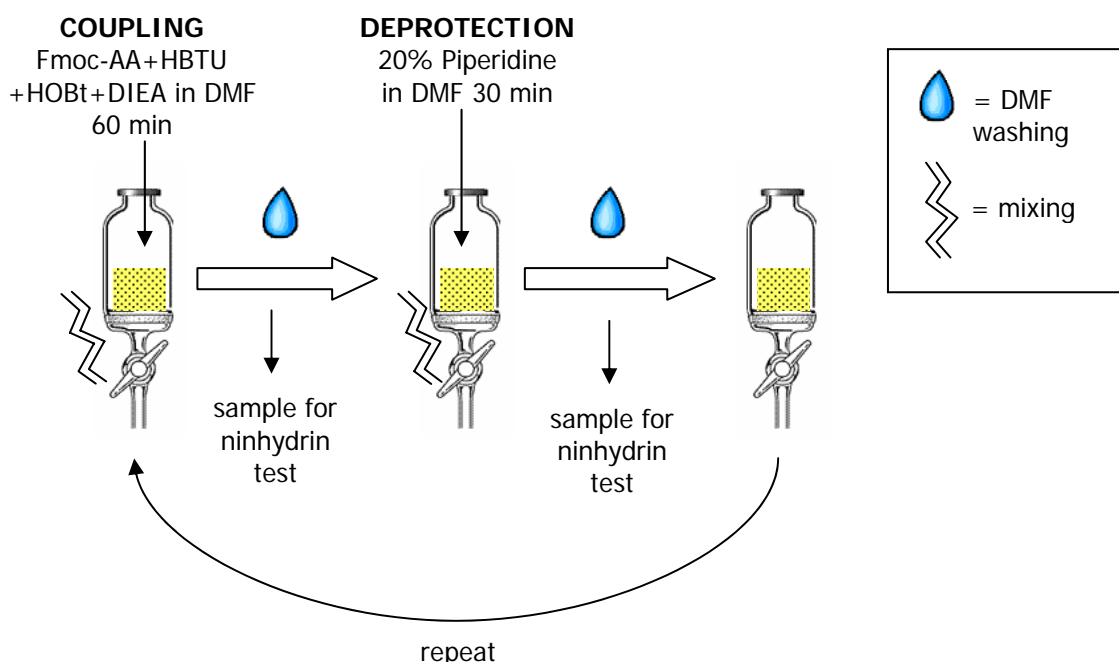


Fig. 3.11: Shake-flask method used for manual solid-phase peptide synthesis.

3.4.2.1 Attachment of the first amino acid

435 mg (0.1 mmol) of Novasyn TGR resin (for the synthesis of peptide amides) or 300 mg (0.075 mmol) Novasyn TGA resin (for the synthesis of peptide acids) was swollen in DMF (20 ml/g) for 30 minutes. The first amino acid (5 eq.)[#] was loaded on the resin using PyBOP[®] (5 eq.), HOBt (5 eq.) and DIEA (10 eq.). The reaction was left to proceed for 4–6 h.

358 mg (0.075 mmol) of Novasyn TGA-Fmoc-Lys(Boc)-OH (pre-loaded resin for the synthesis of peptide acids) were used. The resin was swollen in DMF and then deprotected with piperidine (see Section 3.3.2.4) before proceeding to the elongation step.

3.4.2.2 Capping

After the attachment of the first amino acid, possible free hydroxyl groups on the resin were treated with acetic anhydride (20% v/v in DMF) so as to prevent the growth of incorrect peptide chains. The resin was treated for 20 minutes with the abovementioned mixture and then washed with DMF (15 times, 10 ml/g of resin).

3.4.2.3 Elongation of the peptide chain

Fmoc-amino acids were loaded on the resin using a three times molar excess. HBTU (3 eq.) was used as coupling reagent as a cost-effective alternative to PyBOP[®] (Rautenbach, 1999). HOBt (3 eq.) and DIEA (6 eq.) were also used.

[#] Equivalentents were calculated considering the resin loading capacity.

All the reagents were mixed together using a small amount of DMF (< 1.5 ml) to activate the carboxyl group of the incoming Fmoc-AA and then added to the unprotected growing peptide. The reaction usually lasted for 60 minutes. The completion of the reaction was monitored by performing a ninhydrin test (see Section 3.4.2.6).

Reagents were removed by washing the resin with DMF (15 times, 10 ml/g of resin).

3.4.2.4 Deprotection of the attached Fmoc-amino acid

For the selective removal of Fmoc groups from the attached amino acids a 20% (v/v) piperidine solution in DMF was used. The reaction was left to proceed for 30-45 minutes. The resin was then washed with DMF (24 times, 10 ml/g of resin) so as to remove the excess of piperidine.

3.4.2.5 Cleavage of the peptide from the resin

After the last coupling/deprotection cycle the resin was washed with DMF and prepared for the final cleavage of the peptide. Traces of DMF can interfere with the acid cleavage (Chan and White, 2000b; Novabiochem, 2004), therefore, the resin was washed with different solvents: distilled DCM (20 ml/g of resin), t-amyl alcohol (10 ml/g of resin), glacial acetic acid (10 ml/g of resin), t-amyl alcohol (10 ml/g of resin) and finally with distilled diethyl ether (20 ml/g of resin). It was then dried under vacuum for 4-6 hours, using potassium hydroxide and phosphorous pentoxide as drying agents (Novabiochem, 2004).

The peptide was cleaved from the resin using a solution of 95% TFA (v/v), 2.5% Milli-Q[®] water (v/v) and 2.5% TIS (v/v) for 3 to 4 hours (Paerson et al., 1989). For those peptides containing tyrosine a solution of 92.5% TFA (v/v), 2.5% Milli-Q[®] water (v/v), 2.5% TIS (v/v) and 2.5% phenol (w/v) was used and the cleavage time was extended to 5-6 hours (King et al., 1990).

The cleavage solution containing the peptide was collected and the resin was washed with TFA (20 ml/g of resin). The solvents of the combined filtrates were evaporated under reduced pressure. The crude peptide was dissolved in analytical grade water and lyophilised.

3.4.2.6 Ninhydrin test

The ninhydrin test (also called Kaiser test) (Kaiser et al., 1970) was used to evaluate the completion of the acylation reaction during the coupling of an amino acid and also to monitor the deprotection step after the removal of the Fmoc group.

Three solutions are required to perform the test:

- A. 1 g of ninhydrin in 20 ml 95% ethanol
- B. 80 g of phenol in 20 ml 95% ethanol
- C. 0.5 ml of 1 mM KCN diluted to 25 ml with distilled pyridine.

A few resin beads were taken after the coupling reaction or after the piperidine deprotection, washed with distilled diethyl ether and air dried. Four drops of each solution were added to the

resin and the mixture was heated for 5 minutes in an 85 °C water bath. In the absence of free amino groups no change in colour was noticed (the solution was slightly yellow and the resin beads were colourless). If free primary amino groups were present (i.e. after the removal of the Fmoc group) the resin beads and the solution turned blue. Resin samples were taken twice in every coupling cycle: after the coupling of the amino acid and after the deprotection. The test had to be negative in the first case and positive in the second one. If not, the coupling reaction or the deprotection (respectively) was repeated.

This reaction is very sensitive for free primary amino groups (about 1 µmol/g resin – 99.5% coupling for resins having a loading capacity of 0.2-0.5 mmol/g) (Albericio and Carpino, 1997).

The Kaiser test was also used for quality control on protected amino acids: few milligrams of amino acid derivative were mixed with the three solutions and heated for 5 minutes in an 85 °C water bath. The reagent was used for peptide synthesis if no colour changes were noticed.

3.4.2.7 Chloranil test

This test was used for the detection of free secondary amino groups (i.e. proline) as chloranil (2,3,5,6-tetrachloro-1,4-benzoquinone) reacts with secondary and primary amines – in presence of acetone or acetaldehyde respectively - to give a green-blue colour on the resin beads (Christensen, 1979; Albericio and Kates, 2000). A few resin beads were taken after the coupling reaction and after the piperidine deprotection, placed in a test tube, washed with distilled diethyl ether and dried. Then, 200 µl of acetone and 50 µl of a saturated solution of chloranil in toluene were added. The beads were shaken manually and turned green-blue if free amino groups were present.

The sensitivity for secondary amines is in the range of 2-5 µmol/g resin (97-99% coupling for resins having a loading capacity of 0.2-0.5 mmol/g) (Albericio and Carpino, 1997).

3.4.2.8 Determination of coupling efficiency

As it has already been described in Section 3.1.2.4, the removal of the Fmoc protecting group leads to the production of a benzofulvene derivative characterised by a high UV absorbance.

The piperidine/DMF mixture used for the deprotection step was collected in a clean flask and the absorbance at 301 nm measured. A solution of 20% piperidine in DMF was used as blank. The millimoles of free Fmoc-derivative, hence the millimoles of free amino groups on the resin, were calculated using the following equation^f:

$$\text{mmol/g} = [(A_{301} / \epsilon_{301}) \times (V / g)] \times 1000 \quad (1)$$

^f Modified from the webpage of the Peptide Synthesis Lab of the University of Trieste (Italy), visit: www.bbcm.units.it/~tossi/PepSynt.htm (last accessed 22/05/04).

Where A_{301} is the absorbance of the sample at 301 nm, ϵ_{301} is the extinction coefficient of the fulvene-piperidine adduct ($7800 \text{ M}^{-1}\text{cm}^{-1}$), V the volume of the sample (ml) and g is the total weight of the resin (g).

3.4.3 Peptide purification

The purification of the synthesised peptides was performed by semi-preparative RP-HPLC using a binary solvent system ($A = 95\% \text{ H}_2\text{O}$, $5\% \text{ ACN}$, $0.1\% \text{ TFA}$ and $B = 95\% \text{ ACN}$, $5\% \text{ H}_2\text{O}$, $0.1\% \text{ TFA}$) with a flow rate of 2.5 ml/min . Semi-preparative column and HPLC systems (No. 2) are described in Section 3.3.2.2. Different solvent gradients were developed so as to achieve an optimal separation for the various peptides as described in Tables 3.4, 3.5 and 3.6.

Tab. 3.4: Gradient A

Time (min)	A (%)	B (%)
0	100	0
5	100	0
30	50	50
35	0	100
40	100	100

Tab. 3.5: Gradient B

Time (min)	A (%)	B (%)
0	100	0
7	100	0
35	60	50
37	30	70
40	30	70
45	100	0

Tab. 3.6: Gradient C

Time (min)	A (%)	B (%)
0	100	0
7	100	0
35	60	40
37	50	50
40	50	50
45	100	0

3.4.4 Analysis of purified peptides

Analytical RP-HPLC was used to assess the purity of the synthesised peptides and to confirm their retention times. A binary solvent system was used ($A = 95\% \text{ H}_2\text{O}$, $5\% \text{ ACN}$, $0.1\% \text{ TFA}$ and $B = 95\% \text{ ACN}$, $5\% \text{ H}_2\text{O}$, $0.1\% \text{ TFA}$) with a flow rate of 1 ml/min . Analytical column and HPLC systems (No. 1 and 2) are described in Section 3.2.2.2. The gradients used for this type of analysis are listed below (Tabs. 3.7 and 3.8).

Tab. 3.7: Gradient C₁

Time (min)	A (%)	B (%)
0	100	0
7	100	0
35	60	40
37	50	50
40	50	50
45	100	0

Tab. 3.8: Gradient H₁

Time (min)	A (%)	B (%)
0	100	0
1	100	0
36	0	100
39	0	100
44	100	0

ESI-MS was also used to characterise the purified peptides and peptide hybrids, confirming the mass and giving indications on the achieved purity (refer to Section 3.3.2.3 for details regarding the ESI-MS).

3.5 Results and discussion

3.5.1 Peptide synthesis

SPPS proved to be an excellent technique for the synthesis of the entire set of peptides, made of small amphiphilic molecules. The chosen activation strategy, using PyBOP[®] (or HBTU) and HOBt/DIEA in DMF, gave fast reactions and high yields. Furthermore, as suggested by literature, the use of benzotriazolyl esters as active species during the coupling reaction implied that the chiral centres maintained their natural configurations (no additional studies were performed in this regard) (Gamet et al., 1984). The coupling/deprotection cycles were followed by the ninhydrin test (or by the chloranil test if proline was present): negative results were obtained after the coupling step and positive ones after the Fmoc deprotection, thus confirming the good elongation of the peptide chain. The measurement of the coupling efficiency - according to formula (1) - was successfully performed, determining the released fulvene-adduct by UV spectroscopy. In general it was in the range of 80-95% per coupling step.

The use of the correct protection scheme permitted cleavage of the resin and removal of the side-chain protecting groups from the protected peptide with the same TFA treatment. During the final TFA cleavage different scavengers were employed: H₂O/TIS was employed for most of the peptides, while H₂O/TIS/phenol for tyrosine-containing peptides. They both gave good results and low amounts of impurities were detected in the analysis performed after the synthesis.

Different quantities were used for the synthesis; these ranged from 0.075 mmol to 0.1 mmol, with an average theoretical yield of between about 65 and 90 mg of pure product. Real yields (calculated after purification) were in the range of 70-95%.

The synthesised peptides and peptides hybrids are listed in the following pages: each one is described by its sequence (three-letter code) and reference name, molecular formula, molecular weight, yield (mg, μ mol and percentage), RP-HPLC retention time and method, purity and mass determination by ESI-MS (expected m/z -values were calculated from the monoisotopic mass of the AA residues present in peptides and peptide hybrids).

H-Lys-Leu-Lys-Leu-Leu-Leu-Lys-Leu-Lys-NH₂ (L3)

C₅₄H₁₀₆N₁₄O₉ (1095.81 g/mol)

Yield: *

HPLC analytical (Method H₁): t_R = 28.26 min

Purity HPLC (%): 98

ESI-MS monoisotopic *m/z*: Calculated: 1095.83 [M+H]⁺
 Found: 1095.80 [M+H]⁺

H-Lys-Leu-Lys-Leu-Leu-Leu-Leu-Lys-Leu-Lys-NH₂ (L4)

C₆₀H₁₁₇N₁₅O₁₀ (1208.67 g/mol)

Yield: *

HPLC analytical (Method H₁): t_R = 28.20 min

Purity HPLC (%): 99

ESI-MS monoisotopic *m/z*: Calculated: 1208.92 [M+H]⁺
 Found: 1208.90 [M+H]⁺

H-Lys-Leu-Lys-Leu-Leu-Leu-Leu-Leu-Lys-Leu-Lys-NH₂ (L5)

C₆₆H₁₂₈N₁₆O₁₁ (1321.82 g/mol)

Yield: *

HPLC analytical (Method H₁): t_R = 27.98 min

Purity HPLC (%): 99

ESI-MS monoisotopic *m/z*: Calculated: 1322.00 [M+H]⁺
 Found: 1322.00 [M+H]⁺

H-Lys-Leu-Lys-6-Ahx-Lys-Leu-Lys-OH (KL1)

C₄₂H₈₃N₁₁O₈ (870.18 g/mol)

Yield: 50 mg, 57 μmol (72%)

HPLC analytical (Method C₁): t_R = 24.67 min

Purity HPLC (%): 99

ESI-MS monoisotopic *m/z*: Calculated: 870.65 [M+H]⁺
 Found: 870.51[M+H]⁺

H-Lys-Leu-Lys-9-Anc-Lys-Leu-Lys-OH (KL2)

C₄₅H₈₉N₁₁O₈ (912.26 g/mol)

Yield: 45 mg, 49 μmol (75%)

* Received from Dr M Rautenbach as crude peptides.

HPLC analytical (Method C₁): t_R = 21.29 min

Purity HPLC (%): 99

ESI-MS monoisotopic *m/z*: Calculated: 912.70 [M+H]⁺

Found: 912.63 [M+H]⁺

H-Lys-Leu-Lys-6-Ahx-Lys-Leu-Lys-NH₂ (KL3)

C₄₂H₈₄N₁₂O₇ (869.19 g/mol)

Yield: 82 mg, 94 μmol (95%)

HPLC analytical (Method C₁): t_R = 23.30 min

Purity HPLC (%): 98

ESI-MS monoisotopic *m/z*: Calculated: 869.67 [M+H]⁺

Found: 869.64 [M+H]⁺

H-Lys-Leu-Lys-9-Anc-Lys-Leu-Lys-NH₂ (KL4)

C₄₅H₉₀N₁₂O₇ (911.27 g/mol)

Yield: 51 mg, 56 μmol (67%)

HPLC analytical (Method C₁): t_R = 26.00 min

Purity HPLC (%): 97

ESI-MS monoisotopic *m/z*: Calculated: 911.71 [M+H]⁺

Found: 911.32 [M+H]⁺

H-Orn-Leu-Orn-9-Anc-Orn-Leu-Orn-NH₂ (OL1)

C₄₁H₈₂N₁₂O₇ (855.17 g/mol)

Yield: 59 mg, 69 μmol (75%)

HPLC analytical (Method C₁): t_R = 23.88 min

Purity HPLC (%): 98

ESI-MS monoisotopic *m/z*: Calculated: 855.65 [M+H]⁺

Found: 855.56 [M+H]⁺

H-Orn-Leu-Orn-Gly-Pro-Gly-Orn-Leu-Orn-NH₂ (OL2)

C₄₁H₇₈N₁₄O₉ (911.15 g/mol)

Yield: 62 mg, 68 μmol (94%)

HPLC analytical (Method C₁): t_R = 20.31 min

Purity HPLC (%): 96

ESI-MS monoisotopic *m/z*: Calculated: 911.62 [M+H]⁺

Found: 911.52 [M+H]⁺

H-Orn-Tyr-Orn-9-Anc-Orn-Tyr-Orn-NH₂ (OY1)

C₄₇H₇₈N₁₂O₉ (955.20 g/mol)

Yield: 77 mg, 81 μmol (89%)

HPLC analytical (Method C₁): t_R = 21.43 min

Purity HPLC (%): 99

ESI-MS monoisotopic *m/z*: Calculated: 955.61 [M+H]⁺
 Found: 955.61 [M+H]⁺

H-Orn-Tyr-Orn-Gly-Pro-Gly-Orn-Tyr-Orn-NH₂ (OY2)

C₄₇H₇₄N₁₄O₁₁ (1011.18 g/mol)

Yield: 62 mg, 61 μmol (77%)

HPLC analytical (Method C₁): t_R = 17.33 min

Purity HPLC (%): 99

ESI-MS monoisotopic *m/z*: Calculated: 1011.57 [M+H]⁺
 Found: 1011.52 [M+H]⁺

H-Leu-Orn-Leu-9-Anc-Leu-Orn-Leu-NH₂ (LO1)

C₄₃H₈₄N₁₀O₇ (853.19 g/mol)

Yield: 60 mg, 70 μmol (83%)

HPLC analytical (Method H₁): t_R = 17.70 min

Purity HPLC (%): 100

ESI-MS monoisotopic *m/z*: Calculated: 853.66 [M+H]⁺
 Found: 853.64 [M+H]⁺

H-Leu-Tyr-Leu-9-Anc-Leu-Tyr-Leu-NH₂ (LY1)

C₅₁H₈₂N₈O₉ (951.24 g/mol)

Yield: 77 mg, 81 μmol (91%)

HPLC analytical (Method H₁): t_R = 22.11 min

Purity HPLC (%): 99

ESI-MS monoisotopic *m/z*: Calculated: 951.63 [M+H]⁺
 Found: 951.60 [M+H]⁺

3.5.2 Peptide purification and analysis

The standard purification procedure which includes the diethyl ether precipitation was shown to be inappropriate for the purification of these short amphiphilic peptides (personal communication from Dr Rautenbach). RP-HPLC was hence the method of choice both for analysis and purification of the peptides (Mant et al., 1997). Two different RP-HPLC systems were used for

the analysis of crude and purified peptides (see Section 3.2.2.2 for details). Consistency and reproducibility were showed throughout the various analyses and the use of a C₁₂ column - both for analytical and semi-preparative RP-HPLC - appeared to be a good choice for the separation of these short amphiphilic compounds.

Crude peptides were analysed on different gradients so as to evaluate the best elution conditions for an optimal separation. Gradient C (see Section 3.3.3 for details) was widely used because of the very slow increase in the acetonitrile concentration (from 0 to 40% over 28 minutes) leading to a fast elution of water soluble impurities, better interaction of the peptides with the column and therefore a better separation.

The good protocol followed for the SPPS, the purity of the solvents and the good quality of the chemicals were important elements for synthesizing pure molecules. Pure peptides were synthesised as confirmed by analytical RP-HPLC on crude samples. The use of an EL-SD coupled to the chromatography system was revealed to be an excellent tool for the quantitative detection of impurities regardless of their UV absorbance (Fig. 3.12, A and B).

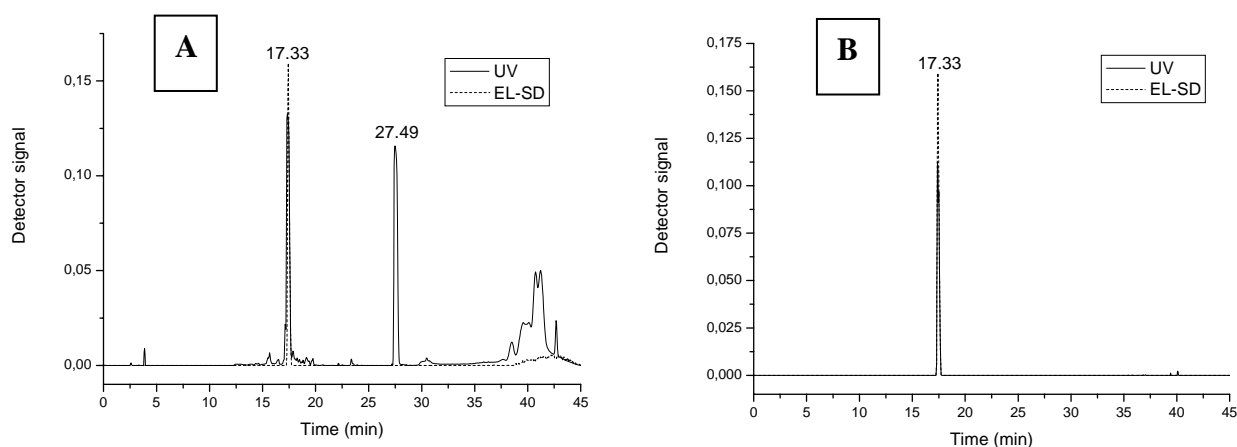


Fig. 3.12: A) RP-HPLC chromatogram of crude OY2 on system 1 (C₁₂ column) eluted with gradient C. Note the difference between the signal of the UV detector and the one from the EL-SD (refer to Section 3.2.2.2 for details about UV/EL-SD settings). B) RP-HPLC chromatogram of pure OY2 (same conditions).

Semi-preparative RP-HPLC was successfully carried out for the purification of the bolaamphiphilic peptides and hybrids thereof (Fig. 3.13). Good separation of the desired peptides was achieved. Two different gradients were employed for the peptides' purifications, taking into account the diverse amino acid composition and the difference in lipophilicity among the synthesised molecules. Gradient C was used for more hydrophilic peptides (KL1, KL2, KL3, KL4, OL1, OL2, OY1, OY2) while gradient B was employed for the purification of more lipophilic peptides (L3, L4, L5, LO1, LY1). The two gradients present different increases in the concentration of the organic modifier, reaching a higher value in gradient B (70%) and a lower value in gradient

C (50%). Purified peptides were further analysed by analytical RP-HPLC for assessing the achieved purity, which was determined to be greater than 96%.

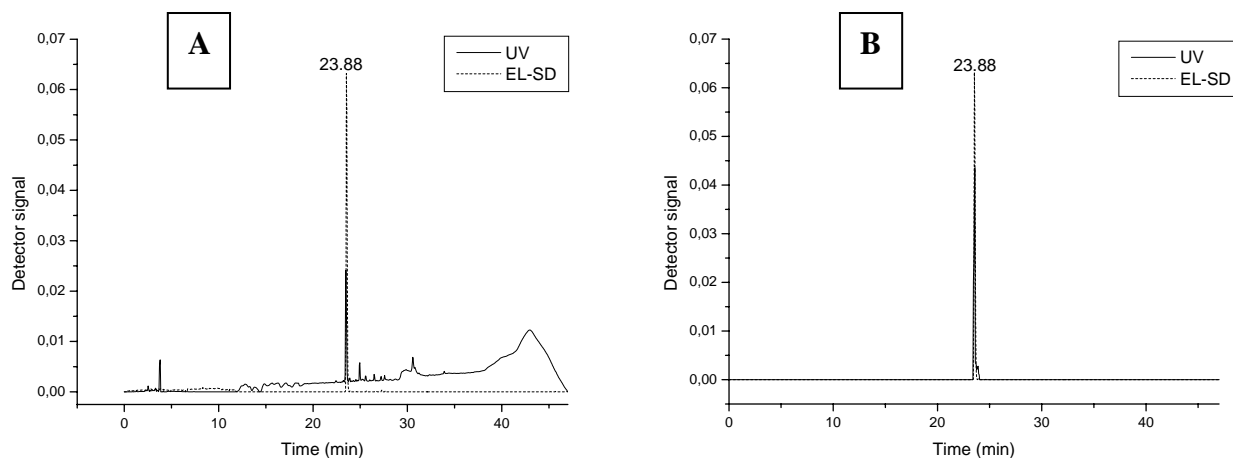


Fig. 3.13: RP-HPLC chromatogram of crude OL1 on system 1 (C_{12} column) eluted with gradient C. B) RP-HPLC chromatogram of pure OL1 (same conditions).

ESI-MS was used directly after the synthesis to confirm the presence of the desired peptide in the crude mixture and to give a first indication on the quality of the synthesis (Burdick and Stults, 1997) (Fig. 3.14).

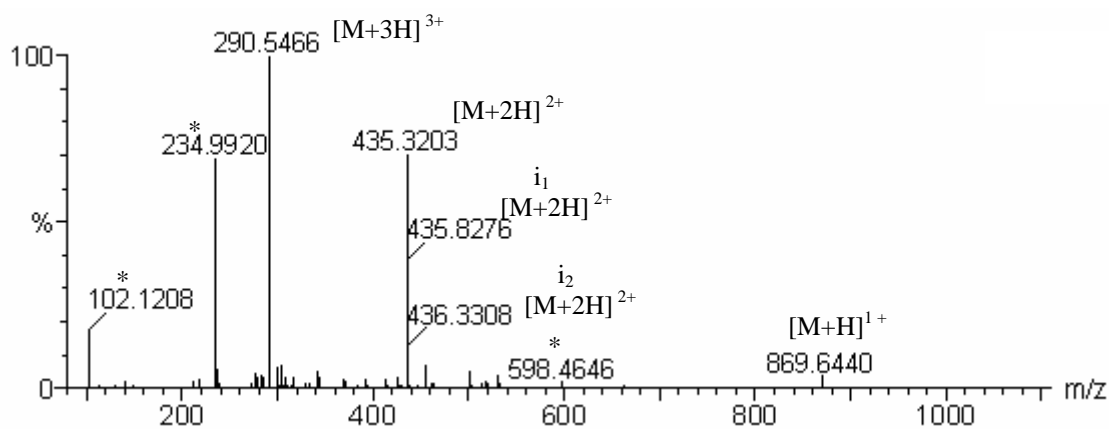


Fig. 3.14: ESI-MS spectrum of crude KL3. Isotope variations are marked by i_1 , i_2 and i_3 corresponding to m/z -values with 1, 2 or 3 amu higher than the mass calculated from the monoisotopic residue mass (unknown fragments are indicated by *).

Mass analysis on crude peptides revealed the presence of contaminants, mostly including deaminated peptides, dimers (Figs. 3.15 and 3.16) (Smith and Light-Wahl, 1993; Loo, 2000) and sodium salts (Fig. 3.17). Mass spectra of the remaining crude compounds are reported in Appendix B. In no cases was the presence of the Fmoc/Boc-protected peptides revealed, thus confirming the successful deprotection of the amino group on the last amino acid and the removal of side-chains protecting groups by TFA cleavage.

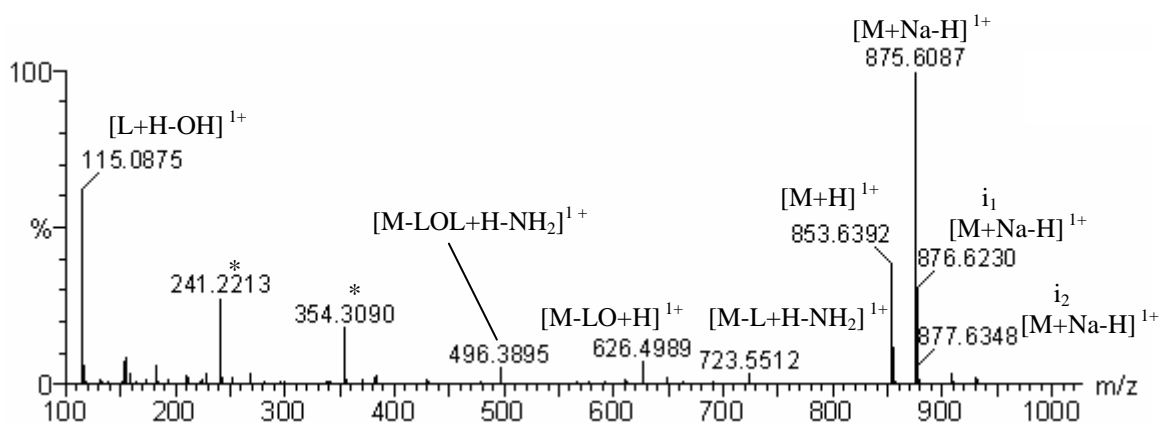


Fig. 3.15: ESI-MS spectrum of crude LO1. Isotope variations are marked by i_1 , i_2 and i_3 corresponding to m/z -values with 1, 2 or 3 amu higher than the mass calculated from the monoisotopic residue mass (unknown fragments are indicated by *).

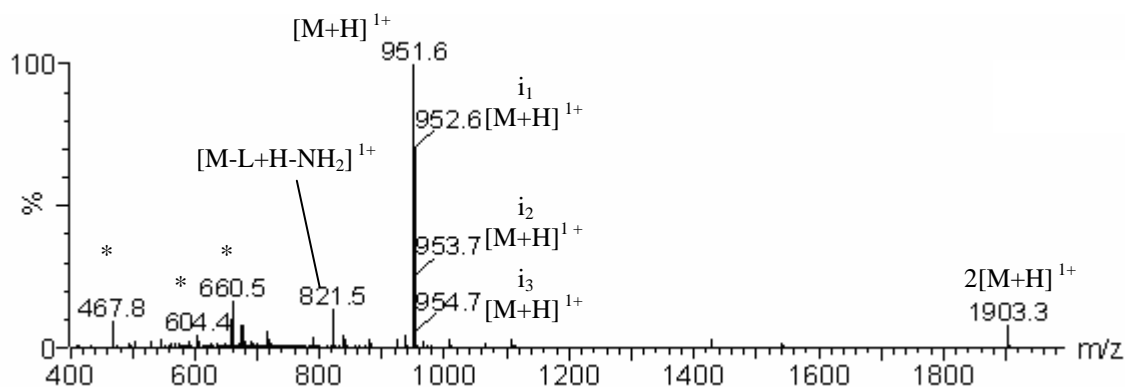


Fig. 3.16: ESI-MS spectrum of crude LY1. Isotope variations are marked by i_1 , i_2 and i_3 corresponding to m/z -values with 1, 2 or 3 amu higher than the mass calculated from the monoisotopic residue mass (unknown fragments are indicated by *).

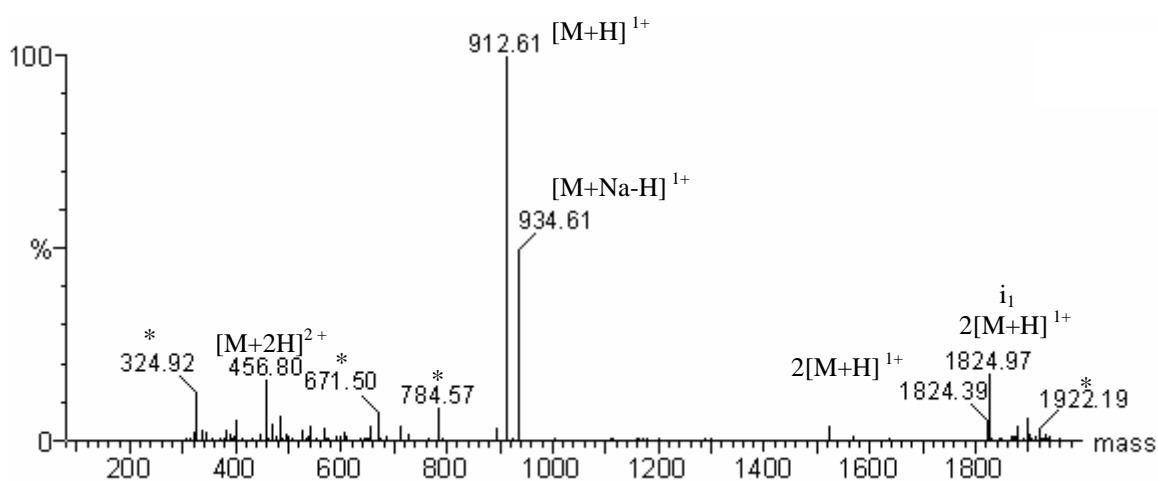


Fig. 3.17: ESI-MS spectrum of crude KL2. Isotope variations are marked by i_1 , i_2 and i_3 corresponding to m/z -values with 1, 2 or 3 amu higher than the mass calculated from the monoisotopic residue mass (unknown fragments are indicated by *).

ESI-MS determination was then repeated after semi-preparative RP-HPLC purification to confirm the mass of the purified peptide and assess its purity (Fig. 3.18).

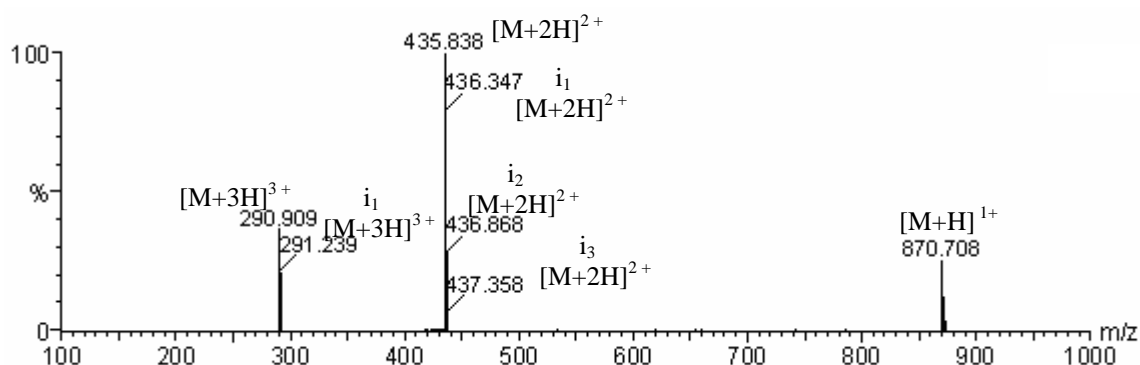


Fig. 3.18: ESI-MS spectrum of pure KL1. Isotope variations are marked by i_1 , i_2 and i_3 corresponding to m/z -values with 1, 2 or 3 amu higher than the mass calculated from the monoisotopic residue mass.

3.6 Conclusions

The designed library of peptides and peptide hybrids was successfully synthesised using a solid-phase approach based on the Fmoc protocol and performed manually with a shake flask procedure. The total yields after purification were generally between 70 and 95%.

SPPS produced quite pure molecules but the entire set of compounds was nonetheless purified by RP-HPLC to achieve a purity greater than 96% (as subsequently determined by RP-HPLC coupled to an EL-SD). This choice was made considering the sensitivity of biological studies (antimicrobial properties, haemolytic activity, interactions with liposomes) and structural characterisation (fluorescence, infrared, circular dichroism) later performed on the same set of peptides.

For each pure peptide, ESI-MS analysis confirmed the presence of the expected mass and also proved the purity of the final products.

3.7 References

- Angell YM, Alsina J, Albericio F and Barany G (2002) Practical protocols for stepwise solid-phase synthesis of cysteine-containing peptides, *Journal of Peptide Research*, 60, 292-299.
- Albericio F and Carpino LA (1997) Coupling reagents and activation, *Methods in Enzymology*, 289, 104-126.
- Albericio F, Bofill JM, El-Faham A and Kates SA (1998) Use of onium salt-based coupling reagents in peptide synthesis, *Journal of Organic Chemistry*, 63, 9678-9683.
- Albericio F and Kates SA (2000) Coupling methods: solid-phase formation of amide and ester bonds, in Kates SA and Albericio F (Eds.) *Solid-phase synthesis. A practical guide*, (pp. 275-330) Marcel Dekker; New York.
- Alvarez-Bravo J, Kurata S and Natori S (1994) Novel synthetic peptides effective against methicillin-resistant *Staphylococcus aureus*, *Biochemical Journal*, 302, 535-538.
- Anzai K, Hamasuna M, Kadono H, Lee S, Aoyagi H and Kirino Y (1991) Formation of ion channels in planar lipid bilayer membranes by synthetic basic peptides, *Biochimica et Biophysica Acta*, 1064, 256-266.
- Atherton E, Cameron LR and Sheppard RC (1988) Peptide synthesis: Part 10. Use of pentafluorophenyl esters of fluorenylmethoxycarbonylamino acids in solid-phase peptide synthesis, *Tetrahedron*, 44, 843-857.
- Atherton E, Gait MJ, Sheppard RC, Williams BJ (1979) The polyamide method of solid-phase peptide and oligonucleotide synthesis, *Bioorganic Chemistry*, 8, 351-370.
- Atherton E and Sheppard RC (1989) *Solid-phase synthesis: a practical approach*, IRL at Oxford University Press; Oxford.
- Bailey PD (1990) Synthesis, in Bailey PD (Ed.) *An introduction to peptide chemistry* (pp. 114-151), Wiley; Chichester.
- Bayer E (1991) Towards the chemical synthesis of proteins, *Angewandte Chemie, International Edition in English*, 30, 113-129.
- Benoiton NL, Lee YC, Steinaur R and Chen FM (1992) Studies on sensitivity to racemization of activated residues in couplings of N-benzyloxycarbonyldipeptides, *International Journal of Peptide and Protein Research*, 40, 559-566.
- Béven L, Castano S, Dufourcq J, Wieslander Å and Wróblewski (2003) The antibiotic activity of cationic linear amphipathic peptides: lessons from the action of leucine/lysine copolymers on bacteria of the class *Mollicutes*, *European Journal of Biochemistry*, 270, 2207-2217.
- Burdick DJ and Stults JT (1997) Analysis of peptide synthesis products by electrospray ionization mass spectrometry, *Methods in Enzymology*, 289, 499-519.
- Carpino LA and Han GY (1970) The 9-Fluorenylmethoxycarbonyl function, a new base sensitive amino-protecting group, *Journal of the American Chemical Society*, 92, 5748-5749.
- Carpino LA and Han GY (1972) The 9-Fluorenylmethoxycarbonyl amino-protecting group, *Journal of Organic Chemistry*, 37, 3404-3409.

Carpino LA, Sadat-Aalae D, Chao HG, DeSelms RH (1990) [(9-Fluorenylmethyl)oxy]carbonyl (Fmoc) amino acid fluorides. Convenient new peptide coupling reagents applicable to the Fmoc/tert-butyl strategy for solution and solid-phase syntheses, *Journal of the American Chemical Society*, 112, 9651-9652.

Chan WC and White PD (2000a) Basic principles, in Chan WC and White PD (Eds.), *Fmoc solid-phase peptide synthesis: a practical approach* (pp. 9-40), in The practical approach series (Series Ed. Hames BD), Oxford University Press; New York.

Chan WC and White PD (2000b) Basic procedures, in Chan WC and White PD (Eds.), *Fmoc solid-phase peptide synthesis: a practical approach* (pp. 41-76), in The practical approach series (Series Ed. Hames BD), Oxford University Press; New York.

Christensen T (1979) A qualitative test for monitoring coupling completeness in solid-phase peptide synthesis using chloranil, *Acta Chemica Scandinavica*, 33B, 763-766.

Dick F (1997) Acid cleavage/deprotection in Fmoc/tBu solid-phase peptide synthesis, in Pennington MW and Dunn BM (Eds.) *Peptide synthesis protocols* (pp. 63-72), in Methods in molecular biology (Series Ed. Walker JM), Humana Press; Totowa.

Fields CG (1991) HBTU activation for automated Fmoc solid-phase peptide synthesis, *Peptide Research*, 4, 95-101.

Fields GB (1997) Methods for removing the Fmoc group, in Pennington MW and Dunn BM (Eds.) *Peptide synthesis protocols* (pp. 17-28), in Methods in molecular biology (Series Ed. Walker JM), Humana Press; Totowa.

Gamet JP, Jacquier R and Verducci J (1984) Etude de la racemisation induite par la DMAP dans les reactions de couplage peptidique, *Tetrahedron*, 40, 1995-2005.

Guy CA and Fields GB (1997) Trifluoroacetic acid cleavage and deprotection of resin-bound peptides following synthesis by Fmoc chemistry, *Methods in Enzymology*, 289, 67-83.

Hirakura Y, Alvarez-Bravo J, Kurata S, Natori S and Kirino Y (1996) Selective interaction of synthetic antimicrobial peptides derived from sapecin B with lipid bilayers, *Journal of Biochemistry*, 120, 1130-1140.

Hong SY, Oh JE and Lee KH (1999) Effect of D-amino acid substitution on the stability, the secondary structure and the activity of membrane-active peptide, *Biochemical Pharmacology*, 58, 1775-1780.

Jones J (2002) Solid-phase peptide synthesis, in *Amino acid and peptide synthesis*, Oxford University Press; New York.

Kaiser E, Colescott RL, Bossinger CD and Cook PI (1970) Color test for detection of free terminal amino groups in the solid-phase synthesis of peptides, *Analytical Biochemistry*, 34, 595-598.

Kisfaludy L and Schön I (1980) Preparation and applications of pentafluorophenyl esters of 9-Fluorenylmethoxycarbonyl amino acids for peptide synthesis, *Analytical Biochemistry*, 108, 325-327.

King DS, Fields CG and Fields GB (1990) A cleavage method which minimizes side reactions following Fmoc solid-phase peptide synthesis, *International Journal of Peptide and Protein Research*, 36, 255-266.

- Lee S, Mihara H, Aoyagi H, Kato T, Izumiya N and Yamasaki N (1986) Relationships between antimicrobial activity and amphiphilic property of basic model peptides, *Biochimica et Biophysica Acta*, 862, 211-219.
- Loo JA (2000) Electrospray ionization mass spectrometry: a technology for studying noncovalent macromolecular complexes, *International Journal of Mass Spectrometry*, 200, 175-186.
- Marder O and Albericio F (2003) Industrial application of coupling reagents in peptides, *Chimica Oggi/Chemistry Today*, May/June, 6-11.
- Mant CT, Kondejewski LH, Cachia PJ, Monera OD and Hodges RS (1997) Analysis of synthetic peptides by high-performance liquid chromatography, *Methods in Enzymology*, 289, 426-469.
- Merrifield B (1963) Solid-phase synthesis. I. The synthesis of a tetrapeptide, *Journal of the American Chemical Society*, 85, 2149-2154.
- Merrifield B (1964) Solid-phase synthesis. III. An improved synthesis for bradykinin, *Biochemistry*, 3, 1385-1390.
- Merrifield B (1969) The total synthesis of an enzyme with ribonuclease A activity, *Journal of the American Chemical Society*, 91, 501-502.
- Merrifield B (1997) Concept and early development of solid-phase peptide synthesis, *Methods in Enzymology*, 289, 3-13.
- Montalbetti CAGN and Falque V (2005) Amide bond formation and peptide coupling, *Tetrahedron*, 61, 10827-10852.
- Nakajima-Shimada J, Natori S and Aoki T (1998) Effects of synthetic undecapeptides on *Trypanosoma cruzi* in vitro, *Parasitology International*, 47, 203-209.
- Naidoo VB (2004) The supramolecular chemistry of novel synthetic biomacromolecular assemblies, PhD thesis, University of Stellenbosch.
- Novabiochem (2004) Catalogue and Peptide Synthesis Handbook 04/05, 3.15-3.17.
- Paerson DA, Blanchette M, Baker ML and Guindon CA (1989) Trialkylsilanes as scavengers for the trifluoroacetic acid deblocking of protecting groups in peptide synthesis, *Tetrahedron Letters*, 40, 2739-2742.
- Park Y, Lee DG, Jang S-H, Woo E-R, Jeong HG, Choi C-H and Hahm K-S (2003) A Leu-Lys-rich antimicrobial peptide: activity and mechanism, *Biochimica et Biophysica Acta*, 1645, 172-182.
- Pennington MW (1997a) HF cleavage and deprotection procedures for peptides synthesised using a Boc/BZL strategy, in Pennington MW and Dunn BM (Eds.) *Peptide synthesis protocols* (pp. 41-62), in *Methods in molecular biology* (Series Ed. Walker JM), Humana Press; Totowa.
- Pennington MW (1997b) Site-specific chemical modifications procedures, in Pennington MW and Dunn BM (Eds.) *Peptide synthesis protocols* (pp. 171-186), in *Methods in molecular biology* (Series Ed. Walker JM), Humana Press; Totowa.
- Rautenbach M (1999) The synthesis and characterisation of analogues of the antimicrobial peptide Iturin A₂, PhD thesis, Chapter 2, University of Stellenbosch.

Rex S (2000) A Pro→Ala substitution in melittin affects self-association, membrane binding and pore-formation kinetics due to changes in structural and electrostatic properties, *Biophysical Chemistry*, 85, 209-228.

Santoso SS and Zhang S (2004) Self-assembled nanomaterials, in Nalwa HS (Ed.) *Encyclopedia of nanoscience and nanotechnology*, Vol. 9, 459-471. American Scientific Publishers; Stevenson Ranch.

Sheehan JC and Hess GP (1955) A new method of forming peptide bonds, *Journal of the American Chemical Society*, 77, 1067-1068.

Sewald N and Jakubke HD (2002) Fundamental chemical and structural principles, in *Peptides: chemistry and biology* (pp. 5-59), Wiley-VCH; Weinheim.

Sheppard R (2003) The fluorenylmethoxycarbonyl group in solid-phase synthesis, *Journal of Peptide Science*, 9, 545-552.

Shimizu T, Kogiso M and Masuda M (1996) Vesicle assembly into microtubes, *Nature*, 383, 487-488.

Smith RD and Light-Wahl KJ (1993) The observation of non-covalent interactions in solution by electrospray ionization mass spectrometry: Promise, pitfalls and prognosis, *Biological Mass Spectrometry*, 22, 493 – 501

Suenaga M, Lee S, Park NG, Aoyagi H, Kato T, Umeda A and Amako K (1989) Basic amphipathic helical peptides induce destabilization and fusion of acidic and neutral liposomes, *Biochimica et Biophysica Acta*, 981, 143-150.

Wellings DA and Atherton E (1997) Standard Fmoc protocols, *Methods in Enzymology*, 289, 44-67.

Zhang S (2003) Fabrication of novel biomaterials through molecular self-assembly, *Nature Biotechnology*, 21, 1171-1178.

Chapter 4

Self-assembly behaviour and structural characterisation of novel bolaamphiphiles

4.1 Introduction

Nanotechnology is a very recent research field and it is growing in importance year after year. Among the different aspects of nanotechnology, the concept of self-assembly or self-organisation of molecules is extremely important. It is especially significant in the “bottom-up” approach, where functional structures are built at the atomic or molecular level to create functional structures (Zhang, 2003). The reason for this interest lies in the possibility to create nanostructured materials, planned to have certain characteristics, physical properties and shapes that are formed by the autonomous association of small molecules under certain conditions (Zhang and Altman, 1999). Nature provides scientists with many examples of self-organisation processes, from protein folding and unfolding to DNA and RNA expression, from lipid vesicles to membranes formation (Rajagopal and Schneider, 2004). Many efforts have been made in the last decade to mimic these processes and create macroscopic structures starting from single atoms.

The creation of new self-assembling molecules with the ability to give novel and useful supramolecular architectures is the focus of many studies in biomaterials engineering (Zhang, 2003). Moreover, a parallel interest is developing around the molecular mechanisms which regulate and trigger the process. To date, different stimuli have been used to activate the self-assembly, including modifications of pH (Aggeli et al., 2003; Claussen et al., 2003; Niece et al., 2003), ionic strength and metal ions (Matsui and Douberly, 2001), light (Collier et al., 2001) and temperature (Pochan et al., 2003).

In this study the investigation into the self-organisational behaviour of the designed library was carried out by using a multifaceted approach. Different techniques were used to look at the self-assembly process from different points of view. Some of them – such as steady-state fluorescence measurements and Fourier-transform infrared spectroscopy – gave a strong physicochemical perspective to the study of peptide assemblies. Others – such as electron

microscopy (EM), Congo red (CR) staining – were used to investigate the peptide assemblies from a morphological perspective.

4.2 Materials

Peptides were synthesised on solid phase using the Fmoc-polyamide protocol and purified by RP-HPLC as previously described (see Chapter 3).

Pyrene (99%) was supplied by Fluka (Buchs, Switzerland). Congo red (99%) was purchased from Saarchem (Wadeville, South Africa).

Triethylamine (TEA, 99%) and trifluoroethanol (TFE, 99%) were supplied by Aldrich (Steinheim, Germany).

Salts for buffers were provided by Saarchem (Wadeville, South Africa), Fluka (Buchs, Switzerland) and Merck (Darmstadt, Germany).

Analytical grade water was obtained by filtering glass-distilled water with a Millipore Milli Q[®] (Bedford, MA, USA) 0.22- μ m filtering system.

4.3 Experimental methods

4.3.1 Steady-state fluorescence measurements

Peptides were dissolved in pyrene/Milli-Q[®] water or pyrene/Milli-Q[®] water/0.1% TEA at a starting concentration of about 45 mM. Samples were diluted with the same solvent directly inside the cuvette reaching a final concentration of about 1×10^{-3} mM. Sufficient time was allowed between dilutions to permit the samples to reach an equilibrium state. Pyrene emission spectra were recorded in a 10 mm path length ultra-micro quartz cuvette (Hellma, Germany) with a LS50B luminescence spectrometer (Perkin Elmer, UK) fitted with a xenon discharge lamp and controlled by FL WinLab software (Perkin Elmer, UK). The excitation wavelength was set at 334 nm and the emission wavelengths recorded at 373 and 384 nm (I_1 and I_3 respectively). Excitation and emission slits were set at 2.5 nm (Ganesh et al., 2003; Bakshi and Kaur, 2005; Yin et al., 2005). Experiments were carried out in triplicate at 25 °C. The ratio I_1/I_3 was automatically calculated by the software and plotted against the concentration of peptides in solutions. Non-linear regression was performed on the concentration-response data and a sigmoidal fit with variable slope was fitted to every data set. Critical aggregation concentration (CAC) values were extrapolated from the experimental data by calculating the derivative of the sigmoidal fit. The minimum of the derivative was taken as the CAC.

4.3.2 Self-assembly experiments

Self-assembly experiments were carried out under different conditions to evaluate the possibility to enforce or inhibit aggregation. Peptides were dissolved in 0.1% TEA (pH 10) (Naidoo, 2004) at a concentration above their CAC and left undisturbed for up to 15 days. Experiments were performed in glass vials at RT. The process was followed by various techniques (electron microscopy, Congo red staining and optical microscopy).

4.3.3 Congo red staining and optical microscopy

A Congo red staining solution was used to detect the presence of β -sheet structure after an aging period up to 15 days. The solution was prepared by dissolving a saturating amount of CR in 80% absolute ethanol saturated with NaCl. The excess dye was filtered off through a 0.45 μ m filter. The staining was performed by letting 10 μ l of peptide solution air-dry on a microscope slide and then adding 20 μ l of CR staining solution for a few seconds (Nilsson, 2004). The stained samples were air-dried and observed with an Axiolab optical microscope (Zeiss, Germany) equipped with 50x, 100x, 200x magnification lenses and a polarised light source. The microscope was connected to a Sony CCD IRIS colour video camera coupled to a PTR Plus image capturing system. A microscope slide with 10 μ l of stained solvent was used as reference.

4.3.4 Scanning electron microscopy (SEM)

SEM was performed on a Leo S440 scanning electron microscope (Department of Physics, University of Cape Town) with an accelerating voltage of 10 kV. Samples of peptide solutions in 0.1% TEA (concentration above CAC) were freeze-dried to preserve the 3D structure and then fixed on a round (1 cm diameter) metal support using a double-sided carbon tape. The preparations were then sputter-coated with a thin gold/palladium layer.

4.3.5 Cryo-fracture scanning electron microscopy (cryo-SEM)

Cryo-SEM was used to observe frozen aqueous samples. Analyses were performed using a Leo S440 scanning electron microscope (Department of Physics, University of Cape Town) with an accelerating voltage of 5 kV. Samples of peptide solutions in 0.1% TEA (concentration above CAC) were placed in a capillary, frozen in liquid N₂, and then the capillary was broken to create a fracture.

4.3.6 Fourier-transform photoacoustic infrared spectroscopy

FT-IR analyses were carried out on a Paragon 1000 spectrometer (Perkin Elmer, UK) fitted with a MTEC 300 photoacoustic detector and controlled by Spectrum 1.00 software (Perkin Elmer, UK). Peptides were dissolved in 0.1% TEA (above their CAC), left undisturbed for sufficient time

to reach an equilibrium state and freeze-dried directly into an aluminium sample holder. Emission spectra were recorded between 4500 and 500 cm^{-1} . For each spectrum 128 interferograms were co-added. Spectra in the amide I region were deconvolved by Spectrum 1.00 software (Perkin Elmer, UK).

4.3.7 Circular dichroism spectroscopy

Circular dichroism was performed on a Jasco J-810 spectrophotometer (Molecular and Cellular Biology, University of Cape Town). CD spectra were recorded in a 2 mm path length quartz cell at 25 °C. Each sample was scanned five times at a scan speed of 100 nm/min, with a band width of 2 nm and a response time of 1 s over the wavelength range 180-260 nm. Peptides were analysed at different concentrations, above and below their CAC. Peptides were dissolved in: (1) 10 mM phosphate buffer pH 6.8, (2) 50% TFE/50% 20 mM phosphate buffer pH 6.8 and (3) 0.1% TEA (pH 10) (Naidoo, 2004). Buffers were filtered through a 0.45 μm filter

Scans were repeated after twelve days to monitor the effect of aging on the aggregation process. Samples were left at RT during this period.

4.4 Results and discussion

4.4.1 Steady-state fluorescence measurements

Fluorescence spectroscopy combined with a fluorescent probe is a technique commonly applied to the determination of the critical micelle concentration (CMC) of surfactants and can also be used to resolve the critical aggregation concentration of aggregating molecules, such as peptide bolaamphiphiles (Ganesh et al., 2003). Many different fluorescent probes can be used but the most diffuse is pyrene, which is very hydrophobic and has a solubility in water of 3.9×10^{-7} mol/l at 25 °C (Ninomiya et al., 2003). The relative intensity of each peak composing its fluorescence spectrum depends strongly on the polarity of the microenvironment. In the presence of micelles and other macromolecular assemblies, the pyrene molecule is preferentially solubilised in the interior hydrophobic regions of these aggregates. This characteristic can be used to monitor modifications in the aggregation status of a certain molecule. As shown below (Fig. 4.1), the relative intensity of the third band (I_3 , at 384 nm) increases with an increased polarity of the environment (i.e. aggregated molecules, curve B) while a diminished effect is seen on the relative intensity of the first band (I_1 , at 373 nm). The ratio I_1/I_3 is therefore used to follow the changes in environmental polarity of aggregating molecules in water, i.e. their status as aggregates or single molecules (Ganesh et al., 2003; Bakshi and Kaur, 2005; Yin et al., 2005).

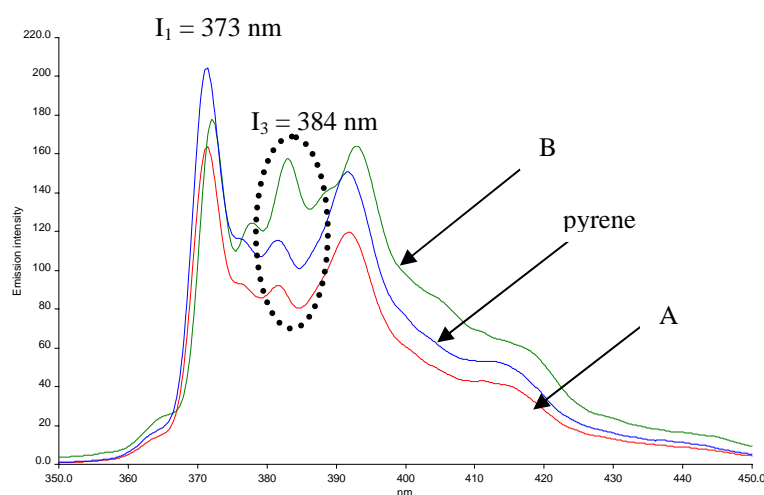


Fig. 4.1: Pyrene fluorescence emission spectra in water, OY1 in 0.1% TEA ($[OY1] < CAC$) [A] and OY1 in 0.1% TEA ($[OY1] > CAC$) [B]. Differences in I_3 intensity are highlighted by the dotted ellipse. $\lambda_{exc} = 334$ nm, emission recorded between 350 and 450 nm on a LS50B Fluorescence Spectrometer (Perkin Elmer, UK), scan speed 500 nm/min.

The CAC values for the synthesised molecules were successfully determined with this technique. The changes of pyrene ratios I_1/I_3 with peptide concentration were followed both in water and 0.1% TEA (pH 10). Significant differences were found within the series of peptides and peptide hybrids and they were strongly related to the different amino acid compositions (Santoso and Zhang, 2004). Sigmoidal curves were successfully fitted to the concentration-response data sets and a correlation factor (R^2) variable between 0.93 ± 0.01 and 0.99 ± 0.01 was found for each curve. The following graphs show the aggregation behaviour in 0.1% TEA for compounds KL1, KL2, KL3, KL4, OL1, OL2, OY1 and OY2 (Fig. 4.2). Because of the low water solubility of compounds LO1 and LY1, it was not possible to follow their aggregation behaviour under the same conditions. The experiments were carried out using a low starting concentration of peptide bolaamphiphile (about 5 mM) which corresponded to already high I_1/I_3 ratios (~ 1.6), thus precluding the determination of the CAC. The same phenomenon occurred for the study of peptide aggregation in water (pH 7), where the probable CAC was much higher than a technically feasible starting concentration. Only for compounds OY1 and OY2 it was possible to accurately establish the CAC value under both conditions.

A summary of the critical aggregation concentration values for peptides and peptide hybrids in water and 0.1% TEA is reported in Table 4.1.

Tab. 4.1: CAC values (in water and 0.1% TEA) for the synthesised compounds determined by fluorescence spectroscopy using pyrene as fluorescent probe (n.d. = not determined)

REF	CAC ^a (mM)	CAC ^b (0.1% TEA) (mM)
KL1	>45	6.50
KL2	>45	8.16
KL3	>45	5.84
KL4	>45	7.45
OL1	>45	3.30
OL2	>45	7.60
OY1	8.64	0.14
OY2	30.02	2.10
LO1	n.d.	n.d.
LY1	n.d.	n.d.

a: pH 7; b: pH 10

The use of two different environments (pH 7 and 10) permitted to study the aggregation behaviour of the compounds in an effort to understand the conditions that trigger the process. Hence, it was possible to determine how to enforce the aggregation, in this case by simply increasing the pH with an organic base (TEA), and how to inhibit it, by lowering the pH to neutral values (mQ water).

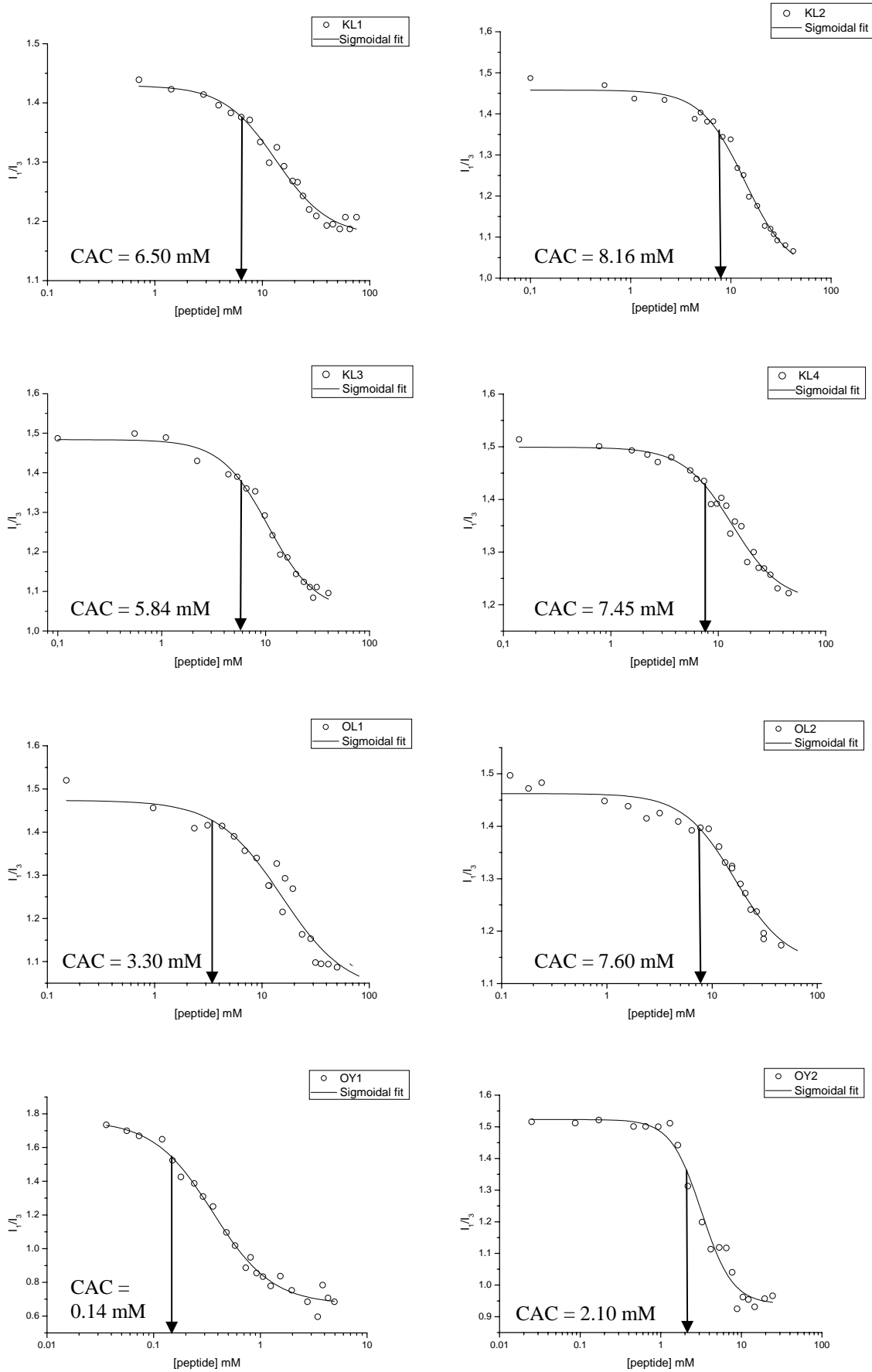


Fig. 4.2: Change of pyrene I_1/I_3 ratios with peptide concentration in 0.1% TEA.
The arrows graphically indicate the CAC values.

Looking at the CAC values it was possible to identify two main classes of parameters which influenced the self-assembly: external parameters (concentration, pH) and internal parameters (three-dimensional structure, amino acid composition).

The concentration of peptides/peptide hybrids in solution was the driving force of the aggregation. All the molecules exhibited higher I_1/I_3 values (i.e. they were present in the aggregated form) at high concentrations than in dilute solutions (Fung et al., 2003; Chen, 2005).

Another important factor which determined the propensity towards aggregation was the pH. Because of the presence of primary amino groups on the side-chains of several AA (such as Orn and Lys), an acidic/neutral pH could be translated into a net positive charge on the molecule. This positive charge could ultimately lead to strong repulsive electrostatic forces, with a resultant high CAC. On the other hand, a basic environment gives a neutral charge on the molecules and facilitates the formation of hydrogen bonds, thus lowering the CAC (Caplan et al., 2000). This tendency is clearly marked by the comparison of the behaviour in water and 0.1% TEA of OY1 and OY2 (Figs. 4.3 and 4.4). For OY1, the shift to higher CAC values is very striking; the CAC in water is more than 60 times greater than in 0.1% TEA (8.64 mM and 0.14 mM respectively). For OY2 the difference is smaller, but there is still a decrease of 15 times in the CAC value going from water to 0.1% TEA (from 30.02 mM to 2.10 mM).

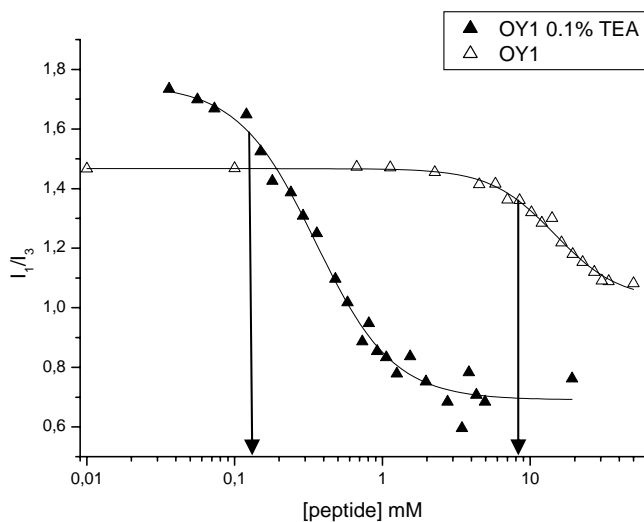


Fig. 4.3: Effect of pH on the aggregation process of OY1.

The arrows graphically indicate the CAC values.

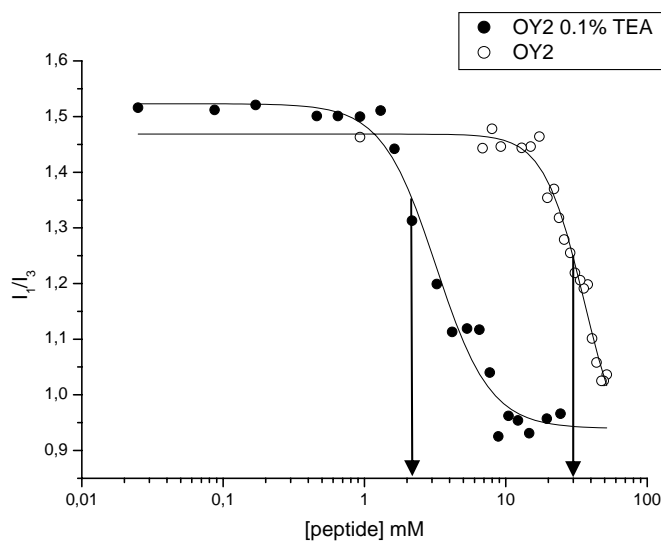


Fig. 4.4: Effect of pH on the aggregation process of OY2.

The arrows graphically indicate the CAC values.

The effect of pH was also considered to be important in the aggregation behaviour of KL1/KL2 and KL3/KL4. These four compounds display a different C terminus functionality, which is acid in the first two and amide in the others. In a basic environment, KL1 and KL2 present negative charges that KL3 and KL4 do not have and they lose the possibility to create intermolecular H bonds at the C terminus. KL1 and KL2 were therefore expected to show higher CAC. Nonetheless, the comparison of the aggregation behaviour of KLx peptides (where x = 1, 2, 3, 4) showed only small differences in the CAC (all comprised between 6 and 8 mM), probably also indicating that the functionality at the C terminus is not a critical factor for the aggregation (Fig. 4.5).

Additionally, the presence of hydrophobic AA (i.e. OY1 and OY2) and the structure of the compounds in solution (i.e. OL2 and OY2) gave other indications of the important parameters that governed the aggregation. Proline strongly influenced the aggregation of the peptides. OY2 and OL2's sequences are similar to the corresponding hybrid peptides OY1 and OL1 except for the presence of the GPG linker between the two charged heads, which is replaced by 9-aminononanoic acid in OY1 and OL1. Nonetheless, they showed a higher CAC than OY1 and OL1 (15 times higher for OY2 and more than twice for OL2). Because of the introduction of a β -turning AA (Pro), the three-dimensional arrangements in solution were altered and molecules were forced into a structure which decreased the possibility of intermolecular interactions. Differences in CAC values and aggregation behaviour of OY1 and OY2, OL1 and OL2 are shown (Figs. 4.6 and 4.7).

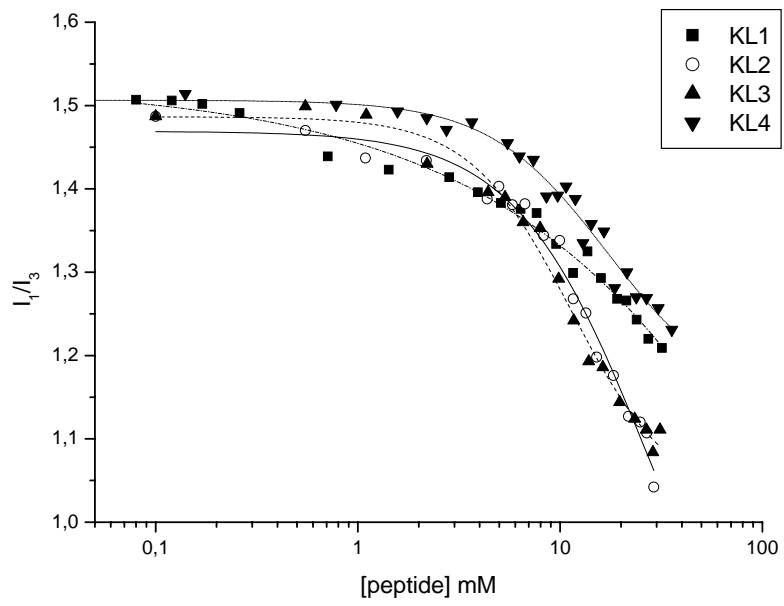


Fig. 4.5: Despite differences in the primary structure KL1, KL2, KL3 and KL4 show a similar behaviour in 0.1% TEA.

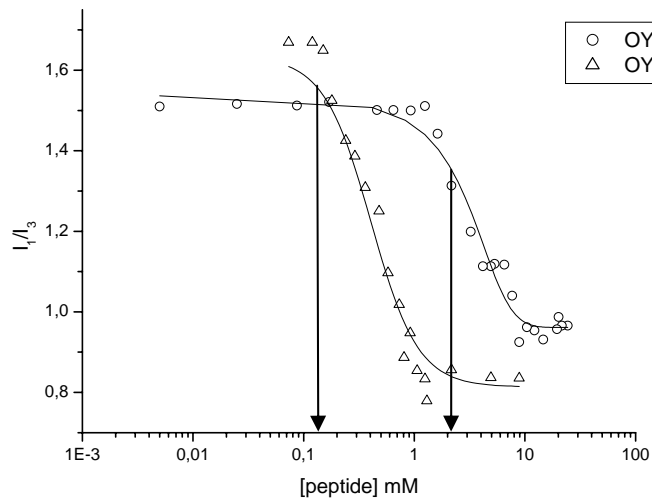


Fig. 4.6: Role of three-dimensional structure on the aggregation behaviour of OY1 and OY2 in 0.1% TEA. The arrows graphically indicate the CAC values.

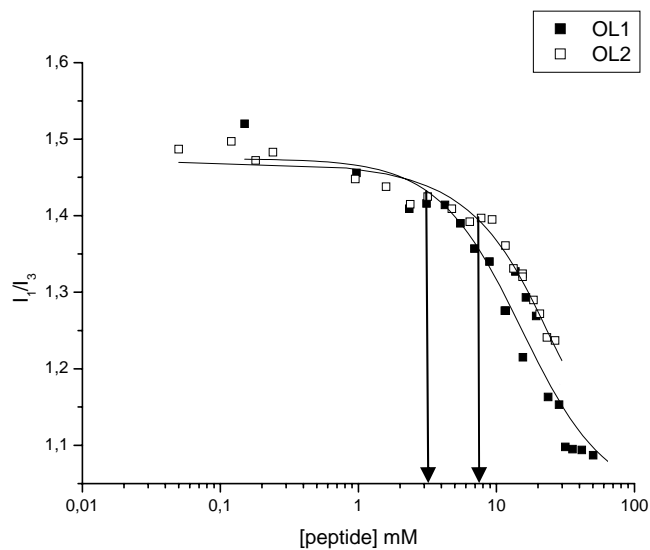


Fig. 4.7: Role of three-dimensional structure on the aggregation behaviour of OL1 and OL2 in 0.1% TEA.
The arrows graphically indicate the CAC values.

As was previously mentioned, the content of hydrophobic AA also affected the aggregation profiles (Zhang et al., 1993; Santoso and Zhang, 2004). Tyrosine-containing compounds aggregated at lower concentrations than the leucine-containing homologues (more than 23 times lower for OY1 and about 4 for OY2) (Figs. 4.8 and 4.9).

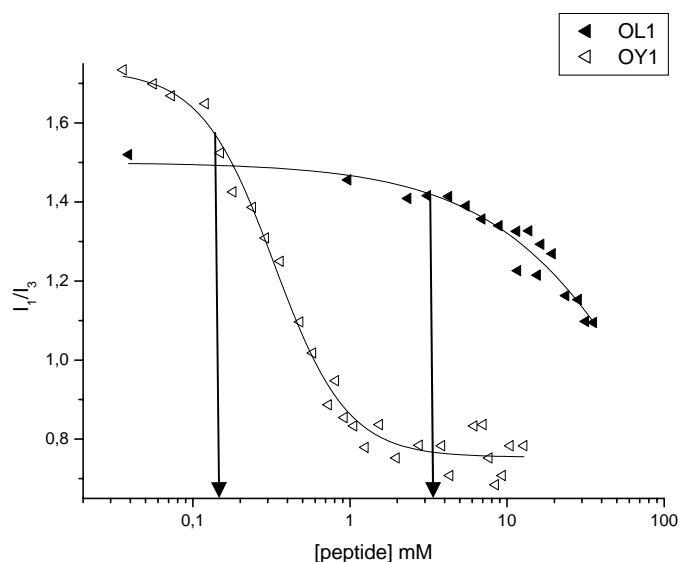


Fig. 4.8: Effect of Leu→Tyr substitution on the aggregation behaviour in 0.1% TEA of OL1 and OY1.
The arrows graphically indicate the CAC values.

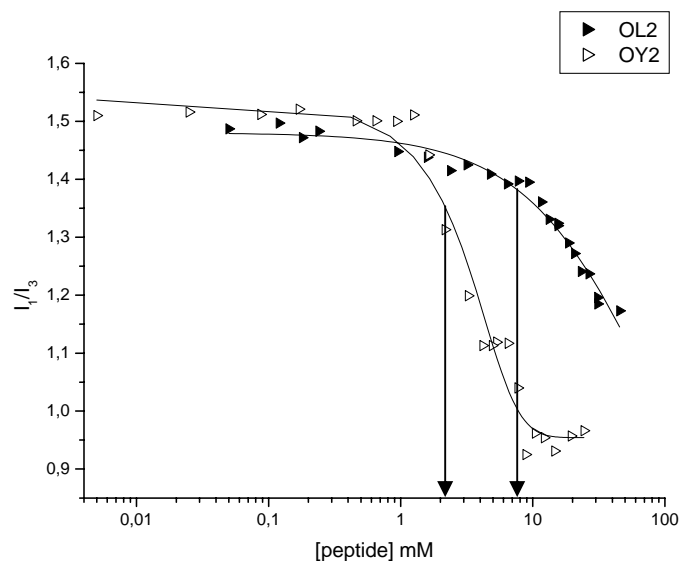


Fig. 4.9: Effect of Leu→Tyr substitution on the aggregation behaviour in 0.1% TEA of OL2 and OY2. The arrows graphically indicate the CAC values.

The use of more hydrophobic AA tends to enhance the self-organisation process of aggregating molecules as hydrophobic interactions are considered one of the driving forces of the process (Wang et al., 2005). This trend was clearly noticed in some of the compounds. OY1 and OY2 are derived from OL1 and OL2 (Leu→Tyr substitution). The presence of a more hydrophobic AA caused a noteworthy decrease in the CAC values because of π -stacking interactions (Caplan et al., 2002; Gazit, 2002).

4.4.2 Self-assembly through microscopy

After the occurrence of aggregation was confirmed by steady-state fluorescence measurements, it was important to study the morphology of such aggregates by using different microscopic tools.

Peptide assemblies were treated with CR and observed with OM. Congo red binds to proteins/peptides assemblies that assume a β -sheet structure and under polarised light they exhibit green birefringence (Nilsson, 2004; Madhavaiah et al., 2005). Peptides assembled into ribbons after 7 days in 0.1% TEA and were detected in the form of red/brown fibres/ribbons. The use of polarised light confirmed the existence of aggregates showing birefringence (Figs. 4.10 and 4.11).

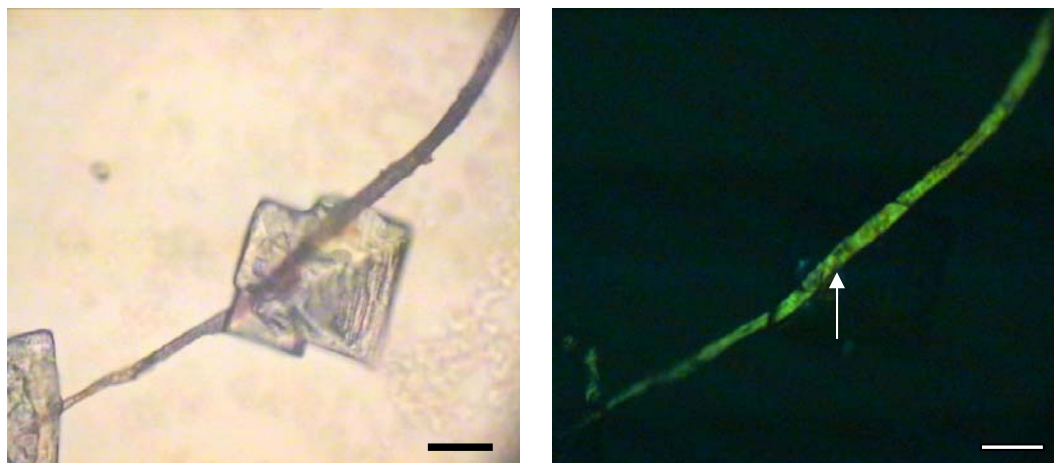


Fig. 4.10: Assembly of OY1 in 0.1% TEA (after 7 days at 25 °C) upon treatment with CR (left) and birefringence under polarised light (right). The scale bar represents 100 μm .

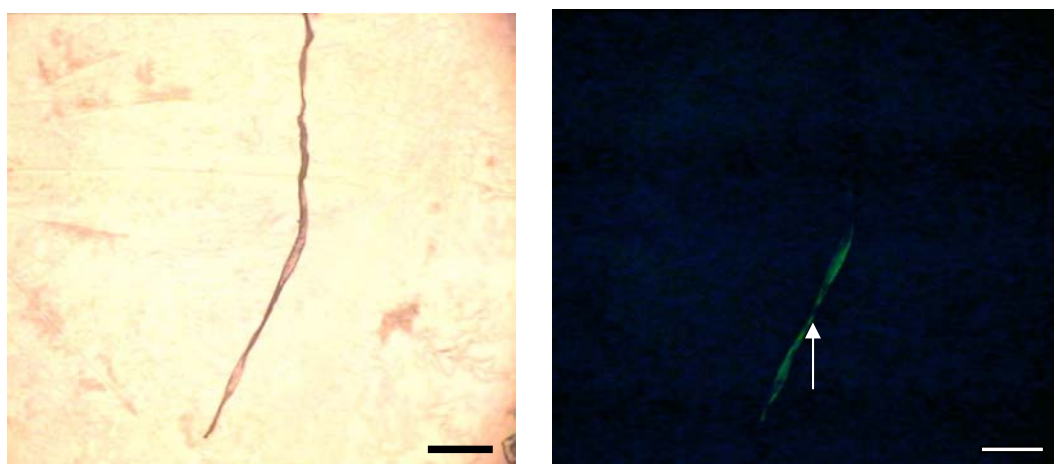


Fig. 4.11: Assembly of OY2 in 0.1% TEA (after 7 days at 25 °C) upon treatment with CR (left) and birefringence under polarised light (right). The scale bar represents 100 μm .

SEM micrographs revealed the presence of a very fine texture in the dried peptide assemblies. The lyophilisation of the samples helped to preserve their 3D structure. Significant SEM micrographs of peptide assemblies are presented in Figures 4.12, 4.13, 4.14 and 4.15. Peptides assembled into microfibrils/microtubes with diameters in the range of 500 nm to 2 μm and lengths of tens of microns. On the other hand the EM work that was performed letting air-dry the samples gave low quality images, possibly because of residual moisture in the samples and/or disorganisation of the supramolecular aggregates due to slow evaporation (results not shown).

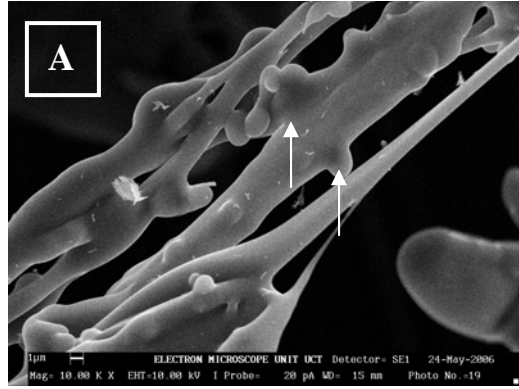
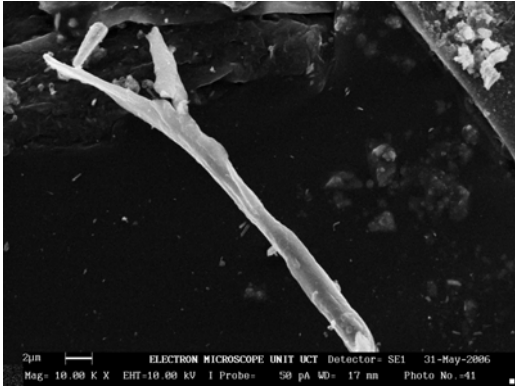


Fig 4.12: SEM images of dried assemblies from KL1. [A] Vesicles budding out of interwoven microtubules.

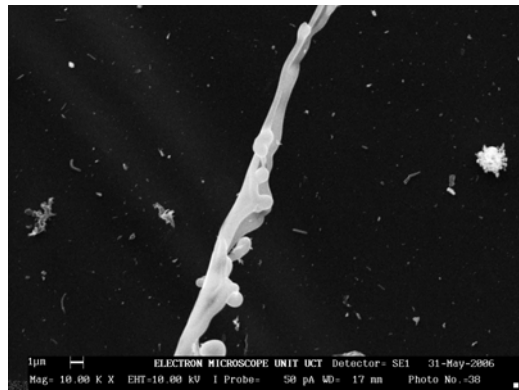
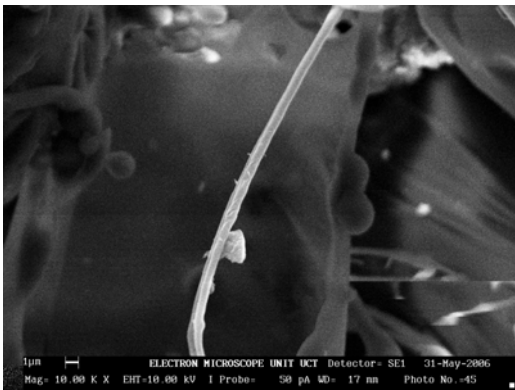


Fig 4.13: SEM images of dried assemblies from KL4.

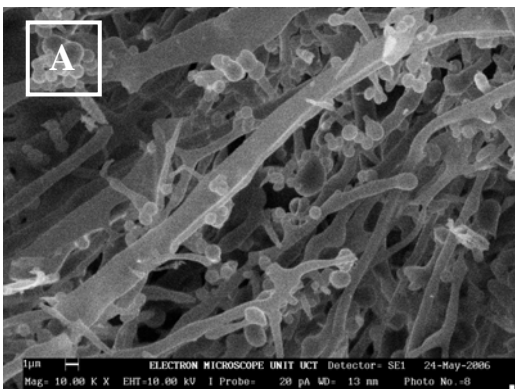


Fig 4.14: SEM images of dried assemblies from OY2. [A] Vesicles budding out of microtubules.

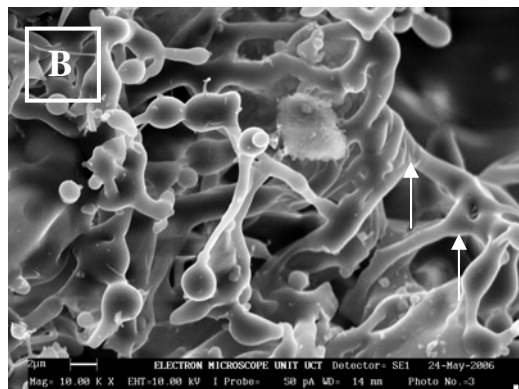
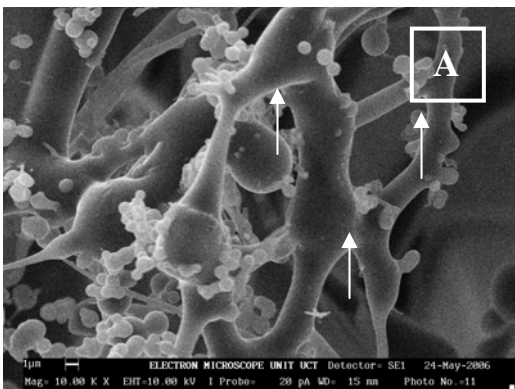


Fig 4.15: SEM images of 3-way junctions (arrows) from dried assemblies: OL2 [A] and OL1 [B].

Cryo-fracture SEM micrographs also revealed fibre-like structures after an incubation time of two weeks at RT in 0.1% TEA (Figs. 4.16, 4.17 and 4.18). Fibres were oriented in different directions: vertically (circles) and horizontally (arrows). The macromolecular assemblies of the peptides consisted mainly of microtubes/microfibres with lengths of several microns and uniform diameters of about 600 nm.

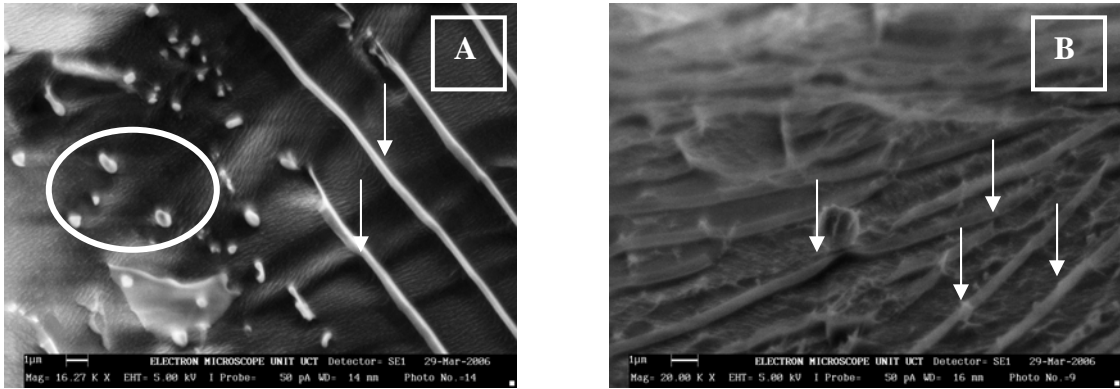


Fig. 4.16: Microtubes from OY1 [A] and OY2 assemblies [B] after 15 days in 0.1% TEA.

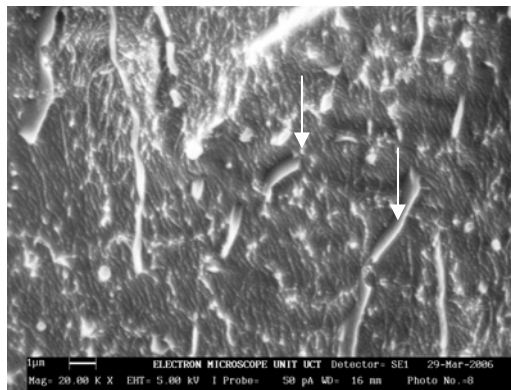


Fig. 4.17: Microtubes from KL4 assemblies after 15 days in 0.1% TEA.



Fig. 4.18: Microtubes from OL1 [A] and OL2 assemblies [[B] after 15 days in 0.1% TEA.

Peptides made of alternating hydrophilic and hydrophobic residues tend to form unusually stable β -sheet structures in water. Polar and non polar AAs are secluded on the two different sides of the β -sheet surface and, therefore, hydrophilic and hydrophobic interactions are much stronger. Moreover, they are added to conventional β -sheet hydrogen bonds along the backbones (Vauthey et al., 2002). Most of the peptide bolaamphiphiles designed for this study present an alternation of polar (Orn, Lys) and non polar (Leu, Tyr, 9-Anc, 6-Ahx) residues and have structural similarities with some compounds developed by Zhang and co-workers (von Maltzahn et al., 2003). Only LO1 and LY1 present an excess of hydrophobic amino acids. The microscopy study that was carried out proved that they self-assemble in response to an increase in pH when the net charge of the peptide molecules is near zero (Caplan et al., 2000). The use of both cryo-fracture SEM and SEM (upon lyophilisation of the samples) permitted to look at the 3D complexes formed in solution. SEM images revealed the presence of microtubes and microvesicles with diameters ranging from 500 nm to 2 μ m. The peptide assemblies were characterised by a network of interwoven fibres. Moreover, 3-way junctions (branches) connecting the microtubes were also observed and resulted in sponge-like three-dimensional arrangements. Such branched supramolecular organisations are attracting significant interest especially because of their effects on rheological properties (Cates, 1987; Shikata and Imai, 2000).

In many cases the peptides created heterogeneous populations of microfibrils, vesicles and entangled rod-like micelles. Furthermore, vesicles budding from the microtubes and developing in 3-way junctions were also noticed. Their presence is often considered as a sign of the dynamic behaviour of the self-assembly process of this kind of molecules (Vauthey et al., 2002).

Cryo-fracture SEM also showed the existence of hollow tubes, at least for some of the peptide bolaamphiphiles. Such an observation is consistent with the presence of branches and vesicles.

4.4.3 Gels from peptide bolaamphiphiles

Except for the formation of microfibrils observed by EM, in some cases the self-assembly had also visible consequences. Peptide hybrid OY1 at high concentration (~ 7 mM or ~ 9 mg/ml or 9% by weight) in 0.1% TEA (clear solution after solubilisation) gave a gel after standing for 7 days at room temperature in a closed glass vial. The gel phase self-supported upon inversion.

The peptide gel was observed with an optical microscope at different magnifications (described in Section 4.3.3) under cross-polarised light, and showed a complex optical texture (Fig. 4.19). OM revealed striations with a parallel development and strong birefringence properties (Fig. 4.19 C and D). Birefringence commonly indicates orientation of the material at the level of tens of microns (Hartgerink et al., 2002). This indication is consistent with the other microscopy observations carried out on the peptide assemblies derived from OY1.

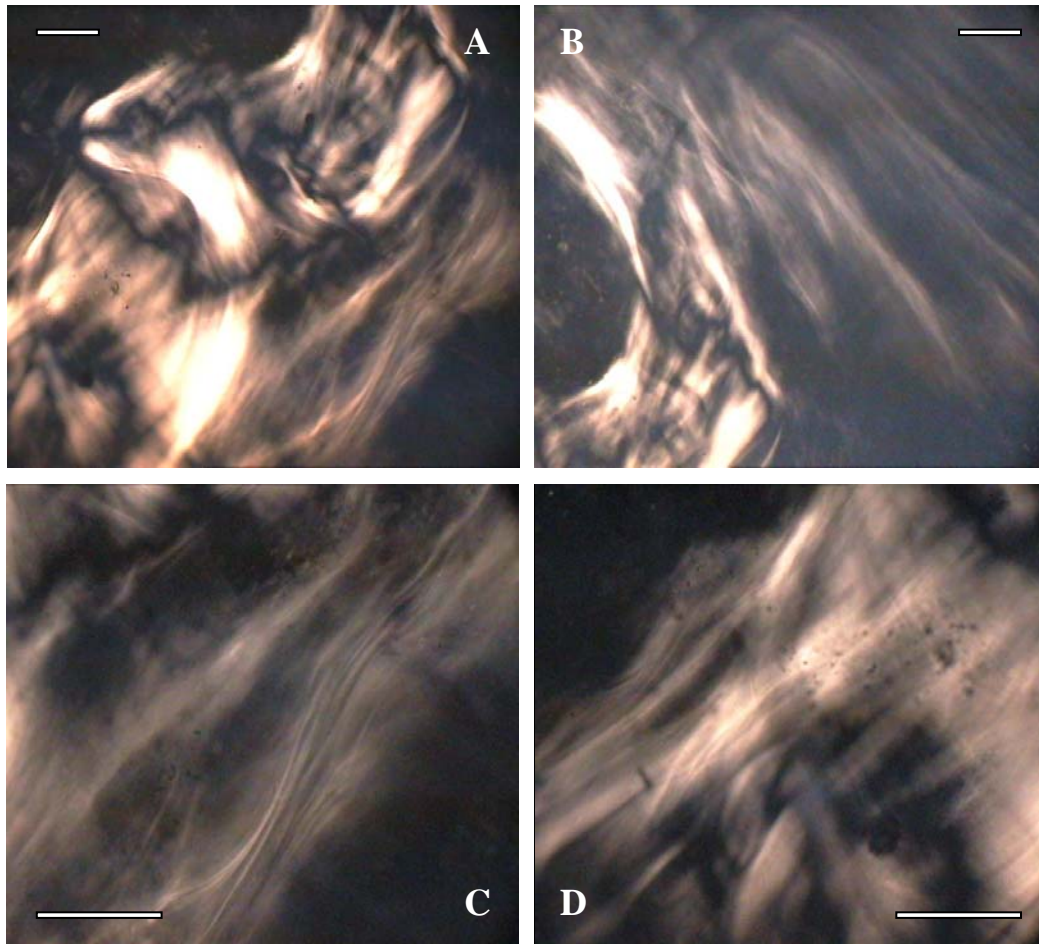


Fig. 4.19: Light microscope images showing birefringence¹ from OY1 gel, observed under cross-polarised light. The bar scale represents 100 μm .

¹ “Birefringence is defined as the double refraction of light in a transparent molecularly ordered material, which is manifested by the existence of orientation-dependent differences in refractive index. [...] Although birefringence is an inherent property of many anisotropic crystals [...] it can also arise from other factors, such as *structural ordering*, physical stress, deformation, [...]. Structural birefringence is a term that applies to a wide spectrum of anisotropic formations, including *biological macromolecular assemblies* such as chromosomes, muscle fibres, microtubules, liquid crystalline DNA and fibrous protein structures such as hair”. From <http://micro.magnet.fsu.edu/primer/lightandcolor/birefringenceintro.html> (accessed 25/05/06).

4.4.4 Fourier-transform photoacoustic infrared spectroscopy

FT-IR PAS was used to study the dried peptide assemblies and especially to evaluate the nature of the hydrogen bonds present in the supramolecular structures. Spectra were dominated by the amide I envelope at 1670 cm^{-1} and amide II band at about 1554 cm^{-1} . Characteristic bands are reported in Table 4.2. Two typical spectra are shown in Figures 4.20 and 4.21 as examples.

Tab. 4.2: FT-IR bands for the dried peptide assemblies (cm^{-1})

<i>assignment</i>	<i>KL1</i>	<i>KL2</i>	<i>KL3</i>	<i>KL4</i>	<i>OL1</i>	<i>OL2</i>	<i>OY1</i>	<i>OY2</i>
Amide A	3270	3286	3270	3272	3289	3287	3286	3252
NH ₂	3077	3082	3052	3069	3084	3069	3087	3066
CH ₂ asymmetric stretching	2954	2932	2930	2936	2930	2940	2932	2924
CH ₂ symmetric stretching	2872	2858	2860	2860	2865	2860	2860	2863
CH ₂ scissoring	1428	1410	1422	1428	1428	1452	1452	1454
Amide II	1554	1546	1554	1552	1554	1552	1556	1556

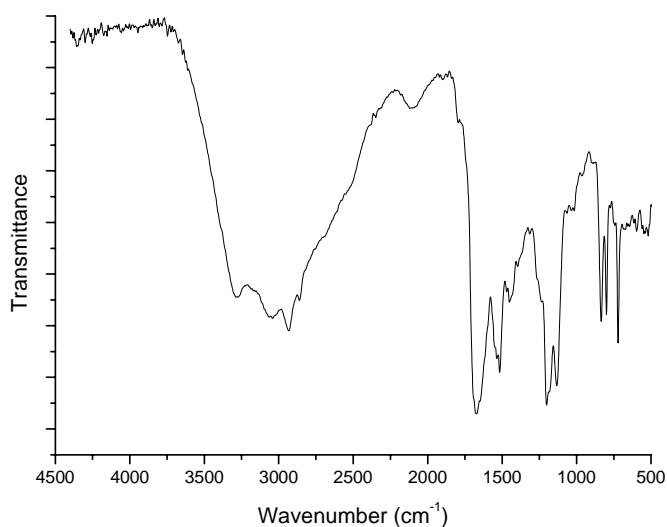


Fig. 4.20: FT-IR spectrum of the dried OY1 assemblies in the region $500\text{-}4500\text{ cm}^{-1}$.

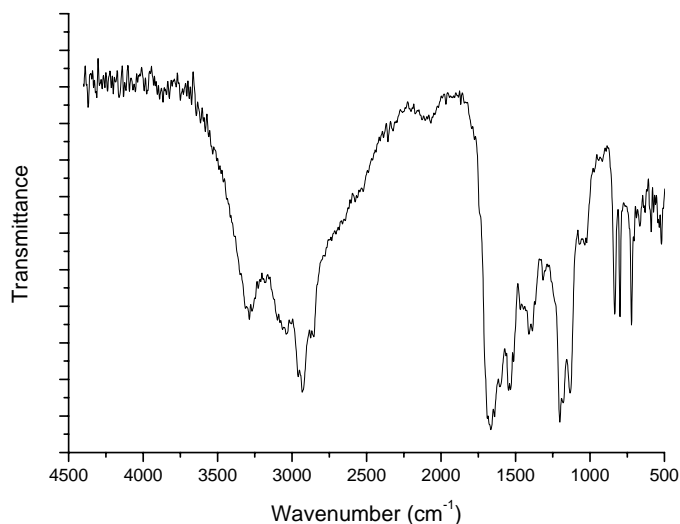


Fig. 4.21: FT-IR spectrum of the dried KL2 assemblies in the region 500-4500 cm^{-1} .

Amide I bands and deconvolved amide I bands (1700-1600 cm^{-1}) gave information on the conformation that peptides took. See Figure 4.22. Most of the peptides adopted a β -sheet conformation with intramolecular hydrogen bonds, as demonstrated by the presence of bands at around 1630-1635 cm^{-1} and 1670-1675 cm^{-1} (Byler and Susi, 1986; Yamada et al., 1998; Stuart, 2004). Amide I bands also gave an indication that the molecules assumed an antiparallel β -sheet conformation as a band around 1690 cm^{-1} was present in almost all the spectra (Yamada et al., 1998; Ganesh et al., 2003). Nonetheless, random/unordered structure and turns were also present, as suggested by a band at around 1640 cm^{-1} (random structures) and one at around 1680 cm^{-1} (turns) (Byler and Susi, 1986). The frequency of amide A bands usually reveals the existence of non-covalent interactions in the molecule (Ganesh et al., 2003). In the peptide bolaamphiphiles' spectra these bands absorb between 3270-3286 cm^{-1} and there is no absorption at around 3400 cm^{-1} , thus indicating that all the peptide amide NHs are involved in intermolecular hydrogen bonding (Ganesh et al., 2003).

C-H stretching vibration bands were also studied as they can provide useful information about the aggregation of peptides (Ricci et al., 2000). Alteration of band stretching, in terms of both position and width, indicate conformational order changes after peptides associate to form aggregates (Ganesh et al., 2003). The C-H asymmetric and symmetric stretching bands of n-octane ($n\text{-C}_8\text{H}_{18}$, comparable to the structure of 9-aminononanoic acid of the peptide hydrophobic core) are located at 2925 and 2855 cm^{-1} respectively. Peptide bolaamphiphiles presented a significant change in frequency (having C-H asymmetric and symmetric bands at around 2930-2940 cm^{-1} and 2860-2870 cm^{-1} respectively), which is consistent with peptide aggregation (Ganesh et al., 2003).

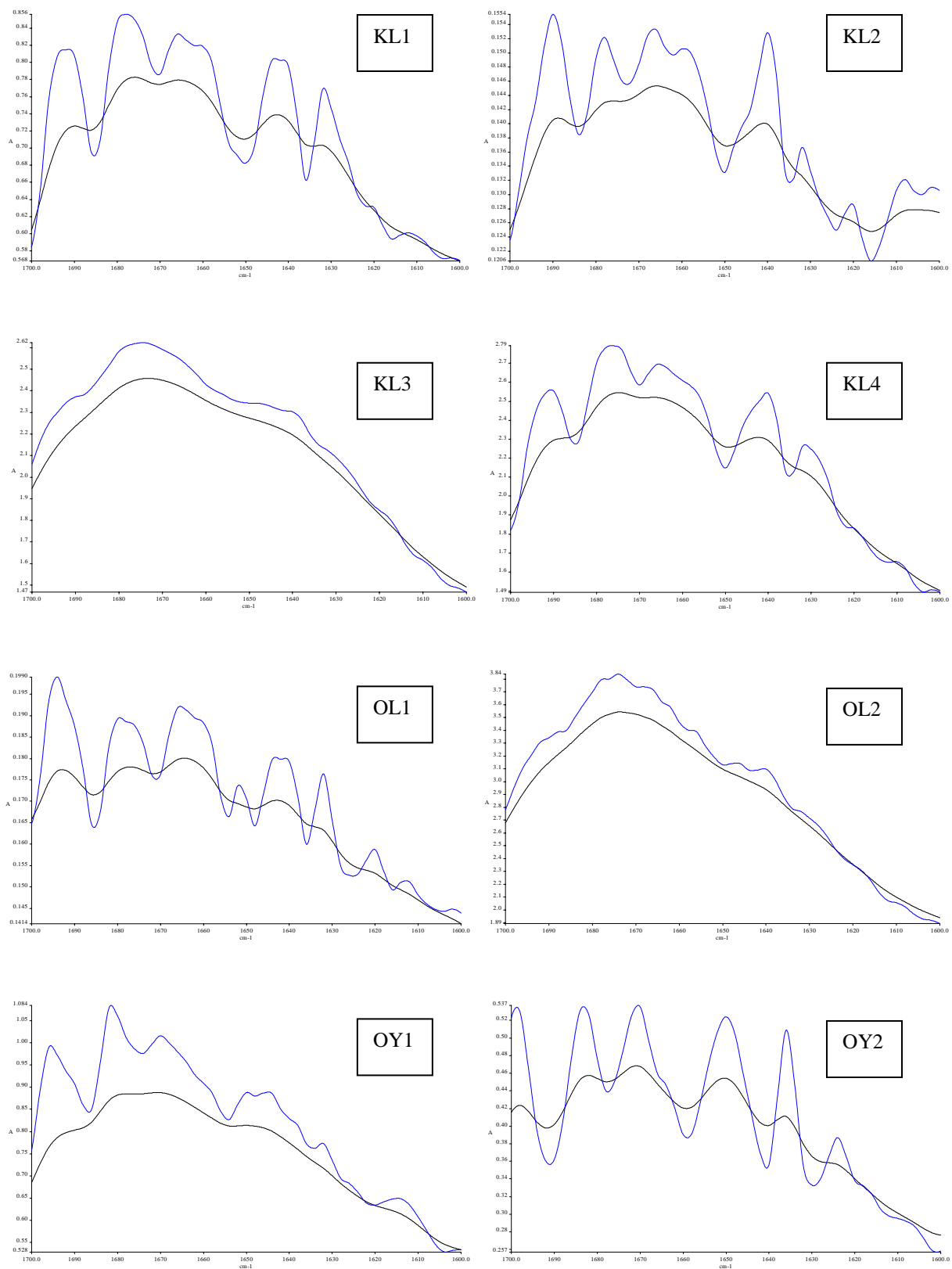


Fig. 4.22: Amide I bands (black) and deconvoluted amide I bands (grey) of dried peptide assemblies ($1700\text{-}1600\text{ cm}^{-1}$).

4.4.5 Circular dichroism spectroscopy

Peptides and peptide hybrids were further analysed by CD in different environments and concentrations. At low concentrations (0.2 mg/ml in 10 mM PBS pH 6.8), all the synthesised molecules showed a random structure (minima at 196-197 nm). Only the parent compounds (L3, L4, L5) showed an α -helical secondary structure in PBS (maxima at 192 nm and minima at 205 and 218 nm) (Naidoo, 2004). Spectra did not change after an aging period of several days (up to twelve) thus indicating that (under those conditions) no significant changes took place in the three-dimensional arrangements of the molecules. At the same concentration, in 20 mM PBS pH 6.8/TFE (1:1), compounds containing ω -AA (KL1, KL2, KL3, KL4, OL1, OY1) presented a different profile, which was very likely induced by the solvent itself. Again, no effects were detected after aging (Figs. 4.23 and 4.24 show CD spectra). In the same environment, peptides OL2 and OY2 (containing proline instead of ω -AA) did not show any difference.

To enforce the aggregation, CD studies were also performed at higher concentrations (~5 mg/ml) dissolving peptides in 0.1% TEA (pH 10). However, under these conditions it was not possible to record noteworthy spectral information because of (i) the high absorption in the far-UV of the solvent itself and (ii) the high peptide concentration which also affected the measurements (Johnson, 1990).

The use of ω -amino acids (6-aminohexanoic acid and 9-aminononanoic acid) in the substitution of the poly-leucine chain proved to heavily affect the helicity, typical of the parent compounds (KLKL_nKLK-NH₂, n = 3, 4, 5). The lack of hydrogen donors and acceptors for the formation of hydrogen bonds was probably fundamental for the modification of the secondary structures in the peptide hybrids (containing 9-Anc and 6-Ahx). Moreover, the use of proline also greatly contributed towards the formation of unordered secondary structures at low concentration.

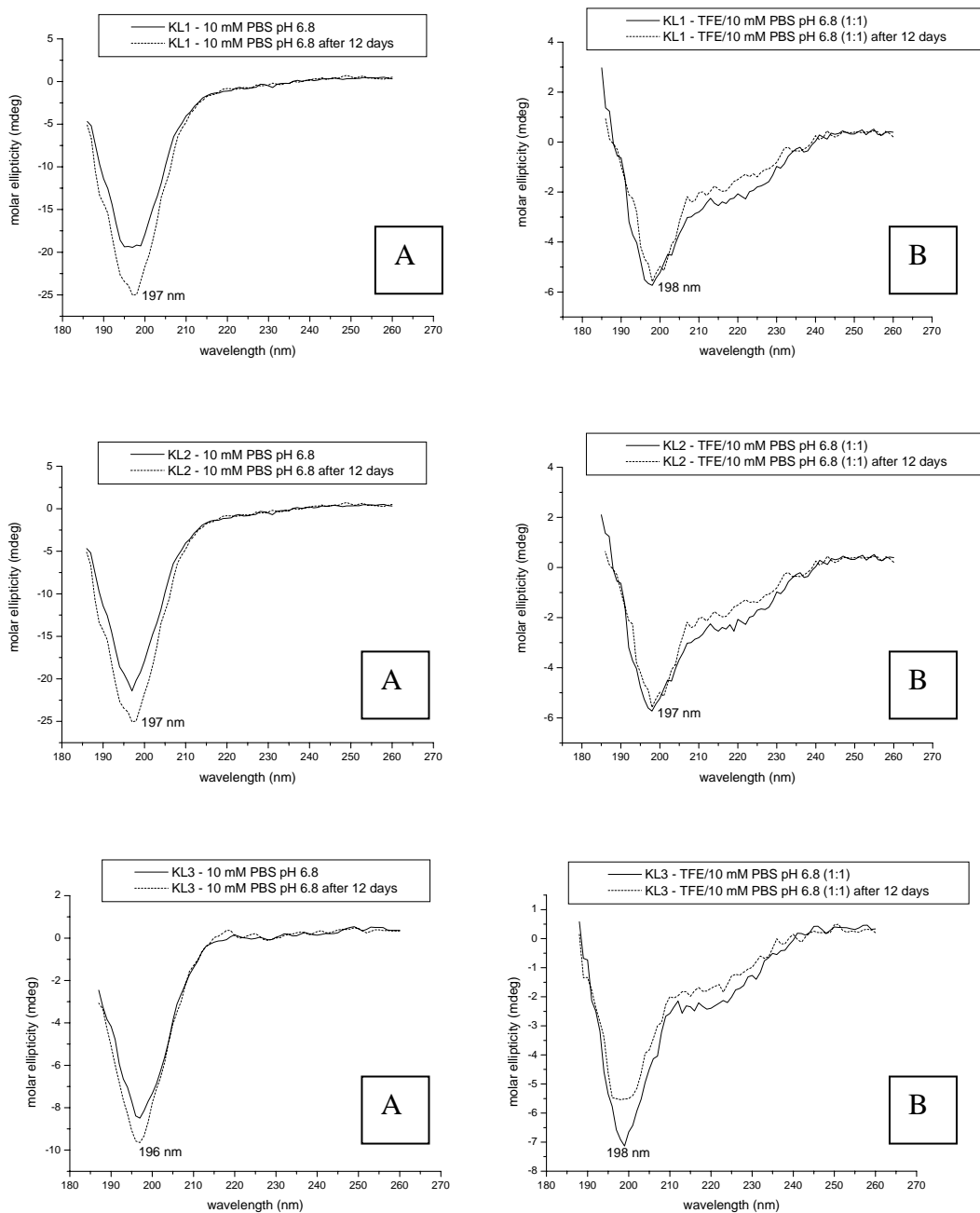


Fig. 4.23: CD spectra of peptide bolaamphiphiles [A] in a watery system and [B] in a more hydrophobic environment.

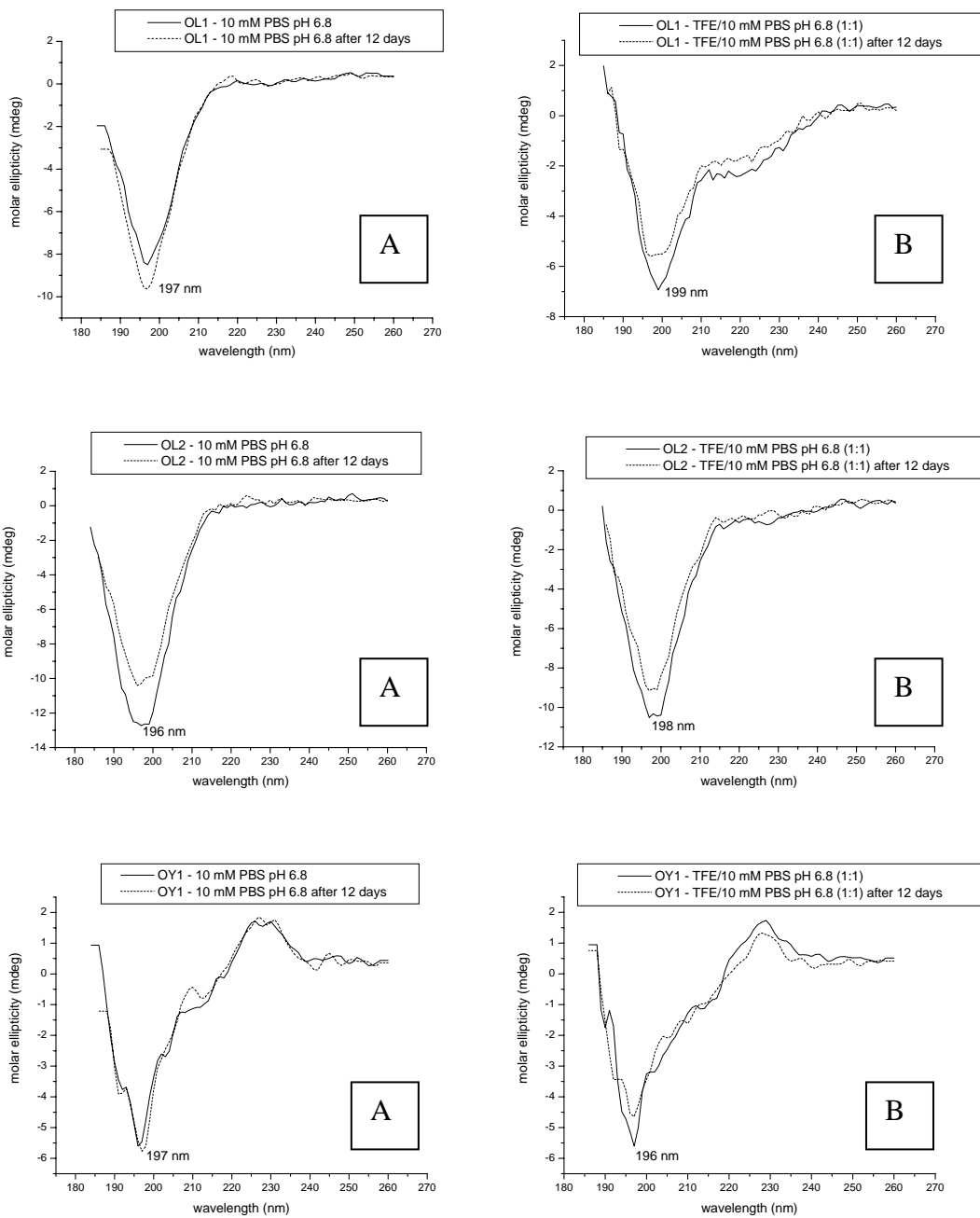


Fig. 4.24: CD spectra of peptide bolaamphiphiles [A] in a watery system and [B] in a more hydrophobic environment.

4.5 Conclusions

The aggregation process of novel bolaamphiphilic peptides was studied both from a physicochemical point of view and from a morphological perspective. The determination of CAC values gave useful guidelines regarding the status of the molecules in solution (as single molecules or aggregates) according to concentrations and other conditions. The comparison of the different behaviours resulted in the possibility to correlate the CAC to the composition in AAs and the 3D structure of the molecules. Factors that are believed to influence the self-assembly (such as the presence of hydrophobic residues) were found to have a primary role in governing the aggregation (Zhang et al., 1993; Santoso and Zhang, 2004). Peptide bolaamphiphiles containing tyrosine showed a lower CAC than leucine containing homologue molecules, especially because of stronger hydrophobic interactions of the side chains due to π -stacking (Gazit, 2002). In addition, the role of the 3D structure was also clarified and established to be fundamental. Proline-containing molecules showed higher CAC values than homologue peptides which had 9-aminononanoic acid, and confirmed the critical importance of single-molecule properties on the aggregation process (Jun et al., 2004).

The morphology studies performed on the assemblies revealed the complex supramolecular architectures formed by these compounds. The aggregation was enforced by pH modifications, while CR staining and OM observation gave evidence of fibre-like structures with birefringence properties under cross-polarised light. SEM and cryo-SEM micrographs also confirmed the formation of fibres with dimensions in the range of several microns (between 500 nm and 2 μ m). The coexistence of microtubes, vesicles, 3-way junctions, branches and vesicles budding out of microtubes revealed that the self-assembly process of these surfactant-like molecules is a dynamic event (Vauthey et al., 2002).

A peptide gel was formed by one of the compounds (OY1, 9% by weight in 0.1% TEA) as a result of the self-assembly. The observation of birefringence by optical microscopy under cross-polarised light revealed a molecular structural organisation at the level of tens of microns. Peptide gels are currently attracting a lot of interest in biomaterials engineering and regenerative medicine because of the structural support combined to the biological activity (Holmes et al., 2000; Kisiday et al., 2002).

The use of FT-IR gave supporting information regarding the aggregation of the molecules. Specific bands related to the presence of antiparallel β -sheet structures were found. Additionally, bands referring to turns and unordered 3D arrangements were also discovered (Byler and Susi, 1986). FT-IR analyses were consistent with the microscopy observations where different kinds of supramolecular architectures were revealed, such as microfibrils, microtubes, vesicles and 3-way junctions.

The self-assembly process could be explained by two hypothetical mechanisms which ultimately coexist and possibly explain the diverse structures detected.

A. The presence of β -sheet structures (FT-IR), microfibrils and microtubules (cryo-SEM) indicated the existence of structured supramolecular architectures created by ordered arrangements of single molecules. Strong intramolecular hydrogen bonds tend to create β -sheets, which turn on themselves to give microtubules (Kogiso et al., 2000; Matsui and Gologan, 2000; Matsui and Douberly, 2001) (Fig. 4.25).

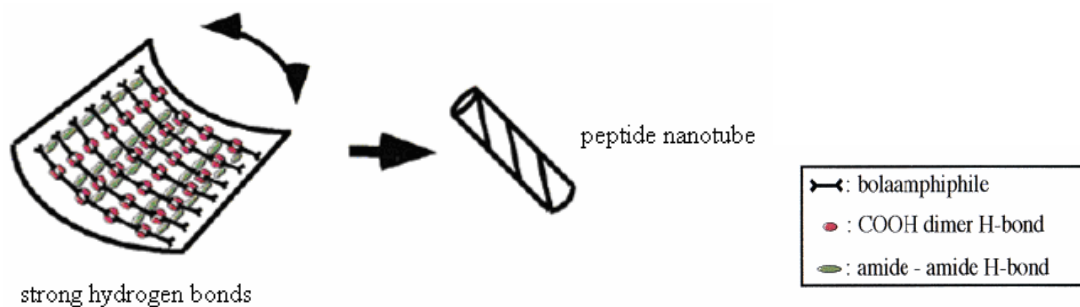


Fig. 4.25: Hypothetical self-assembly mechanism of tubule formation (modified from Matsui and Douberly, 2001).

B. The discovery of turns and unordered structures (FT-IR) and the evidence of the aggregation (CAC by fluorescence measurements) presented a disordered and more dynamic aggregation process. The surfactant-like structure of the molecules could explain the formation of vesicles (micelles) and 3-way junctions (SEM) (Santoso et al., 2002; Vauthey et al., 2002; Masuda and Shimizu, 2004) (Fig. 4.26).

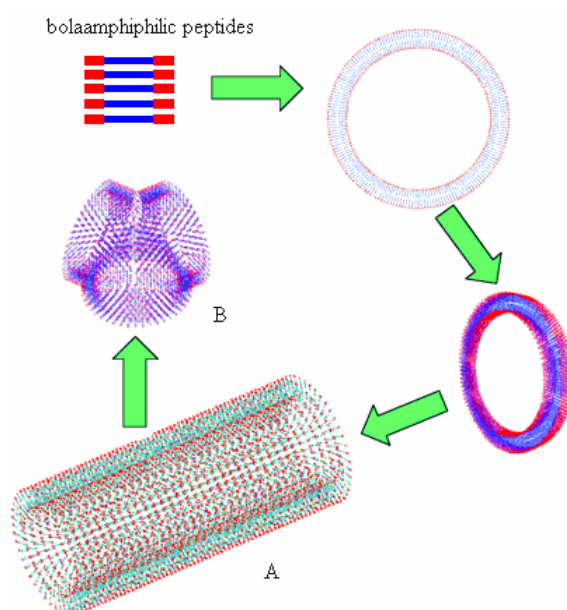


Fig. 4.26: Potential mechanism of tubule formation. Red: hydrophilic; blue: hydrophobic. [A] each peptide may interact with one another to form closed rings, which stack on top of one another to give a nanotube. [B] three nanotubes are connected by a three-way junction (modified from Vauthey et al., 2002).

4.6 References

Aggeli A, Bell M, Carrick LM, Fishwick CWG, Harding R, Mawer PJ, Radford SE, Strong AE and Boden N (2003) pH as a trigger of peptide β -sheet self-assembly and reversible switching between nematic and isotropic phases, *Journal of the American Chemical Society*, 125, 9619-9628.

Bakshi MS and Kaur G (2005) Mixed micelles of series of monomeric and dimeric cationic, zwitterionic, and unequal twin-tail cationic surfactants with sugar surfactants: a fluorescence study, *Journal of Colloid and Interface Science*, 289, 551-559.

Byler DM and Susi H (1986) Examination of the secondary structure of proteins by deconvolved FTIR spectra, *Biopolymers*, 25, 469-487.

Caplan MR, Moore PN, Zhang S, Kamm RD and Lauffenburger DA (2000) Self-assembly of a β -sheet protein governed by relief of electrostatic repulsion relative to van der Waals attraction, *Biomacromolecules*, 1, 627-631.

Caplan MR, Schwartzfarb E, Zhang S, Kamm RD and Lauffenburger DA (2002) Control of self-assembling oligopeptide matrix formation through systematic variation of amino acid sequence, *Biomaterials*, 23, 219-227.

Cates ME (1987) Reptation of living polymers: dynamics of entangled polymers in the presence of reversible chain-scission reactions, *Macromolecules*, 20, 2289-2296.

Chen P (2005) Self-assembly of ionic-complementary peptides: a physicochemical viewpoint, *Colloids and Surfaces A*, 261, 3-24.

Claussen RC, Rabatic BM and Stupp SI (2003) Aqueous self-assembly of unsymmetric peptide bolaamphiphiles into nanofibers with hydrophilic cores and surfaces, *Journal of the American Chemical Society*, 125, 12680-12681.

Collier JH, Hu BH, Ruberti JW, Zhang J, Shum P, Thompson DH and Messersmith PB, Thermally and photochemically triggered self-assembly of peptides hydrogels, *Journal of the American Chemical Society*, 123, 9463-9464.

Fung SY, Keyes C, Duhamel J and Chen P (2003) Concentration effect on the aggregation of a self-assembling oligopeptide, *Biophysical Journal*, 85, 537-548.

Ganesh S, Prakash S and Jayakumar R (2003) Spectroscopic investigation on gel-forming β -sheet assemblage of peptide derivatives, *Biopolymers*, 70, 346-354.

Gazit E (2002) A possible role for π -stacking in the self-assembly of amyloid fibrils, *FASEB Journal*, 16, 77-83.

Hartgerink JD, Beniash E and Stupp SI (2002) Peptide-amphiphile nanofibers: a versatile scaffold for the preparation of self-assembling materials, *Proceedings of the National Academy of Sciences*, 99, 5133-5138.

Holmes TC, de Lacalle S, Su X, Liu G, Rich A and Zhang S (2000) Extensive neurite outgrowth and active synapse formation on self-assembling peptide scaffolds, *Proceedings of the National Academy of Sciences*, 97, 6728-6733.

- Johnson WC jr (1990) Protein secondary structure and circular dichroism: a practical guide, *Proteins: structures, functions and genetics*, 7, 205-214.
- Jun S, Hong Y, Imamura H, Ha BY, Bechhoefer J and Chen P (2004) Self-assembly of the ionic peptide EAK16: the effect of charge distribution on self-assembly, *Biophysical Journal*, 87, 2352-2364.
- Kisiday J, Jin M, Kurz H, Semino C, Zhang S and Grodzinsky (2002) Self-assembling peptide hydrogel fosters chondrocyte extracellular matrix production and cell division: implications for cartilage tissue repair, *Proceedings of the National Academy of Sciences*, 99, 9996-10001.
- Kogiso M, Okada Y, Hanada T, Yase K and Shimizu T (2000) Self-assembled fibers from valylvaline bola-amphiphiles by a parallel β -sheet network, *Biochimica et Biophysica Acta*, 1475, 346-352.
- Madhavaiah C, Krishna Prasad and Verma S (2005) Enforcing aggregation in a dipeptide conjugate, *Tetrahedron Letters*, 46, 3745-3749.
- Masuda M and Shimizu T (2004) Lipid nanotubes and microtubes: experimental evidence for unsymmetrical monolayer membrane formation from unsymmetrical bolaamphiphiles, *Langmuir*, 20, 5969-5977.
- Matsui H and Gologan B (2000) Crystalline glycyglycine bolaamphiphile tubules and their pH-sensitive structural transformation, *Journal of Physical Chemistry B*, 104, 3383-3386.
- Matsui H and Douberly GE (2001) Organization of peptide nanotubes into macroscopic bundles, *Langmuir*, 17, 7918-7922.
- Naidoo VB (2004) The supramolecular chemistry of novel synthetic biomacromolecular assemblies, PhD thesis, University of Stellenbosch.
- Niece KL, Hartgerink JD, Donners JJM and Stupp SI (2003) Self-assembly combining two bioactive peptide-amphiphile molecules into nanofibers by electrostatic attraction, *Journal of the American Chemical Society*, 125, 7146-7147.
- Nilsson MR (2004) Techniques to study amyloid fibril formation in vitro, *Methods*, 34, 151-160.
- Ninomiya R, Matsuoka K and Moroi Y (2003) Micelle formation of sodium chenodeoxycholate and solubilization into the micelles: comparison with other unconjugated bile salts, *Biochimica et Biophysica Acta*, 1634, 116-125.
- Pochan DJ, Schneider JP, Kretsinger J, Ozbas B, Rajagopal K and Haines LB (2003) Thermally reversible hydrogels via intramolecular folding and consequent self-assembly of a *de novo* designed peptide, *Journal of the American Chemical Society*, 125, 11802-11803.
- Rajagopal K and Schneider JP (2004) Self-assembling peptides and proteins for nanotechnological applications, *Current Opinion in Structural Biology*, 14, 480-486.
- Ricci M, Sassi P, Nastruzzi C and Rossi C (2000) Liposome-based formulations for the antibiotic nonapeptide leucenostatin A: Fourier transform infrared spectroscopy characterization and in vivo toxicology study, *AAPS PharmSciTech*, 1, article 2.
- Santoso SS and Zhang S (2004) Self-assembled nanomaterials, in Nalwa HS (Ed.) *Encyclopaedia of nanoscience and nanotechnology*, Vol. 9 (pp. 459-471) American Scientific Publishers; Stevenson Ranch.

Shikata T and Imai S (2000) Entanglements in a threadlike micellar system as studied by dielectric relaxation, *Langmuir*, 16, 4840-4845.

Stuart BH (2004) Biological applications: proteins and peptides, in Stuart BH (Ed.) *Infrared spectroscopy: fundamentals and applications* (pp. 141-151), Analytical techniques in the sciences (Series Ed. Ando DJ), Wiley; Chichester.

Vauthey S, Santoso S, Gong H, Watson N and Zhang S (2002) Molecular self-assembly of surfactant-like peptides to form nanotubes and nanovesicles, *Proceedings of the National Academy of Sciences*, 99, 5535-5360.

von Maltzahn G, Vauthey S, Santoso S and Zhang S (2003) Positively charged surfactant-like peptides self-assemble into nanostructures, *Langmuir*, 19, 4332-4337.

Wang K, Keasling JD and Muller SJ (2005) Effects of the sequence and size of non-polar residues on the self-assembly of amphiphilic peptides, *International Journal of Biological Macromolecules*, 36, 232-240.

Yamada N, Ariga K, Naito M, Matsubara K and Koyama E (1998) Regulation of β -sheet structures with amyloid-like β -sheet assemblage from tripeptide derivatives, *Journal of the American Chemical Society*, 120, 12192-12199.

Yin D, Yang W, Ge Z and Yuan Y (2005) A fluorescence study of sodium hyaluronate/surfactant interactions in aqueous media, *Carbohydrates Research*, 340, 1201-1206.

Zhang S (2003) Fabrication of novel biomaterials through molecular self-assembly, *Nature Biotechnology*, 21, 1171-1178.

Zhang S and Altman M (1999) Peptide self-assembly in functional polymer science and engineering, *Reactive and Functional Polymers*, 41, 91-102.

Zhang S, Holmes T, Locksmith C and Rich A (1993) Spontaneous assembly of self-complementary oligopeptides to form a stable macroscopic membrane, *Proceedings of the National Academy of Sciences*, 90, 3334-3338.

Chapter 5

Hydrophobic characterisation and correlation with self-assembly behaviour

5.1 Hydrophobicity in peptide chemistry

The hydrophobic content of drugs has been historically considered an important parameter for pharmacokinetics studies (Tute, 1996). The prediction of adsorption through membranes such as the skin, blood-brain barrier and gastrointestinal tract (Donnelly et al., 1996; Meng et al., 2001), the interaction with lipid bilayers (Klein et al., 2001) or receptors are all based on a molecule's hydrophobic profile. Therefore, the determination of the hydrophobicity of drugs or biologically active molecules is fundamental for (i) the understanding of their mechanism of action and (ii) the optimisation of SAR parameters (Fauchère, 1996).

A universal tool for the experimental measurement of the hydrophobicity of a given molecule or peptide is its partition coefficient (P) between a non-polar phase and water, where often the non-polar phase is *n*-octanol, as suggested by Fujita et al. (Fujita et al., 1964). Generally the logarithmic form is used ($\text{Log } P$). However, the determination of the $\text{Log } P$ by direct measurements, using the flask-shake equilibration method, faces problems such as poor reproducibility and the long experimental times, besides requiring a reasonable quantity of pure compound (Cimpan et al., 2000). Moreover, the flask-shake technique can produce experimental problems (formation of micelles, accumulation of the compounds at the octanol-water interface) and it is not advisable to use it with amphiphilic compounds (such as surfactants) (Klein et al., 2001). These limitations are overcome by using reversed-phase high performance liquid chromatography, where the stationary phase (generally C_{18} or C_8) mimics the non-polar solvent. The liquid chromatographic method has the advantages of fast determination and better reproducibility, while the purity of the sample is not a necessary condition (Cimpan et al., 2000). Moreover, the quantity used can often be in the range of milligrams or less. In the case of peptides and the determination of their lipophilicity, the advantages offered by RP-HPLC are extremely important and turn this technique into a useful device for their hydrophobic characterisation.

One of the basic parameters for hydrophobicity characterisation by isocratic RP-HPLC is the capacity factor (k'), which can be calculated by the following relationship:

$$k' = (t_R - t_0) / t_0 \quad (2)$$

where t_R is the retention time of the analyte and t_0 is the retention time of an unretained compound (commonly methanol or acetonitrile) (OECD, 1989; vd Waterbeemd, 1996). Frequently, the logarithmic form is used as lipophilicity index ($\text{Log } k$). The capacity factor is independent of the column length and mobile phase flow rate (Meng et al., 2001) but its validity is limited to homologous series of molecules and if the operative conditions are constant for all of them (Pignatello and Puglisi, 2000; Hallgas et al., 2004).

Among the synthesised compounds several differences were present: charge, ratio between hydrophobic and hydrophilic amino acids, three-dimensional structure, number of AA, etc. (Tab. 5.1). Therefore, the use of isocratic HPLC to characterise this variety of structures was considered inappropriate. As suggested by some examples in the literature (Kim et al., 2005), retention times from gradient RP-HPLC can correlate well with the biological activity of antimicrobial peptides (activity intended as ability to lyse membranes) and lipophilicity can be estimated by gradient liquid chromatography (Kaliszan et al., 2002). It was consequently decided to use the t_R obtained by gradient RP-HPLC and study the correlation with theoretically calculated values of lipophilicity and the self-assembly profile of each compound in 0.1% TEA. In order to determine reliable data, t_R values for the synthesised compounds were collected by using different columns and gradients, and the various data sets were compared.

Tab. 5.1: Peptides and peptide hybrids used in this study

<i>PEPTIDE</i>	<i>PROLINE</i>	<i>LINEAR LINKER</i>	<i>MW (g/mol)</i>	<i>NET CHARGE #</i>
L3			1095.81	+5
L4			1208.67	+5
L5			1321.82	+5
KL1		X	870.18	+5
KL2		X	912.26	+5
KL3		X	869.19	+5
KL4		X	911.27	+5
OL1		X	855.17	+5
OL2	X		911.15	+5
OY1		X	955.20	+5
OY2	X		1011.18	+5
LO1		X	853.19	+3
LY1		X	951.24	+1

[#] net charge at pH 7

Theoretical calculations of the hydrophobic content give $\text{Log } P$ values (defined as CLOGP or calculated $\text{Log } P$) which can be compared to the experimental ones. Various mathematical models have been developed since the introduction of the flask-shake method for the $\text{Log } P$ determination

(Leo, 1996; Richards, 1996). The two most widely used in peptide chemistry are (A) the residue addition method and (B) the fragment addition method.

A) Residue addition method

Because peptides and proteins are formed by amino acids one can easily think that their hydrophobicities depend on their amino acid compositions. Therefore it should be possible to theoretically calculate hydrophobicity by knowing the contribution of each single residue. Over the past decades, different hydrophobicity scales have been developed and amino acids categorised accordingly. Two main models were created: the first one only considers the amino acid side-chains' contribution to the overall hydrophobicity (Kyte and Doolittle, 1982; Fauchère and Pliska, 1983), while the second one also takes into account the peptide bonds' contribution (Wimley et al., 1996; Wimley and White, 1996). Thinking about the interactions between a polypeptide and a membrane, it is important to consider that the entire molecule interacts with the phospholipid bilayer and crosses it, not only the side chains. Therefore, the peptide bonds' contribution appears to be as important as the side chains' in the determination of the overall hydrophobicity.

The present study is based on the scale developed by Tao et al. (Tao et al., 1999), which considers the peptide bonds' contribution, includes some non natural AA, and whose values can be adjusted if the peptide is present in the amide or acid form (Fig. 5.1).

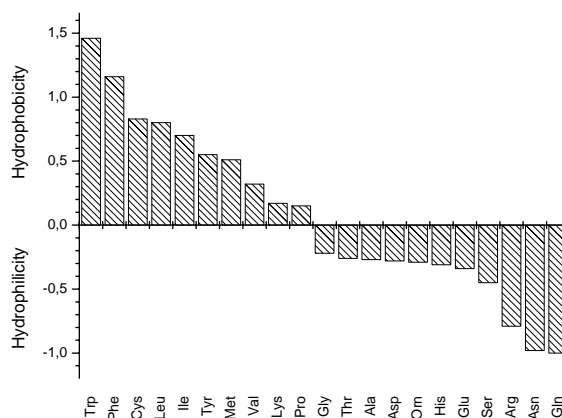


Fig. 5.1: Hydrophobicity contribution of single amino acids (Tao et al., 1999).

According to this model the hydrophobic content of a given peptide can be calculated by the following equation:

$$\text{CLOGP}_{\text{RESIDUE}} = \sum_n a_n R_n^P + bB_P + uU_P \quad (3)$$

where a_n is the incidence of the n th kind of AA, R_n^P is the Log P contribution of the n th type of AA, b and u are indicator variables to account for different forms of the peptides. For blocked

peptides b is set to 1 and u to 0 and vice versa for free peptides. B_P and U_P are the corrections for CLOGP values of blocked and unblocked peptides, respectively (Tao et al., 1999). The contributions to the Log P and the values B_P and U_P are listed in Table 5.2.

Tab. 5.2: [a] Hydrophobicity contributions of common amino acids, [b] for N-acetyl-peptide amides, and [c] for free peptides (adapted from Tao et al., 1999)

Amino acid	Log P contribution [a]	Amino acid	Log P contribution [a]
Ala	-0.27	Met	0.51
Arg	-0.79	Phe	1.16
Asn	-0.98	Pro	0.15
Asp	-0.28	Ser	-0.45
Cys	0.83	Thr	-0.26
Gln	-1.00	Trp	1.46
Glu	-0.34	Tyr	0.55
Gly	-0.22	Val	0.32
His	-0.31	Orn	-0.29
Ile	0.70		
Leu	0.80	Blocked [b]	-1.19
Lys	0.17	Unblocked [c]	-3.25

B) Fragment addition method

According to the fragment addition method molecules can be divided into various elementary chemical fragments (-COOH, -CO-NH-, -CH₂-, -NH₂-, -OH, etc.) which have different contribution to the overall hydrophobic content (Rekker, 1977). The CLOGP value of a certain compound can therefore be determined by summing the contribution of each fragment (Tao et al., 1999), in a process which is commonly computerised.

5.2 Materials

Peptides and peptide hybrids were synthesised on solid phase with the Fmoc-polyamide protocol and purified by RP-HPLC as previously described (see Chapter 3).

Trifluoroacetic acid (99.5%) was supplied by Merck (Hohenbrunn, Germany). Acetonitrile (HPLC grade) was supplied by Riedel-de Haën (Seelze, Germany). Analytical grade water was obtained by filtering glass-distilled water with a Millipore Milli-Q[®] (Bedford, MA, USA) 0.22- μ m filtering system.

5.3 Methods

5.3.1 Theoretical determination of the hydrophobic content

The determination of the hydrophobic content of the synthesised peptides was performed by both the residue addition method and the fragment addition method.

A. For the analysis of the hydrophobic content using the residue addition method the abovementioned formula (3) was used. Values were corrected for peptides present as amides or acids according to the author's instructions (Tao et al., 1999).

B. The CLOGP values corresponding to the fragment addition method were obtained with a computer-based analysis. Bio-Loom software was used (BioByte Corp., CA, USA) [demo version available for download at www.BioByte.com/bb/prod/bioloom.html (last accessed on 15/10/06)]. Structures were first generated with ACD/ChemSketch software (Advanced Chemistry Development Inc., Canada) version 5.12 [www.acdlabs.com last accessed on 15/10/06)], transformed into SMILES (Simplified Molecular Input Line Entry System) and then submitted to the software for the calculation (see Appendix C for details about Bio-Loom analysis).

5.3.2 Experimental determination of the hydrophobic content by RP-HPLC

Reversed-phase high performance liquid chromatography was performed on a Kontron 500 HPLC System (Kontron Instruments, Italy), composed by a Kontron Bio-Tek 522 dual solvent pump, a Kontron HPLC 560 autosampler, a Kontron degasser 3493, a Kontron HPLC 535 dual wavelength UV detector and a PL-ELS 2100 EL-SD (Polymer Laboratories, UK). The column was eluted at 30 °C. The UV detector was set at 220 nm and 254 nm. The parameters for the EL-SD detector were set as follow: nebuliser 70 °C, evaporator 40 °C, gas flow (N₂) 1 l/min. The system was controlled by Geminix software (Goebel-Instrumentelle Analytik, Germany).

Peptides were eluted using gradient C₁ and H₁ (Tabs. 5.3 and 5.4) with a flow rate of 1 ml/min. Analyses were performed using a C₁₂ Proteo Jupiter column (250 x 4.6 mm, 4 µm particle size, 90 Å pore size) (Phenomenex, Torrance, CA, USA) and a C₁₈ Nucleosil column (250 x 4.6 mm, 5 µm particle size, 100 Å pore size) (Supelco, Bellafonte, PA, USA).

Tab. 5.3: Gradient C₁

Time (min)	A (%)	B (%)
0	100	0
7	100	0
35	60	40
37	50	50
40	50	50
45	100	0

Tab. 5.4: Gradient H₁

Time (min)	A (%)	B (%)
0	100	0
1	100	0
36	0	100
39	0	100
44	100	0

Samples were prepared by dissolving peptides in 50% ACN (~0.5 mg/ml) and filtering the solution through a 0.22 μm filter. A 20 μl aliquot of this solution was injected. Average retention times of two runs were taken.

5.3.2 Critical aggregation concentration

CAC values were determined by steady-state fluorescence measurements using pyrene as fluorescent probe, as described in Chapter 4.

5.4 Results and discussion

5.4.1 Theoretical determination of the hydrophobic content

The hydrophobic content of peptide bolaamphiphiles was determined by means of theoretical and experimental methods. Theoretical determination of the peptides' hydrophobicity (CLOGP) was based on two different methods the results of which were compared: the residue addition method (CLOGP_{RESIDUE}) and the fragment addition method (CLOGP_{FRAGMENT}) (Tab. 5.5).

Tab. 5.5: CLOGP values (residue and fragment addition methods) for the synthesised compounds and the parent peptides L3, L4 and L5 (n.d.= not determined)

PEPTIDE	CLOGP _{RESIDUE}	CLOGP _{FRAGMENT}
L3	4.06	4.86
L4	3.26	3.66
L5	2.46	2.46
KL1	n.d.	-1.32
KL2	n.d.	-1.00
KL3	n.d.	-2.59
KL4	n.d.	0.27
OL1	n.d.	-1.85
OL2	-2.07	-5.33
OY1	n.d.	-3.26
OY2	-2.57	-6.75
LO1	n.d.	2.72
LY1	n.d.	5.88

CLOGP_{RESIDUE} values were calculated with formula (3) by simply adding the partial contribution of each amino acid to give the total H. Unfortunately, the recorded values only included natural amino acids, thus making impossible to determine the CLOGP_{RESIDUE} values for

those peptides containing non-natural amino acids (such as 6-Ahx and 9-Anc) (refer to Tab. 5.1). The $CLOGP_{FRAGMENTS}$ values were successfully calculated using Bio-Loom software. As the fragments addition method is based on structural characteristics and not on single amino acid contributions, $CLOGP_{FRAGMENTS}$ values were determined for the entire set of molecules, regardless of the amino acid composition.

The consistency between the two sets of CLOGPs was tested by plotting the values of the one against the other. Figure 5.2 shows the resulting graph, which has a linear correlation between the two sets of data with a correlation coefficient of 0.999 ± 0.001 , thus underlining a good consistency between the data obtained from the two methods.

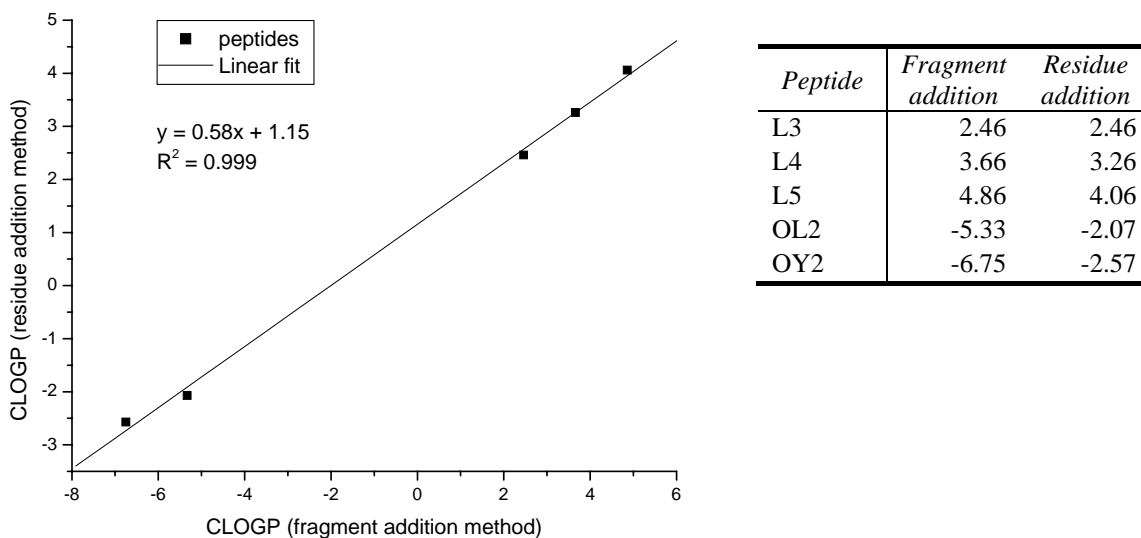


Fig. 5.2: Linear correlation between the two sets of CLOGP values (calculated with the residue addition method and the fragment addition method) for peptides L3, L4, L5, OL2 and OY2.

The two different methods were therefore considered both reliable in terms of determining the hydrophobic content. Because the fragment addition method basically allows the use of any possible amino acid/organic molecules, $CLOGP_{FRAGMENTS}$ were chosen and compared to experimental values (expressed as retention times) obtained by RP-HPLC.

5.4.2 Experimental determination of the hydrophobic content by RP-HPLC

HPLC was chosen for the experimental determination of peptides' lipophilicity, through measurements of the retention times (Kim et al., 2005), especially because of rapidity, sensitivity, the requirement for low amounts of sample and good reproducibility of the determinations. Octadecyl columns (C_{18}) are widely used for this purpose. The results are generally accepted as good estimates of the hydrophobic content of the analyte. In this study the use of a dodecyl column (C_{12}) was investigated and the results obtained compared to those obtained with a C_{18} column with

the same dimensions. Retention times for the synthesised compounds are reported below (Tab. 5.6).

Tab. 5.6: CLOGP_{FRAGMENTS} values and RP-HPLC retention times

PEPTIDE	CLOGP _{FRAGMENT}	t _R (C ₁)	t _R (H ₁)	t _R (C ₁)	t _R (H ₁)
		(min)	(min)	(min)	(min)
		C ₁₂	C ₁₂	C ₁₈	C ₁₈
L3	4.86	36.90	28.26	36.3	20.55
L4	3.66	37.40	28.20	36.27	20.05
L5	2.46	37.30	27.98	36.39	19.8
KL1	-1.32	24.67	11.47	23.26	13.42
KL2	-1.00	21.29	11.00	27.04	14.64
KL3	-2.59	23.30	9.46	22.82	12.57
KL4	0.27	26.00	12.56	29.63	15.35
OL1	-1.85	23.88	11.26	26.17	14.41
OL2	-5.33	20.31	9.39	22.07	12.15
OY1	-3.26	21.43	9.81	23.85	13.18
OY2	-6.75	17.33	8.38	20.12	11.06
LO1	2.72	34.00	17.70	32.59	17.92
LY1	5.88	41.09	22.11	42.52	23.45

Experimental and theoretical analyses of the hydrophobic content were compared by using the RP-HPLC retention times in the two chromatographic columns and the CLOGP_{FRAGMENTS}. The correlation coefficient varied between 0.86 ± 0.01 (gradient H₁) and 0.96 ± 0.01 (gradient C₁) in the dodecyl column (Figs. 5.3 and 5.4) while it was 0.95 ± 0.01 and 0.94 ± 0.01 (respectively) in octadecyl column (Figs. 5.5 and 5.6). Both columns appeared to be suitable for the determination of the hydrophobic content of the synthesised peptides and peptide hybrids. Nonetheless, small differences were noted. The C₁₂ column gave a better correlation when using gradient C₁, which corresponded to a slower increase of the organic modifier (up to 50% B over 33 minutes). On the other hand the correlation was poorer when using gradient H₁, which corresponded to a faster increase of the organic phase (up to 100% B over 35 minutes). Differences in the elution conditions can be translated into diverse interactions between the analyte and the column's hydrophobic phase, which can eventually result in dissimilar values relating to the hydrophobic content of a given molecule. The differences due to the gradients used did not appear to be so important when using a C₁₈ column as the two correlation coefficients were very similar. Hence, this type of column seemed to be less affected by external experimental conditions than the C₁₂ column.

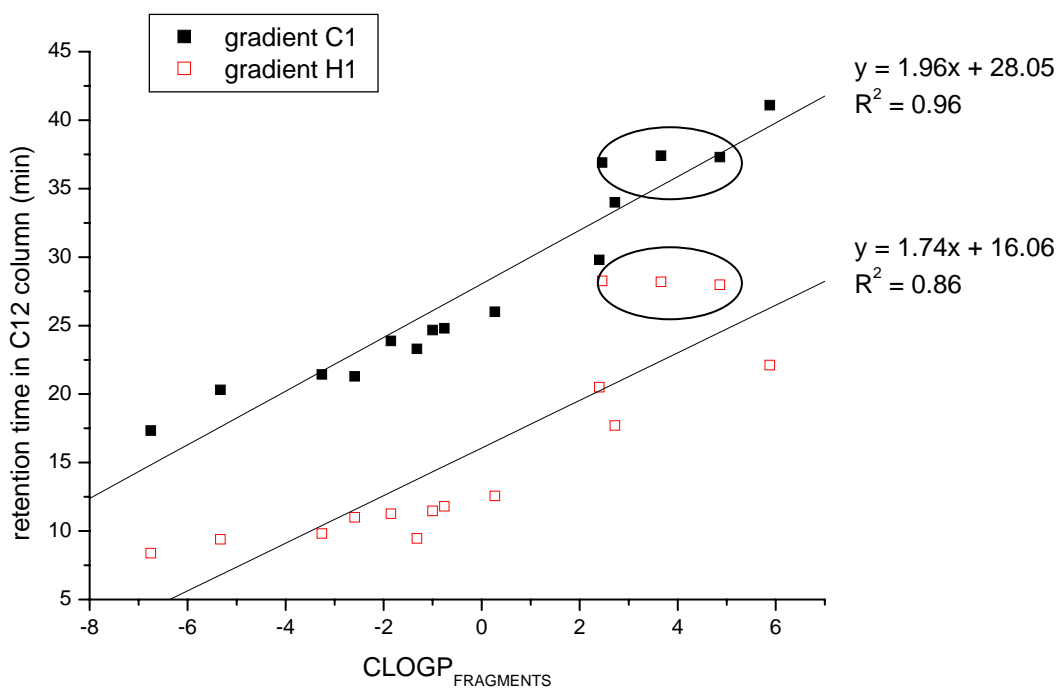


Fig. 5.3: Linear correlation between RP-HPLC retention times of bolaamphiphilic peptides and hybrids in a C₁₂ column and CLOGP values (fragment addition method). The two circles indicate L3, L4 and L5 peptides.

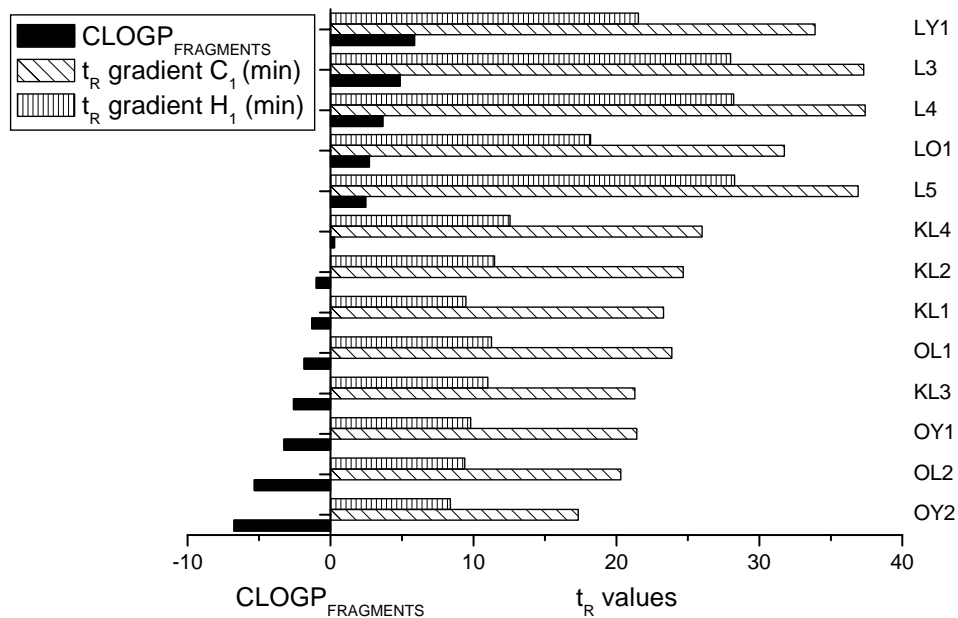


Fig. 5.4: Graphical correlation between RP-HPLC retention times of bolaamphiphilic peptides and hybrids in a C₁₂ column (gradient C₁ and H₁) and CLOGP values (fragment addition method).

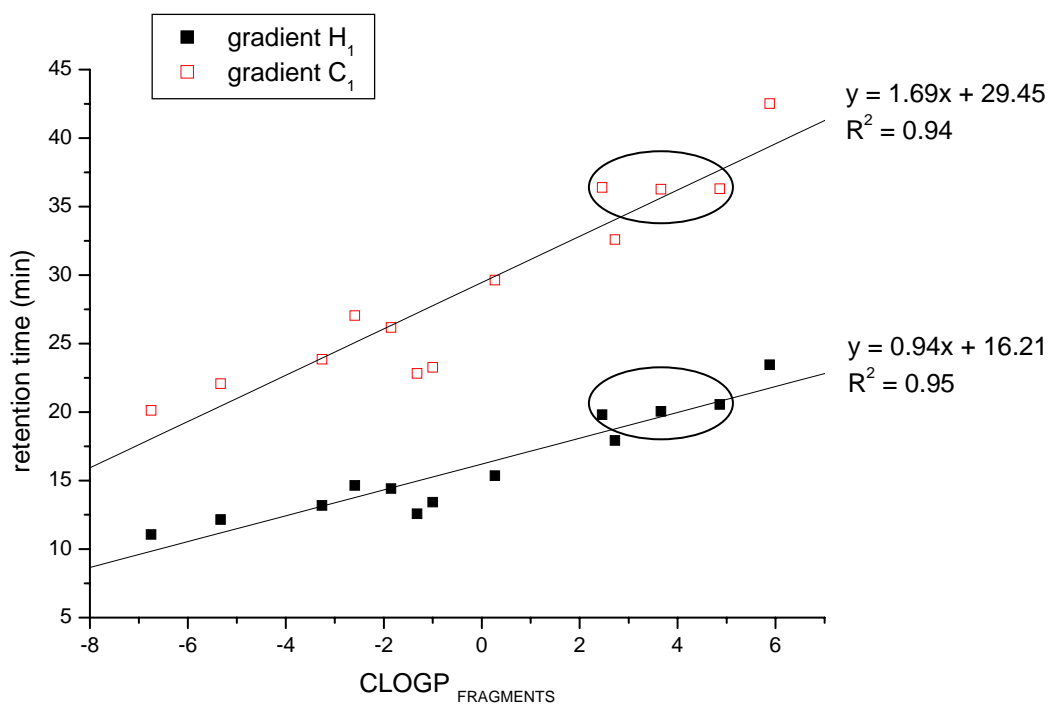


Fig. 5.5: Linear correlation between RP-HPLC retention times of bolaamphiphilic peptides and hybrids in a C₁₈ column and CLOGP values (fragment addition method). The two circles indicate L3, L4 and L5 peptides.

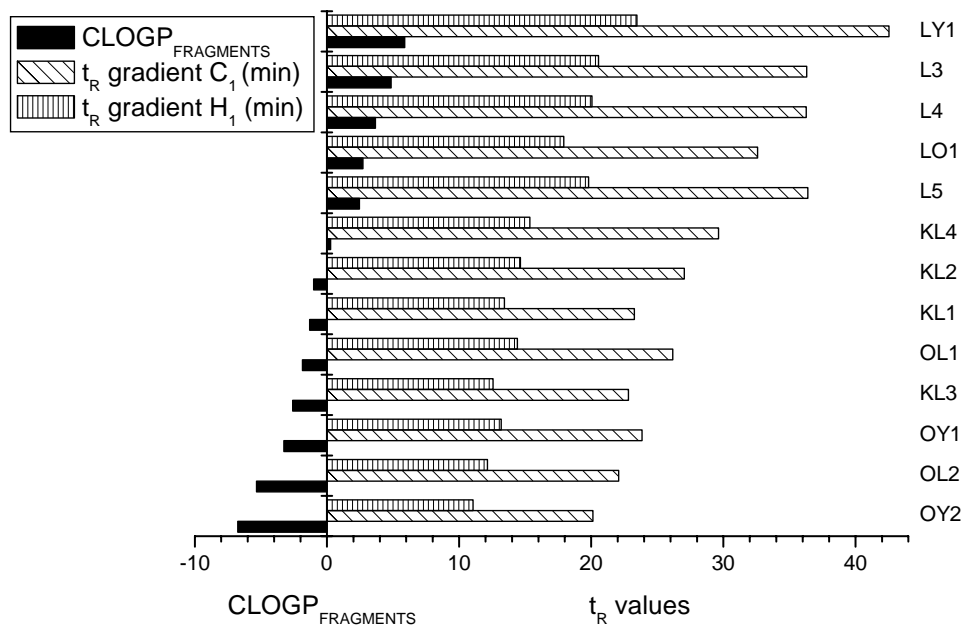


Fig. 5.6: Graphical correlation between RP-HPLC retention times of bolaamphiphilic peptides and hybrids in a C₁₈ column and CLOGP values (fragment addition method).

The chromatographic behaviour of the parent peptides (L3, L4 and L5) was very similar in both columns and gradients. They presented almost the same retention times even if the theoretical hydrophobic content is consistently different (Figs. 5.3 and 5.5, circles). This effect can probably be ascribed to the comparable three-dimensional arrangements of these compounds, as they present an α -helical structure with both hydrophobic and hydrophilic residues (Naidoo, 2004). Possibly the presence of one or two leucine residues more in the poly-leucine chain, which forms the hydrophobic core of these natural bolaamphiphiles, do not change much of the exterior surface that ultimately interacts with the column's hydrophobic phase (Fig. 5.7).

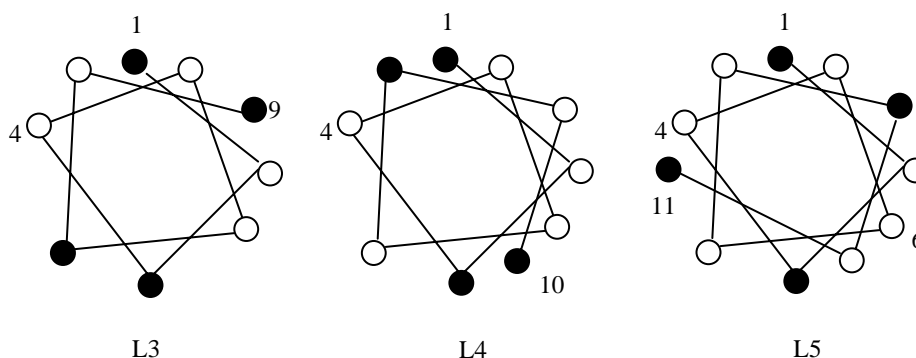


Fig. 5.7: Helical wheel representation of L3, L4 and L5 peptides. Colour designation: black = Lys; white = Leu. Computer-generated helical wheels were obtained by using Peptide Companion software (CSPS, Tucson, AZ, USA).

5.4.3 Correlation between hydrophobicity and aggregation behaviour

Aggregation depends on many factors, among them van der Waals interactions, hydrogen bonds, ionic bonds and hydrophobic interactions (Zhang and Altman, 1999). Some of these forces can prevail over others but the way in which they interfere with each other is not straightforward. Definitely, hydrophobicity plays an important role in the determination of the self-assembly behaviour of organic molecules in solution (Zhang et al., 1993; Gazit, 2002; Santoso and Zhang, 2004). Therefore, peptides rich in hydrophobic amino acids (such as tyrosine, leucine, isoleucine, tryptophan, phenylalanine) are considered to be more likely to self-assemble and aggregate. In this study, peptides rich in tyrosine showed low CAC values, as determined by steady-state fluorescence measurements (see Chapter 4 for details), but the process was influenced by other elements as well. The three-dimensional structure and the possibility to create hydrogen bonds, for example, played a key role in the aggregation/self-assembly process, as testified by different CACs and aggregation profiles of OY1 and OY2 or OL1 and OL2. Therefore, it was important to evaluate the correlation between hydrophobicity (expressed as $\text{CLOGP}_{\text{FRAGMENTS}}$ or t_R) and CAC values (in 0.1% TEA) so as to assess the real influence of hydrophobicity on the self-assembly. The following

graphs show CAC values compared to retention times in HPLC (Fig. 5.8) and $CLOGP_{FRAGMENTS}$ (Fig. 5.9).

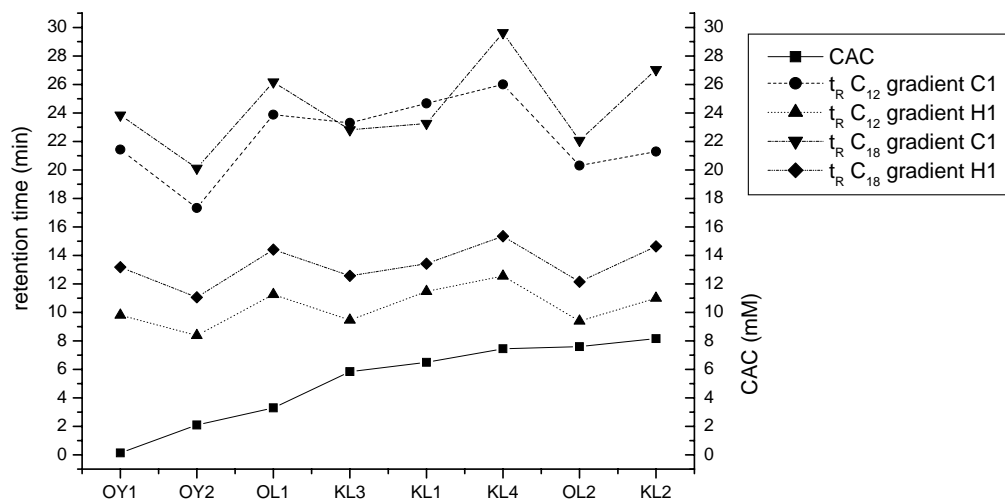


Fig.5.8: Aggregation behaviour (expressed by CAC values) compared to hydrophobic content (expressed by retention times in RP-HPLC).

The good correlation between the four sets of t_R (obtained using different columns and gradients) was once again underlined by the similar pattern of the lines connecting each data point (Fig. 5.8). Nonetheless, it was not possible to establish a direct correlation between the sets of values from HPLC analysis and CAC data. Importantly, increased CACs did not correspond to a proportional increase of HPLC retention times, underlying the limitations of this kind of experimental determination of H.

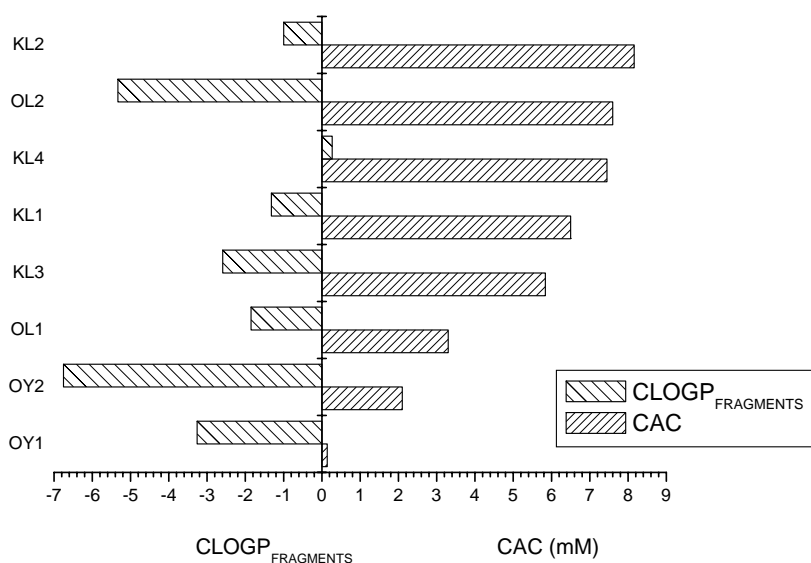


Fig. 5.9: Aggregation behaviour (expressed by CAC values) compared to hydrophobic content (expressed by $CLOGP_{FRAGMENTS}$ values).

The use of $\text{CLOGP}_{\text{FRAGMENTS}}$ values as a hydrophobicity index instead of the HPLC retention times also did not provide a straightforward correlation. In Figure 5.9 some peptide bolaamphiphiles are listed in order of increasing CAC. Bars referring to CLOGP values do not follow a precise order, and especially OL2 and OY2 seem to show no relationship with the aggregation process.

The removal of data related to proline-containing peptides (OL2 and OY2) results in a more meaningful diagram (Fig. 5.10). Peptide bolaamphiphiles containing 9-aminononanoic acid as hydrophobic skeleton between the two charged heads showed a better correlation between the aggregation process and hydrophobicity, the latter as expressed by the $\text{CLOGP}_{\text{FRAGMENTS}}$.

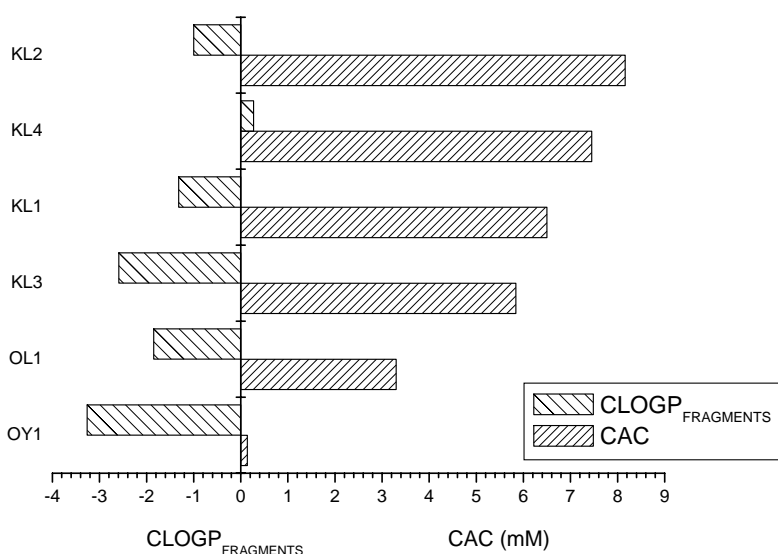


Fig. 5.10: Aggregation behaviour (expressed by CAC values) compared to hydrophobic content (expressed by $\text{CLOGP}_{\text{FRAGMENTS}}$ values) for peptide bolaamphiphiles including 9-Anc.

The tendency shown by ω -AA-containing molecules is consistent with the literature (Santoso and Zhang, 2004): the greater the hydrophobic content, the stronger is the self-assembly, the latter expressed by critical aggregation concentrations. Moreover, aromatic residues played a key role through the π -stacking of their side chains (Gazit, 2002), as was already underlined in Chapter 4. The anomaly which distinguishes the dissimilar behaviours of OY2 and OL2 can possibly be ascribed to the presence of proline. Its effects on the aggregation were discussed in Chapter 4, where it proved to increase the CAC in homologues compounds (such as OY1/OY2 and OL1/OL2). It was therefore confirmed that the modifications of the 3D-structure caused by proline played a key role in determining the aggregation behaviour of proline-containing peptides.

5.5 Conclusions

The hydrophobic content of the synthesised peptide bolaamphiphiles was determined both experimentally and theoretically. RP-HPLC is recognised as a versatile technique for such determination and it proved to work well. Different conditions, columns and elution programmes were used. On the other hand, the theoretical determination was effectively performed by using two different approaches, based on the residue addition method and on the fragment addition method. The latter ($\text{CLOGP}_{\text{FRAGMENTS}}$) was especially useful for the further investigation of the correlation with the data obtained from the experimental technique. Such a correlation revealed a good consistency, although slightly different correlation coefficients were found. The use of an octadecyl column gave similar results with both of the two gradients, thus indicating that it has an inherent strong ability to interact with the analyte regardless of the conditions used. Vice versa, the use of a dodecyl column showed to be influenced by the experimental conditions (such as the gradient). The correlation between $\text{CLOGP}_{\text{FRAGMENTS}}$ and the t_{R} (C_{12}) for the synthesised bolaamphiphilic peptides was shown to vary to some extent with the use of one or the other gradient. Therefore, in the present study, the use of a C_{18} column seemed to give more reliable results in terms of hydrophobic content determination.

Interestingly, it was also possible to investigate the effect of hydrophobicity on the self-assembly behaviour in water. In the previous chapter the relationship between hydrophobic AA and enhanced self-organisation properties was already pointed out (Zhang et al., 1993). The experimental observations made during steady-state fluorescence measurements about the role of hydrophobic residues were confirmed. Compounds showing low CAC were also characterised by a significant hydrophobic content (expressed by $\text{CLOGP}_{\text{FRAGMENTS}}$). On the other hand, compounds with high CACs proved to have a low hydrophobic content. The only exception was represented for proline-containing peptides, where the influence of the 3D structures on the aggregation was much more important than the H.

The current study presented some limitations. As previously discussed, the use of gradient RP-HPLC for hydrophobicity determination is limited to some particular cases and isocratic liquid chromatography is generally preferred. Capacity factors are related to retention times obtained by isocratic elution and therefore were not determined. The lack of a parameter independent from the experimental conditions could possibly be translated into poorer R^2 values when theoretical and experimental data were compared. A similar problem was also found when comparing t_{R} and CAC data, resulting in an absence of direct correlation, which was later found using $\text{CLOGP}_{\text{FRAGMENTS}}$ values.

5.6 References

Cimpan G, Hadaruga M and Miclaus V (2000) Lipophilicity characterisation by reversed-phase liquid chromatography of some furan derivatives, *Journal of Chromatography A*, 869, 49-55.

Donnelly A, Kellaway IW, Farr SJ, Taylor G, Tudball N and Gibson M (1996) The influence of lipophilicity upon the nasal absorption of a series of hexapeptides, *International Journal of Pharmaceutics*, 135, 191-197.

Fauchère J-L and Pliška V (1983) Hydrophobic parameters p of amino acid side chains from the partitioning of N-acetyl amino acid amides, *European Journal of Medicinal Chemistry*, 18, 369-375.

Fauchère J-L (1996) Lipophilicity in peptide chemistry and peptide drug design, in *Lipophilicity in drug action and toxicology* (Pliška V, Testa B and van de Waterbeemd H Eds.) Methods and principles in medicinal chemistry, Vol. 4 (pp. 355-374), VCH; Weinheim.

Fujita T, Iwasa J and Hansch C (1964) A new substituent constant, π , derived from partition coefficients, *Journal of the American Chemical Society*, 86, 5175-5180.

Gazit E (2002) A possible role for π -stacking in the self-assembly of amyloid fibrils, *FASEB Journal*, 16, 77-83.

Kaliszan R, Haber P, Czek TB, Siluk D and Valko K (2002) Lipophilicity and pK_a estimates from gradient high-performance liquid chromatography, *Journal of Chromatography A*, 965, 117-127.

Kim S, Kim SS and Lee BJ (2005) Correlation between the activities of α -helical antimicrobial peptides and hydrophobicities represented as RP-HPLC retention times, *Peptides*, 26, 2050-2056.

Klein CDP, Tabeteh GF, Laguna AV, Holzgrabe U and Mohr K (2001) Lipophilicity and membranes interaction of cationic-amphiphilic compounds: syntheses and structure-property relationships, *European Journal of Pharmaceutical Science*, 14, 167-175.

Kyte J and Doolittle RF (1982) A simple method for displaying the hydrophobic character of a protein, *Journal of Molecular Biology*, 157, 105-132.

Hallgas B, Patonay T, Kiss-Szikszai A, Dobos Z, Hollósy F, Erős D, Órfi L, Kéri G and Idei M (2004) Comparison of measured and calculated lipophilicity of substituted auronones and related compounds, *Journal of Chromatography B*, 801, 229-235.

Leo AJ (1996) The future of log P calculation, in *Lipophilicity in drug action and toxicology* (Pliška V, Testa B and van de Waterbeemd H Eds.) Methods and principles in medicinal chemistry, Vol. 4 (pp. 157-172), VCH; Weinheim.

Meng QC, Zou H, Johansson JS and Eckenhoff RG (2001) Determination of the hydrophobicity of local anesthetic agents, *Analytical Biochemistry*, 292, 102-106.

Naidoo VB (2004) The supramolecular chemistry of novel synthetic biomacromolecular assemblies, PhD thesis, University of Stellenbosch.

OECD – Organisation for Economic Co-operation and Development (1989) Partition coefficient (n-octanol/water), high performance liquid chromatography (HPLC) method, OECD guideline for testing of chemicals; Paris.

Pignatello R and Puglisi G (2000) Lipophilicity evaluation of RP-HPLC of two homologous series of methotrexate derivatives, *Pharmaceutica Acta Helvetiae*, 74, 405-410.

Rekker RF (1977) The hydrophobic fragment constant, *Pharmacochimistry Library*, Vol. 1, Elsevier; New York.

Richards WG (1996) Theoretical calculation of partition coefficients, in *Lipophilicity in drug action and toxicology* (Pliška V, Testa B and van de Waterbeemd H Eds.) *Methods and principles in medicinal chemistry*, Vol. 4 (pp. 173-180), VCH; Weinheim.

Santoso SS and Zhang S (2004) Self-assembled nanomaterials, in Nalwa HS (Ed.) *Encyclopaedia of nanoscience and nanotechnology*, Vol. 9 (pp. 459-471) American Scientific Publishers; Stevenson Ranch.

Tao P, Wang R and Lai L (1999) Calculating partition coefficients of peptides by the addition method, *Journal of Molecular Modeling*, 5, 189-195.

Tute MS (1996) Lipophilicity: a history, in *Lipophilicity in drug action and toxicology* (Pliška V, Testa B and van de Waterbeemd H Eds.) *Methods and principles in medicinal chemistry*, Vol. 4 (pp. 7-26), VCH; Weinheim.

vd Waterbeemd H, Kansy M, Wagner B and Fischer H (1996) Lipophilicity measurements by reversed-phase high performance liquid chromatography (RP-HPLC), in *Lipophilicity in drug action and toxicology* (Pliška V, Testa B and vd Waterbeemd H Eds.) *Methods and principles in medicinal chemistry*, Vol. 4 (pp. 73-87), VCH; Weinheim.

Wimley WC, Creamer TP and White SH (1996) Solvation energies of amino acid side chains and backbone in a family of host-guest pentapeptides, *Biochemistry* 35, 5109-5124.

Wimley WC and White SH (1996) Experimentally determined hydrophobicity scale for proteins at membrane interfaces, *Nature Structural Biology*, 3, 842-848.

Zhang S and Altman M (1999) Peptide self-assembly in functional polymer science and engineering, *Reactive and Functional Polymers*, 41, 91-102.

Zhang S, Holmes T, Locksmith C and Rich A (1993) Spontaneous assembly of self-complementary oligopeptides to form a stable macroscopic membrane, *Proceedings of the National Academy of Sciences*, 90, 3334-3338.

Chapter 6

Determination of biological properties of peptides and peptide hybrids

6.1 Introduction

The interest in bolaamphiphilic compounds as possible new antimicrobial drugs is based on their detergent-like structure, which resembles surfactants. The study of natural-based bolaamphiphiles with biological activity is therefore a very good starting point for the development of active leader molecules. During the 1990s novel peptide-based bolaamphiphilic compounds were de novo designed around an amino acid pattern resulting from a natural antimicrobial peptide (Alvarez-Bravo et al., 1994; Hirakura et al., 1996). The resulting general antimicrobial motif had a bolaamphiphilic structure and was made of different combinations of lysine and leucine (KLKL_nKLK-NH₂, where n = 3, 4, 5) (Alvarez-Bravo et al., 1994). Because of its structure, the poly-leucine chain – which connects the two charged moieties – was replaced by non-natural amino acids to give comparable length (Naidoo, 2004). Still, little was known about the effect on the biological activity of the substitution of leucine with hydrophobic non-natural amino acids. In the present study ω-amino acids were used to create peptide hybrids and their biological properties fully investigated. Further modifications were also used and novel potentially active sequences were designed (refer to Chapter 3 for detailed explanations).

The antimicrobial activity of novel bolaamphiphilic peptides and hybrids was assessed in different ways in order to possibly relate it to structure and AA composition. A general screening was carried out by using the Bauer-Kirby disk diffusion test (radial diffusion assay) (Bauer et al., 1966) and then the minimum inhibitory concentration (MIC) was assessed (Wu and Hancock, 1999; Du Toit and Rautenbach, 2000). Potential toxicity was evaluated using human red blood cells (hRBCs) as model mammalian cells. The selectivity towards bacteria was also investigated using dye-loaded liposomes presenting neutral or negatively charged membranes (Epanand and Epanand, 2003).

6.2 Materials

Peptides and peptide hybrids were synthesised on solid-phase using the Fmoc-polyamide protocol and purified by RP-HPLC as previously described (see Chapter 3).

Acetic acid was supplied by BDH (Poole, UK). Fraction V bovine serum albumin (BSA, 99%) was supplied by Boehringer Mannheim (Mannheim, Germany).

Sterile filter paper disks for the Bauer-Kirby diffusion test, Mueller-Hinton agar (MHA, pH 7.4 ± 0.2), Mueller-Hinton broth (MHB, pH 7.4 ± 0.2) and ATCC bacterial strains were provided by Dr AC Whitelaw (Microbiology, National Health Laboratory Service, Groote Schuur Hospital, University of Cape Town).

Saponin by Aldrich (Steinheim, Germany), hRBCs (2% suspension) and culture medium for the haemolysis tests were kindly provided by Dr HC Hoppe (Clinical Pharmacology, Groote Schuur Hospital, University of Cape Town).

Tryptone soy broth (TSB, soybean-casein digest medium USB, pH 7.3 ± 0.1) and tryptone soy agar (TSA, soybean-casein digest agar medium USB, pH 7.3 ± 0.1) were from Biolab Diagnostics (Midrand, South Africa). Hammersten-casein was from USB Corp. (OH, USA). Polypropylene microtitre plates were from Corning Inc. (NY, USA). Gramicidin S (Gram S) was from Aldrich (Steinheim, Germany). They were all kindly provided by Dr M Rautenbach (Biochemistry, US).

Egg 3-SN-Phosphatidylcholine (EPC, > 99%), egg phosphatidylglycerol (EPG, > 99%) and cholesterol (CHOL, 99%) were bought from Aldrich (Steinheim, Germany). 5(6)-carboxyfluorescein (CF, > 99%), Triton[®] X-100, sodium azide (99%) and Sephadex G50 were supplied by Fluka (Buchs, Switzerland).

Methanol (MeOH, HPLC grade) and isopropyl alcohol (HPLC grade) were from Aldrich (Steinheim, Germany). Technical grade DCM was used after distillation (refer to Section 4.3.1).

Potassium chloride (99%), disodium hydrogenphosphate (99%) and potassium dihydrogenphosphate (99%) were from Merck (Darmstadt, Germany). Tris(hydroxyethyl) amino methane (Tris, 99.7%), sodium chloride (99%), disodium ethylenediaminetetracetate dihydrate ($\text{Na}_2\text{EDTA}\cdot 2\text{H}_2\text{O}$, 99%), ferric chloride hexahydrate (99%) and ammonium thiocyanate (99%) were from Saarchem (Wadeville, South Africa).

Analytical grade water was obtained by filtering glass-distilled water with a Millipore Milli Q[®] (Bedford, MA, USA) 0.22- μm filtering system.

6.3 Experimental methods

6.3.1 Antimicrobial activity

6.3.1.1 Bauer-Kirby disk diffusion test

Peptides were dissolved at a concentration of 50 µg/µl in 0.01% AcOH / 0.2% BSA. An aliquot of 10 µl of the stock solutions (500 µg of peptide) was placed on each disk. The entire set of peptides and hybrids thereof were tested against five different strains of bacteria: *E. coli* (ATCC 25922), *S. aureus* (ATCC 25923), *P. aeruginosa* (ATCC 27853), *E. faecalis* (ATCC 29212) and *S. marcescens* (clinical isolate). Bacteria were plated in MHA. An aliquot of µl 10 of 0.01% AcOH / 0.2% BSA was used as negative control. Positive controls were performed as routine analysis by the National Health Laboratory Service (UCT Hospital).

Peptides and controls were incubated aerobically for 18 h at 35 °C before evaluating the presence of inhibition areas.

6.3.1.2 MIC determination (I)

A first method for the MIC determination was a classical broth microdilution assay modified for cationic antimicrobial peptides according to the recommendations of REW Hancock Laboratory (Wu and Hancock, 1999)^f. MIC was determined against *E. coli* (ATCC 25922), *S. aureus* (ATCC 25923) and *P. aeruginosa* (ATCC 27853). Stock solutions were prepared by dissolving peptides in 0.01% AcOH / 0.2% BSA at a starting concentration of 640 µg/ml, then diluted with the same solution by serial doubling dilutions. Bacterial cultures were diluted in MHB to 5 x 10⁵ CFU/ml and plated in ELISA plates. Peptides were added so as to reach a final concentration 10 times lower than the stock solutions. Peptides were incubated aerobically for 18 h at 37 °C. MIC was represented by the lowest concentration of peptides that clearly inhibited bacterial growth.

6.3.1.3 MIC determination (II)

A second method for the determination of MIC was based on a micro-gel well diffusion assay (Du Toit and Rautenbach, 2000).

A starter culture of *E. coli* HB101 was grown overnight at 37 °C in TSB to mid-log phase (± 0.6 OD unit at 620 nm). A 1% sub-culture was then grown for about three hours (± 0.28 OD unit at 620 nm).

Plates were sterilised with isopropyl alcohol, dried overnight at 60 °C, then blocked for 60 minutes with 200 µl/well sterile 0.5% Hammersten casein in PBS, and finally dried overnight under UV light to ensure sterility.

^f See: www.cmdr.ubc.ca/bobh/methods.php (last accessed on 19/08/05).

Peptides were dissolved in two different solvent systems [(A) Milli-Q[®] water, (B) 0.01% AcOH / 0.2% BSA] to give 0.5 mM stock solutions and then diluted in polypropylene ELISA plates by serial doubling dilutions. An aliquot of 20 μ l of peptide solution was added to 80 μ l of bacterial suspension and the plates incubated aerobically at 37 °C for 18 \pm 0.5 h. Solvents without peptides were used as negative control while Gram S was used as positive control. Sterility and bacterial growth were also monitored. Plates were then read by measuring light dispersion at 620 nm with a Multiscan Plus MKII plate reader (Titertek, AL, USA). The percentage of inhibition was calculated according to the following equation:

$$\% \text{ inhibition} = 100 - [100 \times (\text{LD}_{\text{sample}} - \text{LD}_{\text{bgd}}) / (\text{LD}_{\text{growth}} - \text{LD}_{\text{bgd}})] \quad (4)$$

where $\text{LD}_{\text{sample}}$ is the light dispersion in the well, LD_{bgd} is the background light dispersion in a well containing bacteria and solvent while $\text{LD}_{\text{growth}}$ is the light dispersion of the untreated bacteria.

Experiments were performed in triplicate.

6.3.2 Haemolytic activity

Haemolytic activity was determined against a fresh 2% suspension of hRBCs (type 0+) from healthy donors (Western Province Blood Transfusion Service, South Africa). The cells were washed in RPMI 1640 BioWhittaker[™] culture medium (supplemented with 50 mM glucose, 0.65 mM hypoxanthine, 25 mM Hepes, 0.2% Na_2HCO_3 , 0.048 mg/ml gentamicin and 0.5% Albumax II) by centrifugation at 1000 rpm for 5 min and the pellet stored at 4 °C for up to three weeks.

Peptides were dissolved in a fresh 0.01% AcOH / 0.2% BSA solution with a final concentration of 1 mM. The stock solutions were diluted in ELISA plates with the same solvent by serial doubling dilutions. An aliquot of 10 μ l of the diluted solutions was added to 90 μ l of hRBCs suspension placed into ELISA plates.

Solvent without peptides was used as negative control and saponin (final concentration 0.05%) was used as positive control. Plates were incubated at 37 °C for 24 h and then centrifuged at 1000 rpm for 2 min. An aliquot of 10 μ l of supernatant was transferred into an ELISA plate and diluted 10 times with distilled water. Absorbance of released hemoglobin was recorded at 404 nm with an H72 plate reader (Anthos Labtec, Austria). All experiments were performed in quadruplicate. The percentage of haemolysis was calculated according to the following formula:

$$\% \text{ haemolysis} = [(A_{\text{peptide}} - A_{\text{blank}}) / (A_{\text{Saponin}} - A_{\text{blank}})] / 100 \quad (5)$$

where A_{peptide} is the absorbance of the peptide solution at 404 nm, A_{blank} the absorbance at 404 nm without peptide (0% haemolysis) and A_{Saponin} the absorbance in the presence of saponin (100% haemolysis).

6.3.3 Dye-leakage assay from liposomes

CF-loaded liposomes (80 μl) in buffer (10 mM Tris, 150 mM NaCl, 0.1 mM $\text{Na}_2\text{EDTA}\cdot 2\text{H}_2\text{O}$, pH 7.4) were placed in black 96-well plates. Peptides were dissolved in the same buffer to give 0.5 mM stock solutions and then diluted in polypropylene ELISA plates by serial doubling dilutions. An aliquot of 20 μl was added to the liposome suspension. Triton[®] X-100 (final concentration 0.1%) was used as positive control and the abovementioned buffer as blank. Dye leakage was monitored by fluorescence emission (Duzgünes, 2003). Plates were incubated for 2 h at 37 °C before measuring the fluorescence emission with a FL_X800 Microplate Fluorescence Reader (Kontron Bio-Tek, Italy). An excitation wavelength of 460/40 nm and an emission wavelength of 560/40 nm were used. The percentage of leakage was calculated according to the following formula:

$$\% \text{ leakage} = [(F_{\text{peptide}} - F_{\text{blank}}) / (F_{\text{Triton X-100}} - F_{\text{blank}})] / 100 \quad (6)$$

where F_{peptide} is the fluorescence emission of the peptide solution, F_{blank} the fluorescence without peptide and $F_{\text{Triton X-100}}$ the fluorescence in the presence of Triton[®] X-100 (complete lysis of the liposomes). Experiments were carried out in triplicate.

6.3.3.1 Preparation of liposomes

Large unilamellar vesicles by extrusion technique (LUVETs) were prepared according to literature (Hope et al., 1985; Mui et al., 2003). Two different kinds of liposomes were prepared: negatively charged (EPC:EPG, 10:1 w/w) and neutrally charged (EPC:CHOL, 10:1 w/w). Lipids (11 mg) were dissolved in MeOH/DCM and thoroughly dried under high vacuum to form a thin layer on the vessel wall. The lipid film was then hydrated with 0.5 ml of a buffer (10 mM Tris, 150 mM NaCl, 0.1 mM $\text{Na}_2\text{EDTA}\cdot 2\text{H}_2\text{O}$, pH 7.4) containing 40 mM 5(6)-carboxyfluorescein and vigorously mixed for 1 min to form large multilamellar vesicles (LMVs). Hydration was performed at 25 °C, above the transition temperature (T_c) of the lipid mixtures (which is around 0 °C for both EPC and EPG). The suspension of LMVs was disrupted by five freeze/thaw cycles. The lipid suspension was then extruded through a 100-nm polycarbonate membrane twenty-one times using a stainless steel liposome mini-extruder (Avanti Polar Lipids, AL, USA), according to the manufacturer's instructions. Extrusion was performed at 25 °C. Untrapped dye was removed by gel filtration through a Sephadex G50 column (1 x 20 cm), eluted with 10 mM Tris, 150 mM NaCl, 0.1 mM $\text{Na}_2\text{EDTA}\cdot 2\text{H}_2\text{O}$, pH 7.4. Elution was monitored by visual observation and the collected

fractions were analysed with a Lambda 20 UV-VIS spectrophotometer (Perkin Elmer, UK) measuring absorbance at 490 nm (for CF) and light dispersion at 620 nm (for the liposomes).

Lipid concentration was determined as described in Section 6.3.3.2.

6.3.3.2 Determination of lipid concentration

Lipid concentration of liposomal suspensions was determined by forming a complex between phospholipids and ammonium ferrothiocyanate, according to Stewart (Stewart, 1980). The standard ammonium ferrothiocyanate solution (0.1 N) was prepared by dissolving ferric chloride hexahydrate (27.03 g) and ammonium thiocyanate (30.40 g) in Milli-Q[®] water and making up to one litre.

Duplicate volumes (between 0.1 and 1 ml) of a solution of 10.0 mg of EPC in 100 ml of DCM were mixed with 2 ml of ammonium ferrothiocyanate solution. DCM was added to reach a volume of 4 ml. The biphasic system was shaken for 1 min. The organic phase was removed and the optical density measured at 488 nm with a Lambda 20 UV-VIS spectrophotometer (Perkin Elmer, UK). OD values were plotted against EPC concentration to give a calibration curve with $R^2 = 0.99 \pm 0.01$. Lipid concentration was calculated by using the following equation:

$$\text{concentration } (\mu\text{M}) = [1172.43 \times \text{OD}_{488 \text{ nm}}] - 1.83 \quad (7)$$

where $\text{OD}_{488 \text{ nm}}$ is the optical density of the samples (at known concentration) at 488 nm.

An aliquot of 100 μl of liposome suspension was treated with 2 ml of ammonium ferrothiocyanate solution. DCM (2 ml) was added and the system was shaken for 1 min. The organic phase was removed and the OD measured at 488 nm. The phospholipid content was determined by using formula (7). An average over two determinations was recorded.

6.4 Results and discussion

6.4.1 Antimicrobial properties

The Bauer-Kirby disk diffusion test is a general radial diffusion test for assessing the antimicrobial activity of a broad range of molecules (WHO, 1961; NCCLS, 1975). It is based on the assumption that the diffusion through the disk/gel is the same for every compound tested. The molecules are commonly classified according to the diameter of the inhibition area: active ($d > 10$ mm), non-active (no inhibition detected) or partially active ($0 \text{ mm} < d < 11 \text{ mm}$) (Fig. 6.1).

In this study some peptides were found to be active against *E. coli* (KL2), *S. aureus* (KL2 and OY1) and *P. aeruginosa* (LO1). KL4 was found to be partially active against *E. coli* and *S. aureus*. The actual diameters of the inhibition zones are listed in Table 6.1.

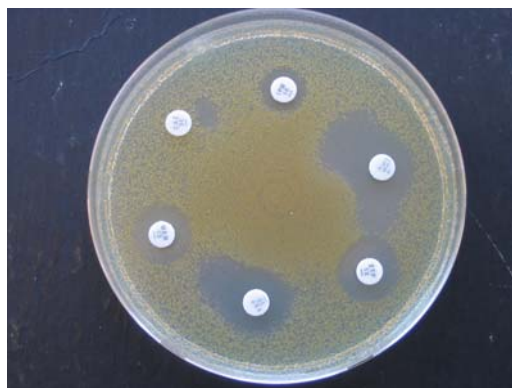


Fig. 6.1: Example of results obtained by Bauer-Kirby test on antimicrobial compounds (kindly provided by Dr AC Whitelaw, Microbiology, UCT).

Tab. 6.1: Antimicrobial activity of the synthesised compounds according to the Bauer-Kirby disk diffusion test performed against [a] *E. coli*, [b] *S. aureus*, [c] *P. aeruginosa*, [d] *E. faecalis* and [e] *S. marcescens* (diameters of inhibition areas are reported in mm; - = no inhibition)

PEPTIDE	disk content (μg)	a	b	c	d	e
KL1	500	-	-	-	-	-
KL2	500	15.0	16.7	-	-	-
KL3	500	-	-	-	-	-
KL4	500	0.4	0.5	-	-	-
OL1	500	-	-	-	-	-
OL2	500	-	-	-	-	-
OY1	500	-	12	-	-	-
OY2	500	-	-	-	-	-
LO1	500	-	-	11.2	-	-
LY1	500	-	-	-	-	-

Nonetheless, most of the compounds did not show any activity with this test, for various reasons. Reduction of antimicrobial activity by aggregation of peptides in different culture media (such as agar and agarose) was reported long ago (Hider et al., 1983). The parent compounds L3, L4 and L5 for example, were also studied in relation with their aggregation in culture medium (Alvarez-Bravo et al., 1994; Rautenbach et al., 2006). Aggregation could also explain the loss of biological activity for the peptides derived from L3. However, the introduction of non-natural AAs and the modification of the secondary structure due to such AAs could also be detrimental to the expression of any biological activity.

Therefore, after the abovementioned general test failed to highlight differences in biological activity, further tests were necessary. MIC values against the same bacterial strains were assessed with a test specifically modified for cationic antimicrobial peptides. This test was performed in solution to highly reduce (if not completely avoid) aggregation due to the medium. Unfortunately, MICs were found to be higher than the highest concentration used (64 µg/ml, approximately 70 µM) for the entire set of peptides tested (Tab. 6.2). Even those peptides which were reported to possess impressively low MICs (Naidoo, 2004), such as KL2 and KL4, did not show noteworthy MIC values.

Tab. 6.2: MIC values for peptides and peptide hybrids
(MIC values in square brackets are taken from Naidoo, 2004)

PEPTIDE		L3*	L4*	L5*	KL1	KL2	KL3	KL4	OL1	OL2	OY1	OY2	LO1	LY1
MIC (µg/ml)	<i>E. coli</i>	8	32	20	> 64	> 64 [16]	> 64	> 64 [4]	> 64	> 64	> 64	> 64	> 64	> 64
	<i>S. aureus</i>	2	2	2	> 64	> 64 [1]	> 64	> 64 [0.5]	> 64	> 64	> 64	> 64	> 64	> 64

* Values taken from Alvarez-Bravo et al., 1994.

To confirm these results, a second MIC protocol was used, based on a micro-well diffusion assay modified from Du Toit and Rautenbach (Du Toit and Rautenbach, 2000). It offered the advantage of determining the bacterial growth inhibition by measuring the OD at 620 nm instead of visually observing the inhibition. In this way it was possible to establish whether the compound tested had any sort of activity (including inhibition lower than 100%), independently from the investigator's optical perception. Moreover, by using this protocol, other studies pointed out the possibility to establish the biological activity of molecules that can aggregate in solution, such as the bolaamphiphilic peptides and peptide hybrids that this study focuses on. Rautenbach et al. (Rautenbach et al., 2006) tested the antimicrobial properties of L3, L4 and L5 peptides with this assay. The data indicate that under these conditions only L3 reaches 100% of bacterial growth inhibition, while L4 and L5 are active up to only 60% (L4) and 20% (L5). See Figure 6.2. At high

concentration, L4 and L5 lose substantial antimicrobial activity and, above 60 μM , the bacterial growth inhibition decreases to less than 50% (around 0% for L5). Such a drastic change in the activity-concentration plot of L4 and L5 was correlated to aggregation in the culture medium (Rautenbach et al., 2006).

The synthesised peptides were tested by a similar method and it was possible to confirm a trend in which the activity slightly increases with increasing concentrations of peptide. However, the activity was found to be modest throughout the range of concentrations used (around 10% of growth inhibition at 100 μM) and it was not possible to determine a minimum inhibitory concentration. Figures 6.3, 6.4 and 6.5 refer to the activity trend for compounds KL2, OY1 and LO1[∞] compared to a typical concentration-response curve of Gram S.

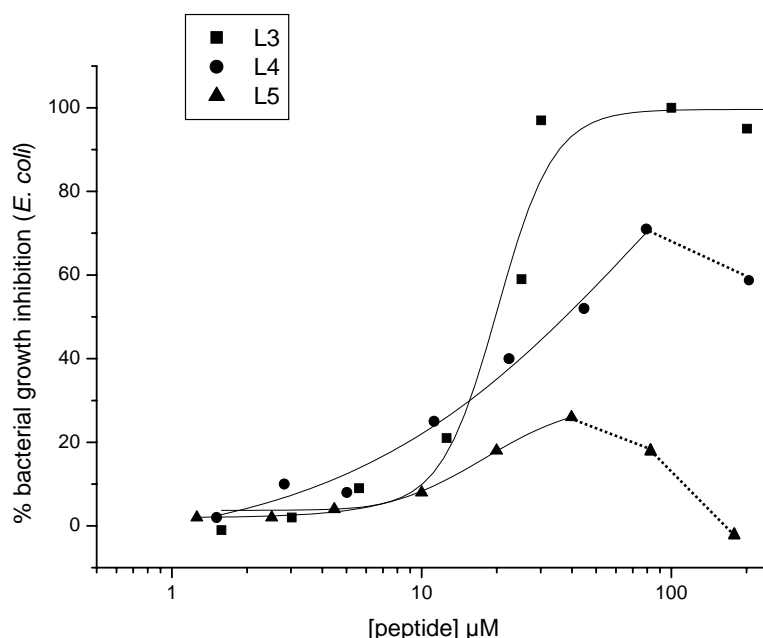


Fig. 6.2: MIC determination of peptides L3, L4 and L5 with a micro-well diffusion assay (modified from Rautenbach et al., 2006).

[∞] Only compounds classified as active with the Bauer-Kirby disk diffusion test were further tested by this method.

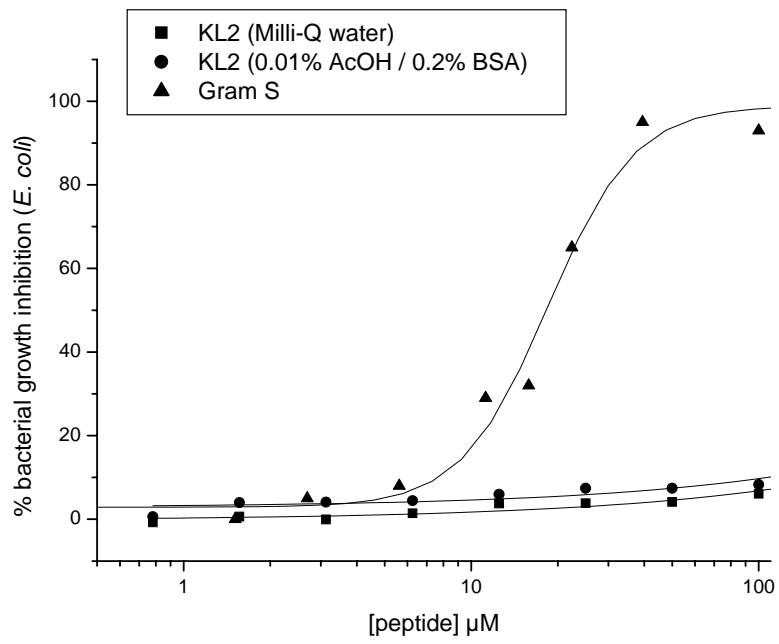


Fig. 6.3: MIC determination of KL2 (Gram S plot adapted from Rautenbach et al., 2006).

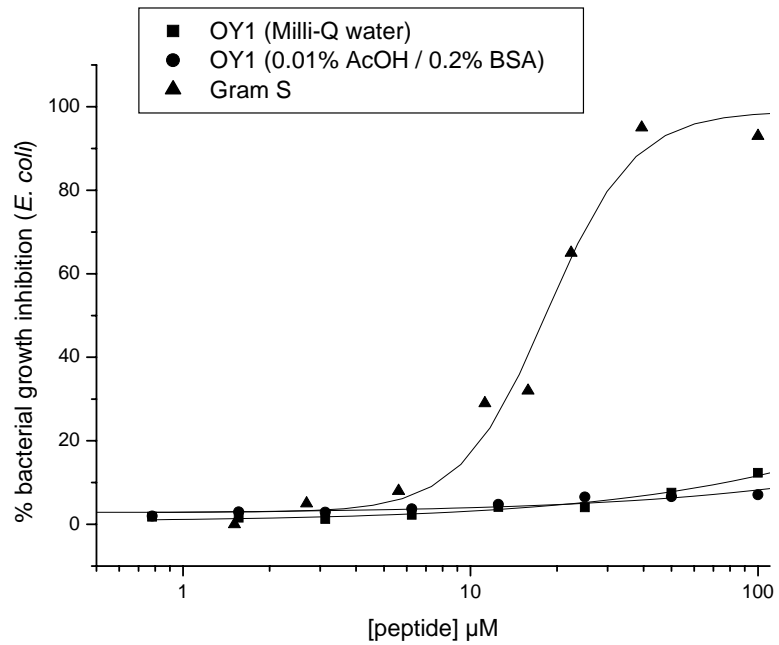


Fig. 6.4: MIC determination of OY1 (Gram S plot adapted from Rautenbach et al., 2006).

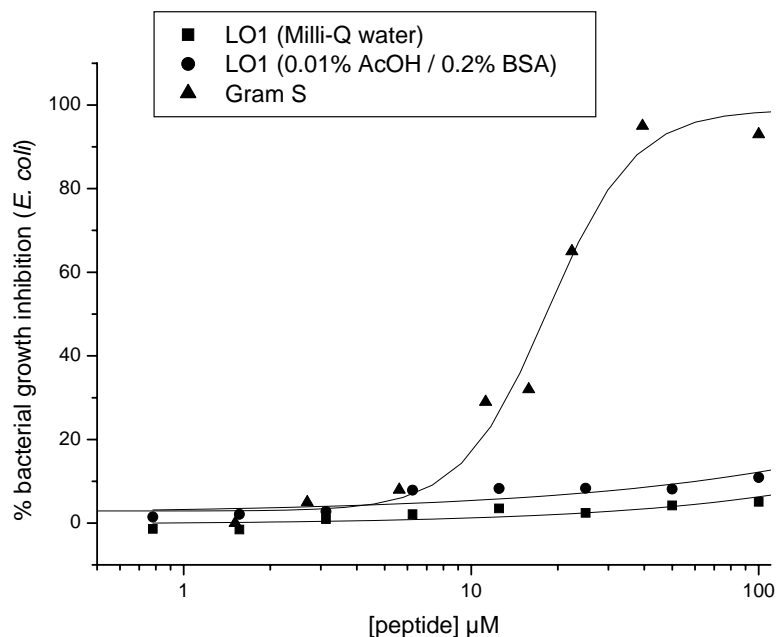


Fig. 6.5: MIC determination of LO1 (Gram S plot adapted from Rautenbach et al., 2006).

The synthesised peptides did not show significant activity in the range of concentrations used (commonly employed for the testing of antimicrobial peptides). According to the aggregation studies in water (see Chapter 4) peptides and peptide hybrids aggregate at much higher concentrations (between 2 and 10 mM, i.e. 20 to 100 times higher than those concentrations used here). It is therefore difficult to attribute the loss of antibacterial activity to the aggregation. The loss of activity seems more likely to be correlated to the AAs introduced into the primary structure, absent in the parent compounds (especially when one considers the ω -AA and the glycyl-prolyl-glycine linkers which drastically modify the peptides' three-dimensional structure) (Zhang et al., 1999). The α -helical structure was therefore assumed to be fundamental for the activity of these compounds (Alvarez-Bravo et al., 1994).

6.4.3 Haemolytic activity

Because of the different lipid compositions of mammalian and bacterial cells, the haemolytic activity commonly indicates the toxicity of CAMPs. In this study peptides were incubated for 24 h at 37 °C in the presence of hRBCs, although the most commonly used incubation time for antimicrobial peptides is around 1 h, and often less (10 to 30 minutes). The use of such a long incubation time was intended to enhance any possible interactions with the erythrocytes and then evaluate the response of the cells in a highly stressful environment. The released hemoglobin was in the range of 2-5% at the highest concentrations of peptides (50-100 μM), and thus confirmed that the peptides and hybrids have no, or very poor, haemolytic activity (Fig. 6.6 and Tab. 6.3).

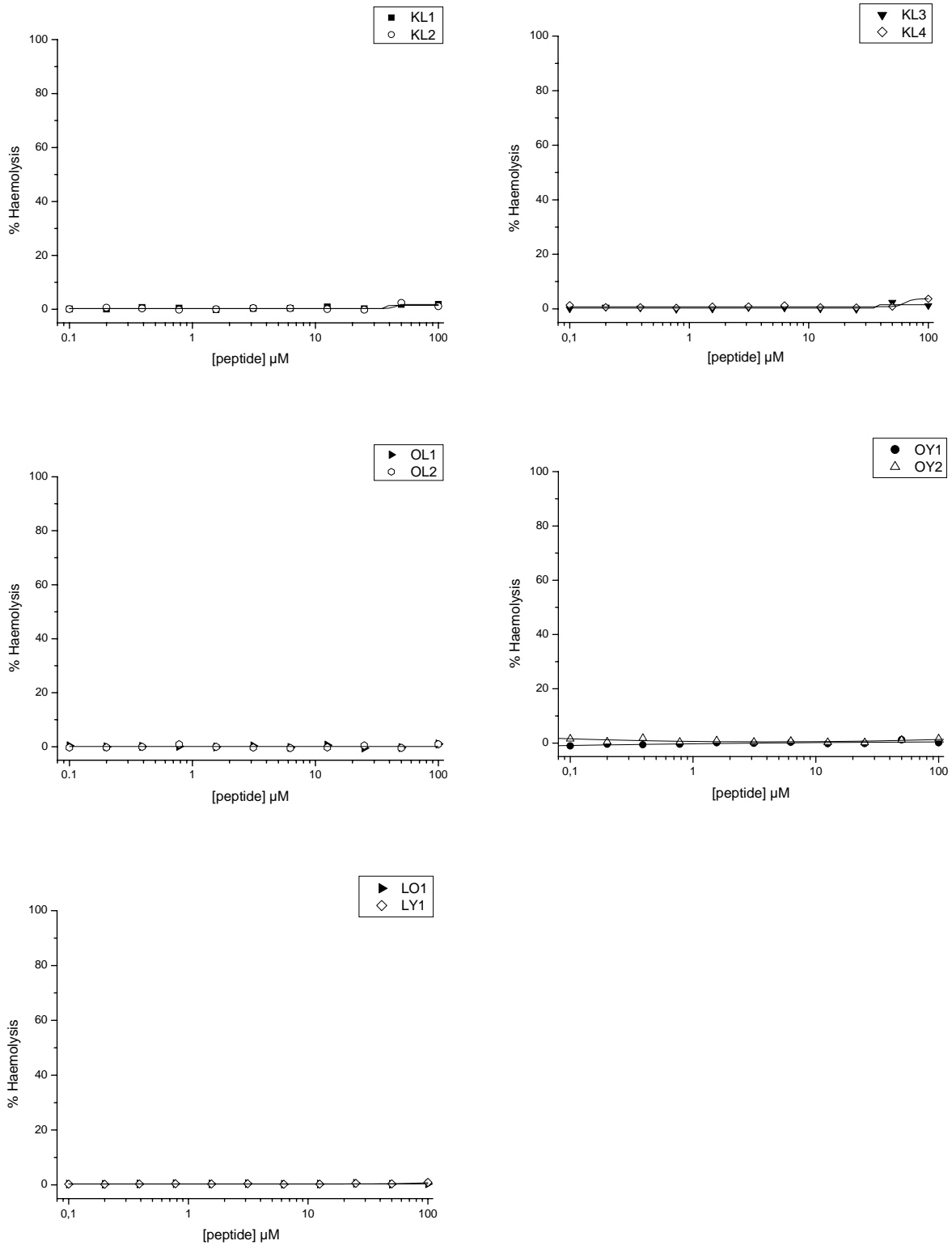


Fig 6.6: Haemolytic activity of the synthesised compounds against hRBCs after 24 h at 37 °C. Saponin (0.5%) and 0.01% AcOH / 0.2% BSA were used as positive and negative controls respectively.

Tab. 6.3: Haemolytic activity of bolaamphiphilic peptides and peptide hybrids

PEPTIDE	L3*	L4*	L5*	KL1	KL1	KL3	KL4
HC ₅₀ (μM) [§]	>100	>100	>100	>100	>100	>100	>100

PEPTIDE	OL1	OL2	OY1	OY2	LO1	LY1
HC ₅₀ (μM) [§]	>100	>100	>100	>100	>100	>100

[§] The HC₅₀ is defined as the concentration of peptide (μM) leading to 50% haemolysis.

* Reported HC₅₀ for L3, L4 and L5 is 143 μM, > 200 μM and > 200 μM respectively (Naidoo, 2004).

6.4.4 Leakage assay from liposomes

The leakage of a fluorescent dye from LUVETs is a very common technique for the assessment of membrane lytic activity (Düzgünes, 2003). The use of artificial membranes to mimic biological membranes is quite widespread and has found many applications in the study of antimicrobial peptides (Epanand and Epanand, 2003). In the literature there is a well established correlation between antimicrobial activity and carboxyfluorescein leakage from liposomes (Hirakura et al., 1996). It has some limitations, however, especially if one considers the complexity of a natural membrane (lipid composition, proteins, ions, membrane potential). On the other hand, it allows one to isolate particular details or characteristics that can be studied independently from others. In this study neutral and negatively charged liposomes were prepared, with the idea to mimic mammalian and bacterial cells, respectively. In this way it would be possible to determine if the compounds tested showed selectivity against a particular kind of cell.

The action of peptides and peptide hybrids against artificial membranes was assessed by monitoring dye leakage from CF-loaded vesicles with an average size of 120 nm, made of PC:CHOL (10:1) and PC:PG (10:1). Graphs showing carboxyfluorescein leakage from liposomes challenged by different peptides are reported in Figures 6.7 and 6.8.

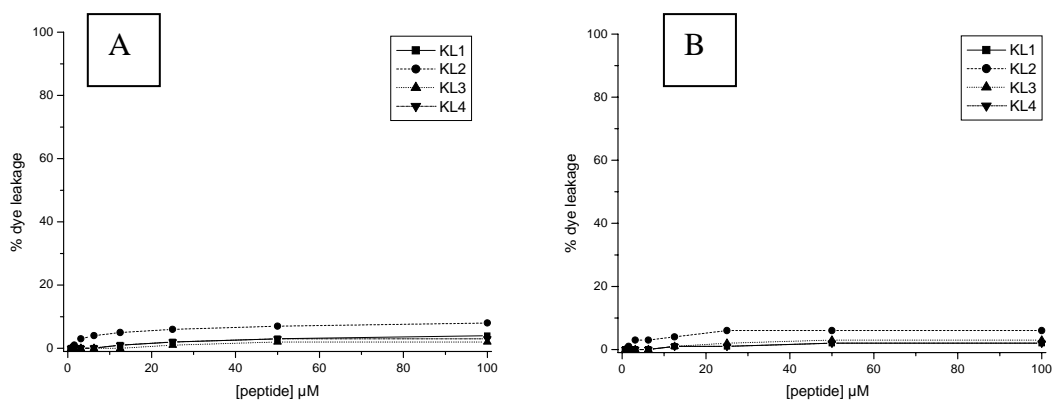


Fig. 6.7: Carboxyfluorescein leakage from liposomes with different lipid composition challenged by KL1, KL2, KL3 and KL4. [A] Negatively charged liposomes (PC:PG, 10:1, lipid concentration 13 μM) and [B] neutrally charged liposomes (PC:CHOL, 10:1, lipid concentration 16 μM).

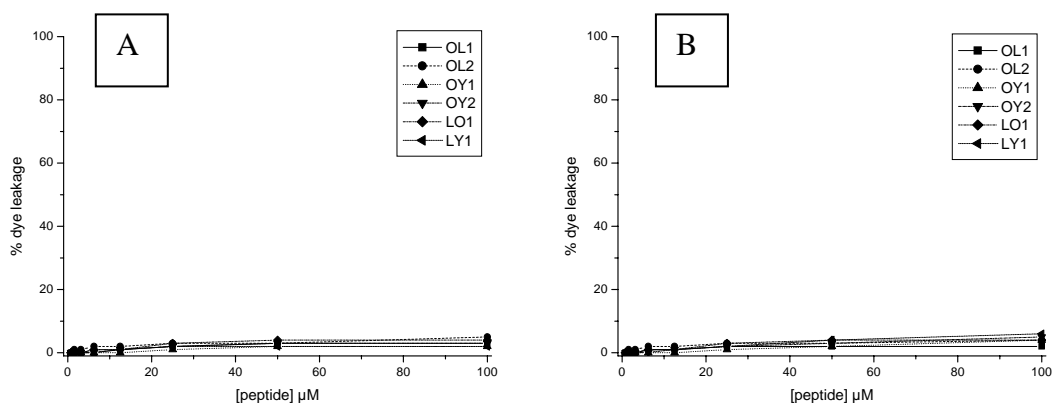


Fig. 6.8: Carboxyfluorescein leakage from liposomes with different lipid composition challenged by OL1, OL2, OY1, OY2, LO1 and LY1. [A] Negatively charged liposomes (PC:PG, 10:1, lipid concentration 13 μM) and [B] neutrally charged liposomes (PC:CHOL, 10:1, lipid concentration 16 μM).

The compounds showed inability to interact with artificial membranes as no significant leakage of fluorescent dye was detected. Moreover, they did not present selectivity and similar trends in the concentration-response curves were observed for both negatively charged and neutral liposomes. The novel compounds did not show the same biological properties typical of the parent compounds. For example, peptide L5 has been reported to possess a strong ability to selectively interact with acidic membranes (Figs. 6.9 [A] and 6.10 [A]) while not provoking leakage from neutral vesicles (Figs. 6.9 [B] and 6.10 [B]). The negative charges on the membrane surface favour initial electrostatic interactions, which are followed by membrane perturbation and leakage of the loaded dye (Hirakura et al., 1996).

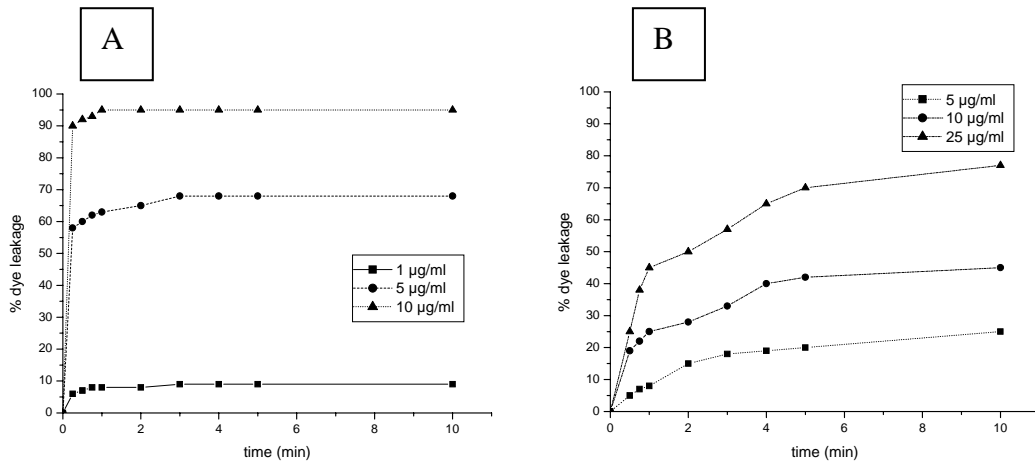


Fig. 6.9: Time course of carboxyfluorescein leakage from liposomes induced by L5. Lipid composition: [A] PE:PG (7:3) and [B] PC:PG (7:3) (after Hirakura et al., 1996).

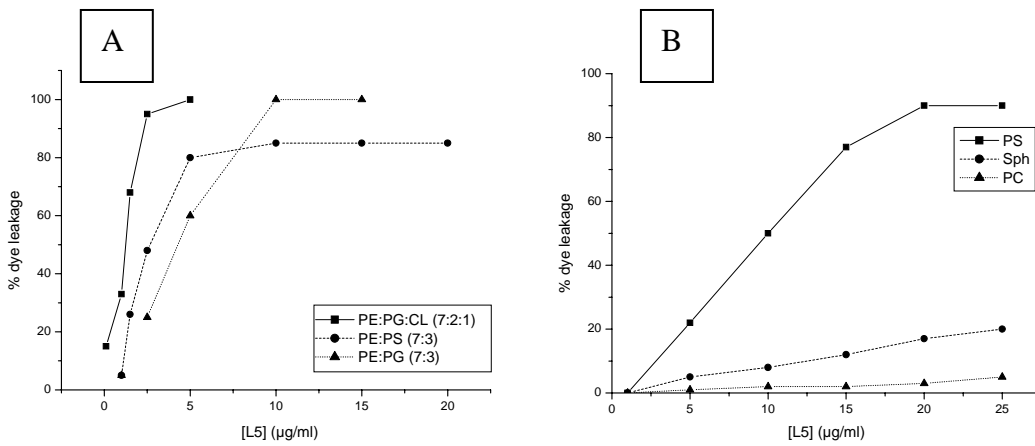


Fig. 6.10: Carboxyfluorescein leakage from liposomes with different lipid composition challenged by L5. [A] Negatively charged liposomes and [B] neutrally charged liposomes (after Hirakura et al., 1996).

Once again, the modifications of the primary structure, the simplification of the parent peptides' sequence and the use of non proteinogenic AA (9-Anc and 6-Ahx) were demonstrated to be critical factors for the loss of lytic properties and selectivity towards negatively charged membranes.

6.5 Conclusions

The determination of the biological properties of the synthesised compounds mainly focused on the ability to interact and disorganise lipid membranes. Many antimicrobial peptides show inhibition areas of 10-20 mm when tested with the Bauer-Kirby disk diffusion assay ^α, even if the disk content is as low as 10-20 µg. In the present study the disk content was 500 µg, and some biological activity was found for compounds KL2, KL4, OY1 and LO1 only. Nonetheless, in these cases such activity was possibly related to a concentration effect more than to a real antimicrobial action due to interaction with the bacterial membranes by one of the mechanisms mentioned earlier (Section 2.1.3). This assumption can be made as other tests (MIC determination I and II) failed to establish MIC values even for the compounds that presented some sort of activity.

As previously discussed, the lack of antimicrobial activity could be ascribed to aggregation in the medium but the range of concentrations in which activity and aggregation occur is rather different, at least for the compounds tested here. Moreover, all the tests performed showed a good consistency: the inability to interact with natural membranes (bacteria, hRBCs) and model membranes (liposomes with different lipid compositions) was proved throughout this chapter.

It therefore appears that the changes applied to sapecin B-derived synthetic peptides did not generate biologically active compounds. A possible explanation lies in the modification of the three-dimensional structure that such alterations produced. Peptides made of Lys/Leu present a typical α -helical structure, which is considered very important for the ability to interact with membranes (Alvarez-Bravo et al., 1994). A poly-leucine chain can form hydrogen bonds which are not formed by the ω -amino acids' hydrocarbon chains. CD results showed that, the use of ω -amino acids deformed the secondary structure and peptides preferentially took a random structure (see Chapter 4 for details). The alteration of structural parameters was stronger in those molecules where the ω -amino acid was replaced by a glycyl-prolyl-glycine tripeptide, introducing a β -turn. The influence of proline residues on the helicity and antibacterial activity of α -helical peptides is well established (Zhang et al., 1999) and the synthesis of proline-containing peptides confirmed the important role of structural parameters (i.e. helicity) for the biological activity of parent peptides L3, L4 and L5. Within the family of compounds, the structural arrangements were represented by α -helices (L_n peptides) \rightarrow distort α -helices (peptides including C5 and C8 linkers) \rightarrow β -turn (GPG linker). The activity followed a similar path, going from active molecules (L3, L4 and L5 peptides) to molecules only active at high concentrations (some peptides including C8 linkers (such as KL2, KL4, OL1 and LO1) and finally to non-active molecules (all the others) (Fig. 6.11).

^α Visit: www.cms.hhs.gov/CLIA/downloads/sc04163.pdf (last accessed 05/04/06).

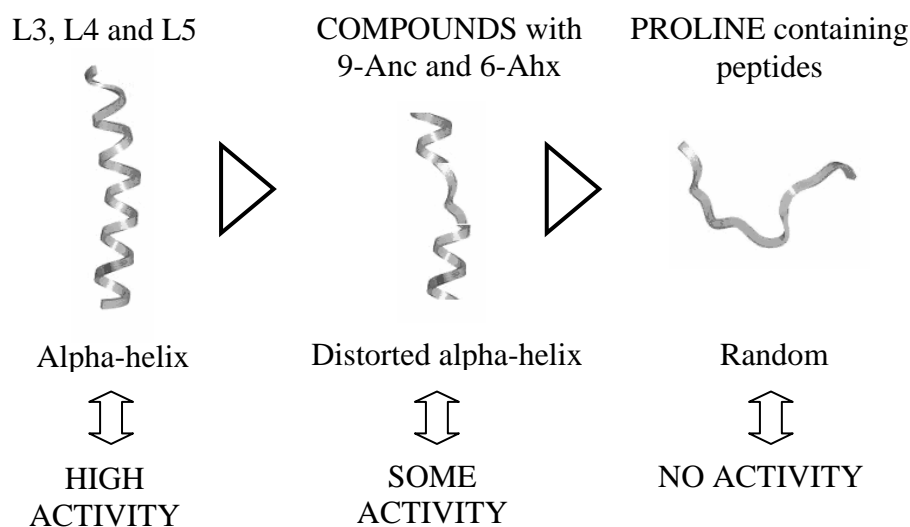


Fig. 6.11: Schematic representation of the correlation between secondary structure and biological activity for the compounds studied. Images were modified from Hancock, 2001.

This study focused on the hydrophobic core of the bolaamphiphilic sapecin B-derived peptides. It especially developed around L3 peptide because of its significant antimicrobial activity (Hirakura et al., 1996; Nakajima et al., 1997). The obtained results showed that the hydrophobic content and the bolaamphiphilic/detergent-like structure was not the only important element for the activity. Three-dimensional structure and the ability to form hydrogen bonds are more likely to play a primary role in the antimicrobial activity of sapecin-derived compounds.

Within CAMPs' broad range of activities, some studies pointed out their ability to stimulate the immune system and decrease the possibility of bacterial infections (Brown and Hancock, 2006). The parent compound L5, for example, was found to protect organisms from methicillin resistant-*S. aureus* infection (Nakajima et al., 1997), activate the generation of reactive species of oxygen (Cho et al., 1990) and induce sustained adaptive immune responses in vivo (Fritz et al., 2004). Research on small peptides with no direct antimicrobial activity but with an immunostimulating influence is at the very early stages (Bowdish et al., 2005b). Nonetheless, several studies pointed out the existence of short peptides which have a strong in vivo immunomodulatory action without having any in vitro antibiotic property (Bowdish et al., 2005a). It is not possible to exclude such a role for the synthesised peptides and peptide hybrids as well, but the determination of any activity on the immune system was far beyond the aim of the current research.

6.6 References

- Alvarez-Bravo J, Kurata S and Natori S (1994) Novel synthetic peptides effective against methicillin-resistant *Staphylococcus aureus*, *Biochemical Journal*, 302, 535-538.
- Bauer AW, Kirby WMM, Sherris JC and Turck M (1966) Antibiotic susceptibility testing by a standardized single disk method, *American Journal of Clinical Pathology*, 45, 493-496.
- Bowdish DME, Davidson DJ, Lau YE, Lee K, Scott MG and Hancock REW (2005a) Impact of LL-37 on anti-infective immunity, *Journal of Leukocyte Biology*, 77, 451-459.
- Bowdish DME, Davidson DJ, Scott MG and Hancock REW (2005b) Immunomodulatory activity of small host defence peptides, *Antimicrobial Agents and Chemotherapy*, 49, 1727-1732.
- Brown KL and Hancock REW (2006) Cationic host defense (antimicrobial) peptides, *Current Opinion in Immunology*, 18, 24-30.
- Cho JH, Homma K, Kanegasaki S and Natori S (1990) Activation of human neutrophils by a synthetic anti-microbial peptide, KLKLLLLLKLK-NH₂ via cell surface calreticulin, *European Journal of Biochemistry*, 266, 878-885.
- Du Toit EA and Rautenbach M (2000) A sensitive standardised micro-gel well diffusion assay for the determination of antimicrobial activity, *Journal of Microbiological Methods*, 42, 159-165.
- Düzgünes N (2003) Fluorescence assays for liposome fusion, *Methods in Enzymology*, 372, 260-274.
- Epanand RM and Epanand RF (2003) Liposomes as models for antimicrobial peptides, *Methods in Enzymology*, 372, 124-133.
- Fritz JH, Brunner S, Birnstiel ML, Buschle M, von Gabain A, Mattner F and Zauner W (2004) The artificial antimicrobial peptide KLKLLLLLKLK induces predominantly a T_H2-type immune response to co-injected antigens, *Vaccine*, 22, 3274-3284.
- Hancock REW (2001) Cationic peptides: effectors in innate immunity and novel antimicrobials, *The Lancet Infectious Diseases*, 1, 156-164.
- Hider RC, Khader F and Tatham AS (1983) Lytic activity of monomeric and oligomeric mellitin, *Biochimica et Biophysica Acta*, 728, 206-214.
- Hirakura Y, Alvarez-Bravo J, Kurata S, Natori S and Kirino Y (1996) Selective interaction of synthetic antimicrobial peptides derived from sapechin B with lipid bilayers, *Journal of Biochemistry*, 120, 1130-1140.
- Hope MJ, Bally MB, Webb G and Cullis PR (1985) Production of large unilamellar vesicles by a rapid extrusion procedure. Characterization of size distribution, trapped volume and ability to maintain a membrane potential, *Biochimica et Biophysica Acta*, 812, 55-65.
- Mui B, Chow L and Hope MJ (2003) Extrusion technique to generate liposomes of defined size, *Methods in Enzymology*, 367, 3-14.
- Naidoo VB (2004) The supramolecular chemistry of novel synthetic biomacromolecular assemblies, PhD thesis, University of Stellenbosch.

Nakajima Y, Alvarez-Bravo J, Cho J, Homma K, Kanegasaki S and Natori S (1997) Chemotherapeutic activity of synthetic antimicrobial peptides: correlation between chemotherapeutic activity and neutrophil-activating activity, *FEBS Letters*, 415, 64-66.

NCCLS – National Committee for Clinical Laboratory Standards (1975) Performance standards for antimicrobial disk susceptibility tests; Approved Standard M2-A7 ASM-2; Villanova, PA.

Rautenbach M, Gerstner GD, Vlok NM, Kulenkampff J and Westerhoff HV (2006) Analyses of dose-response curves to compare the antimicrobial activity of model cationic α -helical peptides highlights the necessity for a minimum of two activity parameters, *Analytical Biochemistry*, 305, 81-90.

Stewart JCM (1980) Colorimetric determination of phospholipids with ammonium ferrothiocyanate, *Analytical Biochemistry*, 104, 10-14.

WHO – World Health Organization (1961) Standardization of Methods for Conducting Microbic Sensitivity Tests, second report of the Expert Committee on Antibiotics. Technical Report Series, No. 210; Geneva.

Wu M and Hancock REW (1999) Interaction of the cyclic antimicrobial cationic peptide bactenecin with the outer and cytoplasmic membrane, *Journal of Biological Chemistry*, 274, 29-35.

Zhang L, Benz R and Hancock REW (1999) Influence of proline residues on the antibacterial and synergistic activities of α -helical peptides, *Biochemistry*, 38, 8102-8111.

Chapter 7

Conclusions and recommendations

7.1 Conclusions

Amphiphilic and bolaamphiphilic peptides with antimicrobial properties represent a potentially new field for the development of antimicrobial leader compounds. The combination of the surfactant-like structure of bolaamphiphilic molecules and the inherent biological activity of short peptides could ultimately turn them into powerful tools mimicking natural materials and tissues (Luk and Abbot, 2002; Fairman and Åkerfeldt, 2005). The current research project developed around the design and synthesis of a library of compounds with a bolaamphiphilic structure, drawn from sapecin-derived synthetic peptides (Alvarez-Bravo et al., 1994). The aims of this research comprised (i) the assessment of the self-assembly tendency of basic bolaamphiphilic peptides and hybrids, (ii) the study of their supramolecular architectures from a morphological point of view, (iii) the characterisation of their hydrophobic profile in relation to the self-assembly and (iv) the study of their biological potentialities.

7.1.1 Understanding of the self-assembly behaviour

Amino acid composition and 3D arrangements of the compounds in solution were correlated to their aggregation profiles by using fluorescence (Chapter 4). This technique allowed the author to study the process while it was occurring. The bolaamphiphile concentration was the driving force of the process but other factors were also fundamental. The external environment, and specifically the pH, was the trigger for the self-assembly. For the same compound, the CAC in 0.1% TEA was much lower than that in water.

The present study also confirmed the key role of amino acid composition in the self-assembly, which was influenced by the type of non-polar AA and the dimensions of the side-chain (Wang et al., 2005). Hydrophobic interactions were another important driving force of the self-assembly (Zhang et al., 1993; Santoso and Zhang, 2004). Hence, the presence of aromatic AA especially promoted the process through the π -stacking of aromatic side-chains (Caplan et al., 2002; Gazit, 2002). Peptide bolaamphiphiles containing tyrosine showed a significant lower CAC than leucine-containing analogue molecules. In addition, the role of the 3D structure was also clarified.

Proline-containing molecules showed much higher CAC values than analogue peptides containing 9-aminononanoic acid.

7.1.2 Morphological study of the supramolecular assemblies

The morphology studies performed on the peptide assemblies revealed the complex supramolecular architectures formed by these compounds (Chapter 4). The aggregation was enforced by a pH modification and it occurred when the net charge of the peptide molecules was close to zero (Caplan et al., 2000). After an aging period of up to 15 days, the structures were clearly observed by means of different microscopes. CR staining and OM observation gave evidence of fibre-like structures characterised by birefringence properties under cross-polarised light. SEM micrographs also confirmed the formation of fibres with dimensions in the range of several microns (between 500 nm and 2 μ m). The coexistence of microtubes/microfibres, vesicles, 3-way junctions/branches and vesicles budding out of microtubes revealed that the self-assembly of these surfactant-like molecules is a dynamic process (Vauthey et al., 2002). Cryo-SEM also revealed the formation of microtubes with consistent dimensions. Two mechanisms of microtube formation were detailed as possible pathways for the self-assembly of these molecules.

7.1.3 Hydrophobic content and its correlation to the self-assembly

The hydrophobic content of the synthesised peptide bolaamphiphiles was determined both experimentally (RP-HPLC) and theoretically (residue addition method and fragment addition method) (Chapter 5). The correlation between experimental and theoretical hydrophobicities revealed a good consistency even if slightly different correlation coefficients were found. The use of an octadecyl column gave similar results with the two gradients used, thus indicating that this type of column has an inherent strong ability to interact with the analyte regardless of the conditions used. On the other hand, the use of a dodecyl column was found to be influenced by the experimental conditions (such as the gradient). The correlation between $CLOGP_{\text{FRAGMENTS}}$ and the t_R (C_{12}) for the synthesised bolaamphiphilic peptides varied to some extent with the use of one or the other gradient. Therefore, in the present study, the use of a C_{18} column seemed to give more reliable results in terms of hydrophobic determination.

Interestingly, it was also possible to investigate the effect of the hydrophobic content on the self-assembly behaviour in water. In Chapter 4 the relationship between hydrophobic AA and enhanced self-organisation properties was already pointed out (Zhang et al., 1993). The experimental observations made during steady-state fluorescence measurements about the role of hydrophobic residues were confirmed. Compounds showing low CAC were characterised by a significant hydrophobic content (expressed by their $CLOGP_{\text{FRAGMENTS}}$) while molecules with high CAC values possessed a low H (Fig. 7.1). The only exception was represented by proline-

containing peptides, where the influence of the 3D arrangements on the aggregation was much more important than the presence of hydrophobic residues.

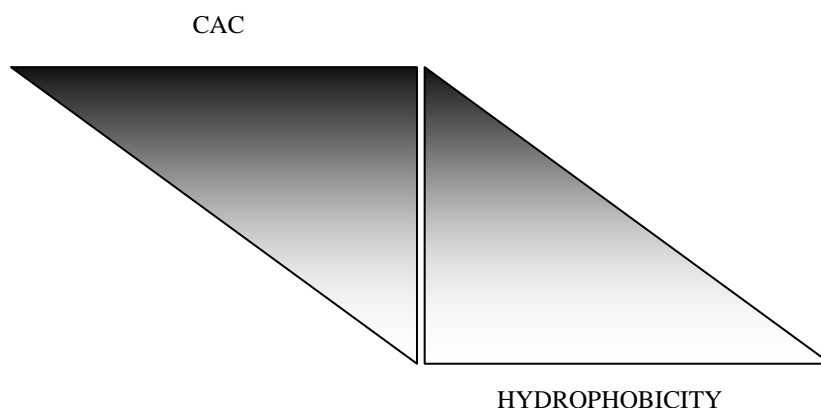


Fig. 7.1: Correlation between hydrophobicity ($\text{CLOGP}_{\text{FRAGMENTS}}$) and CAC for 9-Anc containing molecules.

7.1.4 Influence of non-natural amino acids on the biological activity

These novel peptide-based bolaamphiphiles were developed using a synthetic antimicrobial pattern as template and comprised previously designed – and supposedly active – molecules (such as KL2 and KL4) (Naidoo, 2004). Anyway, the previously reported positive results of Naidoo (Naidoo, 2004) regarding the antimicrobial activity of the bolaamphiphilic peptides were not confirmed (Chapter 6). Multiple tests in the present investigation gave evidence of a complete lack of activity against bacteria and a strong inability to disorganise lipid membranes. The use of an amino acid pattern which presents an alternation of hydrophobic and hydrophilic AA was found not to be an optimal choice. This motif strongly promoted the self-assembly without having any positive effects on the biological activity (Vauthey et al., 2002; von Maltzahn et al., 2003). Especially the use of non natural AA (particularly considering the use of 9-Anc and 6-Ahx) greatly deformed the 3D arrangements and, as already discussed, could possibly explain the loss of activity for those peptide hybrids containing them. Confirmations in this regard were obtained by the use of the glycyl-prolyl-glycine tripeptide instead of 9-Anc, as none of the proline-containing peptides showed any sort of biological activity. Besides that, the use of more hydrophobic AA (such as tyrosine), while strongly increasing the aggregation (Santoso and Zhang, 2004), did not promote any lytic activity. Possibly, the aromatic side-chains, whose hydrophobic interactions significantly promoted the self-assembly, acted against the lysis of the bacterial membrane as none of the compounds containing tyrosine was found to be active.

Furthermore, the use of 9-Anc and 6-Ahx affected the hydrophobic content of the sapecin-derived molecules (expressed as CLOGP). While maintaining the length in terms of C atoms, the aliphatic chain gave a lower contribution to the overall H than the poly-leucine chain of L3, L4 and L5 peptides. The result was a lower hydrophobic content of the newly synthesised compounds, which could possibly be translated into weaker interactions with membranes.

7.2 Limitations

Even if CAMPs are at the centre of the research for new antibiotics some limitations mark a clear boundary between their many possible applications and real uses. In the present study the synthesis of hybrid molecules was still based on SPPS techniques (Chapter 3). Furthermore, the environmental impact of the synthesis and the high costs of production seriously reduce the applications to some restricted areas. Importantly, if the compounds present a low/moderate activity then these costs become prohibitive. These constraints could possibly be overcome by using enzymatic synthesis and by designing simpler molecules such as amino acid-based surfactants (Infante et al., 2004).

The alternation of charged and non-polar AAs (the KLK motif from sapecin-derived L3 peptide) is interesting because of its similarity with some natural antimicrobial patterns. Nonetheless, it was shown to lose importance in the creation of hybrid molecules by including non-proteinogenic AA in the primary structure. Certainly there are tri/pentapeptides that possess bioactivity and which are used for the creation of biomaterials through self-assembly, such as RGD for cell attachment and growth (Hartgerink et al., 2001), [RADA]_n and IKVAV for neurite growth (Holmes et al., 2000; Silva et al., 2004). However, it appears that many parameters influenced the activity of sapecin-derived peptides and the presence of a KLK (or OLO) motif alone was not enough to confer antibiotic properties (Chapter 6).

The fluorescence study in water (pH 6) was limited, by technical difficulties, to concentrations lower than 45 mM. Consequently only two molecules (OY1 and OY2) were fully characterised in water and 0.1% TEA, while the others were only studied in the basic environment (pH 10). Nonetheless, even if it was not possible to evaluate the different aggregation profiles in water, the study in 0.1% TEA allowed the author to obtain a good general idea of the important parameters governing the self-assembly (Chapter 4).

CD results poorly followed the aggregation in water. Technical issues mainly affected the measurements (too high concentration, absorbing buffer, etc.) and the results were only useful to study the 3D structures in solution and confirm the modification of the parent molecules' α -helix (Chapter 4).

The use of gradient RP-HPLC for hydrophobicity determination is usually limited to some particular cases and isocratic liquid chromatography (hence k') is generally preferred. Capacity factors were not determined and the lack of a parameter independent from the experimental conditions was possibly translated into poor R^2 values when theoretical and experimental data were compared (R^2 values were comprised between 0.86 and 0.96). This problem was also noticed when comparing CAC and t_R as a direct relationship was absent. However, the use of $CLOGP_{\text{FRAGMENTS}}$ as H index gave results consistent with the literature, showing a direct correlation between hydrophobicity and self-assembly tendency for 9-Anc-containing molecules (Chapter 5).

7.3 Recommendations for future work

The concept of the bolaamphiphilic molecule could be applied to a new antimicrobial pattern from a natural CAMP and used to design new potentially active compounds. The selection of a novel highly active sequence from a CAMPs database could be the first step towards the development of a new project. The possible activity could then be studied with particular attention to the aggregation profile typical of bolaamphiphiles. Interestingly, it could be possible to evaluate the activity according to the aggregation status and separately test single molecules or peptide assemblies according to diverse experimental conditions (Pérez et al., 1996; Pérez et al., 2002).

This bolaamphiphilic model could lead to the creation of nanostructured biomaterials such as antimicrobial scaffolds for tissue regeneration, antimicrobial patches for burns and tissue healing, antibiotic textile fibers and biodegradable surfactants with biological properties (i.e. soaps).

Moreover, also the self-assembly process could be investigated from a different perspective. Light dispersion measurements could be used to study peptide aggregation in water without any external probe (i.e. pyrene). The use of fluorescent AAs (such as Tyr and Trp) could also offer an interesting way to study bolaamphiphiles' aggregation in water by fluorescence.

7.4 References

- Alvarez-Bravo J, Kurata S and Natori S (1994) Novel synthetic peptides effective against methicillin-resistant *Staphylococcus aureus*, *Biochemical Journal*, 302, 535-538.
- Caplan MR, Moore PN, Zhang S, Kamm RD and Lauffenburger DA (2000) Self-assembly of a β -sheet protein governed by relief of electrostatic repulsion relative to van der Waals attraction *Biomacromolecules*, 1, 627-631.
- Caplan MR, Schwartzfarb E, Zhang S, Kamm RD and Lauffenburger DA (2002) Control of self-assembling oligopeptide matrix formation through systematic variation of amino acid sequence, *Biomaterials*, 23, 219-227.
- Fairman R and Åkerfeldt KS (2005) Peptides as novel smart materials, *Current Opinion in Structural Biology*, 15, 453-463.
- Gazit E (2002) A possible role for π -stacking in the self-assembly of amyloid fibrils, *FASEB Journal*, 16, 77-83.
- Hartgerink JD, Beniash E and Stupp SI (2001) Self-assembly and mineralization of peptide-amphiphile nanofibers, *Science*, 294, 1684-1688.
- Holmes TC, de Lacalle S, Su X, Liu G, Rich A and Zhang S (2000) Extensive neurite outgrowth and active synapse formation on self-assembling peptide scaffolds, *Proceedings of the National Academy of Sciences*, 97, 6728-6733.
- Infante MR, Pérez L, Pinazo A, Clapés P, Morán MC, Angelet M, García MT and Vinardell MP (2004) Amino acid-based surfactants, *CR Chimie*, 7, 583-592.
- Luk YY and Abbot NL (2002) Applications of functional surfactants, *Current Opinion in Colloid and Interface Science*, 7, 267-275.
- Naidoo VB (2004) The supramolecular chemistry of novel synthetic biomacromolecular assemblies, PhD thesis, University of Stellenbosch.
- Pérez L, Torres JL, Manresa A, Solans C and Infante MR (1996) Synthesis, aggregation and biological properties of a new class of gemini cationic amphiphilic compounds from arginine, bis(Args), *Langmuir*, 12, 5296-5301.
- Pérez L, García MT, Ribosa I, Vinardell MP, Manresa A and Infante MR (2002) Biological properties of arginine-based gemini cationic surfactants, *Environmental Toxicology and Chemistry*, 21, 1279-1285.
- Santoso SS and Zhang S (2004) Self-assembled nanomaterials, in Nalwa HS (Ed.) *Encyclopaedia of nanoscience and nanotechnology*, Vol. 9 (pp. 459-471) American Scientific Publishers; Stevenson Ranch.
- Silva GA, Czeisler C, Niece KL, Beniash E, Harrington DA, Kessler JA and Stupp SI (2004) Selective differentiation of neural progenitor cells by high-epitope density nanofibers, *Science*, 303, 1352-1355.

Vauthey S, Santoso S, Gong H, Watson N and Zhang S (2002) Molecular self-assembly of surfactant-like peptides to form nanotubes and nanovesicles, *Proceedings of the National Academy of Sciences*, 99, 5535-5360.

von Maltzahn G, Vauthey S, Santoso S and Zhang S (2003) Positively charged surfactant-like peptides self-assemble into nanostructures, *Langmuir*, 19, 4332-4337.

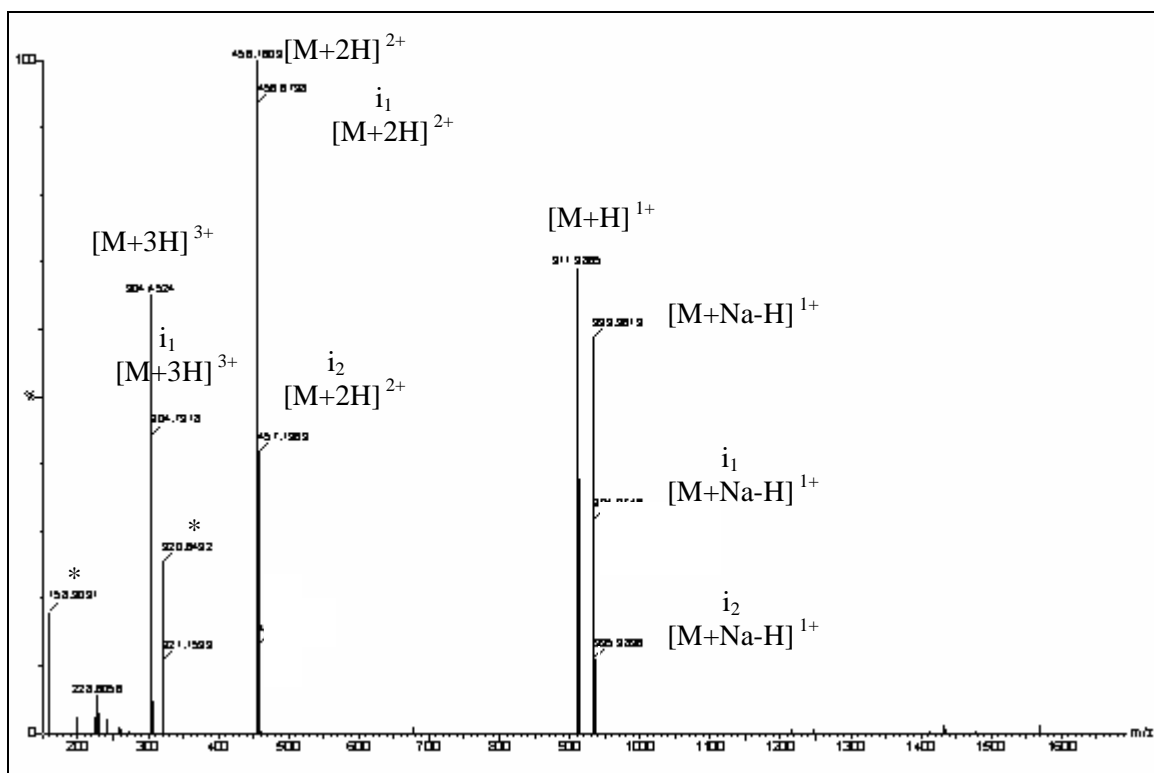
Wang K, Keasling JD and Muller SJ (2005) Effects of the sequence and size of non-polar residues on the self-assembly of amphiphilic peptides, *International Journal of Biological Macromolecules*, 36, 232-240.

Zhang S, Holmes T, Locksmith C and Rich A (1993) Spontaneous assembly of self-complementary oligopeptides to form a stable macroscopic membrane, *Proceedings of the National Academy of Sciences*, 90, 3334-3338.

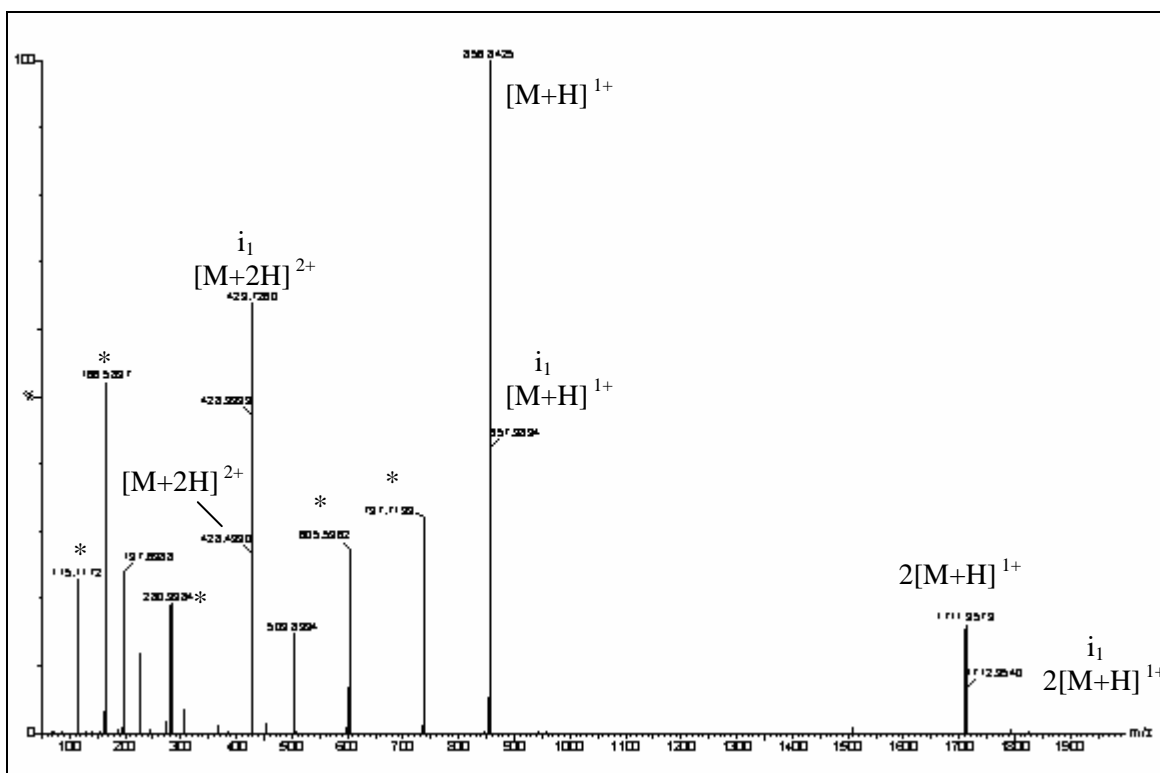
Appendix A – Examples of natural antimicrobial peptides (adapted from Hancock and Powers, 2001)

PEPTIDE	CLASS	HOST/SYNTHETIC	PDB ID
CA-MA	α -Helix	Synthetic	1D9J
CA-MA analogue (P1)	α -Helix	Synthetic	1D9L
CA-MA analogue (P2)	α -Helix	Synthetic	1D9M
CA-MA analogue (P3)	α -Helix	Synthetic	1D9O
CA-MA analogue (P4)	α -Helix	Synthetic	1D9P
Carnobacteriocin B2	α -Helix	<i>Carnobacterium piscicola</i>	1CW5
G-10 Novispirin	α -Helix	Synthetic	1HU6
Magainin 2	α -Helix	<i>Xenopus laevis</i>	2MAG
Magainin 2 analogue	α -Helix	Synthetic	1DUM
Moricin	α -Helix	<i>Bombyx mori</i>	1KV4
Ovispirin-1	α -Helix	Synthetic	1HU5
Sheep myeloid antimicroic peptide (Smap-29)	α -Helix	<i>Ovis aries</i>	1FRY
T-7 Novispirin	α -Helix	Synthetic	1HU7
γ -1-P thionin	β -Sheet	<i>Triticum turgidum</i>	1GPS
θ -Defensin 1	β -Sheet	<i>Macaca mulatta</i>	1HVZ
<i>A. hippocastanum</i> antimicroic protein 1 (Ah-Amp1)	β -Sheet	<i>Aesculus hippocastanus</i>	1BK8
Androctonin	β -Sheet	<i>Androctonus australis</i>	1CZ6
Bovine neutrophil β -defensin 12 (BNBD-12)	β -Sheet	<i>Bos Taurus</i>	1BNB
Circulin A	β -Sheet	<i>Chassalia parviflora</i>	1BH4
Drosomycin	β -Sheet	<i>Drosophila melanogaster</i>	1MYN
Gomesin	β -Sheet	<i>Acanthoscurria gomesiana</i>	1KFP
Heliomicin	β -Sheet	<i>Heliothis virescens</i>	1I2U
Heliomicin analogue	β -Sheet	Synthetic	1I2V
Hepcidin-20	β -Sheet	<i>Homo sapiens</i>	1M4E
Hepcidin-25	β -Sheet	<i>Homo sapiens</i>	1M4F
Human β -defensin 1 (Hbd-1)	β -Sheet	<i>Homo sapiens</i>	1KJ5 & 1E4S & 1IJV
Human β -defensin 2 (Hbd-2)	β -Sheet	<i>Homo sapiens</i>	1E4Q
Human β -defensin 3 (Hbd-3)	β -Sheet	<i>Homo sapiens</i>	1KJ6
Human defensin (HNP-3)	β -Sheet	<i>Homo sapiens</i>	1DFN
Insect defensin A	β -Sheet	<i>Protophormia terraenovae</i>	1ICA
Lactoferricin B	β -Sheet	<i>Bos Taurus</i>	1LFC
Leucocin A	β -Sheet	<i>Leuconostoc gelidum</i>	2LEU & 3LEU
Mediterranean mussel defensin (MGD-1)	β -Sheet	<i>Mytilus galloprovincialis</i>	1FJN
Mouse β -defensin 7 (Mbd-7)	β -Sheet	<i>Mus musculus</i>	1E4T
Mouse β -defensin 8 (Mbd-8)	β -Sheet	<i>Mus musculus</i>	1E4R
<i>P. sativum</i> defensin 1 (Psd-1)	β -Sheet	<i>Pisum sativum</i>	1JKZ
Pafp-S	β -Sheet	<i>Phytolacca Americana</i>	1DKC
Protegrin-1 (Pg1)	β -Sheet	<i>Sus scrofa</i>	1PG1
Rabbit kidney defensin (RK-1)	β -Sheet	<i>Oryctolagus cuniculus</i>	1EWS
Ramoplanin	β -Sheet	<i>Actinoplanes</i> sp.	1DSR
Sapecin	β -Sheet	<i>Sarcophaga peregrina</i>	1LV4
Tachyplesin I	β -Sheet	<i>Tachypleus tridentatus</i>	1MA2 & 1MA5
Tachyplesin I analogue (Tpy4)	β -Sheet	Synthetic	1MA4 & 1MA6
Tachystatin	β -Sheet	<i>Tachypleus tridentatus</i>	1CIX
Ac-AMP2	Extended	<i>Amaranthus caudatus</i>	1MMC
Indolicidin	Extended	<i>Bos Taurus</i>	1G89 & 1G8C
Indolicidin analogue (CP10A)	Extended	Synthetic	1HR1
Pw2	Extended	Synthetic	1M02
Tritrpticin	Extended	Synthetic (potential porcine cathelicidin)	1D6X
Thanatin	Loop	<i>Podisus maculiventris</i>	8TFV

Appendix B – Additional mass spectra of peptide bolamaphiphiles

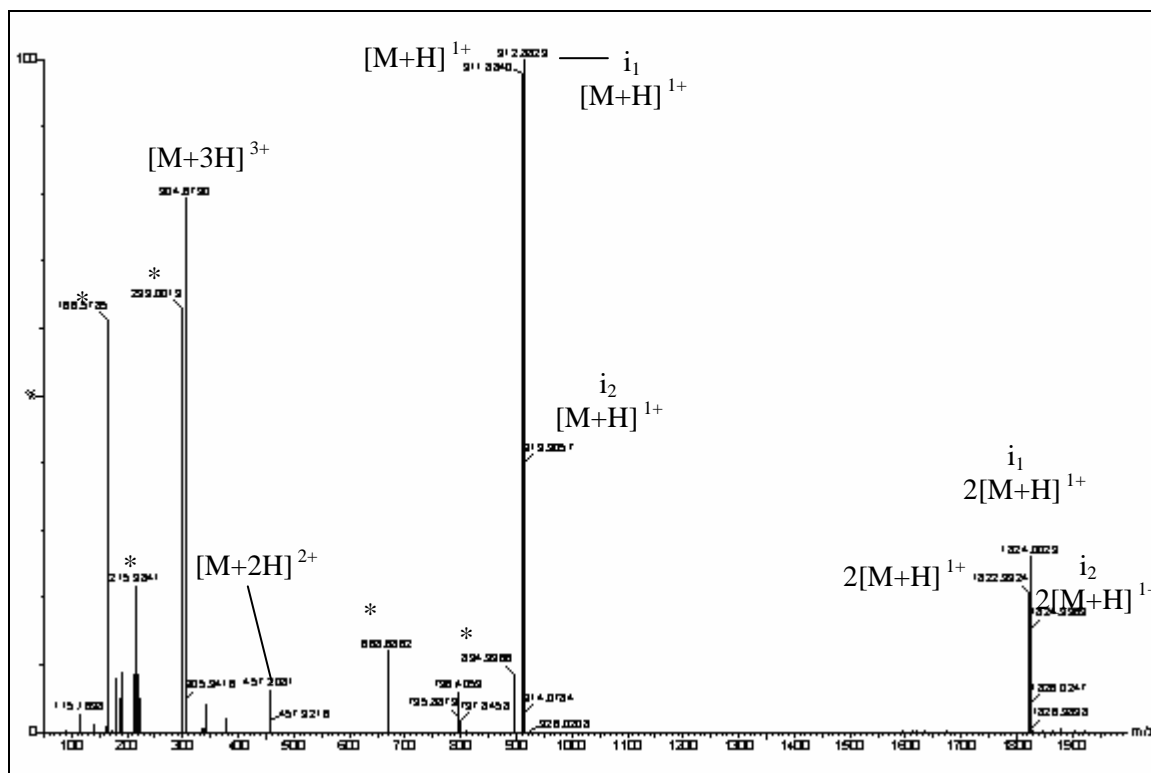


1. ESI-MS spectrum of crude KL4. Isotope variations are marked by i_1 , i_2 and i_3 corresponding to m/z -values with 1, 2 or 3 amu higher than the mass calculated from the monoisotope residue mass (unknown fragments are indicated by *).

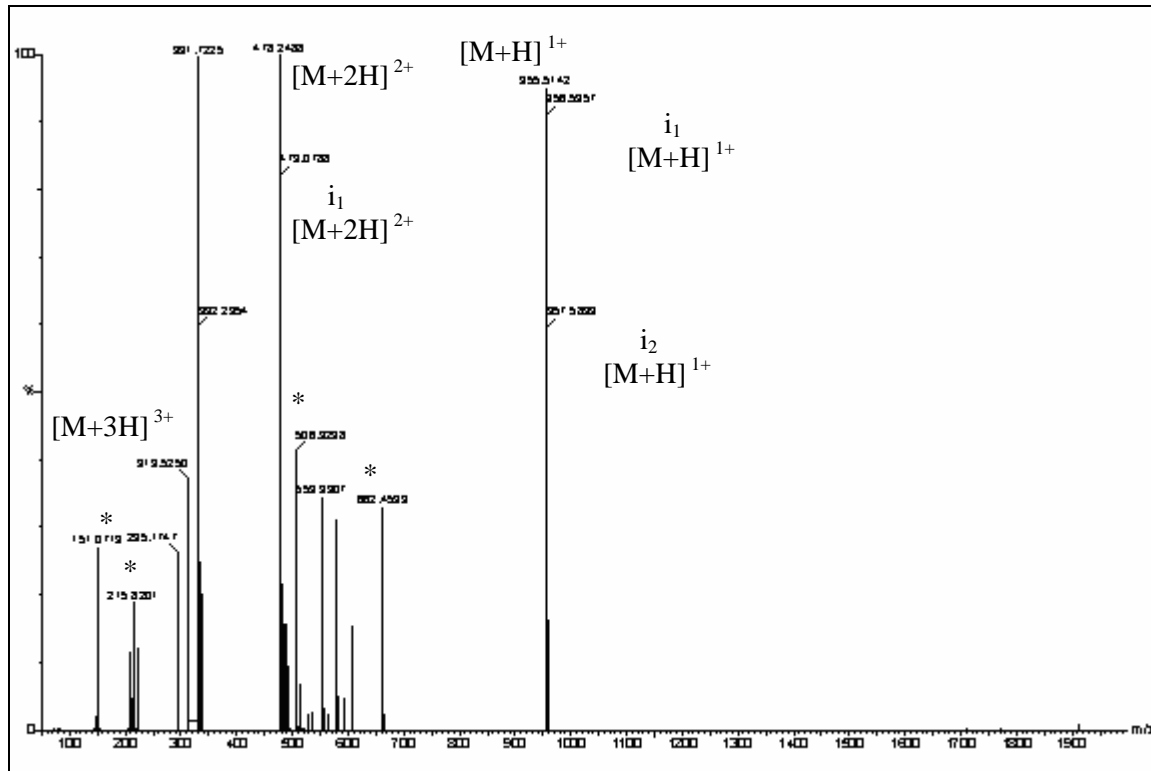


2. ESI-MS spectrum of crude OL1. Isotope variations are marked by i_1 , i_2 and i_3 corresponding to m/z -values with 1, 2 or 3 amu higher than the mass calculated from the monoisotope residue mass (unknown fragments are indicated by *).

Appendix B – Additional mass spectra of peptide bolamaphiphiles

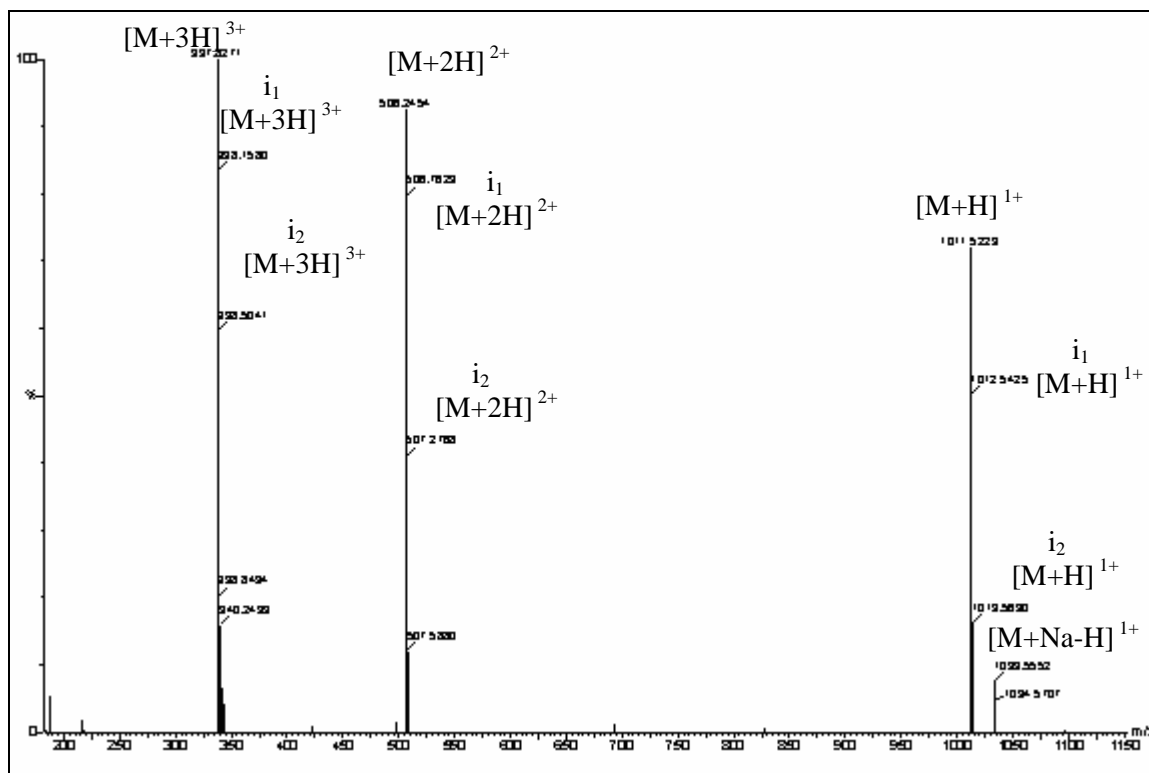


3. ESI-MS spectrum of crude OL2. Isotope variations are marked by i_1 , i_2 and i_3 corresponding to m/z -values with 1, 2 or 3 amu higher than the mass calculated from the monoisotope residue mass (unknown fragments are indicated by *).



4. ESI-MS spectrum of crude OY1. Isotope variations are marked by i_1 , i_2 and i_3 corresponding to m/z -values with 1, 2 or 3 amu higher than the mass calculated from the monoisotope residue mass (unknown fragments are indicated by *).

Appendix B – Additional mass spectra of peptide bolamaphiphiles



5. ESI-MS spectrum of crude OY2. Isotope variations are marked by i_1 , i_2 and i_3 corresponding to m/z -values with 1, 2 or 3 amu higher than the mass calculated from the monoisotope residue mass (unknown fragments are indicated by *).

Appendix C – Bio-Loom determination of the hydrophobic content of synthesised bolaamphiphilic peptides and peptide hybrids (Bio-Loom software is available for download from the internet at www.biobyte.com/prod/bb/bioloom.html).

ExFragment	Bonds	63 chain and 0 alicyclic (net)		-7.560
Proximity	YCY	Fragments 1 & 4: -.32 (-2.71+-2.71)		1.734
Proximity	YCY	Fragments 1 & 2: -.32 (-2.71+-1.54)		1.360
Proximity	YCY	Fragments 4 & 6: -.32 (-2.71+-2.71)		1.734
Proximity	YCY	Fragments 6 & 7: -.32 (-2.71+-2.71)		1.734
Proximity	YCY	Fragments 7 & 8: -.32 (-2.71+-2.71)		1.734
Proximity	YCY	Fragments 8 & 9: -.32 (-2.71+-2.71)		1.734
Proximity	YCY	Fragments 9 & 10: -.32 (-2.71+-2.71)		1.734
Proximity	YCY	Fragments 10 & 12: -.32 (-2.71+-2.71)		1.734
Proximity	YCY	Fragments 12 & 13: -.32 (-2.71+-2.71)		1.734
Proximity	YCY	Fragments 13 & 15: -.32 (-2.71+-1.99)		1.504
RESULT	DB=23	All fragments measured	CLOGP=5	3.661

H-Lys-Leu-Lys-Leu-Leu-Leu-Leu-Lys-Leu-Lys-NH₂ (L5)

C: 4.86

SMILES NOTATION

NC(CCCCN)C(NC(CC(C)C)C(NC(CCCCN)C(NC(CC(C)C)C(NC(CC(C)C)C(NC(CC(C)C)C(NC(CC(C)C)C(NC(CC(C)C)C(NC(CC(C)C)C(NC(CC(C)C)C(NC(CCCCN)C(NC(CC(C)C)C(NC(CCCCN)C(N)=O)=O)=O)=O)=O)=O)=O)=O)=O)=O

Class	Type	Log(P) Contribution Description	Comment	Value
Fragment	# 1	NH-Amide [AA]	Measured	-2.710
Fragment	# 2	Primary Amine [A]	Measured	-1.540
Fragment	# 3	Primary Amine [A]	Measured	-1.540
Fragment	# 4	NH-Amide [AA]	Measured	-2.710
Fragment	# 5	Primary Amine [A]	Measured	-1.540
Fragment	# 6	NH-Amide [AA]	Measured	-2.710
Fragment	# 7	NH-Amide [AA]	Measured	-2.710
Fragment	# 8	NH-Amide [AA]	Measured	-2.710
Fragment	# 9	NH-Amide [AA]	Measured	-2.710
Fragment	#10	NH-Amide [AA]	Measured	-2.710
Fragment	#11	NH-Amide [AA]	Measured	-2.710
Fragment	#12	Primary Amine [A]	Measured	-1.540
Fragment	#13	NH-Amide [AA]	Measured	-2.710
Fragment	#14	NH-Amide [AA]	Measured	-2.710
Fragment	#15	Primary Amine [A]	Measured	-1.540
Fragment	#16	NH ₂ -Amide [A]	Measured	-1.990
Carbon		55 aliphatic isolating carbons		10.725
ExFragment	Branch	7 chain and 0 cluster branches	Chain	-.910
ExFragment	Branch	11 non-halogen, polar group branches	Group	-2.420
ExFragment	Hydrog	106 hydrogens on isolating carbons		24.062
ExFragment	Bonds	69 chain and 0 alicyclic (net)		-8.280
Proximity	YCY	Fragments 1 & 4: -.32 (-2.71+-2.71)		1.734
Proximity	YCY	Fragments 1 & 2: -.32 (-2.71+-1.54)		1.360
Proximity	YCY	Fragments 4 & 6: -.32 (-2.71+-2.71)		1.734
Proximity	YCY	Fragments 6 & 7: -.32 (-2.71+-2.71)		1.734
Proximity	YCY	Fragments 7 & 8: -.32 (-2.71+-2.71)		1.734
Proximity	YCY	Fragments 8 & 9: -.32 (-2.71+-2.71)		1.734
Proximity	YCY	Fragments 9 & 10: -.32 (-2.71+-2.71)		1.734
Proximity	YCY	Fragments 10 & 11: -.32 (-2.71+-2.71)		1.734
Proximity	YCY	Fragments 11 & 13: -.32 (-2.71+-2.71)		1.734
Proximity	YCY	Fragments 13 & 14: -.32 (-2.71+-2.71)		1.734
Proximity	YCY	Fragments 14 & 16: -.32 (-2.71+-1.99)		1.504
RESULT	DB=23	All fragments measured	CLOGP=5	4.861

H-Lys-Leu-Lys-6-Ahx-Lys-Leu-Lys-OH (KL1)

C: -2.59

SMILES NOTATION

NC(C(NC(C(NC(C(NCCCCC(=O)NC(C(NC(C(NC(C(O)=O)CCCCN)=O)CC(C)C)=O)CCCCN)=O)CCCCN)=O)CC(C)C)=O)CCCCN

Class	Type	Log(P) Contribution Description	Comment	Value
-------	------	---------------------------------	---------	-------

Appendix C – Bio-Loom determination of the hydrophobic content of synthesised bolaamphiphilic peptides and peptide hybrids (Bio-Loom software is available for download from the internet at www.biobyte.com/prod/bb/bioloom.html).

Fragment	# 1	NH-Amide [AA]	Measured	-2.710
Fragment	# 2	Primary Amine [A]	Measured	-1.540
Fragment	# 3	Primary Amine [A]	Measured	-1.540
Fragment	# 4	NH-Amide [AA]	Measured	-2.710
Fragment	# 5	Primary Amine [A]	Measured	-1.540
Fragment	# 6	NH-Amide [AA]	Measured	-2.710
Fragment	# 7	NH-Amide [AA]	Measured	-2.710
Fragment	# 8	Primary Amine [A]	Measured	-1.540
Fragment	# 9	NH-Amide [AA]	Measured	-2.710
Fragment	#10	NH-Amide [AA]	Measured	-2.710
Fragment	#11	Primary Amine [A]	Measured	-1.540
Fragment	#12	Carboxy (ZW-) [A]	Measured	-1.070
Carbon		35 aliphatic isolating carbons		6.825
ExFragment	Branch	2 chain and 0 cluster branches	Chain	-.260
ExFragment	Branch	6 non-halogen, polar group branches	Group	-1.320
ExFragment	Hydrog	66 hydrogens on isolating carbons		14.982
ExFragment	Bonds	45 chain and 0 alicyclic (net)		-5.400
Proximity	YCY	Fragments 1 & 4: -.32 (-2.71+-2.71)		1.734
Proximity	YCY	Fragments 1 & 2: -.32 (-2.71+-1.54)		1.360
Proximity	YCY	Fragments 4 & 6: -.32 (-2.71+-2.71)		1.734
Proximity	YCY	Fragments 7 & 9: -.32 (-2.71+-2.71)		1.734
Proximity	YCY	Fragments 9 & 10: -.32 (-2.71+-2.71)		1.734
Proximity	YCY	Fragments 10 & 12: -.42 (-2.71+-1.07)		1.588
Zwitterion	Pairs	1 zwitterion pair		-2.270
RESULT	DB=23	All fragments measured	CLOGP=5	-2.588

H-Lys-Leu-Lys-9-Anc-Lys-Leu-Lys-OH (KL2)

C: -1.00

SMILES NOTATION

NC(C(NC(C(NC(C(NCCCCCCCC(=O)NC(C(NC(C(NC(C(O)=O)CCCCN)=O)CC(C)C)=O)CCCCN)=O)CCCCN)=O)CC(C)C)=O)CCCCN

Class	Type	Log(P) Contribution	Description	Comment	Value
Fragment	# 1	NH-Amide [AA]		Measured	-2.710
Fragment	# 2	Primary Amine [A]		Measured	-1.540
Fragment	# 3	Primary Amine [A]		Measured	-1.540
Fragment	# 4	NH-Amide [AA]		Measured	-2.710
Fragment	# 5	Primary Amine [A]		Measured	-1.540
Fragment	# 6	NH-Amide [AA]		Measured	-2.710
Fragment	# 7	NH-Amide [AA]		Measured	-2.710
Fragment	# 8	Primary Amine [A]		Measured	-1.540
Fragment	# 9	NH-Amide [AA]		Measured	-2.710
Fragment	#10	NH-Amide [AA]		Measured	-2.710
Fragment	#11	Primary Amine [A]		Measured	-1.540
Fragment	#12	Carboxy (ZW-) [A]		Measured	-1.070
Carbon		38 aliphatic isolating carbons			7.410
ExFragment	Branch	2 chain and 0 cluster branches		Chain	-.260
ExFragment	Branch	6 non-halogen, polar group branches		Group	-1.320
ExFragment	Hydrog	72 hydrogens on isolating carbons			16.344
ExFragment	Bonds	48 chain and 0 alicyclic (net)			-5.760
Proximity	YCY	Fragments 1 & 4: -.32 (-2.71+-2.71)			1.734
Proximity	YCY	Fragments 1 & 2: -.32 (-2.71+-1.54)			1.360
Proximity	YCY	Fragments 4 & 6: -.32 (-2.71+-2.71)			1.734
Proximity	YCY	Fragments 7 & 9: -.32 (-2.71+-2.71)			1.734
Proximity	YCY	Fragments 9 & 10: -.32 (-2.71+-2.71)			1.734
Proximity	YCY	Fragments 10 & 12: -.42 (-2.71+-1.07)			1.588
Zwitterion	Pairs	1 zwitterion pair			-2.270
RESULT	DB=23	All fragments measured		CLOGP=5	-1.001

Appendix C – Bio-Loom determination of the hydrophobic content of synthesised bolaamphiphilic peptides and peptide hybrids (Bio-Loom software is available for download from the internet at www.biobyte.com/prod/bb/bioloom.html).

H-Lys-Leu-Lys-6-Ahx-Lys-Leu-Lys-NH₂ (KL3)

C: -1.32

SMILES NOTATION

NC(CCCCN)C(NC(CC(C)C)C)C(NC(CCCCN)C(NCCCCC(NC(CCCCN)C(NC(CC(C)C)C)C(NC(CCCCN)C(N)=O)=O)=O)=O)=O

Class	Type	Log(P) Contribution Description	Comment	Value
Fragment	# 1	NH-Amide [AA]	Measured	-2.710
Fragment	# 2	Primary Amine [A]	Measured	-1.540
Fragment	# 3	Primary Amine [A]	Measured	-1.540
Fragment	# 4	NH-Amide [AA]	Measured	-2.710
Fragment	# 5	Primary Amine [A]	Measured	-1.540
Fragment	# 6	NH-Amide [AA]	Measured	-2.710
Fragment	# 7	NH-Amide [AA]	Measured	-2.710
Fragment	# 8	Primary Amine [A]	Measured	-1.540
Fragment	# 9	NH-Amide [AA]	Measured	-2.710
Fragment	#10	NH-Amide [AA]	Measured	-2.710
Fragment	#11	Primary Amine [A]	Measured	-1.540
Fragment	#12	NH2-Amide [A]	Measured	-1.990
Carbon		35 aliphatic isolating carbons		6.825
ExFragment	Branch	2 chain and 0 cluster branches	Chain	-.260
ExFragment	Branch	6 non-halogen, polar group branches	Group	-1.320
ExFragment	Hydrog	66 hydrogens on isolating carbons		14.982
ExFragment	Bonds	45 chain and 0 alicyclic (net)		-5.400
Proximity	YCY	Fragments 1 & 4: -.32 (-2.71+-2.71)		1.734
Proximity	YCY	Fragments 1 & 2: -.32 (-2.71+-1.54)		1.360
Proximity	YCY	Fragments 4 & 6: -.32 (-2.71+-2.71)		1.734
Proximity	YCY	Fragments 7 & 9: -.32 (-2.71+-2.71)		1.734
Proximity	YCY	Fragments 9 & 10: -.32 (-2.71+-2.71)		1.734
Proximity	YCY	Fragments 10 & 12: -.32 (-2.71+-1.99)		1.504
RESULT	DB=23	All fragments measured	CLOGP=5	-1.321

H-Lys-Leu-Lys-9-Anc-Lys-Leu-Lys-NH₂ (KL4)

C: 0.27

SMILES NOTATION

NC(CCCCN)C(NC(CC(C)C)C)C(NC(CCCCN)C(NCCCCCCCC(NC(CCCCN)C(NC(CC(C)C)C)C(NC(CCCCN)C(N)=O)=O)=O)=O)=O

Class	Type	Log(P) Contribution Description	Comment	Value
Fragment	# 1	NH-Amide [AA]	Measured	-2.710
Fragment	# 2	Primary Amine [A]	Measured	-1.540
Fragment	# 3	Primary Amine [A]	Measured	-1.540
Fragment	# 4	NH-Amide [AA]	Measured	-2.710
Fragment	# 5	Primary Amine [A]	Measured	-1.540
Fragment	# 6	NH-Amide [AA]	Measured	-2.710
Fragment	# 7	NH-Amide [AA]	Measured	-2.710
Fragment	# 8	Primary Amine [A]	Measured	-1.540
Fragment	# 9	NH-Amide [AA]	Measured	-2.710
Fragment	#10	NH-Amide [AA]	Measured	-2.710
Fragment	#11	Primary Amine [A]	Measured	-1.540
Fragment	#12	NH2-Amide [A]	Measured	-1.990
Carbon		38 aliphatic isolating carbons		7.410
ExFragment	Branch	2 chain and 0 cluster branches	Chain	-.260
ExFragment	Branch	6 non-halogen, polar group branches	Group	-1.320
ExFragment	Hydrog	72 hydrogens on isolating carbons		16.344
ExFragment	Bonds	48 chain and 0 alicyclic (net)		-5.760
Proximity	YCY	Fragments 1 & 4: -.32 (-2.71+-2.71)		1.734
Proximity	YCY	Fragments 1 & 2: -.32 (-2.71+-1.54)		1.360
Proximity	YCY	Fragments 4 & 6: -.32 (-2.71+-2.71)		1.734
Proximity	YCY	Fragments 7 & 9: -.32 (-2.71+-2.71)		1.734
Proximity	YCY	Fragments 9 & 10: -.32 (-2.71+-2.71)		1.734
Proximity	YCY	Fragments 10 & 12: -.32 (-2.71+-1.99)		1.504
RESULT	DB=23	All fragments measured	CLOGP=5	.266

Appendix C – Bio-Loom determination of the hydrophobic content of synthesised bolaamphiphilic peptides and peptide hybrids (Bio-Loom software is available for download from the internet at www.biobyte.com/prod/bb/bioloom.html).

H-Orn-Leu-Orn-9-Anc-Orn-Leu-Orn-NH₂ (OL1)

C: -1.85

SMILES NOTATION

NC(CCCN)C(NC(CC(C)C)C(NC(CCCN)C(NCCCCCCCC(NC(CCCN)C(NC(CC(C)C)C(NC(CCCN)C(N)=O)=O)=O)=O)=O)=O)=O

Class	Type	Log(P) Contribution	Description	Comment	Value
Fragment	# 1		NH-Amide [AA]	Measured	-2.710
Fragment	# 2		Primary Amine [A]	Measured	-1.540
Fragment	# 3		Primary Amine [A]	Measured	-1.540
Fragment	# 4		NH-Amide [AA]	Measured	-2.710
Fragment	# 5		Primary Amine [A]	Measured	-1.540
Fragment	# 6		NH-Amide [AA]	Measured	-2.710
Fragment	# 7		NH-Amide [AA]	Measured	-2.710
Fragment	# 8		Primary Amine [A]	Measured	-1.540
Fragment	# 9		NH-Amide [AA]	Measured	-2.710
Fragment	#10		NH-Amide [AA]	Measured	-2.710
Fragment	#11		Primary Amine [A]	Measured	-1.540
Fragment	#12		NH2-Amide [A]	Measured	-1.990
Carbon			34 aliphatic isolating carbons		6.630
ExFragment	Branch		2 chain and 0 cluster branches	Chain	-.260
ExFragment	Branch		6 non-halogen, polar group branches	Group	-1.320
ExFragment	Hydrog		64 hydrogens on isolating carbons		14.528
ExFragment	Bonds		44 chain and 0 alicyclic (net)		-5.280
Proximity	YCY		Fragments 1 & 4: -.32 (-2.71+-2.71)		1.734
Proximity	YCY		Fragments 1 & 2: -.32 (-2.71+-1.54)		1.360
Proximity	YCY		Fragments 4 & 6: -.32 (-2.71+-2.71)		1.734
Proximity	YCY		Fragments 7 & 9: -.32 (-2.71+-2.71)		1.734
Proximity	YCY		Fragments 9 & 10: -.32 (-2.71+-2.71)		1.734
Proximity	YCY		Fragments 10 & 12: -.32 (-2.71+-1.99)		1.504
RESULT	DB=23		All fragments measured	CLOGP=5	-1.850

H-Orn-Leu-Orn-Gly-Pro-Gly-Orn-Leu-Orn-NH₂ (OL2)

C: -5.33

SMILES NOTATION

NC(CCCN)C(NC(CC(C)C)C(NC(CCCN)C(NC([H])C(N1C(C(NC([H])C(NC(CCCN)C(NC(CC(C)C)C(NC(CCCN)C(N)=O)=O)=O)=O)=O)CC1)=O)=O)=O

Class	Type	Log(P) Contribution	Description	Comment	Value
Fragment	# 1		[H]* [A]	Calculated	-1.316
Fragment	# 2		NH-Amide [AA]	Measured	-2.710
Fragment	# 3		Amide [RRA]	Derived	-3.600
Fragment	# 4		[H]* [A]	Calculated	-1.316
Fragment	# 5		NH-Amide [AA]	Measured	-2.710
Fragment	# 6		Primary Amine [A]	Measured	-1.540
Fragment	# 7		NH-Amide [AA]	Measured	-2.710
Fragment	# 8		NH-Amide [AA]	Measured	-2.710
Fragment	# 9		Primary Amine [A]	Measured	-1.540
Fragment	#10		Primary Amine [A]	Measured	-1.540
Fragment	#11		NH-Amide [AA]	Measured	-2.710
Fragment	#12		Primary Amine [A]	Measured	-1.540
Fragment	#13		NH-Amide [AA]	Measured	-2.710
Fragment	#14		NH-Amide [AA]	Measured	-2.710
Fragment	#15		Primary Amine [A]	Measured	-1.540
Fragment	#16		NH2-Amide [A]	Measured	-1.990
Carbon			32 aliphatic isolating carbons		6.240
ExFragment	Branch		2 chain and 0 cluster branches	Chain	-.260
ExFragment	Branch		9 non-halogen, polar group branches	Group	-1.980
ExFragment	Hydrog		57 hydrogens on isolating carbons		12.939
ExFragment	Bonds		41 chain and 5 alicyclic (net)	Combined	-5.370
Proximity	YCY		Fragments 1 & 2: -.32 (-1.32+-2.71)		1.288
Proximity	YCY		Fragments 1 & 11: -.32 (-1.32+-2.71)		1.288

Appendix C – Bio-Loom determination of the hydrophobic content of synthesised bolaamphiphilic peptides and peptide hybrids (Bio-Loom software is available for download from the internet at www.biobyte.com/prod/bb/bioloom.html).

Proximity	YCY	Fragments 2 & 3: -0.32 (-2.71+-3.60)	2.019
Proximity	YCY	Fragments 3 & 4: -0.32 (-3.60+-1.32)	1.573
Proximity	YCY	Fragments 3 & 5: -0.32 (-3.60+-2.71)	2.019
Proximity	YCY	Fragments 5 & 7: -0.32 (-2.71+-2.71)	1.734
Proximity	YCY	Fragments 7 & 8: -0.32 (-2.71+-2.71)	1.734
Proximity	YCY	Fragments 8 & 9: -0.32 (-2.71+-1.54)	1.360
Proximity	YCY	Fragments 11 & 13: -0.32 (-2.71+-2.71)	1.734
Proximity	YCY	Fragments 13 & 14: -0.32 (-2.71+-2.71)	1.734
Proximity	YCY	Fragments 14 & 16: -0.32 (-2.71+-1.99)	1.504
RESULT	DB=23	Calculated fragment value	CLOGP=5 -5.333

H-Orn-Tyr-Orn-9-Anc-Orn-Tyr-Orn-NH₂ (OY1)

C: -3.26

SMILES NOTATION

NC(CCCN)C(NC(CC1=CC=C(O)C=C1)C(NC(CCCN)C(NCCCCCCCC(NC(CCCN)C(NC(CC2=CC=C(O)C=C2)C(NC(CCCN)C(N)=O)=O)=O)=O)=O)=O)=O

Class	Type	Log(P) Contribution Description	Comment	Value
Fragment	# 1	Primary Amine [A]	Measured	-1.540
Fragment	# 2	Primary Amine [A]	Measured	-1.540
Fragment	# 3	NH-Amide [AA]	Measured	-2.710
Fragment	# 4	Alcohol or Hydroxy [a]	Measured	-0.440
Fragment	# 5	NH-Amide [AA]	Measured	-2.710
Fragment	# 6	Primary Amine [A]	Measured	-1.540
Fragment	# 7	NH-Amide [AA]	Measured	-2.710
Fragment	# 8	NH-Amide [AA]	Measured	-2.710
Fragment	# 9	Primary Amine [A]	Measured	-1.540
Fragment	#10	NH-Amide [AA]	Measured	-2.710
Fragment	#11	Alcohol or Hydroxy [a]	Measured	-0.440
Fragment	#12	NH-Amide [AA]	Measured	-2.710
Fragment	#13	Primary Amine [A]	Measured	-1.540
Fragment	#14	NH2-Amide [A]	Measured	-1.990
Carbon		28 aliphatic isolating carbons		5.460
Carbon		12 aromatic isolating carbons		1.560
ExFragment	Branch	6 non-halogen, polar group branches	Group	-1.320
ExFragment	Hydrog	58 hydrogens on isolating carbons		13.166
ExFragment	Bonds	40 chain and 0 alicyclic (net)		-4.800
Benzylbond	Simple	2 benzyl bonds to simple aromatics		-0.300
Proximity	YCY	Fragments 2 & 3: -0.32 (-1.54+-2.71)		1.360
Proximity	YCY	Fragments 3 & 5: -0.32 (-2.71+-2.71)		1.734
Proximity	YCY	Fragments 5 & 7: -0.32 (-2.71+-2.71)		1.734
Proximity	YCY	Fragments 8 & 10: -0.32 (-2.71+-2.71)		1.734
Proximity	YCY	Fragments 10 & 12: -0.32 (-2.71+-2.71)		1.734
Proximity	YCY	Fragments 12 & 14: -0.32 (-2.71+-1.99)		1.504
RESULT	DB=23	All fragments measured	CLOGP=5	-3.262

H-Orn-Tyr-Orn-Gly-Pro-Gly-Orn-Tyr-Orn-NH₂ (OY2)

C: -6.75

SMILES NOTATION

NC(CCCN)C(NC(CC1=CC=C(O)C=C1)C(NC(CCCN)C(NC([H])C(N2C(C(NC([H])C(NC(CCCN)C(NC(CC3=CC=C(O)C=C3)C(NC(CCCN)C(N)=O)=O)=O)=O)CCC2)=O)=O)=O) # Calculated fragment value

Class	Type	Log(P) Contribution Description	Comment	Value
Fragment	# 1	[H]* [A]	Calculated	-1.316
Fragment	# 2	NH-Amide [AA]	Measured	-2.710
Fragment	# 3	Amide [RRA]	Derived	-3.600
Fragment	# 4	[H]* [A]	Calculated	-1.316
Fragment	# 5	NH-Amide [AA]	Measured	-2.710
Fragment	# 6	Primary Amine [A]	Measured	-1.540

Appendix C – Bio-Loom determination of the hydrophobic content of synthesised bolaamphiphilic peptides and peptide hybrids (Bio-Loom software is available for download from the internet at www.biobyte.com/prod/bb/bioloom.html).

Fragment	# 7	NH-Amide [AA]	Measured	-2.710
Fragment	# 8	Alcohol or Hydroxy [a]	Measured	-.440
Fragment	# 9	NH-Amide [AA]	Measured	-2.710
Fragment	#10	Primary Amine [A]	Measured	-1.540
Fragment	#11	Primary Amine [A]	Measured	-1.540
Fragment	#12	NH-Amide [AA]	Measured	-2.710
Fragment	#13	Primary Amine [A]	Measured	-1.540
Fragment	#14	NH-Amide [AA]	Measured	-2.710
Fragment	#15	Alcohol or Hydroxy [a]	Measured	-.440
Fragment	#16	NH-Amide [AA]	Measured	-2.710
Fragment	#17	Primary Amine [A]	Measured	-1.540
Fragment	#18	NH2-Amide [A]	Measured	-1.990
Carbon		26 aliphatic isolating carbons		5.070
Carbon		12 aromatic isolating carbons		1.560
ExFragment	Branch	9 non-halogen, polar group branches	Group	-1.980
ExFragment	Hydrog	51 hydrogens on isolating carbons		11.577
ExFragment	Bonds	37 chain and 5 alicyclic (net)	Combined	-4.890
Benzylbond	Simple	2 benzyl bonds to simple aromatics		-.300
Proximity	YCY	Fragments 1 & 2: -.32 (-1.32+-2.71)		1.288
Proximity	YCY	Fragments 1 & 12: -.32 (-1.32+-2.71)		1.288
Proximity	YCY	Fragments 2 & 3: -.32 (-2.71+-3.60)		2.019
Proximity	YCY	Fragments 3 & 4: -.32 (-3.60+-1.32)		1.573
Proximity	YCY	Fragments 3 & 5: -.32 (-3.60+-2.71)		2.019
Proximity	YCY	Fragments 5 & 7: -.32 (-2.71+-2.71)		1.734
Proximity	YCY	Fragments 7 & 9: -.32 (-2.71+-2.71)		1.734
Proximity	YCY	Fragments 9 & 10: -.32 (-2.71+-1.54)		1.360
Proximity	YCY	Fragments 12 & 14: -.32 (-2.71+-2.71)		1.734
Proximity	YCY	Fragments 14 & 16: -.32 (-2.71+-2.71)		1.734
Proximity	YCY	Fragments 16 & 18: -.32 (-2.71+-1.99)		1.504
RESULT	DB=23	Calculated fragment value	CLOGP=5	-6.745

H-Leu-Orn-Leu-9-Anc-Leu-Orn-Leu-NH₂ (LO1)

C: 2.72

SMILES NOTATION

NC(CC(C)C)C(NC(CCCN)C(NC(CC(C)C)C(NCCCCCCCC(NC(CC(C)C)C(NC(CCCN)C(NC(CC(C)C)C(NC(=O)=O)=O)=O)=O)=O)=O)=O

Class	Type	Log(P) Contribution	Description	Comment	Value
Fragment	# 1	Primary Amine [A]		Measured	-1.540
Fragment	# 2	NH-Amide [AA]		Measured	-2.710
Fragment	# 3	Primary Amine [A]		Measured	-1.540
Fragment	# 4	NH-Amide [AA]		Measured	-2.710
Fragment	# 5	NH-Amide [AA]		Measured	-2.710
Fragment	# 6	NH-Amide [AA]		Measured	-2.710
Fragment	# 7	NH-Amide [AA]		Measured	-2.710
Fragment	# 8	Primary Amine [A]		Measured	-1.540
Fragment	# 9	NH-Amide [AA]		Measured	-2.710
Fragment	#10	NH2-Amide [A]		Measured	-1.990
Carbon		36 aliphatic isolating carbons			7.020
ExFragment	Branch	4 chain and 0 cluster branches		Chain	-.520
ExFragment	Branch	6 non-halogen, polar group branches		Group	-1.320
ExFragment	Hydrog	70 hydrogens on isolating carbons			15.890
ExFragment	Bonds	44 chain and 0 alicyclic (net)			-5.280
Proximity	YCY	Fragments 1 & 2: -.32 (-1.54+-2.71)			1.360
Proximity	YCY	Fragments 2 & 4: -.32 (-2.71+-2.71)			1.734
Proximity	YCY	Fragments 4 & 5: -.32 (-2.71+-2.71)			1.734
Proximity	YCY	Fragments 6 & 7: -.32 (-2.71+-2.71)			1.734
Proximity	YCY	Fragments 7 & 9: -.32 (-2.71+-2.71)			1.734
Proximity	YCY	Fragments 9 & 10: -.32 (-2.71+-1.99)			1.504
RESULT	DB=23	All fragments measured		CLOGP=5	2.722

Appendix C – Bio-Loom determination of the hydrophobic content of synthesised bolaamphiphilic peptides and peptide hybrids (Bio-Loom software is available for download from the internet at www.biobyte.com/prod/bb/bioloom.html).

H-Leu-Tyr-Leu-9-Anc-Leu-Tyr-Leu-NH₂ (LY1)

C: 5.88

SMILES NOTATION

NC(CC(C)C)C(NC(CC1=CC=C(O)C=C1)C(NC(CC(C)C)C(NCCCCCCCC(NC(CC(C)C)C(NC(CC2=CC=C(O)C=C2)C(NC(CC(C)C)C(N)=O)=O)=O)=O)=O)=O

Class	Type	Log(P) Contribution Description	Comment	Value
Fragment	# 1	Primary Amine [A]	Measured	-1.540
Fragment	# 2	NH-Amide [AA]	Measured	-2.710
Fragment	# 3	Alcohol or Hydroxy [a]	Measured	- .440
Fragment	# 4	NH-Amide [AA]	Measured	-2.710
Fragment	# 5	NH-Amide [AA]	Measured	-2.710
Fragment	# 6	NH-Amide [AA]	Measured	-2.710
Fragment	# 7	NH-Amide [AA]	Measured	-2.710
Fragment	# 8	Alcohol or Hydroxy [a]	Measured	- .440
Fragment	# 9	NH-Amide [AA]	Measured	-2.710
Fragment	#10	NH2-Amide [A]	Measured	-1.990
Carbon		32 aliphatic isolating carbons		6.240
Carbon		12 aromatic isolating carbons		1.560
ExFragment	Branch	4 chain and 0 cluster branches	Chain	- .520
ExFragment	Branch	6 non-halogen, polar group branches	Group	-1.320
ExFragment	Hydrog	70 hydrogens on isolating carbons		15.890
ExFragment	Bonds	40 chain and 0 alicyclic (net)		-4.800
Benzylbond	Simple	2 benzyl bonds to simple aromatics		- .300
Proximity	YCY	Fragments 1 & 2: -.32 (-1.54+-2.71)		1.360
Proximity	YCY	Fragments 2 & 4: -.32 (-2.71+-2.71)		1.734
Proximity	YCY	Fragments 4 & 5: -.32 (-2.71+-2.71)		1.734
Proximity	YCY	Fragments 6 & 7: -.32 (-2.71+-2.71)		1.734
Proximity	YCY	Fragments 7 & 9: -.32 (-2.71+-2.71)		1.734
Proximity	YCY	Fragments 9 & 10: -.32 (-2.71+-1.99)		1.504
RESULT	DB=23	All fragments measured	CLOGP=5	5.882